The role of pneumococcal carbon metabolism in colonisation and invasive disease

Ana Laura Paixão

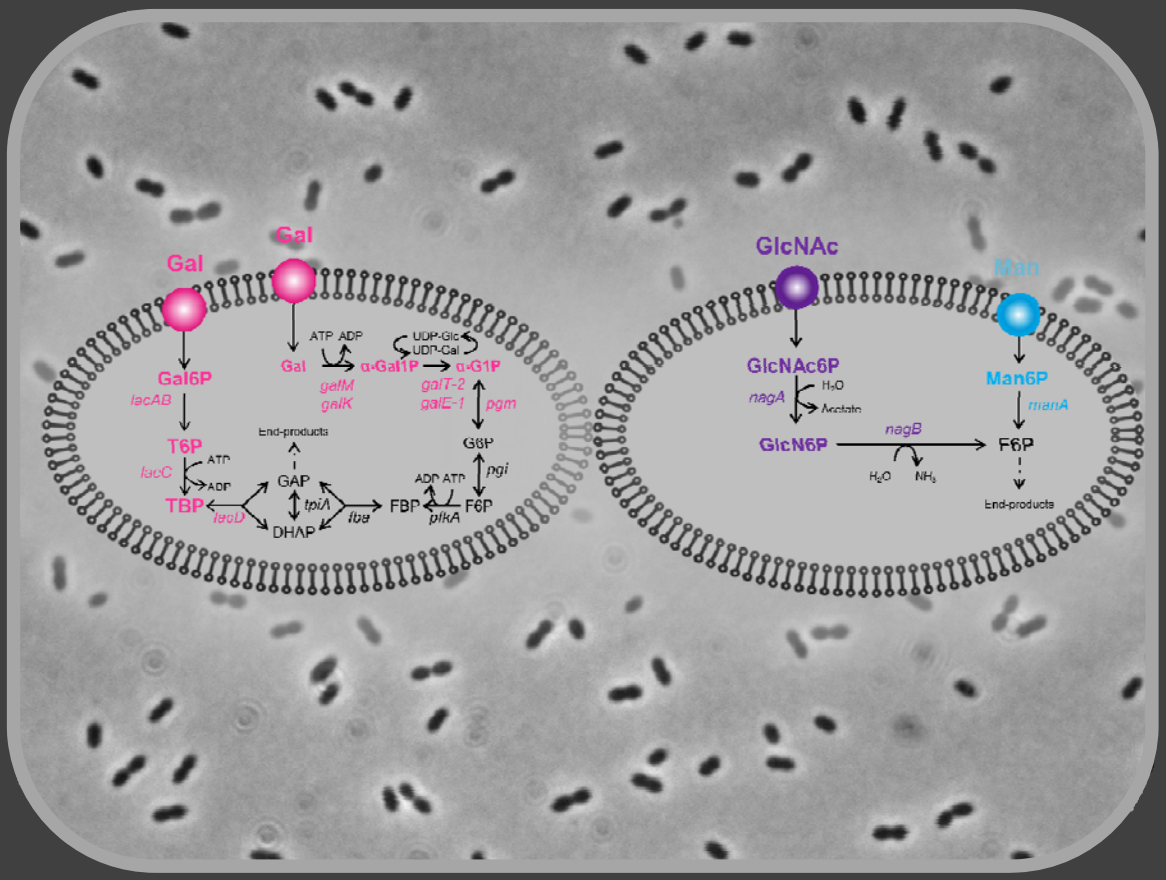

Dissertation presented to obtain the Ph.D degree in Biochemistry

Instituto de Tecnologia Química e Biológica António Xavier | Universidade Nova de Lisboa

Oeiras,
March, 2015

INSTITUTO DE TECNOLOGIA QUÍMICA E BIOLÓGICA ANTÓNIO XAVIER / UNL

Knowledge Creation

The role of pneumococcal carbon metabolism in colonisation and invasive disease

Ana Laura Paixão

Supervisor: Dr. Ana Rute Neves

Co-Supervisors: Professor Peter William Andrew and Dr. Hasan Yesilkaya

Interim Co-Supervisor: Professor Adriano Oliveira Henriques (2012-2015)

Dissertation presented to obtain the Ph.D degree in Biochemistry

Instituto de Tecnologia Química e Biológica António Xavier | Universidade Nova de Lisboa

Oeiras, March, 2015

From left to right: Patrick Maria Franciscus Derkx, Raquel Sá Leão Domingues da Silva, Karina de Bívar Xavier, Cecília Maria Pais de Faria de Andrade Arraiano, Ana Laura Paixão, Ana Rute Neves, Adriano Oliveira Henriques and Sofia Rocha Pauleta.
Oeiras, March 27th, 2015

Apoio financeiro da Fundação para a Ciência e Tecnologia e do FSE no âmbito do Quadro Comunitário de apoio, Bolsa de Doutoramento com a referência SFRH/BD/46997/2008.

Cover page: Schematic representation of *S. pneumoniae* and catabolic pathways for galactose, mannose and N-acetylglucosamine. Background: phase contrast image of *S. pneumoniae*.

Acknowledgments

It was a long journey since I started my PhD, in the end of 2009. A full life experience. A path full of mixed feelings. The energy and motivation of a new beginning and the fear of failing such a challenge. The happiness of achieving the goals of this work, the surprise of reaching unexpected results and the frustration of failed experiments. The winnings and losses, laughs and tears, and the discovery of different worlds. And now? A new beginning. But before, I would like to express my gratitude to those that enriched this work and personal experience.

First, I would like to thank my supervisor, Dr. Rute Neves, for the opportunity I was given to conduct my PhD in the LAB & *in vivo* NMR laboratory. Thank you for giving me the conditions to accomplish this work until the end, for the guidance, the scientific mentoring and the critical support in reviewing and writing this thesis. I thank the final effort to conclude this thesis in time. The encouragement to share my results in several European meetings and the opportunity to travel to amazing places.

I thank my co-supervisors, Prof. Peter William Andrew and Dr. Hasan Yesilkaya, for accepting me as a PhD student. For the openness to discuss my work and reviewing the first manuscript, contributing to a fruitful collaboration.

To Prof. Adriano Henriques, my “borrowed” co-supervisor, who accepted me in a very difficult period. For all the wise advices and for helping me not to give up. For contributing to my serenity in the most

troublesome times. I am thankful for being always open to discuss my work and for teach me to do one thing at a time.

To Dr. Jan-Willem Veening who received me in his lab (Molecular Genetics - Groningen Institute of Biomolecular Sciences & Biotechnology) and supervised my work during my stay in Groningen. The best work experience I ever had. Thank you for running such a nice lab, full of interesting people, who received me so well.

To my dearest post-doc, Morten Kjos, the kindest person I have ever met. Always concerned with my work and my well-being while I was in Groningen. Thank you for all the support and help in the complementation assays, especially when I left Groningen and there were still experiments to be concluded.

To Prof Helena Santos for the valuable discussions held in her lab meeting presentations during the first years of my PhD.

To Ana Lúcia Carvalho for her tireless help. For her support and effort to conclude all the *in vivo* NMR experiments with me before leaving to her new professional challenge. For teaching me everything she knew about HPLC and *in vivo* NMR. And most importantly, for her friendship. Thank you for all the good moments in and outside the lab.

To José Caldas I thank all the help, dedication and interest in the microarrays analysis. Thank you for such a fruitful collaboration.

To Nuno Borges, for being always available to help both by giving technical tips to conduct my experiments and by showing openness to share lab material.

To Luis Gafeira, for being such an enthusiastic, passionate about science, who contributes with creative ideas to the work of everyone, including mine. Always willing to help. I will remember him for being a good listener and a friend.

To Paula Gaspar for sharing her knowledge and technical support.

To all the past and present members of Cell Physiology and NMR group (because you are so many I won't enumerate – I could fail someone), for being always available to help and for sharing good parties with the LAB & *in vivo* NMR laboratory.

To Joana Oliveira for doubling my hands in the growth experiments. Thank you for the effort.

To all my colleagues in the in the LAB & *in vivo* NMR that contributed to this experience in so many ways.

To Dr. Susana Vinga and André Veríssimo for the modelling of the growth curves and statistical analysis.

To Dr. Rita Ventura and Eva Lourenço for the synthesis of phosphorylated compounds.

To all the other collaborators that contributed in different ways to this thesis: Dr. Tomas Kloosterman, Dr. Vitor Fernandes and Prof. Dr. Oscar Kuipers.

To Dr. Mariana Pinho and her students Pedro, Pedrinho and Raquel, that moved to our laboratory without disturbing my ongoing work.

To Teresa Maio, Ana Mingote, Sónia Estêvão, Teresa Ferreira, Tiago Pais and Marta Rodrigues for contributing to the most hilarious times in and outside the lab.

To all my colleagues from the 2010 PhD classes with whom I shared good moments.

To Fundação para a Ciência e a Tecnologia for the financial support that made this doctoral work possible (SFRH / BD / 46997 / 2008).

With the greatest gratitude, I dedicate this thesis to my parents and my husband, Gonçalo. This experience was also yours. I am grateful for your unconditional support, comprehension, love, and advices. Without them, it would have been much more difficult. Thank you for being always there when I needed the most.

A special word to my siblings Tiago, Afonso and Mariana: love you guys. Thank you for sharing the most important times with me.

Abstract

Streptococcus pneumoniae is a common asymptomatic commensal of the human nasopharynx. However, it is better known as a threatening pathogen that causes serious diseases such as pneumonia, meningitis and sepsis, as well as other less severe but more prevalent infections (*e.g*. otitis media). With the increase of antibiotic resistance and the limited efficacy of vaccines, pneumococcal infections remain a major problem. Therefore, the discovery of new therapeutic targets and preventive drugs are in high demand. Given this panorama, much attention has been dedicated to classical aspects of virulence (*e.g.* toxins, capsule or cell wall components), but the knowledge of *in vivo* physiology and metabolism of *S. pneumoniae* is still limited. This is intriguing, considering that to a large extent, pneumococcal pathogenesis relies on efficient acquisition and metabolism of the nutrients required for growth and survival in the host niches. In line with this view, recent work uncovers substantial interdependencies between carbohydrate metabolism and virulence. These findings denote a far greater importance of basic pneumococcal physiology than previously imagined. However, a scarcity of data on sugar metabolism and its regulation in *S. pneumoniae* hampers a comprehensive understanding of the connections between these processes.

The ultimate goal of this thesis is to improve our understanding of *S. pneumoniae* basic physiology and discover links between carbohydrate metabolism and the ability of the bacterium to colonise and cause disease.

S. pneumoniae is a strictly fermentative microorganism that relies on glycolytic metabolism to obtain energy, but free monosaccharides are limited in the airways. The most abundant sugars present in the natural niche of *S. pneumoniae* are the glycoproteins mucins, which are generally

composed of N-acetylglucosamine (GlcNAc), N-acetylgalactosamine (GalNAc), N-acetylneuraminic acid (NeuNAc), galactose (Gal), fucose (Fuc) and sulphated sugars linked to the protein core. Importantly, *S. pneumoniae* possesses a large set of extracellular glycosidases that act over glycans and release free sugars that can potentially be used for grow. Therefore, we hypothesised that the pneumococcus depends on one or multiple glycan-derived sugars to grow.

To disclose prevalent pathways during growth on mucin we resorted to a transcriptome analysis comparing transcript levels during growth on the model glycoprotein porcine gastric mucin and glucose (Glc). The gene expression profile revealed Gal, Man and GlcNAc as the most probable glycan-derived sugars to be used as carbon sources by *S. pneumoniae* D39. Accordingly, D39 was able to grow on these sugars, but not on other host-derived glycan monosaccharides (Fuc, NeuNAc, GalNAc), as expected from its genomic potential. An in depth characterization of growth profiles on a chemically defined medium supplemented with each carbohydrate using two different sugar concentrations (30 and 10 mM) was performed. *S. pneumoniae* displayed a preference for GlcNAc, whereas Gal was the least preferable carbohydrate for growth, but energetically the most favourable. The inefficient Gal catabolism could be partially explained by the absence of a high affinity Gal transporter. Gal caused a remarkable metabolic shift from homolactic to a truly mixed acid fermentation. The *in silico* predicted pathways for the catabolism of each sugar were experimentally validated at the biochemical level by determining sugar-specific intracellular metabolites and pathway specific enzyme activities. Furthermore, mutants were generated in each pathway by inactivation of a gene encoding a pathway specific enzyme, and their analysis proved at the genetic level the biochemical analyses. Curiously, inactivation of *galK* (Leloir pathway) rendered a strain unable to grow on Gal even though an alternative pathway for Gal processing is available

(tagatose 6-phosphate pathway), suggesting a subtle regulatory link between the two pathways.

Intranasal mouse infection models of pneumococcal colonisation and disease (bronchopneumonia with bacteraemia) showed that mutants in the Gal catabolic genes (Δ*lacD*, Δ*galK,* Δ*lacD*Δ*galK*) were attenuated, but mutants on Man (Δ*manA*) and GlcNAc (Δ*nagA*) pathways were not. Our data identified Gal as a key nutrient for growth in the respiratory tract. Strengthening this view is the large fraction of genes committed to Gal catabolism induced by mucin (25%) as well as the considerable group of virulence genes (8.2%) displaying altered expression in response to Gal.

The response to Gal, GlcNAc and Man (test sugars) was also evaluated at the transcriptional and metabolic levels. The transcriptional response was substantial and sugar-specific. Gal, GlcNAc and Man affected the expression of up to 8.4%, 11.4%, and 14.2% of the genome, respectively, covering multiple cellular processes, including specific sugar pathways, central metabolism and virulence. An overview of the transcriptional response of central carbon metabolism functions (sugar transport and sugar specific pathways, glycolysis and fermentation pathways) to growth on the glycan-derived sugars as compared to Glc is presented. A complete correlation between expression profiles and pneumococcal phenotypic traits was not observed, denoting regulation at other cellular layers, such as post-transcriptional and/or metabolic levels. Hence, the glycolytic dynamics of *S. pneumoniae* D39 during catabolism of the glycan-derived sugars were monitored in resting cells by *in vivo* ^{13}C-NMR. The rate of GlcNAc utilization was similar to that of the fast metabolizable sugar Glc, and likewise the glycolytic metabolite fructose 1,6-bisphosphate (FBP), a metabolic activator of homolactic metabolism, accumulated to considerably high concentrations (*circa* 30 mM). In line, this sugar displayed a fully homolactic end-product profile. In contrast, the rates of Gal and Man utilization were 2-fold lower, the accumulation of

FBP was considerably reduced to *circa* 12 mM, and a mixed-acid fermentation profile was observed. In addition, specific metabolic intermediates (α-galactose 6-phosphate and mannose 6-phosphate) accumulated, suggesting metabolic bottlenecks in the specific steps converting Gal and Man to glycolytic intermediates. On Man, the metabolic constriction most likely occurs at the level of mannose 6-phosphate isomerase, since growth is improved when this activity is positively modulated by varying the gene expression.

In the host *S. pneumoniae* has to cope with fluctuating concentrations of carbon sources. While free sugars, particularly Glc, are scarce in the nasopharynx, in the bloodstream and during infection Glc is comparatively higher. Therefore, we hypothesised that during the transition from colonisation to invasive disease *S. pneumoniae* adapts to the nutritional changes through a specific response to a Glc stimulus that result in changes in gene regulation and metabolism.

Thus, cells growing in glycan-derived sugars or in a sugar mixture of Gal, GlcNAc and Man were challenged in exponential phase with a Glc pulse. The response to this stimulus was evaluated at the transcriptional, physiological and metabolic (for Gal-adapted cells) levels. Glc was readily consumed independently of the initial substrate adaptation, strengthening the view that Glc is the preferred carbohydrate for pneumococcal growth. The transcriptional response to a Glc stimulus was large, the most represented COG category being carbohydrate metabolism and transport. Except for Man-adapted cells, Glc exerted mostly negative regulation over the majority of genes encoding central carbon metabolism functions. Additionally, Glc induced shifts to more homolactic profiles and, which on Gal was accompanied by an increase on the FBP concentration following the Glc pulse.

The expression of classical virulence factors was also sugar dependent, but Glc consistently exerted a repressive effect over virulence

genes. Interestingly, cells adapted to grow on a sugar mixture (Gal, Man and GlcNAc) displayed the smallest transcriptional response to Glc, suggesting improved fitness of *S. pneumoniae* when exposed to varied sugars. We suggest that the nasopharynx is the reservoir for the development of niche-specific virulence traits, essential for successful colonisation of the niche. In addition, the majority of these virulence factors are downregulated by a Glc stimulus, and are therefore not required in disease. The link between sugar metabolism and virulence is herein reinforced.

Overall, the findings of this thesis substantially contribute to the comprehension of the interdependency between carbohydrate metabolism, adaptation to host niches and virulence. Furthermore, the "omic" data collected at different regulatory layers can in the future be used to fuel multi-scale metabolic models. Such mathematical representations of metabolism are expected to provide robust platforms for data integration and interpretation, and thus generate testable hypothesis, which in the future will facilitate the identification of novel targets for alternative therapeutic and preventive drugs.

Resumo

Streptococcus pneumoniae é um organismo comensal assintomático comummente encontrado na nasofaringe humana. Contudo, é mais conhecido no seu papel patogénico ameaçador que causa doenças como a pneumonia, a meningite ou septicémia, bem como outras infeções menos severas mas mais recorrentes (*e.g.* otite média). Com o aumento da resistência a antibióticos e a eficácia limitada das vacinas, as infeções pneumocócicas permanecem um importante problema. Assim sendo, há uma grande necessidade em descobrir novos alvos terapêuticos e drogas preventivas. Neste contexto, a atenção tem-se focado em aspetos clássicos da virulência (*e.g.*, toxinas, cápsula ou componentes da parede celular). No entanto, o conhecimento da fisiologia *in vivo* e do metabolismo de *Streptococcus pneumoniae* é ainda limitado. Esta situação é intrigante, considerando que em grande medida, a patogenicidade pneumocócica baseia-se na aquisição eficiente e subsequente metabolismo de nutrientes necessários para o crescimento e a sobrevivência em nichos no hospedeiro. A corroborar esta afirmação, estudos recentes revelam interdependências substanciais entre o metabolismo dos hidratos de carbono e a virulência, e sugerem que o conhecimento sólido da fisiologia pneumocócica básica é mais importante do que antecipado. Contudo, a escassez de dados relativos ao metabolismo de açúcares e a sua regulação em *S. pneumoniae* limita a compreensão das ligações entre estes processos.

O objetivo último desta tese é o de melhorar o conhecimento da fisiologia básica de *S. pneumoniae* e descobrir relações entre o metabolismo dos hidratos de carbono e a capacidade da bactéria em colonizar e causar doença.

S. pneumoniae é um microrganismo estritamente fermentativo que depende do metabolismo glicolítico para obter energia, mas os monossacáridos livres são escassos nas vias respiratórias. Os açúcares mais abundantes presentes no nicho natural de *S. pneumoniae* são as glicoproteínas mucinas, compostas geralmente por N-acetylglucosamina (GlcNAc), N-acetylgalactosamina (GalNAc), ácido N-acetilneuramínico (NeuNAc), galactose (Gal), fucose (Fuc) e açúcares sulfatados ligados a um núcleo proteico. De realçar que *S. pneumoniae* possui um grande conjunto de glicosidases extracelulares que atuam sobre os glicanos e libertam açúcares que podem potencialmente ser utilizados para crescimento. Por conseguinte, colocámos e testámos a hipótese de que os pneumococos podem depender, para crescimento, de um ou de múltiplos açúcares derivados destes glicanos.

Para revelar as vias predominantes durante o crescimento em mucinas recorremos a uma análise de transcriptómica comparando os níveis de transcrição durante o crescimento na presença de mucina gástrica de suíno, enquanto glicoproteína modelo, e na presença de glucose (Glc). O perfil de expressão génica revelou que a Gal, Man e GlcNAc são os açúcares derivados de glicano mais provavelmente utilizados como fontes de carbono por *S. pneumoniae* D39. Em consonância, a estirpe D39 cresce nestes açúcares, mas não em outros monossacáridos derivados de glicanos do hospedeiro (Fuc, NeuNAc, GalNAc), como antecipado do seu potencial genómico. Realizou-se uma caracterização aprofundada dos perfis de crescimento em meio quimicamente definido suplementado com cada hidrato de carbono usando duas concentrações de açúcar (30 e 10 mM). *S. pneumoniae* demonstrou preferência por GlcNAc, enquanto Gal foi o hidrato de carbono menos preferido para crescimento, mas energeticamente mais favorável. O ineficiente catabolismo de Gal pode ser parcialmente explicado pela ausência de um transportador de Gal de alta afinidade. A

galactose causou um desvio pronunciado da fermentação homolática para ácidos mistos. As vias catabólicas previstas *in silico* para cada açúcar foram experimentalmente validadas ao nível bioquímico, pela determinação de metabolitos intracelulares específicos de cada açúcar e atividades enzimáticas específicas de cada via. Adicionalmente, geraram-se mutantes por inativação de um gene que codifica uma enzima específica de cada via, e a sua análise confirmou ao nível genético a análise bioquímica. Curiosamente, a inativação de *galK* (via Leloir) originou uma estirpe incapaz de crescer em Gal, apesar de ter uma via alternativa disponível para o processamento deste açúcar (via da tagatose 6-fosfato), sugerindo uma conexão subtil na regulação das duas vias.

Modelos de infeção intranasal de ratinhos de colonização pneumocócica e doença (broncopneumonia com bacteriemia) demonstraram que mutantes em genes catabólicos da Gal (Δ*lacD*, Δ*galK,* Δ*lacD*Δ*galK*) são atenuados, mas mutantes nas vias da Man (Δ*manA*) e GlcNAc (Δ*nagA*), não. Os nossos estudos identificaram a Gal como um nutriente crucial para o crescimento no trato respiratório. A grande fração de genes do catabolismo da Gal induzida pela mucina (25%) bem como um grupo considerável de genes de virulência (8.2%) com expressão alterada em Gal, reforçam esta conclusão.

A resposta à Gal, GlcNAc e Man (açúcares teste) foi também avaliada aos níveis transcricional e metabólico. A resposta transcricional foi substancial e dependente do açúcar. Gal, GlcNAc e Man afetaram a expressão até 8.4%, 11.4% e 14.2% do genoma, respetivamente, abrangendo múltiplos processos, incluindo vias específicas de açúcar, metabolismo central e virulência. Apresenta-se uma visão geral da resposta transcricional de funções do metabolismo central de carbono (transporte de açúcar e vias específicas de açúcares, glicólise e vias fermentativas) no crescimento em açúcares derivados de glicanos, em

comparação com a Glc. Não foi observada uma correlação completa entre os perfis de expressão e as características fenotípicas do pneumococo, demonstrando a existência de outros níveis de regulação, incluindo regulação pós-transcricional e/ou metabólica. Consequentemente, a dinâmica glicolítica de *S. pneumoniae* D39 durante o catabolismo de açúcares derivados de glicanos foi monitorizada em células em suspensão por *in vivo* ^{13}C-NMR. A taxa de consumo de GlcNAc foi semelhante à do açúcar rapidamente metabolizado Glc e, do mesmo modo o metabolito glicolítico frutose 1,6-bifosfato (FBP), um ativador do metabolismo homolático, acumulou em concentrações elevadas (cerca de 30 mM). Em concordância, este açúcar apresentou um perfil de produtos finais totalmente homolático. Em contraste, as taxas de consumo de Gal e Man foram 2 vezes inferiores, a acumulação de FBP foi consideravelmente reduzida a aproximadamente 12 mM, e o perfil de fermentação de ácidos mistos foi observado. Além disso, foi detectada a acumulação de intermediários metabólicos específicos (α-galactose 6-fosfato e manose 6-fosfato), sugerindo estrangulamentos metabólicos em passos específicos da conversão de Gal e Man a intermediários glicolíticos. Em Man, a constrição metabólica muito provavelmente ocorre ao nível da manose 6-fosfato isomerase, uma vez que o crescimento é melhorado quando esta atividade é positivamente modulada por alteração da expressão do gene.

No hospedeiro, *S. pneumoniae* tem que lidar com concentrações variáveis de fontes de carbono. Enquanto os açúcares livres, particularmente Glc, são escassos na nasofaringe, na corrente sanguínea e durante a infeção, a Glc é comparativamente elevada. Deste modo, colocámos a hipótese que durante a transição de colonização para doença invasiva *S. pneumoniae* adapta-se às variações nutricionais através de uma resposta específica a um estímulo de Glc que resulta em variações na regulação génica e no metabolismo.

Deste modo, células a crescerem em açúcares derivados de glicanos ou numa mistura de Gal, GlcNAc e Man foram sujeitas, durante o crescimento exponencial, a um pulso de Glc. A resposta a este estímulo foi avaliada aos níveis transcricional, fisiológico e metabólico (para células adaptadas a Gal). A Glc foi prontamente consumida independentemente da adaptação inicial ao substrato, reforçando que a Glc é o hidrato de carbono preferido para o crescimento dos pneumococos. A resposta transcricional ao estímulo de Glc foi ampla, sendo a categoria COG mais representada a do metabolismo de hidratos de carbono e do transporte. À exceção de células adaptadas a Man, a Glc exerceu principalmente uma regulação negativa sobre a maioria dos genes que codificam funções do metabolismo central de carbono. Adicionalmente, a Glc induziu desvios para perfis mais homoláticos e, em Gal foi acompanhado por um aumento da concentração de FBP após o pulso de Glc.

A expressão de fatores de virulência clássicos foi também dependente do açúcar, mas a Glc exerceu consistentemente um efeito repressivo sobre os genes de virulência. De interesse, notámos que as células adaptadas ao crescimento numa mistura de açúcares (Gal, Man e GlcNAc) originaram uma menor resposta transcricional à Glc, sugerindo uma melhor aptidão de *S. pneumoniae* quando exposto a uma variedade de açúcares. Sugerimos que a nasofaringe é o reservatório para o desenvolvimento de traços específicos de virulência, essenciais para a colonização bem-sucedida deste nicho. Adicionalmente, a maioria destes fatores de virulência são reprimidos pelo estímulo de Glc, não sendo por conseguinte necessários na doença. A ligação entre metabolismo de açúcares e virulência é aqui reforçada.

Globalmente, as descobertas desta tese contribuem substancialmente para a compreensão da interdependência entre o metabolismo de hidratos de carbono, a adaptação aos nichos do hospedeiro e a

virulência. Além disso, os dados “ómicos” recolhidos a diferentes níveis de regulação podem no futuro ser utilizados em modelos metabólicos multi-escala. É esperado que tais representações matemáticas do metabolismo constituam plataformas robustas para a integração e a interpretação de dados e, por conseguinte, para a geração de hipóteses que no futuro facilitarão a identificação de novos alvos para terapêuticas alternativas e drogas preventivas.

Contents

Thesis outline

Pneumococcal infections have high socio-economic impact, and are therefore a major burden worldwide. According to the WHO, *S. pneumoniae* causes over 1 million deaths per year in children under 5 years of age. Moreover, this high mortality is exacerbated by the rate at which the organism acquires resistance to traditional antibiotics and by the re-emergence of non-vaccine type strains. Therefore, the development of new therapeutic and preventive agents demands an increasing understanding of *S. pneumoniae* physiology and virulence. The overall goal of this thesis is to gain new insights regarding *S. pneumoniae* adaptive response to sugar availability and the link to *in vivo* fitness and virulence.

Chapter 1 starts with a brief introduction to the main phenotypic traits of *S. pneumoniae*, its ability to colonise the nasopharynx and cause disease, and provides an overview of the traits of the bacterium in the perspective of a commensal and a pathogen. An overview of the major virulence factors is given as well as its link to carbohydrate metabolism. The catabolism, of monosaccharides (galactose, mannose, N-acetylglucosamine, N-acetylgalactosamine, N-acetylneuraminic acid and fucose) is reviewed. The relevance of these sugars in the lifestyle of different bacteria is discussed. Lastly, the current knowledge concerning central metabolism in *S. pneumoniae* is overviewed.

In Chapter 2 we identified the sugar catabolic pathways likely used during growth on a model glycoprotein, porcine gastric mucin, by a whole-genome transcriptome analysis. An in depth characterization of pneumococcal growth on the glycan-derived sugars galactose, mannose

and N-acetylglucosamine is provided. The catabolic pathways of those sugars were, for the first time, experimentally validated at genetic and biochemical levels, confirming the *in silico* predictions. Finally, the relevance of sugar-specific catabolic genes to *in vivo* fitness was assessed in murine models of colonisation (nasopharyngeal carriage) and pneumococcal disease (bronchopneumonia with bacteraemia).

Chapter 3 describes the transcriptional and metabolic responses in the presence of galactose, mannose and N-acetylglucosamine, by DNA microarrays and *in vivo* ^{13}C-NMR, respectively. Glucose is used as the reference sugar.

The effect of adding the fast metabolizable sugar glucose to *S. pneumoniae* cells actively growing on galactose, mannose, N-acetylglucosamine or in a mixture thereof is evaluated at the transcriptional, physiological and metabolic levels.

Furthermore, the influence of the carbohydrate source and the glucose pulse in the gene expression of known virulence factors is examined at the transcriptional level by DNA microarrays.

Chapter 4 provides an integrative discussion of the findings reported in this work.

Abbreviations

ABC	ATP-binding cassette
BgaA	β-galactosidase A
CAP	Community-acquired pneumonia
CcpA	Carbon catabolite protein A
CCR	Carbon catabolite repression
CDM	Chemically defined medium
COG	Clusters of orthologous groups
CRE	Catabolite response elements
DHAP	Dihydroxyacetone phosphate
DW	Dry weight
EI	Enzyme I
EMP	Embden-Meyerhof-Parnas
Eno	Enolase
F6P	Fructose 6-phosphate
Fba	Fructose-bisphosphate aldolase
Fuc	Fucose
FucA	L-fuculose phosphate aldolase
FucI	L-fucose isomerase
FucK	L-fuculose kinase
FucO	L-1,2-propanediol oxidoreductase
FucU	Fucose mutarotase
G6P	Glucose 6-phosphate
Gal	Galactose
Gal6P	Galactose 6-phosphate
GalE	UDP-glucose 4-epimerase
GalK	Galactokinase
GalM	Aldolase 1-epimerase (galactose mutarotase)
GalN	Galactosamine

GalN6P	Galactosamine 6-phosphate
GalNAc	N-acetylgalactosamine
GalNAc6P	N-acetylgalactosamine 6-phosphate
GalP	Galactose permease
GalT	Galactose 1-phosphate uridylyltransferase
Gap	Glyceraldehyde 3-phosphate
Glc	Glucose
GlcN	Glucosamine
GlcN6P	Glucosamine 6-phosphate
GlcNAc	N-acetylglucosamine
GlcNAc6P	N-acetylglucosamine 6-phosphate
HPLC	High performance liquid chromatography
Hpr	Histidine phosphocarrier protein HPr
IPD	Invasive pneumococcal disease
LacAB	Galactose 6-phosphate isomerase subunits LacA and LacB
LacC	Tagatose 6-phosphate kinase
LacD	Tagatose 1,6-diphosphate aldolase
Lcto	Lactate oxidase
LDH	Lactate dehydrogenase
Man	Mannose
Man6P	Mannose 6-phosphate
ManA	Mannose 6-phosphate isomerase
ManNAc	N-acetylmannosamine
ManNAc6P	N-acetylmannosamine 6-phosphate
NagA	N-acetylglucosamine 6-phosphate deacetylase
NagB	Glucosamine 6-phosphate isomerase
NAD^+	Nicotinamide adenine dinucleotide
NADH	Dihydronicotinamide adenine dinucleotide
NanA	Neuraminidase A
NanE	N-acetylmannosamine 6-phosphate epimerase
NanK	N-acetylmannosamine kinase

NBD	ATP- or nucleotide-binding domains
NeuNAc	N-acetylneuraminic acid
NMR	Nuclear magnetic resonance
OD_{max}	Maximum optical density
PCV	Pneumococcal conjugate vaccine
PDHC	Pyruvate dehydrogenase complex
PFL	Pyruvate formate-lyase
PFL-AE	Pyruvate formate-lyase activating enzyme
Pgk	Phosphoglycerate kinase
Pgm	Phosphoglucomutase
PME	Phosphomonoester
PTS	Phosphoenolpyruvate-dependent carbohydrate phosphotransferase system
Pyk	Pyruvate kinase
SBP	Solute-binding proteins
Adh	Alcohol dehydrogenase
SpxB	Pyruvate oxidase
StrH	β-N-acetylglucosaminidase
T6P	Tagatose 6-phosphate
TBP	Tagatose 1,6-bisphosphate
TMD	Transmembrane domains
WHO	World Health Organization
α-G1P	α-glucose 1-phosphate
α-Gal1P	α-galactose 1-phosphate
α-Gal6P	α-galactose 6-phosphate
μ_{max}	Maximum specific growth rate

Chapter 1

General introduction

Chapter 1 - Contents

Streptococcus pneumoniae

At the core of great discoveries

Streptococcus pneumoniae, also known as the pneumococcus, was discovered in 1881 by Louis Pasteur and George Miller Sternberg in two independent studies [1,2]. Shortly after its isolation *S. pneumoniae* was identified as a major causative agent of human lobar pneumonia [1,2]. Due to its morphology (pairs of coccoid bacteria) and the involvement in pneumonia the bacterium was then named *Diplococcus pneumoniae* [1]. The present nomenclature remains since 1974 [1].

The story of *S. pneumoniae* is intertwined with the history of different fields of research that range from microbiology, molecular biology, biochemistry to immunology (reviewed in [1,2]). Indeed, the study of the pneumococcus was at the centre of critical important discoveries. In 1928, Griffith demonstrated that when mice were inoculated with a mixture of dead virulent pneumococcal strains and live avirulent pneumococci, virulent phenotype strains could be recovered from the pneumonia dead animals. This phenomenon was denominated the “transforming principle” [3], and preceded the discovery of DNA as the hereditary material. Indeed, in 1944, Avery, McLeod and McCarthy proved, that the DNA was the transforming principle responsible for the phenotypic changes [4].

Importantly, the discovery that pneumococci were “coated” by a polysaccharide capsule (“sugar-coated microbe” as called by Avery) with serological reactivity provided the basis for the development of the current polysaccharide vaccines [5–10]. Furthermore, the pneumococcus is behind the comprehension of antibiotic resistance. It was one of the first microorganisms recognized to develop resistance to antibiotics [1]. The pneumococcus is also closely associated with key discoveries in

molecular processes such as quorum sensing, autolysis and opsonisation, as well as to the development of molecular tools, the Gram's stain technique and other identification methods (*e.g.* Quellung reaction and bile solubility test) still in use today [1,2].

General characteristics

Streptococcus pneumoniae is a low-GC (40%), Gram-positive, lanceolate cocci (elongated ellipsoid-shape) [11]. These ovoid cells are commonly designated ovococci (Fig. 1.1) [12,13]. It is usually arranged in pairs (diplococci), but can occur as single cells or in short chains. Individual cells can range from 0.5 to 1.25 micrometres in size. *S. pneumoniae* is non-motile and a non-spore forming bacterium. It is an aerotolerant anaerobe and a strictly fermentative microorganism that mainly converts carbohydrates to lactic acid (homolactic fermentation) [11].

S. pneumoniae is a fastidious bacterium that requires nutritionally rich media for growth. Its nutritional requirement for choline is a unique characteristic of this microorganism [14]. It grows optimally at 37ºC in a pH range of 6.5-7.5. When cultured until stationary phase of growth the bacterium displays a tendency to undergo autolysis due to the presence of efficient autolysins, such as autolysin, LytA [15]. The pneumococci are also naturally transformable, taking up DNA from the medium (other bacteria), a phenomenon that contributes to a highly variable genome [16].

The genus *Streptococcus* belongs to the phylum Firmicutes, Lactobacillales order, and Streptococcaceae family. Based on 16S ribosomal RNA, the pneumococcus belongs to the mitis group alongside with other bacteria that can be isolated from the human oro-nasopharynx (*e.g. Streptococcus oralis*, *Streptococcus gordonii*, *Streptococcus mitis, Streptococcus infantis, S. pseudopneumoniae*) [17,18]. The genome

similarity within this group of microorganisms together with frequent events of horizontal gene transfer makes it difficult to differentiate *S. pneumoniae* from other closely related commensals (*S. mitis, S. oralis, S. infantis, S. pseudopneumoniae*) [18–20].

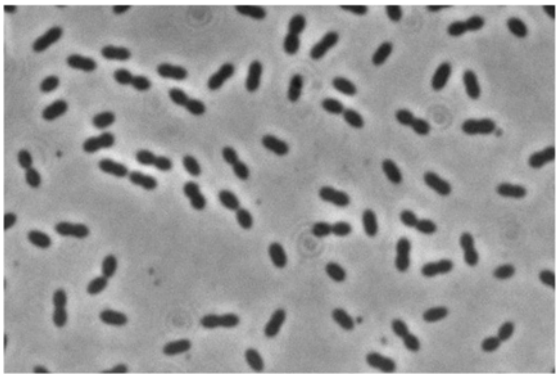

Figure 1.1. *Streptococcus pneumoniae*.

Phase contrast image of *S. pneumoniae* D39 grown in chemically defined medium supplemented with 10 mM glucose, until exponential phase of growth.

Traditionally, *S. pneumoniae* has been identified based on colony morphology and on phenotypic tests [21]. Two properties generally assessed are the pneumococcal alpha-hemolytic activity when cultured on blood agar plates and its catalase-negative phenotype [11]. Commonly, optochin susceptibility and/or bile solubility are used to distinguish *S. pneumoniae* from other viridans streptococci [20]. In addition, the ability to ferment inulin has also been used as a differentiating parameter [11].

Some pneumococci are encapsulated and according to the polysaccharide composition more than 93 different serotypes have been identified [22]. The antigenic properties of the capsule are the basis for serotyping (Quellung reaction, agglutination with anti-pneumococcal polysaccharide antibodies), important for epidemiological surveillance and vaccine impact studies [21,23,24].

Despite the application of different phenotypic and genotypic techniques (*e.g.* PCR targeting virulence genes, pulsed-field gel electrophoresis, multilocus sequence typing (MLST), multilocus sequence analysis (MLSA)), and recently proteomic profiling (MALDI-TOF MS), identification and classification of *S. pneumoniae* has been problematic and is still controversial [18,20,21,25,26]. Atypical reactions to standard identification tests are documented [18,25]. Part of this struggle stems out from the pneumococcus' vast pan-genome and its genomic plasticity.

S. pneumoniae, a commensal and a pathogen

The scientific interest on *S. pneumoniae* was primarily raised because the organism has been a leading cause of mortality worldwide. In the beginning of the 20th century, Sir William Osler referred to it as the "captain of the men of death" [27,28], and pneumonia was the "natural end of elderly people" [29]. Nowadays, *S. pneumoniae* is also recognized as a commensal microorganism, which resides in the mucosal surface lining the upper respiratory tract, *i.e*. the nasopharynx of humans [30,31]. Pneumococci are members of the respiratory tract microflora alongside with other prominent opportunistic pathogens such as *Haemophilus influenzae*, *Moraxella catarrhalis* and *Staphylococcus aureus* [32].

Colonisation is usually asymptomatic and, for that reason, an important vehicle for dissemination within the community, which occurs through direct contact with contaminated secretions or aerosols of healthy or sick carriers [29,30,33,34]. Colonisation is more frequent in small children, which are usually colonised during the first year of life [33]. Carriage rates are age-related, with higher incidence in the childhood (2-3 years) [33], decreasing to less than 10% in the adult age [30]. The close contact with children increases the carriage rates in adults [29]. In developing countries the frequency of carriage in children is 2-3 times higher than in developed countries [31]. Risk factors associated with higher incidences

of pneumococcal carriage and disease are: ethnicity, crowding (*e.g.* attendance to day-care centres, hospitals, schools, contact with older siblings and children), environmental (*e.g.* smoking) and socioeconomic (*e.g.* living circumstances, income) ([33], reviewed in [35,36]).

Colonisation is a dynamic process in terms of duration and colonising serotypes in the lifetime of an individual. Carriage with one or more serotypes can occur simultaneously or sequentially. It is a transient stage and its duration is serotype-dependent and influenced by past carriage episodes [31]. It is longer in young than older children [37,38]. Most often pneumococcal infections occur following a newly-acquired strain [31]. Some serotypes are more commonly involved in carriage while others, a relatively small number, are more related with invasive pneumococcal disease [16,39,40]. This finding suggests that the latter clones have specific genes that facilitate progression to disease [41]. Interestingly, high mortality rates were found within serotypes of lower invasive potential [16,39].

The establishment of a carrier state is a pre-requisite for pneumococcal disease with the colonising homologous strain, which usually occurs when the bacterium spreads to other parts of the human body [30,33]. Indeed, the pneumococcus is an opportunistic bacterium and children, elderly (>65 years old) and immunocompromised people are at increased risk of pneumococcal disease [33,42]. *S. pneumoniae* is an etiological agent of mild respiratory mucosal infections such as sinusitis or otitis media (non-invasive diseases), but also less prevalent but more serious invasive pneumococcal diseases (IPD), when the pneumococcus gains access to normally sterile areas of the human body, such as bacteremic pneumonia or pneumonia with empyema, meningitis or sepsis [33].

With the advent of antibiotics in the 1950s, there was a general belief that bacterial infections could be controlled [2]. However, the emergence of antibiotic resistant phenotypes, the genomic plasticity of the

pneumococcus, the limited efficacy of pneumococcal vaccines, the aging of populations and difficulties in clinical diagnosis of pneumococcal diseases makes *S. pneumoniae* a re-emergent infectious agent and a matter of concern. Currently, the impact of pneumococcal disease on society is still large, with the pathogen being responsible for high mortalities and morbidities worldwide. It was estimated, by the WHO (World Health Organization), that the pneumococcus is responsible for approximately 700 000 to 1 000 000 children deaths every year worldwide [43]. Among children, pneumococcus is the primary cause of acute otitis media; this illness is the most common manifestation of pneumococcal infection and of antibiotic prescription in the United States of America (USA). Although complications resultant from otitis media are rare the economic costs are high [44].

The pneumococcus is the most common cause of community-acquired pneumonia (CAP), and the clinical and economic burden of CAP is documented [45]. According to the WHO, pneumonia is the largest infectious cause of death in children worldwide, with high incidence in South Asia and sub-Saharan Africa countries [46].

Considering this scenario, it is urgent to circumvent pneumococcal disease. While antibiotic treatment is of key importance to fight pneumococcal disease, exclusive reliance on this strategy is not prudent and prevention is mandatory to minimise the disease burden. Currently, there are three pneumococcal conjugate vaccines (PCV) available for children (especially younger than 2 years). In 2000, a 7-valent vaccine (PCV7, Prevnar) was licensed, containing the 7 serotypes most commonly associated with IPD and antibiotic resistance in children of North America [29,47]. The immunization with PCV reduced the incidence of carriage and pneumococcal disease of vaccine serotypes among vaccinated children, but also reduced transmission, carriage and disease in non-vaccinated population (children and adults) – the herd effect

[29,48]. This indirect effect promoted a positive impact on public health systems and economy [48]. However, immunization with PCV accounted for replacement by non-vaccine serotypes (serotype replacement), contributing to a unaltered colonisation prevalence [48]. Moreover, an increase of drug resistant clones not included in PCV7 has also been reported [29,49]. Approximately nine years after the launch of PCV7, a 10- and 13-valent PCV were licensed, PCV10 (Synflorix) and PCV13 (Prevnar13), respectively, expanding the serotype coverage [47]. Despite the availability and positive impact of PCVs, only few countries with high incidence rates of pneumococcal disease have introduced the PCV in their immunization programmes [47,48]. Today PCV13 is recommended for children, and additionally some studies point towards the beneficial use of this vaccine for adults (reviewed in [45]). The use of PCV13 in adults older than 50 was approved by FDA in 2011 [45]. In a very recent study [50], the use of PCV13 was found to have an added benefit in diminishing carriage of antibiotic-nonsusceptible *S. pneumoniae* over PCV7, in infants.

The 23-valent pneumococcal polysaccharide vaccine (PPV), which includes the main serotypes that have developed antibiotic resistance and causative agents of IPD, is commonly used in adults [29]. This vaccine has cross-reactivity with serotypes not included in PPV and therefore potentially protects against more than 23 serotypes [51].

The development of protein-based vaccines has emerged as an alternative to the currently available vaccines (reviewed in [45]). Currently, a number of these protein based vaccines are in clinical trial phase I [45]. These products are based in pneumococcal surface proteins (*e.g.* pneumolysin, autolysin) and are expected to be cheaper, elicit protection in all age groups in a serotype-independent way [33].

Despite the intrinsic limitations of vaccines (*e.g.* number of serotypes coverage, costs, serotype replacement), it was estimated that

pneumococcal vaccination could prevent more than 7 million deaths by 2030 at a global scale [52].

Transition from colonisation to disease

While the exact circumstances that trigger the transition from colonisation to disease are still largely unknown, it is surely a multifactorial event that results from an imbalance of the equilibrium between the host, the pathogen and the other niche residents. Pneumococcal disease starts with a successful colonisation, which relies on the adherence of the pneumococcus to host structures, the ability to acquire nutrients in fluctuating conditions to replicate, compete with co-colonisers (*e.g.* resist to toxic molecules such as bacteriocins produced by other microorganisms) and evasion from the host immune system (innate or acquired immunity) [42,53]. Several experimental animal models of pneumococcal colonisation and disease have been used to study different aspects of host-pathogen interactions (*e.g.* inflammatory host responses, bacterial virulence factors) (reviewed in [16,30,54]).

During colonisation the expression of specific pneumococcal genes contributes to its commensal lifestyle and persistence in the airways but, simultaneously, might influence the virulence potential of this microorganism. Indeed, virulence can only be seen in the context of host-pathogen interactions, as it is an outcome of these relations [55]. Since nasopharynx provides a suitable environment for pneumococcal growth and proliferation it is likely that disease is accidental as it can result in a dead end for the microorganism. Therefore, some of the virulence factors promote pneumococcal lifestyle and for that reason are also considered colonisation determinants [34,56].

In the following section the classical factors of pneumococcal virulence will be briefly described.

Virulence factors

The pneumococcal capsule is recognized as a major virulence factor. The polysaccharide capsule produced by *S. pneumoniae* is protective against host defences. This structure is covalently linked to the outer surface of the cell wall peptidoglycan and is, in general, negatively charged [30]. At first, capsule prevents the entrapment in the airway mucus to allow subsequence access to epithelial surfaces [57]. However, once in this surface, capsule seems to be disadvantageous because it masks pneumococcal molecules that recognize host receptors. Therefore, the pneumococcus spontaneously undergoes a phase variation phenotype between two forms distinguishable by different colony morphologies: opaque and transparent [58]. In the initial stages of colonisation transparent variants express a thinner capsule promoting adherence to host tissues by expressing higher amounts of surface-exposed proteins. In contrast to opaque variants which display increased amounts of capsule that mask pneumococcal molecules recognizing host receptors. These variants are usually isolated from the blood, indicating that are selected to cross the epithelial barriers [56,59–62]. Part of this peculiarity is due to enhanced opsonophagocytic resistance [63]. Indeed, the capsule is highly anti-phagocytic [64], preventing antibodies (*e.g.* Fc of IgG) and complement (*e.g.* iC3b component) associated with bacterial cell surfaces, from interacting with the correspondent receptors on the phagocytic cells [65,66]. Moreover, capsule diminishes the spontaneous or antibiotic-induced autolysis contributing to antibiotic tolerance and has been associated with reduction of natural competence [30,67–69].

Capsule is regarded as a *sine qua non* factor for virulence, as clinical isolates from sterile areas of humans are encapsulated whereas non-encapsulated derivatives are largely non-virulent [30,70]. Strains with reduced expression of capsule were avirulent in mouse models of disease

[71]. Furthermore, the capsular thickness and serotype are associated with different degrees of virulence [64,72]. In summary, the capsule allows *S. pneumoniae* to evade the host immune system during inflammation and “invade” the host [56].

Besides the polysaccharide capsule, *S. pneumoniae* possesses an incredible array of surface-exposed proteins that enable adherence in various degrees to host structures (glycoconjugates), either directly or by modulating the functional properties of other pneumococcal proteins, and thus influencing the colonisation and invasive effectiveness of this microorganism (reviewed in [57]).

Three main clusters of surface-exposed proteins were identified in *S. pneumoniae*: 1) proteins carrying a LPxTG motif covalently linked to the cell wall peptidoglycan, 2) the lipoproteins, embedded in the phospholipidic bilayer and 3) choline-binding proteins (CBPs), non-covalently linked to phosphorylcholine (ChoP) of the cell wall and to lipid-anchored teichoic acids [14,62,73]. Besides this classification, the cell wall is decorated with other proteins that do not fulfil these features (moonlighting proteins) [62,73] (Fig. 1.2).

The LPxTG-anchored proteins encompass a variety of glycosidases (*e.g.* neuraminidase (NanA), β-galactosidase (BgaA), β-*N*-acetylglucosaminidase (StrH), pullulanase (SpuA), endo-β-*N*-acetylglucosaminidase (EndoD), endo-α-*N*-acetylgalactosaminidase (Eng)), proteases (*e.g.* PrtA, ZmpABC), one lyase (SpnHL), among others [14].

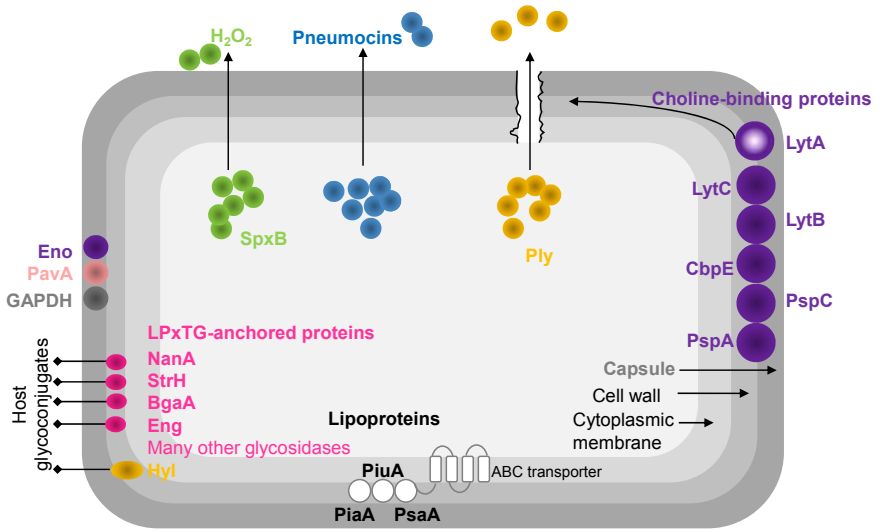

Figure 1.2. Schematic representation of pneumococcal virulence factors.

Abbreviations: NanA, neuraminidase A; StrH, β-*N*-acetylglucosaminidase; BgaA, β-galactosidase; Eng, endo-α-*N*-acetylgalactosaminidase; Hyl, hyaluronate lyase; Eno, enolase; PavA, pneumococcal adherence and virulence factor A; GAPDH, glyceraldehyde 3-phosphate dehydrogenase; SpxB, pyruvate oxidase; Ply, pneumolysin; LytA, autolysin; LytC, 1,4-β-N-acetylmuramidase; LytB, endo-β-N-acetylglucosamidase; CbpE, choline-binding protein E; PspC, pneumococcal surface protein C; PspA, pneumococcal surface protein A; PiaA, pneumococcal iron acquisition A, PiuA, pneumococcal iron uptake A, PsaA, pneumococcal surface antigen A, H_2O_2, hydrogen peroxide (adapted from Kadioglu *et al.* [30]).

Adherence of the pneumococcus appears to occur through binding to human glycoconjugates [74]. Pneumococcal glycosidases might be implicated in such process [75]. At least 10 extracellular exoglycosidases have already been identified in *S. pneumoniae* with different specificities for sugar structures present in human airways. Their activity contribute in different ways to the lifestyle of the pneumococcus and has broad implications in colonisation and the virulence potential of the bacterium (reviewed in King [75]). For example, the sequential cleaving activity of terminal sugars from human glycoconjugates by NanA, BgaA and StrH results in reduction of mucus viscosity, reveals receptors for adherence, releases sugars for growth and promotes resistance to

opsonophagocytosis by neutrophils [75–77]. Recently, BgaA was found to work as an adhesin promoting adherence to epithelial cells [78]. Another glycosidase, hyaluronidase (Hyl), acts over hyaluronic acid of the extracellular matrix, and is believed to assist in dissemination through tissues and colonisation [79,80] (Fig. 1.2).

The exact role of the serine protease, PrtA, in virulence is still unknown, but PrtA-deficient mutants were attenuated in a murine model of disease and all clinical isolates possessed this protein [81].

Among the lipoproteins identified (listed in [14]), PsaA (pneumococcal surface antigen A) is the substrate-binding lipoprotein of an ABC transporter for manganese. Mutations in this protein caused reduced adhesion and virulence and increased sensitivity to oxidative stress [82,83]. Other metal-binding lipoproteins (PiuA and PiaA) were identified to play role in virulence [30].

ChoP is an uncharacteristic component of cell wall that binds to host innate immune system components such as receptor for platelet-activating factor (rPAF) of human epithelial surfaces of nasopharynx and C-reactive protein [30,73]. ChoP anchors a diversity of CBPs (listed in [14]). Among these are the hydrolytic enzymes autolysin LytA, endo-β-N-acetylglucosamidase LytB, 1,4-β-N-acetylmuramidase LytC and CbpE. LytA degrades the cell wall, leading to the release of highly inflammatory cell wall components, and pneumolysin (Ply) from the cytoplasm (reviewed in [30,82,84]). Mutants in the CBPs LytB, LytC, CbpE, CbpD and CpbG were attenuated in colonisation models and CpbG also played a role in sepsis [85]. Other members of CBP family are the pneumococcal surface proteins A (PspA) and C (PspC, also known as CbpA or SpsA). PspA interferes with complement activation, preventing binding of C3 component on pneumococcal cells, and also binds to lactoferrin and apolactoferrin protecting the bacterium from the bactericidal activity of these molecules. Additionally, PspA has high immunogenicity and elicits

antibody response that increase complement deposition, conferring protection in diverse models of pneumococcal infection. PspC acts as an adhesin and binds to the complement regulatory protein factor H and to the human secretory IgA receptor, providing resistance to complement. PspC mutants presented attenuated virulence in different models of infection. Both PspA and PspC, are considered good candidates for protein-based vaccines (reviewed by Nieto *et al*., 2013 [84] and by Kadioglu *et al.* [30]).

S. pneumoniae also have other surface proteins, lacking conventional anchoring motifs or secretory signals (reviewed in [14]). These “non-classical surface proteins” display moonlighting functions. They are usually cytoplasmic with intracellular roles but when they reach the cell surface have other functions. Among these are, the pneumococcal adherence and virulence factor A (PavA) and the glycolytic enzymes enolase (Eno) and glyceraldehyde 3-phosphate dehydrogenase (GAPDH). PavA is an adhesin that binds to fibronectin, a component of the extracellular matrix. PavA mutants were attenuated in diverse models of pneumococcal disease and therefore is considered a crucial virulence factor [86,87]. Eno and GAPDH are plasmin(ogen)-binding proteins that allow transmigration through the basement membrane. Interaction of Eno with plasminogen was found to promote adherence in epithelial and endothelial cells [88–91].

Pneumolysin (Ply) is a potent virulence factor of *S. pneumoniae* which has been extensively studied (reviewed in [30,82]). It is a cytoplasmic pore forming toxin of the cholesterol-dependent cytolysins [30], released independently of autolysin activity [92]. Its high toxicity arises from the ability to bind host cholesterol, thereby leading to the formation of pores and subsequent lysis of mammalian cells. Ply also inhibits the mucociliary beat of respiratory epithelium and complement deposition in pneumococcal surface [93,94]. Ply is presumably essential for the

development of pneumonia, as mutants lacking Ply were attenuated in models of pneumococcal pneumoniae [30] (Fig. 1.2).

Other aspect influencing the pneumococcal virulence potential is the competitive interactions with other microorganisms occupying the same niche during colonisation. Pneumococci produce bacteriocins (pneumocins), small antimicrobial peptides to target other bacteria from the same or closely species that do not produce the cognate immunity factor. This phenomenon has been hypothesised as the mechanism behind serotype replacement due to PCV administration [95]. Chemical warfare is also thought to contribute to the virulence potential. *S. pneumoniae* can produce a range of end-products, among them hydrogen peroxide (H_2O_2). This metabolite, produced by pyruvate oxidase (SpxB) as a by-product of pyruvate aerobic metabolism, is known to damage host tissues and to kill other organisms in the same niche [96–98]. The high insensitivity of *S. pneumoniae* to H_2O_2 is well described [99]. In sum, the vast diversity of pneumococcal virulence factors endows the bacterium with an “armory” to survive in the host and compete with other bacteria.

Virulence and carbohydrate metabolism

Several studies, using signature target mutagenesis (STM) [100–102], microarrays analysis of gene expression [103–106], and Tn-seq [107] have consistently revealed a link between carbohydrate metabolism and virulence of *S. pneumoniae*. Importantly these studies have shown the dynamics and pattern of gene expression in different stages of pneumococcal infection, providing a means to evaluate the role of different genes in colonisation and disease. Carbohydrate uptake systems (*e.g. msmK*, *satABC*, *SPD_0295-6-7*, *scrT*, *susT1T2X*) [108–111] and glycosidases (*e.g. nanA*, *nanB*, *eng*, *bgaC*) [112–117] were established as important for *in vivo* fitness of *S. pneumoniae* by testing mutants of these proteins in different mouse models. Moreover, in addition to Eno

and GAPDH, other central metabolic functions such as pyruvate formate-lyase (PFL) [118], lactate dehydrogenase (LDH) [119], pyruvate oxidase (SpxB) [120], have been associated with pathogenicity, as mutant strains were attenuated or avirulent in the ability to colonise or cause disease in different mouse models (Fig. 1.3). The PFL mutant phenotype likely resulted from reduced synthesis of ATP and alterations of membrane lipid composition [118]. A LDH-deficient mutant was avirulent after intravenous inoculation and attenuated post intranasal infection. These features were explained as arising from the different environmental conditions (carbohydrate availability) encountered in the two niches [119]. SpxB was found important in adaptation to different host environments. It enhances colonisation by competing with other host co-colonisers through H_2O_2 production or biofilm formation. In contrast its role in virulence is still controversial. Some studies showed that downregulation of *spxB* is beneficial for survival in the bloodstream, but this behaviour is in contradiction to the study by Spellerberg *et al.*, [120] that attributed the virulence of an SpxB mutant to reduced acetyl-P levels and repression of several adhesive properties (reviewed in [121]). More recently, a relation between SpxB expression and capsule production (the major virulence factor of the pneumococcus) was established [99].

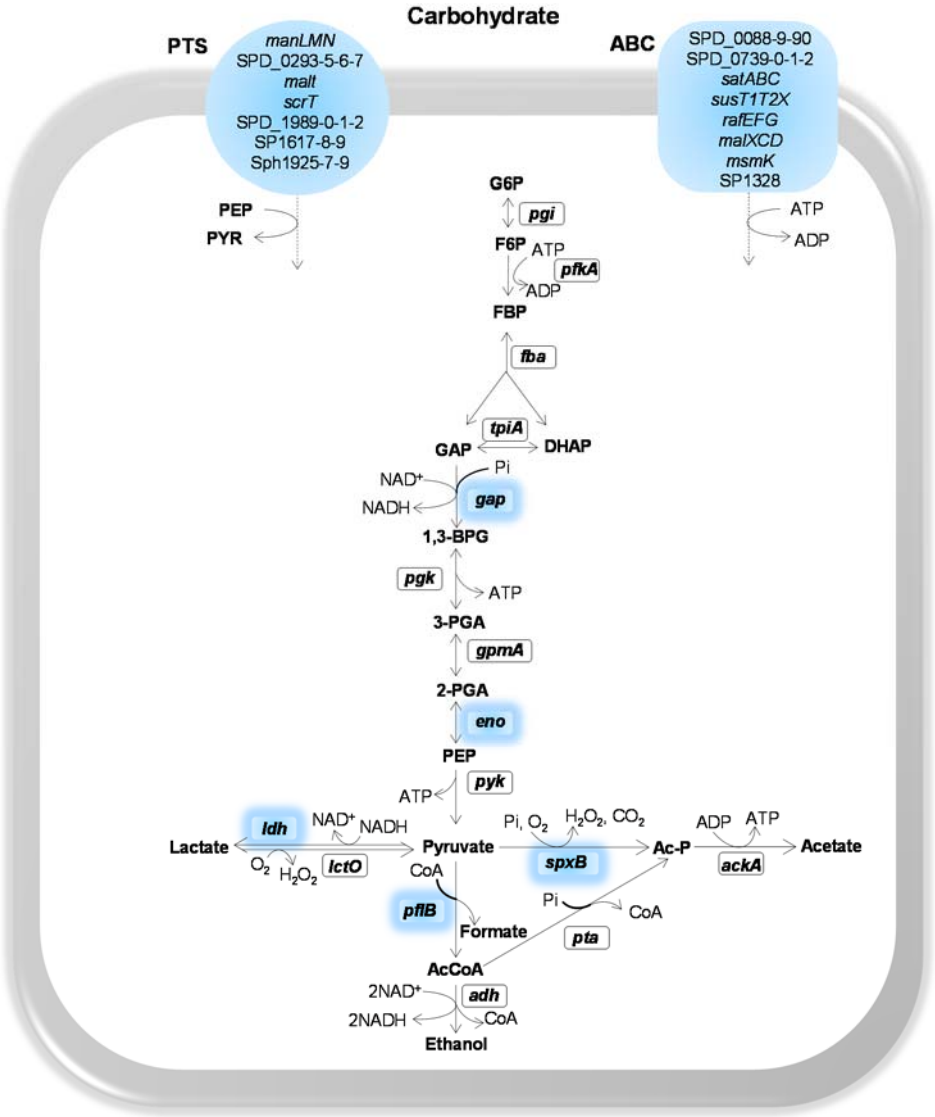

Figure 1.3. Schematic representation of sugar transporters and central carbon metabolism highlighting proteins implied in virulence of *S. pneumoniae*, as assessed by *in vivo* studies (except for Eno and GAPDH).

Reactions are catalysed by the following protein encoding genes: *gki*, glucokinase; *pgi*, glucose 6-phosphate isomerase; *pfkA*, 6-phosphofructokinase; *fba*, fructose-biphosphate aldolase; *tpiA*, triosephosphate isomerase; *gap*, glyceraldehyde 3-phosphate dehydrogenase; *pgk*, phosphoglycerate kinase; *gpmA*, phosphoglyceromutase; *eno*, enolase; *pyk*, pyruvate kinase; *ldh*, L-lactate dehydrogenase; *spxB*, pyruvate oxidase; *lcto*, lactate oxidase; *pflB*, pyruvate formate-lyase; *pta*, phosphotransacetylase; *ackA*, acetate kinase; adh, bifunctional acetaldehyde-coA/alcohol dehydrogenase (SPD_1834).

Intermediates: G6P, glucose 6-phosphate; F6P, fructose 6-phosphate; FBP, fructose 1,6-biphosphate; GAP, glyceraldehyde 3-phosphate; DHAP, dihydroxyacetone phosphate; BPG, 1,3-biphosphoglycerate; 3-PGA, 3-phosphoglycerate; 2-PGA, 2-phosphoglycerate; PEP, phosphoenolpyruvate.

In Gram-positive bacteria, the transcriptional regulator carbon catabolite protein A (CcpA) plays a major role in carbon catabolite control, *i.e*., the hierarchical and highly regulated utilization of carbon sources [122]. CcpA has been reported to contribute to pneumococcal colonisation and virulence [123,124]. The involvement of CcpA has been rationalized as a consequence of regulation of enzymes of central metabolism, impaired capsule production and/or attachment to the cell envelope, and influencing the binding of cell wall components [123–125].

Glycans at the interface of bacteria-host interactions

Glycoconjugates are widespread in nature and encompass a wide variety of molecules consisting of carbohydrates covalently linked to a non-sugar backbone. The principal categories are glycoproteins (N- or O-linked to a protein core) and glycopeptides (linked to an oligopeptide), peptidoglycans (bound to amino acids), glycolipids and lipopolysaccharides (linked to a lipid moiety) [126]. Despite the vast diversity of host glyconjugates, their glycan portions are often composed of the monosaccharides N-acetylglucosamine (GlcNAc), N-acetylgalactosamine (GalNAc), N-acetylneuraminic acid (NeuNAc), galactose (Gal) and fucose (Fuc), mannose (Man), glucose (Glc) and fructose. While the first five sugars are widespread in both N- and O-glycans (*e.g*. mucins), the other three are generally restricted to N-glycans.

These molecules contribute to important biological functions in different kingdoms of life (reviewed in [127,128]). The bacterial glycome (*e.g.* capsule, exopolysaccharides, lipolysaccharides, peptidoglycan, teichoic acids and lipoteichoic acids) is far more diverse than that of animals and is usually located at the cell surface (exception polysaccharides used as energy reserves). As many bacteria (commensal or pathogens) reside in mucosal surfaces, the glycoconjugates on the cell envelope play important roles in bacteria-host interactions [128]. From the bacteria perspective these molecules are highly important for *in vivo* fitness. On the other hand, in animals, and particularly in humans, a glycoconjugate barrier often prevents direct contact between bacteria and host cells. Among these, mucins are highly important in the mucosal surfaces (*e.g.* respiratory, gastrointestinal tracts). Mucins are major components of the mucus that cover the epithelial surfaces [129]. They are high molecular weight glycoproteins, heavily O-glycosylated [130,131], composed of a protein backbone enriched with threonine or serine (apomucin) containing one or multiple tandem repeats (TR) to which a diversity of oligosaccharides are linked via a GalNAc residue [129–131]. The structure and composition of oligosaccharides in mucins are varied; generally, the carbohydrate fraction is composed of GlcNAc, GalNAc, NeuNAc, Gal, Fuc and sulphated sugars. Sulphation confers protection to the epithelium as it increases resistance against mucin-degrading enzymes [131]. N-glycosylation is also found on mucins but it is a small contribution to the mucins molecular size when compared to the O-glycosylation [131]. The oligosaccharide content of mucins can reach up to 80% of their total weight [130]. Mucins are produced by eukaryotic cells and can be cell surface associated or secreted (gel-forming or non-gel forming). Gel-forming mucins, are the major constituents of mucus and confer viscoelastic properties [130,132].

Mucus and mucins have a dualistic role. On one hand represent a first defence barrier (innate defensive barrier) by trapping the microbes and protecting the underlying host surfaces from interaction with bacteria, facilitating their removal through mucociliary transport. On the other hand, the carbohydrate content of mucins provide adhesion sites and nutrients for bacteria enabling their survival and colonisation at these surfaces [130,131].

Interactions between mucin and microbes are broad in nature. For example, expression of mucin can be induced by probiotic bacteria, likely limiting the infection by pathogens [133]; the lipopolysaccharides of *Helicobacter pylori*, decrease mucin synthesis in gastric epithelial cells *in vitro*, modulating the mucus barrier [134]; *Bacteroides thetaiotaomicron* induces fucosylation of mucin oligosaccharides, subsequently using fucose as nutrient [135]. Also, microbes have developed strategies to overcome this barrier: adhesins to bind oligosaccharides (*H. pylori*, possesses four adhesins with different specificities) [136]; motility (flagella) or production of mucin degrading enzymes (proteases and glycosidases) that destabilize mucus and release carbohydrates that can be used for growth [75,137,138].

Pneumococcal carbohydrate metabolism

Carbohydrate metabolism and its importance for pneumococcal lifestyle

The incidence and impact of pneumococcal infections have prompt intense research on the identification of factors that contribute to *S. pneumoniae* pathogenesis. In particular, factors that directly impinge on host-pathogen interactions, such as toxins, cell wall components,

adhesins and capsule [30]. Even though the relevance of carbohydrate metabolism has been recognized for *in vivo* fitness, only recently the underlying mechanisms have been systematically addressed [109–111,118,125]. With the availability of the pneumococcal genome the relevance of carbohydrates for pneumococcal fitness became apparent [139]. *S. pneumoniae* is a strictly fermentative bacterium that relies on glycolytic metabolism to obtain energy [139]. It lacks a complete set of respiratory genes and is, for that reason, unable to generate energy by respiration [139,140]. Among the bacteria sharing the same niche, *S. pneumoniae* possesses the highest number of transport systems, and of those more than 30% were predicted to be involved in the uptake of sugars [140]. A recent functional genomics approach validated the majority of the homology based predictions, and identified 32 carbohydrates that can be used by pneumococci [141]. It has been postulated that the vast diversity in terms of sugar utilization is driven by adaptations to host niches as a means to proliferate [142–144]. Additionally, it has been reported that sugar transporters contribute to *S. pneumoniae* colonisation and disease [103,109–111]. Furthermore, numerous studies have revealed a consistent link between genes involved in sugar catabolism and virulence [100–102,105–107,145].

In the human airway free carbohydrates are scarce, being the Glc concentration below 1 mM, in contrast to its content in blood (~4-6 mM) [145,146]. Hexoses, and in particular Glc, are generally the preferred carbon sources for several bacteria and the same seems to be true for the pneumococcus [125,141]. Therefore, *in vivo* growth in the nasopharynx requires alternative carbon sources. The host glycoproteins (O- and N-linked glycans, and glycosaminoglycans), secreted or lining the epithelial surfaces appear as good candidates to serve as carbon and energy sources for pneumococcal growth. *S. pneumoniae* can grow on each of the former glycan types as sole carbon source [75,110,147,148].

Furthermore, it is able to grow on mucin as the sole carbon source [147]. In addition to mucins and other glycans, carbohydrates might also be provided by the host diet and other microbial residents of the same niche [143].

S. pneumoniae is equipped with at least 10 extracellular (exo- or endo) glycosidases with a broad range of specificities (reviewed by King [75]). These enzymes can break down O-linked glycans (*e.g.* BgaC, Eng) [114–116], N-linked glycans (*e.g.* NanA, StrH, BgaA, NanB) [77,148], and glycosaminoglycans (hyaluronic acid) (*e.g.* Hyl) [110], providing free sugars that can potentially be used by the pneumococcus to grow [110,148].

Sugar transport systems in *S. pneumoniae*

Sugar transport across the membrane is the first step in catabolism. In *Streptococcaceae* there are three types of transport systems: the secondary carriers, the primary active transporters ATP-binding cassette superfamily (ABC transporters) and the phospho*enol*pyruvate-dependent carbohydrate phosphotransferase systems (PTS systems) (Fig. 1.4).

Secondary carriers couple the translocation of the carbohydrate to an electrochemical gradient and comprise symporters (a carbohydrate is imported together with a solute), antiporters (carbohydrate and solute are transported in opposite directions) and uniporters (catalyse the unidirectional translocation of the sugar across the cytoplasmic membrane) [149].

ABC transporters take up carbohydrate at the expense of ATP, which is intracellularly hydrolysed to ADP and inorganic phosphate (Pi) [150].

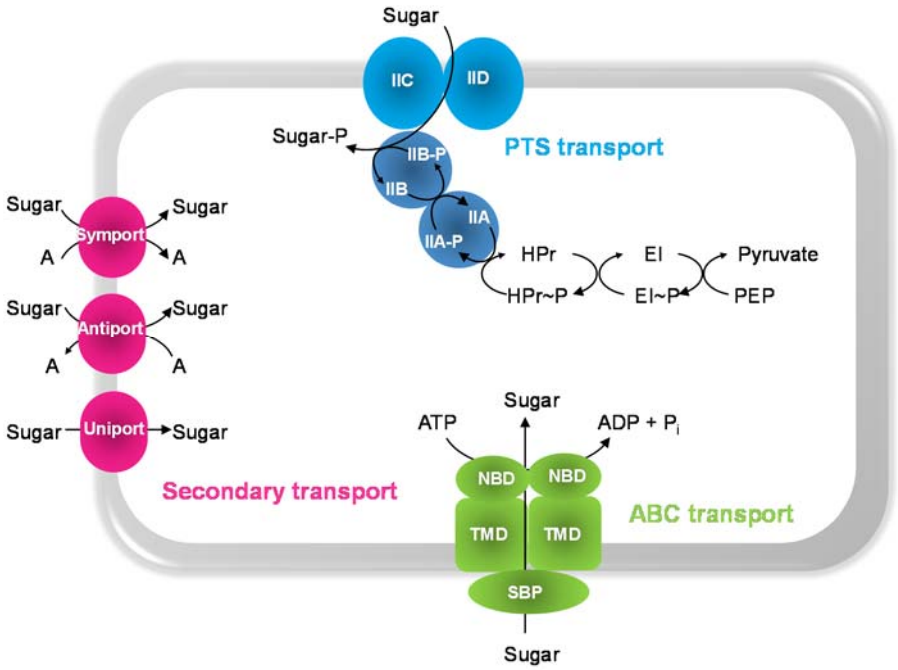

Figure 1.4. Schematic representation of sugar transport systems in *S. pneumoniae*.
Abbreviations: A, general solute; SBP, solute-binding protein; NBD, nucleotide-binding domains; TMD, transmembrane domains; ABC, ATP-Binding Cassette transporter; PEP, phospho*enol*pyruvate; PTS, phospho*enol*pyruvate-dependent-carbohydrate phosphotransferase systems; EI, enzyme I and HPr, histidine phosphocarrier protein are general components of the PTS system; IIAB cytoplasmic proteins and IICD, transmembrane domains of the PTS system. The occurrence of IID component is typical of mannose type-PTS transporter. P~ corresponds to the phosphorylated form of each component.

In general, an ABC is composed of four core domains: two transmembrane domains (TMD) spanning in the membrane, forming the pathway of entry of the solute and defining the specificity of the transporter through the substrate-binding site and two ATP- or nucleotide-binding domains (NBD) associated with the inner face of the membrane, that energize the transport via ATP hydrolysis. ABC importers require auxiliary proteins, the solute-binding proteins (SBP), anchored outside the cell via lipid groups, that confer high affinity, specificity and directionality to the transporter [151].

In *S. pneumoniae* there are 1 CUT2 family ABC transporter and 6-7 CUT1 ABC transporters, differing in the nature of the substrate and structure. Each locus of the CUT1 family ABC transporter lacks the predicted ATPase [141]. Recently, a single ATPase (MsmK), was found to energize multiple carbohydrate ABC transporters, that are involved in the uptake of sialic acid, raffinose and maltotetraose [108].

The PTS system involves uptake and concomitant phosphorylation of the incoming sugar via a phosphorylation cascade that transfers a phosphate group from PEP. It consists of a series of cytoplasmic and membrane-bound proteins [152]. The PTS permeases (EII complexes), generally comprise 3 or 4 domains (the cytoplasmic subunits IIA, IIB and membrane-bound subunits IIC, IID) arranged in different ways, which allow the transport and phosphorylation of the substrate. While IIAB domains participate in the phosphorylation of the substrate, IICD correspond to the membrane permeases. The PTS is also composed by two PTS energy-coupling proteins, Enzyme I (EI) and the heat stable histidine phosphocarrier protein HPr, encoded by *ptsI* and *ptsH,* respectively. While the EII subunits are usually substrate-specific, the EI and HPr are common to all PTS carbohydrates and therefore denominated general proteins [153,154]. PTS systems are energetically more favourable since transport and phosphorylation occurs in one step spending a PEP molecule instead of ATP. PEP is energetically equivalent to one molecule of ATP as one ATP is formed from PEP to pyruvate in glycolysis. In non-PTS systems more ATP is expended in both processes. This likely explains the high number of these systems in anaerobic bacteria [154].

In *S. pneumoniae,* the functional genomics approach conducted by Bidossi *et al.* [141], identified twenty-one PTS systems, six to seven CUT1 ABC transporters, one CUT2 ABC transporter, one sodium solute symporter and three aquaporin/glycerol permeases potentially involved in

carbohydrate uptake. The total number of transporters varies with the strain [141]. At the time, only a few transporters (beta-glucosides, sucrose, sialic acid, maltose and raffinose) had been partially characterized in *S. pneumoniae* [141]. Thirty-two carbohydrates can be metabolized by the pneumococcus. Some of these were internalized by more than one transporter and the same transporter could take up different sugars [141]. Even though the complement of transporters is well covered in Bidossi *et al*. [141], the specificity for substrates is only fully elucidated for a reduced number of transport systems. More in-depth studies combining biochemical and genetic approaches are needed to establish the specificity range of pneumococcal transport systems.

Glycan-derived monosaccharides: pathways and functions

In this section, catabolic pathways for the assimilation of selected carbohydrates, *i.e.* monosaccharides present in host glycans, will be described. The focus will be on *S. pneumoniae* and closely related organisms, but alternative pathways in other bacteria are also presented.

In *S. pneumoniae* the pathways for the catabolism of monosaccharides can be deduced from genome annotations, but their functionality remains largely to be proven. In this work we focused on the six carbohydrates constituents of the highly available glycoprotein, mucin.

Galactose

Galactose is abundant in the airway glycoconjugates (*e.g.* mucins) [116]. Available as a monosaccharide through the action of pneumococcal galactosidases (BgaA, BgaC) [77,115,116,155]. However, it is usually regarded as a less efficiently metabolized sugar and the type of transport system dictates, at some extent, the catabolic pathway to be followed. It has been postulated that its efficient uptake could determine the outcome of interspecies competition between streptococcus [156,157].

Galactose catabolism

In several *Streptococcaceae*, metabolism by the Leloir pathway is preceded by the entry of Gal in the cell through the secondary carrier galactose permease (GalP) [158–160]. However, homologues of this protein were not found in the pneumococcus. Recently, Bidossi *et al*. [141], implicated the CUT1-family ABC transporter SPD_0088-9-0 in the uptake of Gal, but the evidence presented was relatively weak, since inactivation of the transporter resulted in a very mild reduction in Gal utilization. Possible explanations can be that the inactivation of the ABC transporter is masked by the activity of other transporters or Gal is exclusively taken up via PTS-type transporters.

Metabolism of Gal via tagatose 6-phosphate (T6P) pathway is preceded by transport via a PTS system. In other *Streptococcaceae* it occurs through a lactose-specific PTS (PTS^{lac}), encoded by *lacFE* genes, albeit with a low efficiency [161–164]. In *S. pneumoniae*, duplication of *lacFE* genes appears to have occurred, but the involvement of these transporters is not yet disclosed. Nevertheless, our team showed that *lacFE* genes were induced by Gal, suggesting a potential contribution of the lactose-PTS to the uptake of the sugar [125]. Transport of Gal by a PTS complex other than PTS^{lac} was proposed for *Lactococcus lactis*, *Streptococcus mutans, Streptococcus gordonii* and *Streptococcus oligofermentans* (*e.g*. galactose-specific PTS and/or PTS^{Man}) [156,157,163,165,166].

In the pneumococcus Gal uptake was attributed to the galactitol-PTS SPD_0559-1 [141,167]. This seems to be the major Gal uptake system [141]. Two additional PTS systems were then allocated to Gal, the mannose-family PTS (ManMNL) and probably a mannose-family PTS (SPD_0066-7-8-9) [141]. The latter, was assigned based on the presence of a beta-galactosidase (*bgaC*) with specificity for Galβ1-3GlcNAc [115,116].

In *S. pneumoniae* genes for the catabolism of Gal through the T6P and Leloir pathways are encoded in the genome (Fig. 1.5). The product of PTS transport, galactose 6-phosphate (Gal6P), is metabolized by the T6P pathway. Briefly, Gal6P is converted to tagatose 6-phosphate (T6P), by the heteromeric galactose-6-phosphate isomerase (LacAB), which is subsequently converted to tagatose 1,6-biphosphate (TBP) by tagatose 6-phosphate kinase (LacC) and finally to the glycolytic intermediates glyceraldehyde 3-phosphate (GAP) and dihydroxyacetone phosphate (DHAP) by the tagatose 1,6-diphosphate aldolase (LacD). The non-PTS transport leads the incoming Gal to the Leloir pathway, in which Gal is phosphorylated to α-galactose 1-phosphate (α-Gal1P) through the sequential activity of galactose mutarotase (GalM) and galactokinase (GalK). Through the galactose 1-phosphate uridylyltransferase (GalT)/UDP-glucose 4-epimerase (GalE) activities α-Gal1P is then converted to α-glucose 1-phosphate (α-G1P), which is then converted to glucose 6-phosphate (G6P) by the phosphoglucomutase (PGM), thus entering in the Embden-Meyerhof-Parnas (EMP) pathway.

Interestingly, in *L. lactis* and *S. mutans* a phosphatase that converts the PTS product, Gal6P to Gal, allowing its processing through the Leloir has been described, but its identity remains elusive [163,165] (Fig. 1.5). In contrast to *L. lactis*, *S. mutans* apparently does not possess homologues of *galP* and *galM* and therefore Gal enters the exclusively via PTS [163].

In *S. pneumoniae*, both pathways seem to be simultaneous active [125], but the relative contribution of each and conditions that trigger the prevalence of one pathway over the other remains to be elucidated.

In *S. mutans*, *S. oligofermentans* and *S. gordonii* both pathways are present but T6P seems to be the preponderant route for Gal catabolism [156,163,166]. In contrast, in the dairy bacterium *L. lactis* this feature seems to be strain dependent [165]. While laboratorial strains possess the

Leloir, dairy strains have and express both pathways [165]. Other microorganisms possess only one pathway. *Streptococcus salivarius* uses Gal exclusively via the Leloir, because it lacks a galactose-lactose PTS and therefore Gal likely enters through a symport-driven permease, whereas *Streptococcus thermophilus* does not grow on Gal unless GalK is expressed in sufficient amounts [168,169].

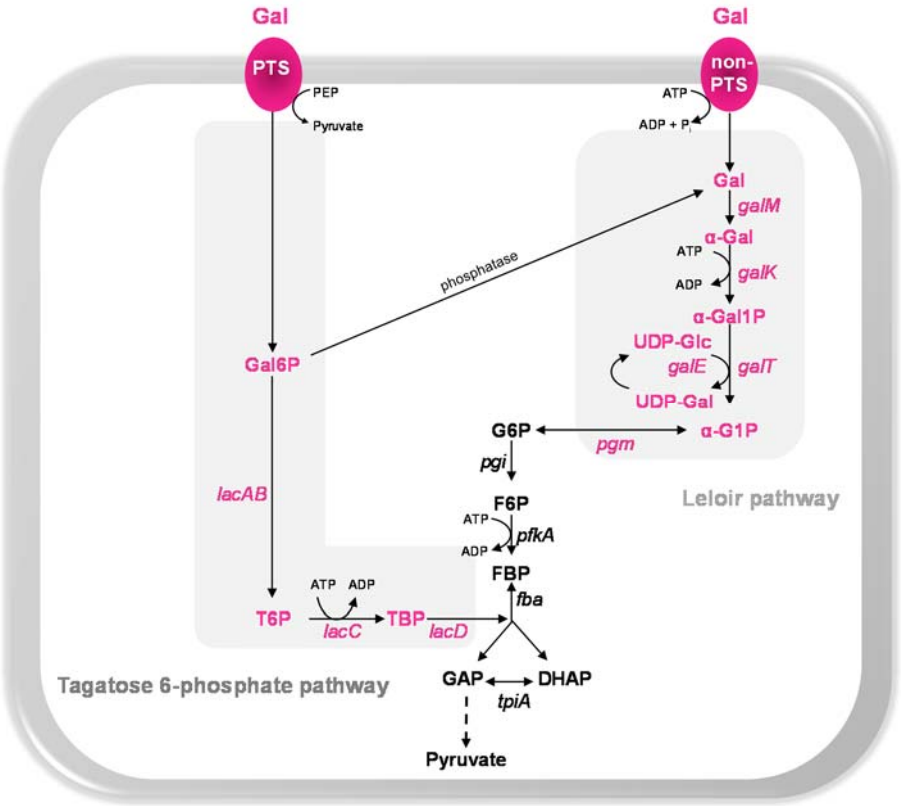

Figure 1.5. Schematic representation of pathways for the dissimilation of galactose (Gal) in bacteria.

Reactions are catalysed by the following protein encoding genes: *galM*, galactose mutarotase; *galK,* galactokinase; *galT*, galactose 1-phosphate uridylyltransferase; *galE*, UDP-glucose 4-epimerase; *pgm*, phosphoglucomutase; *lacA*, galactose 6-phosphate isomerase subunit LacA; *lacB*, galactose 6-phosphate isomerase subunit LacB; *lacC*, tagatose 6-phosphate kinase; *lacD*, tagatose 1,6-diphosphate aldolase; *pgi*, glucose 6-phosphate isomerase; *pfkA*, 6-phosphofructokinase; *fba*, fructose-biphosphate aldolase;

tpiA, triosephosphate isomerase. The lower glycolytic pathway is represented by a dashed arrow.
Intermediates: Gal, galactose; α-Gal, α-galactose; α-Gal1P, α-galactose 1-phosphate; α-G1P, α-glucose 1-phosphate; UDP-Glc, UDP-glucose; UDP-Gal, UDP-galactose; Gal6P, galactose 6-phosphate; T6P, tagatose 6-phosphate; TBP, tagatose 1,6-diphosphate; G6P, glucose 6-phosphate; F6P, fructose 6-phosphate; FBP, fructose 1,6-biphosphate; GAP, glyceraldehyde 3-phosphate; DHAP, dihydroxyacetone phosphate.
In rose are depicted the intermediates and genes committed specifically to galactose catabolism.
For the sake of simplicity transporters other than PTS are designated generically as non-PTS.

While the necessary genes for T6P pathway (*lacABCD*) are organized in one operon the Leloir genes are dispersed in the pneumococcal genome. The organization of Leloir genes seems to be species-specific probably reflecting the genomic plasticity among LAB [170,171]. Various combinations of the *gal* and *lac* genes have been reported among streptococci, lactococci and lactobacilli [166].

Mannose

Mannose is the major component of N-glycans [172]. High-mannose-type glycoproteins are present in host tissues and are components of the extracellular matrix (*e.g.* laminin) [173]. Mannosidase activity over glycoconjugates has been reported in *viridans* group streptococci and in particular in *S. pneumoniae* [173]. The exact role of these enzymes has not yet been determined but it is possible that their action provides substrates for growth. In contradiction *S. pneumoniae*, but not *S. mitis* and *S. oralis*, expose mannose residues of host glycoproteins defence molecules, through the sequential action of NanA, BgaA and StrH, that bind pneumococcus and protect the airway, likely allowing its persistence in the nasopharynx [77]. According to King *et al.* [77]., the lack of further deglycosylation through mannosidase is likely due to the of low efficiency (activity) of this enzyme, it is only present in some isolates or is not expressed under the conditions used where other sugars were present.

Man metabolism also provides the phosphorylated intermediate mannose 6-phosphate (Man6P), which is a precursor of GDP-mannose, important for biosynthesis of glycosylated components of cell wall in several microorganisms [174].

Mannose catabolism

In *S. pneumoniae* Man likely enters into the cell via a PTS system and the resultant Man6P is converted to fructose 6-phosphate (F6P) by the mannose 6-phosphate isomerase (ManA) (Fig. 1.6), in a pathway similar to that described in *E. coli* [175,176]. Two PTSs (Man-PTS and Lac-PTS, the latter with a very mild phenotype) were identified as putative Man uptake systems [141]. The involvement of other PTSs (fructose-PTS) has been reported for other bacteria [174,177–179]. Whether this is true for *S. pneumoniae* remains to be elucidated. Nevertheless, the existence of non-PTS transporters for Man uptake cannot be excluded [141].

Man catabolism has been studied in *Escherichia coli* [175,176]. More recently, the same pathway was characterized in the gram-positive bacteria *Corynebacterium glutamicum* and *Bacillus subtilis* [174,180]. In these microorganisms, mannose 6-phosphate isomerase was essential for growth on mannose as sole carbon source.

Different types (based on amino acid sequence similarity and domain organization) of this enzyme were described in *Xanthomonas campestris* and *Rhizobium meliloti* [181,182]. In these microorganisms deletion of ManA did not hamper growth on Man. In *R. meliloti* a different Man catabolic route was proposed involving active transport of Man (whether is mediated by an ABC or by a secondary carrier was not disclosed), subsequent phosphorylation by mannokinase and isomerization to F6P by mannose 6-phosphate isomerase [183].

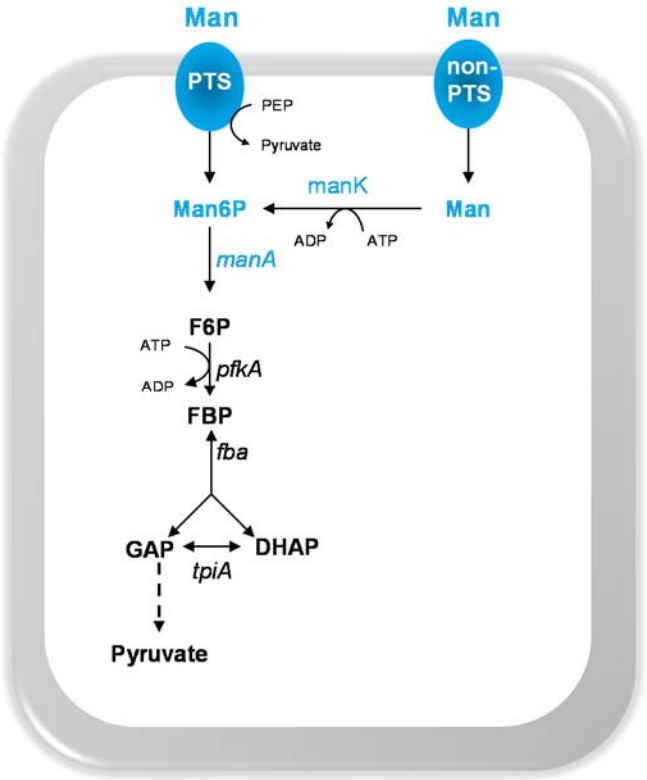

Figure 1.6. Schematic representation of pathways for the dissimilation of mannose (Man) in bacteria.

Reactions are catalysed by the following protein encoding genes: *manA*, mannose 6-phosphate isomerase; *manK*, mannose kinase; *pfkA*, 6-phosphofructokinase; *fba*, fructose-biphosphate aldolase; *tpiA*, triosephosphate isomerase. The lower glycolytic pathway is represented by a dashed arrow.
Intermediates: Man6P, mannose 6-phosphate; F6P, fructose 6-phosphate; FBP, fructose 1,6-biphosphate; GAP, glyceraldehyde 3-phosphate; DHAP, dihydroxyacetone phosphate.
In blue are depicted the intermediates and genes committed specifically to mannose catabolism.

Recently, two loci for mannoside catabolism were predicted in two species of *Shewanella*. These pathways are different from that descried in *E. coli* and its experimental validation is required [184]. According to this study these loci are restricted to Alteromonadales lineage.

Amino sugars: N-acetylneuraminic acid, N-acetylglucosamine and N-acetylgalactosamine

The amino sugars NeuNAc, GlcNAc and GalNAc are valuable carbon and nitrogen sources for growth and are present in high content in mucins, as determined in the model glycoprotein, porcine gastric mucin: 30% (wt/v) GlcNAc, 15% (wt/v) GalNAc and 2.6% (wt/v) NeuNAc [116]. The presence of pneumococcal extracellular glycosidases, with specificity for GlcNAc (StrH) and NeuNAc (NanA and NanB) residues, contributing to growth on human glycoconjugates, further supports this claim [148,185–187]. Besides the mucins, there are other glycan sources of these sugars. NeuNAc (or generically sialic acid) is copious as a terminal sugar of eukaryotic surface-exposed glycoconjugates but also in prokaryotes surfaces [188,189]. GlcNAc can be provided from host diet and secretions, as well as from peptidoglycan recycling (GlcNAc is a building block of this structure and also of lipopolysaccharides) and is present in the extracellular matrix of mammals and chito-oligosaccharides [190–192]. GalNAc is widespread in host receptors and glycoconjugates and is a component of bacterial cell wall, lipopolysaccharides and exopolysaccharides [114,193,194].

Nevertheless, the importance of these sugars goes beyond their nutritional value. For instances, these sugars contribute to cell wall synthesis. More recently, NeuNAc was found to act as a signalling molecule in the pneumococcus, promoting increased colonisation, invasion of the host's lower respiratory tract and biofilm formation *in vitro* [109,195,196]. In other pathogenic bacteria the presence of NeuNAc in the bacterial cell surfaces permits evasion from immune system (*e.g. H. influenzae*) and is important for interaction with host-cell surfaces (reviewed in [188]).

Similarly, GlcNAc has been found to act as a signalling molecule in different kingdoms (reviewed in [190]). In bacteria GlcNAc ensures

regulation between its catabolism and anabolism ensuring the desired quantities of UDP-GlcNAc necessary for peptidoglycan synthesis. In *E. coli* it is responsible for regulation of virulence factors (*e.g.* fimbriae) and its catabolism is important for gut colonisation ([197], reviewed in [190]). In soil bacteria, such as streptomycetes, it is involved in morphogenesis regulation namely sporulation and antibiotic production [198–200]. Under adverse conditions (famine) development (leading to sporulation) and antibiotic production are triggered whereas under feast periods these mechanisms are blocked [200]. In addition, the ubiquity of GlcNAc across kingdoms has revealed a multiplicity of interspecies communication mediated by this amino sugar (reviewed in [190]).

Adherence of *S. pneumoniae* and other viridans group streptococci via carbohydrate-containing receptors of host glycoconjugates has been demonstrated [193,201,202]. GalNAc-containing receptors were identified as important for the pneumococcus adherence [203,204]. An O-glycosidase, Eng, endo-α-*N*-acetylgalactosaminidase, with specificity for Galβ1-3GalNAc from core-1 O-linked glycans was characterized. In conjunction with NanA these glycosidases sequentially deglycosylate the sialylated core-1 O-linked glycans of glycoconjugates. Moreover, a role in colonisation of respiratory tract and adherence to human epithelial cells was established [114].

GalNAc-sensitive coaggregations have also been shown between viridans group streptococci and between streptococci and actinomyces [193].

NeuNAc and GlcNAc catabolism

In *S. pneumoniae* the transport of NeuNAc remains largely unknown, even though putative sugar transporters are annotated in *nanA*, *nanB* and *nanC* loci. In the *nanAB* locus two ABC transporters are encoded (SPD_1493-4-5 and SPD_1500-1-2) [205]. The first was recently

identified as the main NeuNAc transporter contributing to growth on a human glycoprotein and colonisation *in vivo* [109,141]. In this region a third transporter, Glc-PTS SPD_1496, was allocated to glucosamine [141]. A major facilitator superfamily (MFS) sodium solute symporter (SSS) (SP_1328) was identified, in some pneumococcal strains, in the *nanC* locus [141,188,206]. This region also comprises a neuraminidase (*nanC*), a kinase, a lyase and an epimerase [141]. D39 does not possess this locus and alternatively carries a putative oligopeptide ABC transporter, a mutarotase and an epimerase [141]. In opposition, the *nanAB* cluster is conserved and was proposed as the responsible for the uptake and metabolism of NeuNAc [141,205–208], but little is known about the *nanC* locus. A relation of *nanC* presence and invasive phenotypes in a tissue-specific manner was established and mutations in *nanC* locus did not influence the growth on NeuNAc [141,209].

There is a great diversity of NeuNAc transport systems widespread among bacteria and even in bacteria belonging to the same genus (*e.g.* genus *Streptococcus*) [206]. The first system to be studied in detail was in *E. coli*, the NanT, which is a single component system, secondary transporter, of the MFS [206,210].

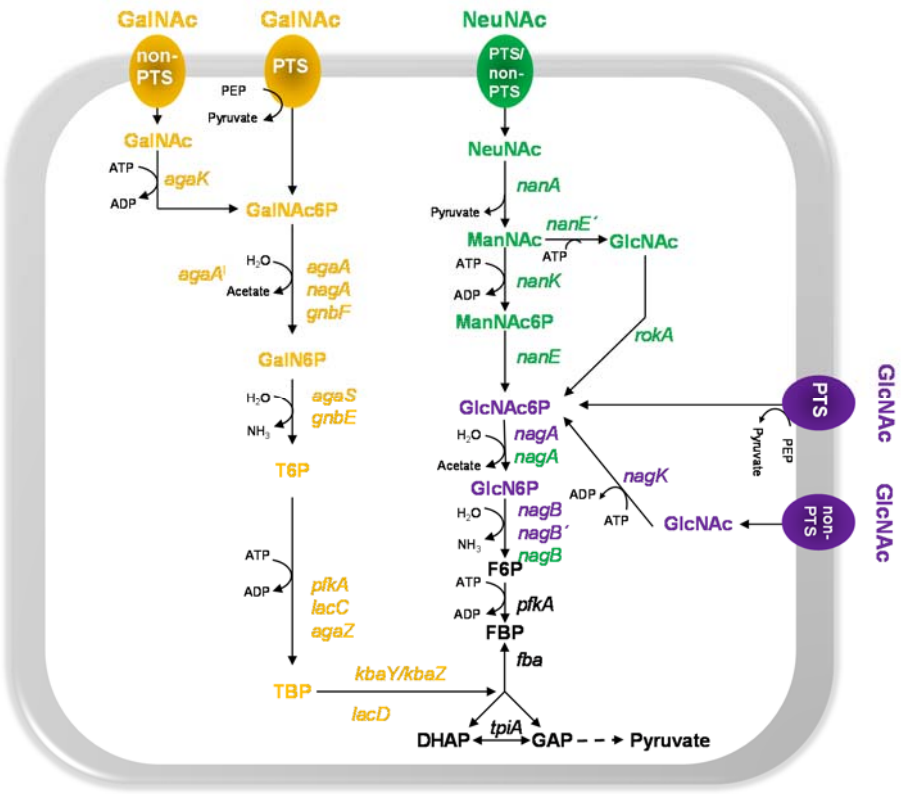

Figure 1.7. Schematic representation of pathways for the dissimilation of the amino sugars N-acetylglucosamine (GlcNAc), N-acetylneuraminic acid (NeuNAc) and N-acetylgalactosamine (GalNAc) in bacteria.

Reactions are catalysed by the following protein encoding genes: *nanA*, N-acetylneuraminate lyase; *nanK*, N-acetylmannosamine kinase; *nanE*, N-acetylmannosamine 6-phosphate epimerase; *rokA*, hexokinase; *nagA*, N-acetylglucosamine 6-phosphate deacetylase; *nagB*, glucosamine 6-phosphate isomerase; *nagB'*, glucosamine 6-phosphate isomerase non-homologues of *nagB*; *nagK,* N-acetylglucosamine kinase*; agaK,* N-acetylgalactosamine kinase; *agaA or gnbF*, N-acetylgalactosamine 6-phosphate deacetylase; *agaA*^{I} non-orthologous variants of *agaA; agaS* or *gnbE,* galactosamine 6-phosphate deaminase/isomerase; *agaZ* or *lacC*, tagatose 6-phosphate kinase; *kbaZ/kbaY or lacD,* tagatose 1,6-biphosphate aldolase; *pfkA*, 6-phosphofructokinase; *fba*, fructose-biphosphate aldolase; *tpiA*, triosephosphate isomerase. The lower glycolytic pathway is represented by a dashed arrow.
Intermediates: NeuNAc, N-acetylneuraminic acid; ManNAc, N-acetylmannosamine; ManNAc6P, N-acetylmannosamine 6-phosphate; GlcNAc6P, N-acetylglucosamine 6-phosphate; GlcN6P, glucosamine 6-phosphate; GalNAc6P, N-acetyl-galactosamine 6-phosphate; GalN6P, galactosamine 6-phosphate; T6P, tagatose 6-phosphate; TBP, tagatose 1,6-biphosphate; F6P, fructose 6-phosphate; FBP, fructose 1,6-biphosphate; GAP, glyceraldehyde 3-phosphate; DHAP, dihydroxyacetone phosphate.

In green, purple and orange are depicted the intermediates and genes committed to NeuNAc, GlcNAc and GalNAc catabolism.
For the sake of simplicity transporters other than PTS are designated generically as non-PTS.

In *H. influenzae* and *Pasteurella multocida* another type of secondary transporter was characterized: a tripartite ATP-independent periplasmic (TRAP) transporter (SiaPQM). This is a multicomponent system with an additional substrate-binding protein (SBP, SiaP) [211–213]. An ATP-binding cassette (ABC) transporter (SatABCD) was described in *Haemophilus ducreyi* [214]. More recently, a secondary carrier of the sodium solute symporter (SSS) family was reported [205,215].

Opposite to the NeuNAc transporters, for which bacteria have evolved multiple systems, the catabolic genes of the *nan* cluster (comprising a lyase (*nanA*), a kinase (*nanK*) and an epimerase (*nanE*)) seem to be shared among bacteria, despite the diversity in its organization, and are confined to human pathogens and commensals. Many of them occupying mucus rich regions (*e.g.* gut and respiratory tract) [205]. As demonstrated in oral streptococci which share the core metabolic activity for NeuNAc processing [208,216].

One exception is *Bacteroides fragilis* which lacks NanK and for which a new epimerase was described, with activity over unphosphorylated N-acetylmannosamine converting it to GlcNAc, using ATP as a cofactor. The latter is then phosphorylated by a RokA kinase and the concomitant product proceeds through the NagAB pathway. Hence a different catabolic route was established [217,218]. A similar pathway was predicted in the periodontal pathogen *Tannerella forsythia* [219] (Fig. 1.7).

The enzymes required for NeuNAc catabolism are encoded in the pneumococcal genome [140,205]. Catabolism of N-acetylneuraminic acid involves five specific steps (Fig. 1.7). A pyruvate group is first removed from the intracellular NeuNAc by N-acetylneuraminate lyase (NanA)

yielding N-acetylmannosamine (ManNAc). A subsequent phosphorylation step, mediated by N-acetylmannosamine kinase (NanK), originates N-acetylmannosamine 6-phosphate (ManNAc6P). ManNAc6P is then epimerized to N-acetylglucosamine 6-phosphate (GlcNAc6P) by N-acetylmannosamine 6-phosphate epimerase (NanE). The sequential removal of the acetyl group by N-acetylglucosamine 6-phosphate deacetylase (NagA) and removal of amino group and isomerization by glucosamine 6-phosphate isomerase/deaminase (NagB), yields glucosamine 6-phosphate (GlcN6P) and the glycolytic intermediate fructose 6-phosphate (F6P), respectively. The enzymes NagA and NagB are also involved in the degradation route of GlcNAc, with GlcNAc6P and GlcN6P as common intermediates of both pathways. Interestingly, in different bacteria, the *nagAB* orthologues are not coded closely to the *nan* system (except for *H. influenzae*) [206]. In *S. pneumoniae,* GlcNAc6P arises most likely as a product of PTS-mediated transport, as recently demonstrated by Bidossi *et al.* [141]. These authors found that *ptsI* mutants of strains G54 and the D39 rough derivative DP1004, which lack PTS activity, were unable to utilize GlcNAc. Similarly, in the closely related *S. mutans* UA159, GlcNAc is imported exclusively by a PTS system, with *manLMN* playing a dominant role. In contrast, in *S. gordonii* strain DL1 other GlcNAc transport systems must be present [191]. As for NeuNAc the diversity in transport systems is wide among bacteria. In *E. coli* is well described the PTS-mediated uptake of GlcNAc (NagE) [220,221]. And recently the same type of transport has been shown for *Bacillus subtilis* (NagP) [222]. In contrast, in *Streptomyces olivaceoviridis* and *Xanthomonas campestris* pv. *campestris* an ABC transporter (Ngc) and a secondary active transporter from the MFS (NagP), respectively, were described [192,223]. Novel permeases (NagP and presumably NagX) were identified in the genome of Alteromonadales (*e.g. Shewanella oneidensis*) and Xanthomonadales, lacking GlcNAc-PTS or GlcNAc-ABC

systems [224]. NagP functionality was experimentally validated in *S. oneidensis* MR-1 [184]. In these cases, the existence of GlcNAc specific kinases (NagK) that phosphorylate the incoming sugar is pivotal for GlcNAc catabolism, and therefore an alternative pathway was proposed that includes this step before the action of NagAB [192,224]. Indeed, GlcNAc kinases were identified and characterized in *S. oneidensis* and *X. campestris* pv. *campestris* [192,224]. In addition, NagB enzymes (NagB-II), non-homologous to the one found in *E. coli*, were also characterized in these microorganisms [192,224] (Fig. 1.7). In contrast, NagA orthologous are conserved across bacteria and eukaryotes [224]. Genomic reconstruction of GlcNAc catabolism was made for several proteobacteria [224].

GalNAc catabolism

The transport and catabolism of GalNAc in the pneumococcus is unknown. Genes for a full catabolic route are not annotated in the genome. In opposition, GalNAc catabolism has been studied in *E. coli* K-12 and C [225–227]. However, K-12 does not grow on GalNAc, due to deletion and truncation of genes comprising a transporter (*agaW'EF*) and a deacetylase (*agaA'*) [226]. Although this pathway has been proposed *in silico* many years ago [225,226], only recently it was experimentally validated [226–229]. In *E. coli*, GalNAc enters the cell via a PTS (coded by *agaVWEF)*, and the concomitant phosphorylated product is deacetylated by GalNAc deacetylase (AgaA) to form galactosamine 6-phosphate (GalN6P). The NagA, involved in GlcNAc catabolic pathway, is seemingly a surrogate for AgaA [227,230]. GalN6P is then deaminated and isomerised by AgaS to yield T6P. The latter is phosphorylated by 6-phosphofructokinase (PfkA) yielding TBP, which is then converted to the glycolytic intermediates DHAP and GAP by a dimeric aldolase

(KbaY/KbaZ). It was proposed that KbaZ subunit is needed for full activity and stability of KbaY [226–229] (Fig. 1.7).

A different variant of GalNAc catabolic pathway was proposed for *Shewanella* strains and more recently some of those enzyme activities were experimentally validated for *Shewanella* sp ANA-3, which grows on GalNAc [184,230]. In *Shewanella* the PTS system is substituted by a permease (AgaP) and a subsequent phosphorylation step mediated by a GalNAc kinase (AgaK). A nonorthologous GalNAc deacetylase ($AgaA^{II}$) converts GalNA6P to GalN6P and AgaS (*E. coli* like-enzyme) functions as the main GalN6P isomerase [184,230]. While *Shewanella* possesses a gene encoding AgaZ (*E. coli* like-T6P kinase) genes coding for AgaY (predicted TBP aldolase) are missing and likely this activity is replaced by fructose biphosphate aldolase, but confirmation is required [230] (Fig. 1.7).

The genomic GalNAc pathway reconstruction was extended for other bacteria of the Proteobacteria philum [230]. The initial steps of GalNAc catabolism are the most variable among proteobacteria, whereas AgaS is the most conserved. The identities of the enzymes mediating the two final steps of GalNAc catabolism are not totally disclosed and experimental validation is needed, as differential patterns of distribution of these genes was observed among Proteobacteria. Whether AgaZ acts in conjunction with AgaY or separately or are replaced by other enzymes needs to be addressed [230].

The first example of a GalNAc pathway in Firmicutes was studied more recently in *Lactobacillus casei* [194]. The GalNAc gene cluster (*gnbREFGBCDA*) differs from that of proteobacteria studied so far [230]. It comprises a mannose-type PTS (encoded by *gnbBCDA*, PTS^{Gnb}) involved in transport of GalNAc and the enzymes for subsequent GalNAc6P catabolism, GalNAc6P deacetylase (GnbF) and GalN6P deaminase (GnbE). Interestingly it was shown that NagA is also required

for full growth on GalNAc. The genes for T6P processing are encoded in a different cluster (lacR1ABD2C) comprising a T6P kinase (LacC) and TBP aldolase (LacD), subsequently leading to triose phosphates (DHAP and GAP) [194] (Fig. 1.7). However, the *gnb* cluster is only present in three lactobacilli species [194].

Fucose

Fucose differs from the other monosaccharides by lacking the hydroxyl group at position C6 and possessing an L-configuration. It is a widespread and abundant sugar found in mammalian cells as a major component of glycoconjugates (N- and O-linked glycans and glycolipids), usually localized at terminal positions of glycan structures [231]. The diversity of fucosylated glycoconjugates is wide [231]. Fucose is highly abundant in the mucins ranging from 4-14% according to the origin of the glycoprotein [116,232], in the ABO blood group antigens [231,233,234], in intestine epithelial surfaces and in dietary polysaccharides (*e.g.* pectin, human milk oligosaccharides) [235,236], but it can also be found in bacterial polysaccharides [237]. Therefore it is likely a potential sugar for bacterial growth. Indeed, both pathogenic and commensal bacteria are able to grow on Fuc (*e.g. Bacteroides thetaiotaomicron* [238], *Salmonella enterica* serovar *Typhimurium* LT2 [239], *Roseburia inulinivorans* [235] or *E. coli* [240]).

Interestingly, *S. pneumoniae* seems unable to use this sugar for growth despite possessing the genes required to assemble a catabolic pathway which suggests a non-metabolic role of Fuc metabolism [41,234,241]. In support, different reports reveal the implication of Fuc metabolic genes in pneumococcal virulence. A STM analysis implicated two transporter subunits, a fuculose kinase and an extracellular hydrolase of the Fuc operon, in pneumococcal virulence [102]. Later, deletion of the whole operon resulted in attenuated virulence in a mouse model of pneumonia

but does not have a role in colonisation [241]. More recently it was suggested that the strain dependency ability to scavenge distinct fucosylated glycans antigens might play a role in virulence in the interaction with the host, in a strain-dependent manner [233,242]. Higgins *et al*., [234] suggested that Fuc pathway in *S. pneumoniae* could act as a mechanism for sensing Fuc-containing oligosaccharides, conducting Fuc through the pathway being one intermediate, likely fuculose, the signalling molecule.

Similarly, in other bacteria, non-metabolic functions were described for Fuc. The enterohemorragic bacteria *E. coli* (EHEC) uses a Fuc sensing mechanism to regulate gut colonisation (TCST, FusKR), by modulating the expression of virulence genes in EHEC [243]. The regular intestinal coloniser *B. thetaiotaomicron*, coordinates the expression of Fuc utilization pathway with expression of a locus regulating the production of fucosylated glycans in the intestinal enterocytes of the host, controlling the supply and demand of Fuc [238,244]. Additionally, fucosylated glycans are adherence targets for bacteria (*e.g. Helicobacter pylori*, *Campylobacter jejuni* [245,246]) and Fuc was found to be a chemoattractant in *C. jejuni* [232]. More interestingly *H. pilory* induces host cells to produce α-L-fucosidase activity and can attach Fuc to the bacterial cell surface [247].

All these examples highlight the relevance of fucose for bacteria at a variety of levels.

Fucose catabolism

Two types of Fuc utilization operons were identified in the pneumococcal genomes [41,233,234]. Type 1 operon, disclosed by homology to *E. coli* and *H. influenzae* fucose metabolic proteins, is widespread among pneumococcal genomes (*e.g.* TIGR4, R6, D39) whereas Type 2 seems to be confined to a fewer strains (*e.g.* SP3-BS71)

[41,233]. The general operon (Type 1) codes a fucose regulator (FucR, a repressor controlling the whole operon), a fucose mutarotase (FucU) that likely accelerates the conversion of the β and α forms of L-fucose, a L-fucose isomerase (FucI) that acts over α-L-fucose to yield L-fuculose, a L-fuculose kinase (FucK) that phosphorylates L-fuculose to L-fuculose 1-phosphate and a L-fuculose phosphate aldolase (FucA) converts the latter into DHAP and L-lactaldehyde. DHAP then enters in the glycolysis [233,234] (Fig. 1.8). Both operons possess conserved features: the regulator and the fucose processing genes *fucI*, *fucK* and *fucA* [233,234]. The main differences rely on the transport system - the PTS (EIIABCD) of Type 1 operon is replaced by an ABC transporter in the Type 2 operon -, and in the extra- and intracellular glycan-processing enzymes. The extracellular family 98 glycoside hydrolases (GH98) with endo-β-D-galactosidase activity, present in both operons, have different substrate specificities. GH98 of Type 1 acts over Lewis^{y} antigen to release H-disaccharide and GH98 of Type 2 operon cleaves A- and B- blood group antigens to yield A/B trisaccharide products. Moreover, while Type 1 operon encodes a putative intracellular α-1,2-fucosidase GH95A, in alternative, Type 2 operon codes GH29 and two additional glycosidases: GH36A (putative α-N-acetylgalactosaminidase) and GH36B (putative α-galactosidase) [233,234,242]. The different glycan substrate specificities of GH98 enzymes of both operons, lead to the formulation of two models for fucosylated-glycan uptake and metabolism [242]. In brief, in Type 1 model, H-disaccharide is transported and concomitantly phosphorylated via PTS. The intracellular product is then cleaved to β-Fuc and Gal6P, by GH95A. β-Fuc is converted to α-Fuc by FucU entering in Fuc catabolic route [242,248]. In Type 2 model the trisaccharides enter the cell without modification, by an ABC transporter, and are subject to GH36A/GH29 activities yielding α-Fuc, Gal and GalNAc or subject to GH29/GH36B to yield Gal and α-Fuc [242,248].

Higgins *et al*. [234], suggested that Fuc transport is mediated by a non-specific permease, but the identity of such transporter is not yet known.

The pathway for Fuc metabolism is well established in *E. coli* [240,249–251]. The major distinct features between Fuc catabolism in *E. coli* and in the pneumococcus are the transport system, *E. coli* possesses a fucose permease (H^+-symporter [252]) not present in pneumococcal genomes, and different glycoside hydrolases [234]. Moreover, while FucU catalyzes the first step in Fuc catabolism in *E. coli*, in *S. pneumoniae* it links glycoside hydrolase activity to bacterial Fuc catabolism [248].

More recently *Campylobacter jejuni* was found to grow on Fuc in a strain dependent manner [253,254]. A new pathway, with no homologous genes (except the permease for Fuc transport and lactaldehyde dehydrogenase for aerobic degradation of lactaldehyde) to those described in the enteric bacteria, was proposed, but is yet uncharacterized [254,255]. Experimental evidence suggest that Fuc enters the cell by a FucP, but is not phosphorylated, as in *E. coli* or *Bacteroides* [254]. Surrounding FucP a set of genes, with homology to those of the plant pathogen *Xanthomonas campestris* which code a new Fuc pathway, was identified suggesting that Fuc is likely metabolized by a similar route [254,256].

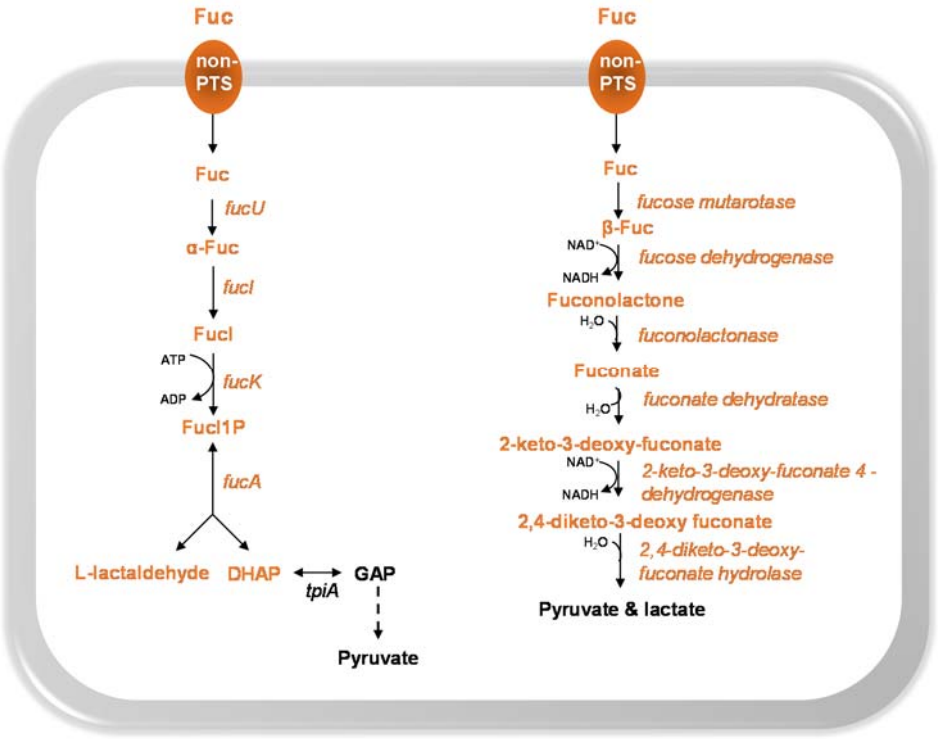

Figure 1.8. Schematic representation of pathways for the dissimilation of fucose (Fuc) in bacteria.

Reactions are catalysed by the following protein encoding genes*: fucU,* fucose mutarotase; *fucI*, L-fucose isomerase; *fucK*, L-fuculose kinase; *fucA*, L-fuculose phosphate aldolase; *tpiA*, triosephosphate isomerase.
Intermediates: Fucl, fuculose; Fucl1P, fuculose 1-phosphate; DHAP, dihydroxyacetone phosphate; GAP, glyceraldehyde 3-phosphate.
In orange are depicted the intermediates and genes committed specifically to Fuc catabolism.

The general Fuc degradation pathway, comprising an isomerase, a kinase, and an aldolase has been identified/proposed in several microorganisms (*e.g. E. coli* [240,249–251], *R. inulinivorans* [235], *B. thetaiotaomicron* [238], *Clostridium phytofermentans* [257]). Under anaerobic conditions, the resultant L-lactaldehyde is reduced to L-1,2-propanediol by a L-1,2-propanediol oxidoreductase (*fucO*) [240]. But whereas in *E. coli* and *B. thetaiotaomicron*, L-1,2-propanediol is likely excreted [235,240], in other microorganisms it is further metabolized.

Salmonella serovar *Typhimurium LT2* encodes an operon (*pdu*) for propanediol utilization [258–260]. A different organization of *pdu* genes, and with some distinct enzymatic features, was found in *R. inulinivorans* [235,257]. Alternatively, in aerobiosis, L-lactaldeheyde is metabolized to lactate by a lactaldehyde dehydrogenase (*ald*), and the latter to pyruvate, in *E. coli* [260].

Opposite to the previous bacteria several strains of *Lactobacillus* were unable to use or only moderately use Fuc [261]. *Lactobacillus casei* BL23 lacks genes for Fuc catabolism but expresses three α-fucosidases. This bacterium grows on the fucosylated glycan Fuc-α-1,3-GlcNAc, but uses only the GlcNAc moiety. The liberated Fuc is released to the environment by a yet unknown mechanism [262].

Glycolysis, glucose and pyruvate metabolism

Glucose is the preferred carbon and energy sources of the majority of the *Streptococcaceae. S. pneumoniae* seems to be no exception [125,141].

Glucose enters the cell usually by PTS systems and is concomitantly phosphorylated to glucose 6-phosphate (G6P). Bidossi *et al*. [141] proposed the PTS-Man, ManLMN (PTS^{Man}) as the main Glc uptake system in *S. pneumoniae*, but transport through other PTSs was not ruled out. Glc can also be up taken by non-PTS transporters and phosphorylated by a glucokinase (GKI) yielding G6P. This hypothesis is in line with the ability of *ptsI* mutants of *S. pneumoniae* to use glucose as sole carbon source for growth [141] (Fig. 1.9). The presence of more than one transporter for Glc internalization is widespread in bacteria (*e.g. L. lactis, E. coli or B. subtilis*) [263–265]. The further processing of G6P into pyruvate occurs via the Embden-Meyerhof-Parnas depicted in Fig. 1.9. The net gain of Glc catabolism is two pyruvate molecules, two NADH and two ATP´s per mole of Glc.

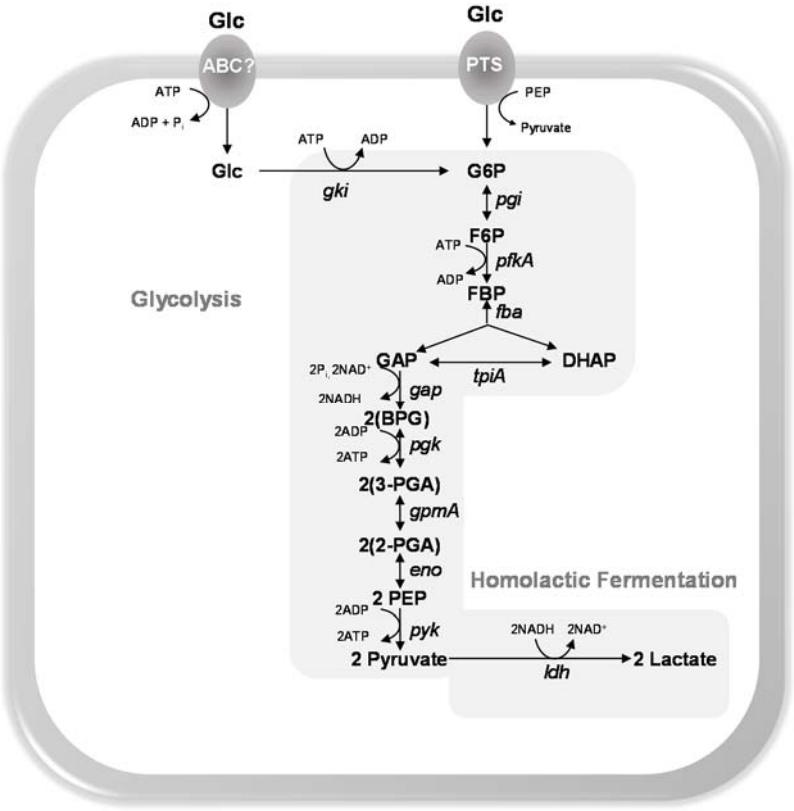

Figure 1.9. Schematic representation of the glucose uptake and catabolism via the Embden-Meyerhof-Parnas (EMP) pathway, and homolactic fermentation in *S. pneumoniae*.

Reactions are catalysed by the following protein encoding genes: *gki*, glucokinase; *pgi*, glucose 6-phosphate isomerase; *pfkA*, 6-phosphofructokinase; *fba*, fructose-biphosphate aldolase; *tpiA*, triosephosphate isomerase; *gap*, glyceraldehyde 3-phosphate dehydrogenase; *pgk*, phosphoglycerate kinase; *gpmA*, phosphoglyceromutase; *eno*, enolase; *pyk*, pyruvate kinase; *ldh*, L-lactate dehydrogenase.
Intermediates: G6P, glucose 6-phosphate; F6P, fructose 6-phosphate; FBP, fructose 1,6-biphosphate; GAP, glyceraldehyde 3-phosphate; DHAP, dihydroxyacetone phosphate; BPG, 1,3-biphosphoglycerate; 3-PGA, 3-phosphoglycerate; 2-PGA, 2-phosphoglycerate; PEP, phosphoenolpyruvate.

Generally pyruvate is converted to lactate, by lactate dehydrogenase (LDH), with oxidation of NADH to NAD^+ - homolactic fermentation (Fig. 1.10). While LDH is encoded by multiple genes in other bacteria [266–

268], *S. pneumoniae* possesses only a single copy of the gene [140]. Recently, successful construction of a pneumococcal *ldh* mutant was attained resulting in total abrogation of lactate production [119]. In this study the importance of LDH for NAD^+ regeneration and maintenance of redox balance was established. LDH was suggested as the most efficient enzyme for pyruvate consumption [119].

However, under certain conditions, such as the presence of slow metabolizable carbohydrates (*e.g.* galactose), sugar limitation, aerobiosis, and in the LDH mutant described above, a shift to mixed acid fermentation profile is observed with production of ethanol, acetate or formate [269–272].

Pyruvate metabolism involves several enzymes (Fig. 1.10). Besides LDH, pyruvate can be processed by pyruvate oxidase (SpxB) or pyruvate formate-lyase (PFL). SpxB catalyses the conversion of pyruvate, in presence of O_2 and inorganic phosphate, to acetyl-P, H_2O_2 and CO_2. This enzyme has been extensively studied in *S. pneumoniae* and its involvement in several important biological processes was established (*e.g.* competitive advantage over co-colonisers, streptococcal resistance to H_2O_2) (reviewed in [99,121]). Part of these features are connected with the high amounts (in mM range) of H_2O_2 produced. Recently, a relation between SpxB and sugar utilization capabilities was established, under microaerobic conditions [99].

Yesilkaya *et al*. [118] identified the pneumococcal genes responsible for PFL activity and demonstrated its relevance for mixed acid fermentation under microaerobic and anaerobic conditions, in *S. pneumoniae*. PFL converts pyruvate to formate and acetyl-CoA. The latter can be further metabolized to ethanol or acetate by alcohol dehydrogenase (*adh*) or phosphotransacetylase/acetate kinase (*pta*/*ackA*), respectively. While acetate production leads to an additional molecule of ATP, ethanol regenerates two NAD^+ (Fig. 1.10).

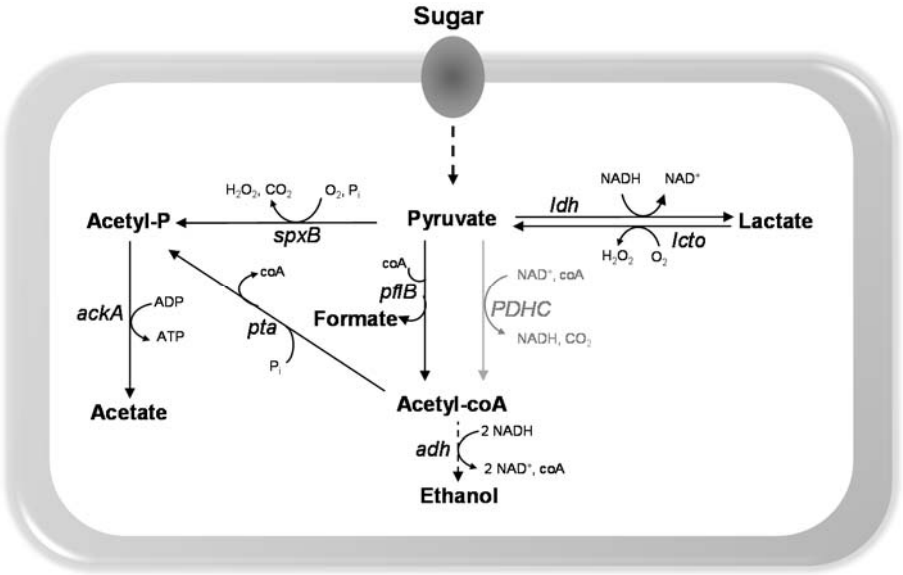

Figure 1.10. Schematic representation of pyruvate metabolism in *S. pneumoniae*.

Reactions are catalysed by the following protein encoding genes: *spxB*, pyruvate oxidase; *ldh*, L-lactate dehydrogenase; *lcto*, lactate oxidase; *pflB*, pyruvate formate-lyase; *pta*, phosphotransacetylase; *ackA*, acetate kinase; *adh*, bifunctional acetaldehyde-coA/alcohol dehydrogenase (SPD_1834); PDHC, pyruvate dehydrogenase complex.
The occurrence of the reaction catalysed by PDHC is unknown and therefore is depicted in grey.

Several *Streptococcaceae* also possess the pyruvate dehydrogenase complex (PDHC), which canalizes the oxidative decarboxylation of pyruvate to acetyl-CoA and CO_2, under aerobic conditions. *S. pneumoniae* lacks genes homologous to those encoding PDHC [139,140,273]. However, the presence of a functional pyruvate dehydrogenase in the pneumococcus is still controversial [118,274].

The versatility of pyruvate metabolism has been proposed to be a way for effective pneumococcal *in vivo* fitness [99,119].

In this thesis, we study the transcriptional response of *S. pneumoniae* to mucin. In addition, we assess which monosaccharides, present in the representative airway glycan mucin, are utilized by the pneumococcus to grow and how it benefits from the diversity of sugars generated from its deglycosylation. The biochemical routes predicted *in silico* for the catabolism of mannose, galactose and N-acetylglucosamine in *S. pneumoniae* D39 are experimentally validated (Chapter 2).

The importance of sugar-specific catabolic genes in galactose, mannose and N-acetylglucosamine pathways is studied in mouse models of pneumococcal colonisation and disease (Chapter 2). Furthermore, we address the impact of carbohydrate availability (nasopharynx carbohydrates and glucose) in the expression of known virulence factors (Chapter 3).

We study, at transcriptional and metabolic levels, the response of the pneumococcus to carbohydrates present in the airways and how *S. pneumoniae* responds to the presence of the fast metabolizable sugar, glucose, existing in comparatively high abundance in blood (Chapter 3).

References

1. Watson DA, Musher DM, Jacobson JW, Verhoef J. A brief history of the pneumococcus in biomedical research: a panoply of scientific discovery. Clin Infect Dis Off Publ Infect Dis Soc Am. 1993;17: 913–924.
2. López R. Pneumococcus: the sugar-coated bacteria. Int Microbiol Off J Span Soc Microbiol. 2006;9: 179–190.
3. Griffith, F. The significance of pneumococcal types. J Hyg. 1928;27: 113–159.
4. Avery OT, Macleod CM, McCarty M. Studies on the chemical nature of the substance inducing transformation of pneumococcal types: induction of transformation by a desoxyribonucleic acid fraction isolated from pneumococcus type III. J Exp Med. 1944;79: 137–158.
5. Dochez A, Avery OT. The elaboration of specific soluble substance by pneumococcus during growth. J Exp Med. 1917;26: 477–493.

6. Dochez AR, Avery OT. Soluble substance of pneumococcus origin in the blood and urine during lobar pneumonia. Exp Biol Med. 1917;14: 126–127. doi:10.3181/00379727-14-75
7. Avery OT. Immunological relationships of cell constituents of pneumococcus: second paper. J Exp Med. 1925;42: 367–376. doi:10.1084/jem.42.3.367
8. Avery OT, Goebel WF. Chemoimmunological studies on the soluble specific substance of pneumococcus: I. The isolation and properties of the acetyl polysaccharide of pneumococcus type I. J Exp Med. 1933;58: 731–755.
9. M Heidelberger, Avery OT. The soluble specific substance of pneumococcus. J Exp Med. 1923;38: 73–79.
10. Heidelberger M. Immunologically specific polysaccharides. Chem Rev. 1927;3: 403–423. doi:10.1021/cr60012a004
11. Tuomanen E. Streptococcus pneumoniae. In: Dworkin M, Falkow S, Rosenberg E, Schleifer K-H, Stackebrandt E, editors. The Prokaryotes. New York, NY: Springer US; 2006. pp. 149–162. Available: http://link.springer.com/10.1007/0-387-30744-3_4
12. Zapun A, Vernet T, Pinho MG. The different shapes of cocci. FEMS Microbiol Rev. 2008;32: 345–360. doi:10.1111/j.1574-6976.2007.00098.x
13. Pinho MG, Kjos M, Veening J-W. How to get (a)round: mechanisms controlling growth and division of coccoid bacteria. Nat Rev Microbiol. 2013;11: 601–614. doi:10.1038/nrmicro3088
14. Pérez-Dorado I, Galan-Bartual S, Hermoso JA. Pneumococcal surface proteins: when the whole is greater than the sum of its parts: Structural biology of pneumococcal surface proteins. Mol Oral Microbiol. 2012;27: 221–245. doi:10.1111/j.2041-1014.2012.00655.x
15. Martner A, Skovbjerg S, Paton JC, Wold AE. *Streptococcus pneumoniae* autolysis prevents phagocytosis and production of phagocyte-activating cytokines. Infect Immun. 2009;77: 3826–3837. doi:10.1128/IAI.00290-09
16. Henriques-Normark B, Tuomanen EI. The pneumococcus: epidemiology, microbiology, and pathogenesis. Cold Spring Harb Perspect Med. 2013;3: a010215–a010215. doi:10.1101/cshperspect.a010215
17. Nobbs AH, Lamont RJ, Jenkinson HF. *Streptococcus* adherence and colonization. Microbiol Mol Biol Rev MMBR. 2009;73: 407–450, Table of Contents. doi:10.1128/MMBR.00014-09
18. Arbique JC, Poyart C, Trieu-Cuot P, Quesne G, Carvalho M d. GS, Steigerwalt AG, et al. Accuracy of phenotypic and genotypic testing for identification of *Streptococcus pneumoniae* and description of *Streptococcus pseudopneumoniae* sp. nov. J Clin Microbiol. 2004;42: 4686–4696. doi:10.1128/JCM.42.10.4686-4696.2004
19. Doern CD, Burnham C-AD. It's not easy being green: the viridans group streptococci, with a focus on pediatric clinical manifestations. J Clin Microbiol. 2010;48: 3829–3835. doi:10.1128/JCM.01563-10
20. Facklam R. What happened to the streptococci: overview of taxonomic and nomenclature changes. Clin Microbiol Rev. 2002;15: 613–630. doi:10.1128/CMR.15.4.613-630.2002
21. Reller LB, Weinstein MP, Werno AM, Murdoch DR. Laboratory diagnosis of invasive pneumococcal disease. Clin Infect Dis. 2008;46: 926–932. doi:10.1086/528798

22. Song J-H, Dagan R, Klugman KP, Fritzell B. The relationship between pneumococcal serotypes and antibiotic resistance. Vaccine. 2012;30: 2728–2737. doi:10.1016/j.vaccine.2012.01.091
23. Vernet G, Saha S, Satzke C, Burgess DH, Alderson M, Maisonneuve J-F, et al. Laboratory-based diagnosis of pneumococcal pneumonia: state of the art and unmet needs: Laboratory-based diagnosis of pneumococcal pneumonia. Clin Microbiol Infect. 2011;17: 1–13. doi:10.1111/j.1469-0691.2011.03496.x
24. Habib M, Porter BD, Satzke C. Capsular serotyping of *Streptococcus pneumoniae* using the quellung reaction. J Vis Exp. 2014; doi:10.3791/51208
25. Leegaard TM, Bootsma HJ, Caugant DA, Eleveld MJ, Mannsaker T, Froholm LO, et al. Phenotypic and genomic characterization of pneumococcus-like streptococci isolated from HIV-seropositive patients. Microbiology. 2010;156: 838–848. doi:10.1099/mic.0.035345-0
26. Bandettini R, Melioli G. Laboratory diagnosis of *Streptococcus pneumoniae* infections: past and future. J Prev Med Hyg. 2012;53: 85–88.
27. Koornhof HJ, Madh SA, Feldman C, Gottberg A von, Klugman KP. A century of South African battles against the pneumococcus –"the Captain of Death." South Afr J Epidemiol Infect. 2009;24: 7–19.
28. Gennaris A, Collet J-F. The "captain of the men of death", *Streptococcus pneumoniae* , fights oxidative stress outside the "city wall": A novel antioxidant surface defence. EMBO Mol Med. 2013;5: 1798–1800. doi:10.1002/emmm.201303482
29. Braido F, Bellotti M, De Maria A, Cazzola M, Canonica GW. The role of pneumococcal vaccine. Pulm Pharmacol Ther. 2008;21: 608–615. doi:10.1016/j.pupt.2008.04.001
30. Kadioglu A, Weiser JN, Paton JC, Andrew PW. The role of *Streptococcus pneumoniae* virulence factors in host respiratory colonization and disease. Nat Rev Microbiol. 2008;6: 288–301. doi:10.1038/nrmicro1871
31. Obaro S, Adegbola R. The pneumococcus: carriage, disease and conjugate vaccines. J Med Microbiol. 2002;51: 98–104.
32. Bosch AATM, Biesbroek G, Trzcinski K, Sanders EAM, Bogaert D. Viral and bacterial interactions in the upper respiratory tract. Hobman TC, editor. PLoS Pathog. 2013;9: e1003057. doi:10.1371/journal.ppat.1003057
33. Bogaert D, de Groot R, Hermans P. *Streptococcus pneumoniae* colonisation: the key to pneumococcal disease. Lancet Infect Dis. 2004;4: 144–154. doi:10.1016/S1473-3099(04)00938-7
34. Hava DL, LeMieux J, Camilli A. From nose to lung: the regulation behind *Streptococcus pneumoniae* virulence factors: Virulence gene regulation in S. pneumoniae. Mol Microbiol. 2003;50: 1103–1110. doi:10.1046/j.1365-2958.2003.03764.x
35. Lynch JP, Zhanel GG. Streptococcus pneumoniae: epidemiology, risk factors, and strategies for prevention. Semin Respir Crit Care Med. 2009;30: 189–209. doi:10.1055/s-0029-1202938
36. Feldman C, Anderson R. New insights into pneumococcal disease. Respirology. 2009;14: 167–179. doi:10.1111/j.1440-1843.2008.01422.x
37. Hill PC, Cheung YB, Akisanya A, Sankareh K, Lahai G, Greenwood BM, et al. Nasopharyngeal carriage of Streptococcus pneumoniae in Gambian infants: a longitudinal study. Clin Infect Dis Off Publ Infect Dis Soc Am. 2008;46: 807–814. doi:10.1086/528688

38. Högberg L, Geli P, Ringberg H, Melander E, Lipsitch M, Ekdahl K. Age- and serogroup-related differences in observed durations of nasopharyngeal carriage of penicillin-resistant pneumococci. J Clin Microbiol. 2007;45: 948–952. doi:10.1128/JCM.01913-06
39. Sandgren A, Sjostrom K, Olsson-Liljequist B, Christensson B, Samuelsson A, Kronvall G, et al. Effect of clonal and serotype-specific properties on the invasive capacity of *Streptococcus pneumoniae*. J Infect Dis. 2004;189: 785–796. doi:10.1086/381686
40. Brueggemann AB, Peto TEA, Crook DW, Butler JC, Kristinsson KG, Spratt BG. Temporal and geographic stability of the serogroup-specific invasive disease potential of *Streptococcus pneumoniae* in children. J Infect Dis. 2004;190: 1203–1211. doi:10.1086/423820
41. Chan PF, O'Dwyer KM, Palmer LM, Ambrad JD, Ingraham KA, So C, et al. Characterization of a novel fucose-regulated promoter (PfcsK) suitable for gene essentiality and antibacterial mode-of-action studies in *Streptococcus pneumoniae*. J Bacteriol. 2003;185: 2051–2058. doi:10.1128/JB.185.6.2051-2058.2003
42. Nobbs AH, Jenkinson HF, Everett DB. Generic determinants of *Streptococcus* colonization and infection. Infect Genet Evol. 2014; doi:10.1016/j.meegid.2014.09.018
43. O'Brien KL, Wolfson LJ, Watt JP, Henkle E, Deloria-Knoll M, McCall N, et al. Burden of disease caused by *Streptococcus pneumoniae* in children younger than 5 years: global estimates. The Lancet. 2009;374: 893–902. doi:10.1016/S0140-6736(09)61204-6
44. Advisory Committee on Immunization Practices. Preventing pneumococcal disease among infants and young children. Recommendations of the Advisory Committee on Immunization Practices (ACIP). MMWR Recomm Rep Morb Mortal Wkly Rep Recomm Rep Cent Dis Control. 2000;49: 1–35.
45. Feldman C, Anderson R. Review: Current and new generation pneumococcal vaccines. J Infect. 2014;69: 309–325. doi:10.1016/j.jinf.2014.06.006
46. Wardlaw TM, Johansson EW, Hodge MJ, UNICEF, Division of Communication, World Health Organization. Pneumonia: the forgotten killer of children. New York: UNICEF : Geneva, Switzerland : World Health Organization; 2006.
47. Johnson HL, Deloria-Knoll M, Levine OS, Stoszek SK, Freimanis Hance L, Reithinger R, et al. Systematic evaluation of serotypes causing invasive pneumococcal disease among children under five: the pneumococcal global serotype project. Cohen J, editor. PLoS Med. 2010;7: e1000348. doi:10.1371/journal.pmed.1000348
48. Davis SM, Deloria-Knoll M, Kassa HT, O'Brien KL. Impact of pneumococcal conjugate vaccines on nasopharyngeal carriage and invasive disease among unvaccinated people: Review of evidence on indirect effects. Vaccine. 2013;32: 133–145. doi:10.1016/j.vaccine.2013.05.005
49. Frazão N, Hiller NL, Powell E, Earl J, Ahmed A, Sá-Leão R, et al. Virulence potential and genome-wide characterization of drug resistant *Streptococcus pneumoniae* clones selected in vivo by the 7-valent pneumococcal conjugate vaccine. Miyaji EN, editor. PLoS ONE. 2013;8: e74867. doi:10.1371/journal.pone.0074867
50. Dagan R, Juergens C, Trammel J, Patterson S, Greenberg D, Givon-Lavi N, et al. Efficacy of 13-valent versus 7-valent pneumococcal conjugate vaccine against

nasopharyngeal colonization of antibiotic-nonsusceptible *Streptococcus pneumoniae*. J Infect Dis. 2014; doi:10.1093/infdis/jiu576

51. El-Solh A, Assaad, El-Masri, Porhomayon J. Pneumonia immunization in older adults: review of vaccine effectiveness and strategies. Clin Interv Aging. 2012; 453. doi:10.2147/CIA.S29675
52. Improving global health by preventing pneumococcal disease. Report from the all-party parliamentary group on pneumococcal disease prevention in the developing world. 2008.
53. Jenkinson HF, Lamont R. Streptococcal adhesion and colonization. Crit Rev Oral Biol Med. 1997;8: 175–200. doi:10.1177/10454411970080020601
54. Catterall JR. *Streptococcus pneumoniae*. Thorax. 1999;54: 929–937. doi:10.1136/thx.54.10.929
55. Casadevall A, Pirofski L. Host-pathogen interactions: the attributes of virulence. J Infect Dis. 2001;184: 337–344. doi:10.1086/322044
56. Weiser JN. The pneumococcus: why a commensal misbehaves. J Mol Med Berl. 2010;88: 97–102. doi:10.1007/s00109-009-0557-x
57. Nelson AL, Roche AM, Gould JM, Chim K, Ratner AJ, Weiser JN. Capsule enhances pneumococcal colonization by limiting mucus-mediated clearance. Infect Immun. 2007;75: 83–90. doi:10.1128/IAI.01475-06
58. Weiser JN, Austrian R, Sreenivasan PK, Masure HR. Phase variation in pneumococcal opacity: relationship between colonial morphology and nasopharyngeal colonization. Infect Immun. 1994;62: 2582–2589.
59. Cundell DR, Weiser JN, Shen J, Young A, Tuomanen EI. Relationship between colonial morphology and adherence of *Streptococcus pneumoniae*. Infect Immun. 1995;63: 757–761.
60. Weiser JN, Bae D, Epino H, Gordon SB, Kapoor M, Zenewicz LA, et al. Changes in availability of oxygen accentuate differences in capsular polysaccharide expression by phenotypic variants and clinical isolates of *Streptococcus pneumoniae*. Infect Immun. 2001;69: 5430–5439.
61. Hammerschmidt S, Wolff S, Hocke A, Rosseau S, Müller E, Rohde M. Illustration of pneumococcal polysaccharide capsule during adherence and invasion of epithelial cells. Infect Immun. 2005;73: 4653–4667. doi:10.1128/IAI.73.8.4653-4667.2005
62. Voß S, Gámez G, Hammerschmidt S. Impact of pneumococcal microbial surface components recognizing adhesive matrix molecules on colonization: Impact of pneumococcal MSCRAMMs on colonization. Mol Oral Microbiol. 2012;27: 246–256. doi:10.1111/j.2041-1014.2012.00654.x
63. Kim JO, Romero-Steiner S, Sørensen UB, Blom J, Carvalho M, Barnard S, et al. Relationship between cell surface carbohydrates and intrastrain variation on opsonophagocytosis of *Streptococcus pneumoniae*. Infect Immun. 1999;67: 2327–2333.
64. Austrian R. Some observations on the pneumococcus and on the current status of pneumococcal disease and its prevention. Rev Infect Dis. 1981;3 Suppl: S1–17.
65. Musher DM. Infections caused by *Streptococcus pneumoniae*: clinical spectrum, pathogenesis, immunity, and treatment. Clin Infect Dis Off Publ Infect Dis Soc Am. 1992;14: 801–807.
66. Winkelstein JA. The role of complement in the host's defense against *Streptococcus pneumoniae*. Rev Infect Dis. 1981;3: 289–298.

67. Van der Poll T, Opal SM. Pathogenesis, treatment, and prevention of pneumococcal pneumonia. Lancet. 2009;374: 1543–1556. doi:10.1016/S0140-6736(09)61114-4
68. Fernebro J, Andersson I, Sublett J, Morfeldt E, Novak R, Tuomanen E, et al. Capsular expression in *Streptococcus pneumoniae* negatively affects spontaneous and antibiotic-induced lysis and contributes to antibiotic tolerance. J Infect Dis. 2004;189: 328–338. doi:10.1086/380564
69. Weiser JN, Kapoor M. Effect of intrastrain variation in the amount of capsular polysaccharide on genetic transformation of *Streptococcus pneumoniae*: implications for virulence studies of encapsulated strains. Infect Immun. 1999;67: 3690–3692.
70. Iannelli F, Pearce BJ, Pozzi G. The type 2 capsule locus of *Streptococcus pneumoniae*. J Bacteriol. 1999;181: 2652–2654.
71. Shainheit MG, Mule M, Camilli A, Pirofski L. The core promoter of the capsule operon of *Streptococcus pneumoniae* is necessary for colonization and invasive disease. Infect Immun. 2014;82: 694–705. doi:10.1128/IAI.01289-13
72. MacLEOD CM, Kraus MR. Relation of virulence of pneumococcal strains for mice to the quantity of capsular polysaccharide formed in vitro. J Exp Med. 1950;92: 1–9.
73. Bergmann S. Versatility of pneumococcal surface proteins. Microbiology. 2006;152: 295–303. doi:10.1099/mic.0.28610-0
74. Hammerschmidt S. Adherence molecules of pathogenic pneumococci. Curr Opin Microbiol. 2006;9: 12–20. doi:10.1016/j.mib.2005.11.001
75. King SJ. Pneumococcal modification of host sugars: a major contributor to colonization of the human airway? Mol Oral Microbiol. 2010;25: 15–24. doi:10.1111/j.2041-1014.2009.00564.x
76. Dalia AB, Standish AJ, Weiser JN. Three surface exoglycosidases from *Streptococcus pneumoniae*, NanA, BgaA, and StrH, promote resistance to opsonophagocytic killing by human neutrophils. Infect Immun. 2010;78: 2108–2116. doi:10.1128/IAI.01125-09
77. King SJ, Hippe KR, Weiser JN. Deglycosylation of human glycoconjugates by the sequential activities of exoglycosidases expressed by *Streptococcus pneumoniae*. Mol Microbiol. 2006;59: 961–974. doi:10.1111/j.1365-2958.2005.04984.x
78. Limoli DH, Sladek JA, Fuller LA, Singh AK, King SJ. BgaA acts as an adhesin to mediate attachment of some pneumococcal strains to human epithelial cells. Microbiology. 2011;157: 2369–2381. doi:10.1099/mic.0.045609-0
79. Kostyukova NN, Volkova MO, Ivanova VV, Kvetnaya AS. A study of pathogenic factors of *Streptococcus pneumoniae* strains causing meningitis. FEMS Immunol Med Microbiol. 1995;10: 133–137.
80. Zwijnenburg PJ, van der Poll T, Florquin S, van Deventer SJ, Roord JJ, van Furth AM. Experimental pneumococcal meningitis in mice: a model of intranasal infection. J Infect Dis. 2001;183: 1143–1146. doi:10.1086/319271
81. Bethe G, Nau R, Wellmer A, Hakenbeck R, Reinert RR, Heinz HP, et al. The cell wall-associated serine protease PrtA: a highly conserved virulence factor of *Streptococcus pneumoniae*. FEMS Microbiol Lett. 2001;205: 99–104.
82. Mitchell AM, Mitchell TJ. *Streptococcus pneumoniae*: virulence factors and variation. Clin Microbiol Infect. 2010;16: 411–418. doi:10.1111/j.1469-0691.2010.03183.x
83. Berry AM, Paton JC. Sequence heterogeneity of PsaA, a 37-kilodalton putative adhesin essential for virulence of *Streptococcus pneumoniae*. Infect Immun. 1996;64: 5255–5262.

84. Nieto PA, Riquelme SA, Riedel CA, Kalergis AM, Bueno SM. Gene elements that regulate *Streptococcus pneumoniae* virulence and immunity evasion. Curr Gene Ther. 2013;13: 51–64.
85. Gosink KK, Mann ER, Guglielmo C, Tuomanen EI, Masure HR. Role of novel choline binding proteins in virulence of *Streptococcus pneumoniae*. Infect Immun. 2000;68: 5690–5695. doi:10.1128/IAI.68.10.5690-5695.2000
86. Holmes AR, McNab R, Millsap KW, Rohde M, Hammerschmidt S, Mawdsley JL, et al. The *pavA* gene of *Streptococcus pneumoniae* encodes a fibronectin-binding protein that is essential for virulence. Mol Microbiol. 2001;41: 1395–1408.
87. Pracht D, Elm C, Gerber J, Bergmann S, Rohde M, Seiler M, et al. PavA of *Streptococcus pneumoniae* modulates adherence, invasion, and meningeal inflammation. Infect Immun. 2005;73: 2680–2689. doi:10.1128/IAI.73.5.2680-2689.2005
88. Eberhard T, Kronvall G, Ullberg M. Surface bound plasmin promotes migration of *Streptococcus pneumoniae* through reconstituted basement membranes. Microb Pathog. 1999;26: 175–181. doi:10.1006/mpat.1998.0262
89. Bergmann S, Rohde M, Chhatwal GS, Hammerschmidt S. alpha-enolase of *Streptococcus pneumoniae* is a plasmin(ogen)-binding protein displayed on the bacterial cell surface. Mol Microbiol. 2001;40: 1273–1287.
90. Bergmann S, Rohde M, Hammerschmidt S. Glyceraldehyde-3-phosphate dehydrogenase of *Streptococcus pneumoniae* is a surface-displayed plasminogen-binding protein. Infect Immun. 2004;72: 2416–2419. doi:10.1128/IAI.72.4.2416-2419.2004
91. Bergmann S, Schoenen H, Hammerschmidt S. The interaction between bacterial enolase and plasminogen promotes adherence of Streptococcus pneumoniae to epithelial and endothelial cells. Int J Med Microbiol. 2013;303: 452–462. doi:10.1016/j.ijmm.2013.06.002
92. Balachandran P, Hollingshead SK, Paton JC, Briles DE. The autolytic enzyme LytA of *Streptococcus pneumoniae* is not responsible for releasing pneumolysin. J Bacteriol. 2001;183: 3108–3116. doi:10.1128/JB.183.10.3108-3116.2001
93. Yuste J, Botto M, Paton JC, Holden DW, Brown JS. Additive inhibition of complement deposition by pneumolysin and PspA facilitates *Streptococcus pneumoniae* septicemia. J Immunol Baltim Md 1950. 2005;175: 1813–1819.
94. Feldman C, Mitchell TJ, Andrew PW, Boulnois GJ, Read RC, Todd HC, et al. The effect of *Streptococcus pneumoniae* pneumolysin on human respiratory epithelium in vitro. Microb Pathog. 1990;9: 275–284.
95. Dawid S, Roche AM, Weiser JN. The blp bacteriocins of *Streptococcus pneumoniae* mediate intraspecies competition both in vitro and in vivo. Infect Immun. 2007;75: 443–451. doi:10.1128/IAI.01775-05
96. Pericone CD, Overweg K, Hermans PW, Weiser JN. Inhibitory and bactericidal effects of hydrogen peroxide production by *Streptococcus pneumoniae* on other inhabitants of the upper respiratory tract. Infect Immun. 2000;68: 3990–3997.
97. Regev-Yochay G, Trzcinski K, Thompson CM, Malley R, Lipsitch M. Interference between *Streptococcus pneumoniae* and *Staphylococcus aureus*: In vitro hydrogen peroxide-mediated killing by *Streptococcus pneumoniae*. J Bacteriol. 2006;188: 4996–5001. doi:10.1128/JB.00317-06

98. Hoffmann O, Zweigner J, Smith SH, Freyer D, Mahrhofer C, Dagand E, et al. Interplay of pneumococcal hydrogen peroxide and host-derived nitric oxide. Infect Immun. 2006;74: 5058–5066. doi:10.1128/IAI.01932-05
99. Carvalho SM, Farshchi Andisi V, Gradstedt H, Neef J, Kuipers OP, Neves AR, et al. Pyruvate oxidase influences the sugar utilization pattern and capsule production in *Streptococcus pneumoniae*. Chi J-TA, editor. PLoS ONE. 2013;8: e68277. doi:10.1371/journal.pone.0068277
100. Lau GW, Haataja S, Lonetto M, Kensit SE, Marra A, Bryant AP, et al. A functional genomic analysis of type 3 *Streptococcus pneumoniae* virulence. Mol Microbiol. 2001;40: 555–571.
101. Polissi A, Pontiggia A, Feger G, Altieri M, Mottl H, Ferrari L, et al. Large-scale identification of virulence genes from *Streptococcus pneumoniae*. Infect Immun. 1998;66: 5620–5629.
102. Hava DL, Camilli A. Large-scale identification of serotype 4 *Streptococcus pneumoniae* virulence factors. Mol Microbiol. 2002;45: 1389–1406.
103. Ogunniyi AD, Mahdi LK, Trappetti C, Verhoeven N, Mermans D, Van der Hoek MB, et al. Identification of genes that contribute to the pathogenesis of invasive pneumococcal disease by *in vivo* transcriptomic analysis. Infect Immun. 2012;80: 3268–3278. doi:10.1128/IAI.00295-12
104. LeMessurier KS. Differential expression of key pneumococcal virulence genes in vivo. Microbiology. 2006;152: 305–311. doi:10.1099/mic.0.28438-0
105. Orihuela CJ, Radin JN, Sublett JE, Gao G, Kaushal D, Tuomanen EI. Microarray analysis of pneumococcal gene expression during invasive disease. Infect Immun. 2004;72: 5582–5596. doi:10.1128/IAI.72.10.5582-5596.2004
106. Song X-M, Connor W, Hokamp K, Babiuk LA, Potter AA. *Streptococcus pneumoniae* early response genes to human lung epithelial cells. BMC Res Notes. 2008;1: 64. doi:10.1186/1756-0500-1-64
107. Van Opijnen T, Camilli A. A fine scale phenotype-genotype virulence map of a bacterial pathogen. Genome Res. 2012;22: 2541–2551. doi:10.1101/gr.137430.112
108. Marion C, Aten AE, Woodiga SA, King SJ. Identification of an ATPase, MsmK, which energizes multiple carbohydrate ABC transporters in *Streptococcus pneumoniae*. Infect Immun. 2011;79: 4193–4200. doi:10.1128/IAI.05290-11
109. Marion C, Burnaugh AM, Woodiga SA, King SJ. Sialic acid transport contributes to pneumococcal colonization. Infect Immun. 2011;79: 1262–1269. doi:10.1128/IAI.00832-10
110. Marion C, Stewart JM, Tazi MF, Burnaugh AM, Linke CM, Woodiga SA, et al. *Streptococcus pneumoniae* can utilize multiple sources of hyaluronic acid for growth. Infect Immun. 2012;80: 1390–1398. doi:10.1128/IAI.05756-11
111. Iyer R, Camilli A. Sucrose metabolism contributes to *in vivo* fitness of *Streptococcus pneumoniae*. Mol Microbiol. 2007;66: 1–13. doi:10.1111/j.1365-2958.2007.05878.x
112. Tong HH, Blue LE, James MA, DeMaria TF. Evaluation of the virulence of a *Streptococcus pneumoniae* neuraminidase-deficient mutant in nasopharyngeal colonization and development of otitis media in the chinchilla model. Infect Immun. 2000;68: 921–924.
113. Manco S, Hernon F, Yesilkaya H, Paton JC, Andrew PW, Kadioglu A. Pneumococcal neuraminidases A and B both have essential roles during infection of the respiratory tract and sepsis. Infect Immun. 2006;74: 4014–4020. doi:10.1128/IAI.01237-05

114. Marion C, Limoli DH, Bobulsky GS, Abraham JL, Burnaugh AM, King SJ. Identification of a pneumococcal glycosidase that modifies O-linked glycans. Infect Immun. 2009;77: 1389–1396. doi:10.1128/IAI.01215-08
115. Jeong JK, Kwon O, Lee YM, Oh D-B, Lee JM, Kim S, et al. Characterization of the Streptococcus pneumoniae BgaC protein as a novel surface β-galactosidase with specific hydrolysis activity for the Galβ1-3GlcNAc moiety of oligosaccharides. J Bacteriol. 2009;191: 3011–3023. doi:10.1128/JB.01601-08
116. Terra VS, Homer KA, Rao SG, Andrew PW, Yesilkaya H. Characterization of novel β-galactosidase activity that contributes to glycoprotein degradation and virulence in *Streptococcus pneumoniae.* Infect Immun. 2010;78: 348–357. doi:10.1128/IAI.00721-09
117. Brittan JL, Buckeridge TJ, Finn A, Kadioglu A, Jenkinson HF. Pneumococcal neuraminidase A: an essential upper airway colonization factor for *Streptococcus pneumoniae*: *Streptococcus pneumoniae* neuraminidase. Mol Oral Microbiol. 2012;27: 270–283. doi:10.1111/j.2041-1014.2012.00658.x
118. Yesilkaya H, Spissu F, Carvalho SM, Terra VS, Homer KA, Benisty R, et al. Pyruvate formate lyase is required for pneumococcal fermentative metabolism and virulence. Infect Immun. 2009;77: 5418–5427. doi:10.1128/IAI.00178-09
119. Gaspar P, Al-Bayati FAY, Andrew PW, Neves AR, Yesilkaya H. Lactate dehydrogenase is the key enzyme for pneumococcal pyruvate metabolism and pneumococcal survival in blood. Infect Immun. 2014;82: 5099–5109. doi:10.1128/IAI.02005-14
120. Spellerberg B, Cundell DR, Sandros J, Pearce BJ, Idanpaan-Heikkila I, Rosenow C, et al. Pyruvate oxidase, as a determinant of virulence in *Streptococcus pneumoniae*. Mol Microbiol. 1996;19: 803–813.
121. Hakansson AP. Pneumococcal adaptive responses to changing host environments. J Infect Dis. 2014;210: 1–3. doi:10.1093/infdis/jiu084
122. Deutscher J, Francke C, Postma PW. How phosphotransferase system-related protein phosphorylation regulates carbohydrate metabolism in bacteria. Microbiol Mol Biol Rev. 2006;70: 939–1031. doi:10.1128/MMBR.00024-06
123. Giammarinaro P, Paton JC. Role of RegM, a homologue of the catabolite repressor protein CcpA, in the virulence of *Streptococcus pneumoniae*. Infect Immun. 2002;70: 5454–5461.
124. Iyer R, Baliga NS, Camilli A. Catabolite Control Protein A (CcpA) Contributes to virulence and regulation of sugar metabolism in *Streptococcus pneumoniae*. J Bacteriol. 2005;187: 8340–8349. doi:10.1128/JB.187.24.8340-8349.2005
125. Carvalho SM, Kloosterman TG, Kuipers OP, Neves AR. CcpA ensures optimal metabolic fitness of *Streptococcus pneumoniae*. Horsburgh MJ, editor. PLoS ONE. 2011;6: e26707. doi:10.1371/journal.pone.0026707
126. Sharon N. Nomenclature of glycoproteins, glycopeptides and peptidoglycans (Recommendations 1985). Pure Appl Chem. 1988;60. doi:10.1351/pac198860091389
127. Sasaki N, Toyoda M. Glycoconjugates and related molecules in human vascular endothelial cells. Int J Vasc Med. 2013;2013: 1–10. doi:10.1155/2013/963596
128. Tytgat HLP, Lebeer S. The sweet tooth of bacteria: common themes in bacterial glycoconjugates. Microbiol Mol Biol Rev. 2014;78: 372–417. doi:10.1128/MMBR.00007-14

129. Rose MC, Voynow JA. Respiratory tract mucin genes and mucin glycoproteins in health and disease. Physiol Rev. 2006;86: 245–278. doi:10.1152/physrev.00010.2005
130. Thornton DJ. From mucins to mucus: toward a more coherent understanding of this essential barrier. Proc Am Thorac Soc. 2004;1: 54–61. doi:10.1513/pats.2306016
131. Derrien M, van Passel MW, van de Bovenkamp JH, Schipper RG, de Vos WM, Dekker J. Mucin-bacterial interactions in the human oral cavity and digestive tract. Gut Microbes. 2010;1: 254–268. doi:10.4161/gmic.1.4.12778
132. Linden SK, Sutton P, Karlsson NG, Korolik V, McGuckin MA. Mucins in the mucosal barrier to infection. Mucosal Immunol. 2008;1: 183–197. doi:10.1038/mi.2008.5
133. Mack DR, Michail S, Wei S, McDougall L, Hollingsworth MA. Probiotics inhibit enteropathogenic *E. coli* adherence *in vitro* by inducing intestinal mucin gene expression. Am J Physiol. 1999;276: G941–950.
134. Slomiany BL, Slomiany A. Cytosolic phospholipase A2 activation in *Helicobacter pylori* lipopolysaccharide-induced interference with gastric mucin synthesis. IUBMB Life. 2006;58: 217–223. doi:10.1080/15216540600732021
135. Bry L, Falk PG, Midtvedt T, Gordon JI. A model of host-microbial interactions in an open mammalian ecosystem. Science. 1996;273: 1380–1383.
136. Lindén SK, Wickström C, Lindell G, Gilshenan K, Carlstedt I. Four modes of adhesion are used during *Helicobacter pylori* binding to human mucins in the oral and gastric niches. Helicobacter. 2008;13: 81–93. doi:10.1111/j.1523-5378.2008.00587.x
137. Corfield AP, Wagner SA, Clamp JR, Kriaris MS, Hoskins LC. Mucin degradation in the human colon: production of sialidase, sialate O-acetylesterase, N-acetylneuraminate lyase, arylesterase, and glycosulfatase activities by strains of fecal bacteria. Infect Immun. 1992;60: 3971–3978.
138. Homer KA, Whiley RA, Beighton D. Production of specific glycosidase activities by *Streptococcus intermedius* strain UNS35 grown in the presence of mucin. J Med Microbiol. 1994;41: 184–190.
139. Hoskins J, Alborn WE, Arnold J, Blaszczak LC, Burgett S, DeHoff BS, et al. Genome of the bacterium *Streptococcus pneumoniae* strain R6. J Bacteriol. 2001;183: 5709–5717. doi:10.1128/JB.183.19.5709-5717.2001
140. Tettelin H, Nelson KE, Paulsen IT, Eisen JA, Read TD, Peterson S, et al. Complete genome sequence of a virulent isolate of *Streptococcus pneumoniae*. Science. 2001;293: 498–506. doi:10.1126/science.1061217
141. Bidossi A, Mulas L, Decorosi F, Colomba L, Ricci S, Pozzi G, et al. A functional genomics approach to establish the complement of carbohydrate transporters in *Streptococcus pneumoniae*. Miyaji EN, editor. PLoS ONE. 2012;7: e33320. doi:10.1371/journal.pone.0033320
142. Rohmer L, Hocquet D, Miller SI. Are pathogenic bacteria just looking for food? Metabolism and microbial pathogenesis. Trends Microbiol. 2011;19: 341–348. doi:10.1016/j.tim.2011.04.003
143. Buckwalter CM, King SJ. Pneumococcal carbohydrate transport: food for thought. Trends Microbiol. 2012;20: 517–522. doi:10.1016/j.tim.2012.08.008
144. Price CE, Zeyniyev A, Kuipers OP, Kok J. From meadows to milk to mucosa - adaptation of *Streptococcus* and *Lactococcus* species to their nutritional environments. FEMS Microbiol Rev. 2012; 36(5):949-71. doi:10.1111/j.1574-6976.2011.00323.x

145. Shelburne SA, Davenport MT, Keith DB, Musser JM. The role of complex carbohydrate catabolism in the pathogenesis of invasive streptococci. Trends Microbiol. 2008;16: 318–325. doi:10.1016/j.tim.2008.04.002
146. Philips BJ, Meguer J-X, Redman J, Baker EH. Factors determining the appearance of glucose in upper and lower respiratory tract secretions. Intensive Care Med. 2003;29: 2204–2210. doi:10.1007/s00134-003-1961-2
147. Yesilkaya H, Manco S, Kadioglu A, Terra VS, Andrew PW. The ability to utilize mucin affects the regulation of virulence gene expression in *Streptococcus pneumoniae*. FEMS Microbiol Lett. 2008;278: 231–235. doi:10.1111/j.1574-6968.2007.01003.x
148. Burnaugh AM, Frantz LJ, King SJ. Growth of *Streptococcus pneumoniae* on human glycoconjugates is dependent upon the sequential activity of bacterial exoglycosidases. J Bacteriol. 2008;190: 221–230. doi:10.1128/JB.01251-07
149. Konings WN, Poolman B, van Veen HW. Solute transport and energy transduction in bacteria. Antonie Van Leeuwenhoek. 1994;65: 369–380.
150. Davidson AL, Dassa E, Orelle C, Chen J. Structure, function, and evolution of bacterial ATP-binding cassette systems. Microbiol Mol Biol Rev. 2008;72: 317–364. doi:10.1128/MMBR.00031-07
151. Higgins CF. ABC transporters: physiology, structure and mechanism – an overview. Res Microbiol. 2001;152: 205–210.
152.Postma PW, Lengeler JW. Phosphoenolpyruvate:carbohydrate phosphotransferase system of bacteria. Microbiol Rev. 1985;49: 232–269.
153. Lorca GL, Barabote RD, Zlotopolski V, Tran C, Winnen B, Hvorup RN, et al. Transport capabilities of eleven gram-positive bacteria: Comparative genomic analyses. Biochim Biophys Acta BBA - Biomembr. 2007;1768: 1342–1366. doi:10.1016/j.bbamem.2007.02.007
154. Postma PW, Lengeler JW, Jacobson GR. Phosphoenolpyruvate:carbohydrate phosphotransferase systems of bacteria. Microbiol Rev. 1993;57: 543–594.
155. Zähner D, Hakenbeck R. The *Streptococcus pneumoniae* beta-galactosidase is a surface protein. J Bacteriol. 2000;182: 5919–5921.
156. Cai J, Tong H, Qi F, Dong X. CcpA-dependent carbohydrate catabolite repression regulates galactose metabolism in *Streptococcus oligofermentans*. J Bacteriol. 2012;194: 3824–3832. doi:10.1128/JB.00156-12
157. Zeng L, Xue P, Stanhope MJ, Burne RA. A galactose-specific sugar: phosphotransferase permease is prevalent in the non-core genome of *Streptococcus mutans*. Mol Oral Microbiol. 2013;28: 292–301. doi:10.1111/omi.12025
158. Grossiord BP, Luesink EJ, Vaughan EE, Arnaud A, de Vos WM. Characterization, expression, and mutation of the *Lactococcus lactis galPMKTE* genes, involved in galactose utilization via the Leloir pathway. J Bacteriol. 2003;185: 870–878. doi:10.1128/JB.185.3.870-878.2003
159. Thomas TD, Turner KW, Crow VL. Galactose fermentation by Streptococcus lactis and *Streptococcus cremoris*: pathways, products, and regulation. J Bacteriol. 1980;144: 672–682.
160. Thompson J. Galactose transport systems in *Streptococcus lactis*. J Bacteriol. 1980;144: 683–691.
161. De Vos WM, Vaughan EE. Genetics of lactose utilization in lactic acid bacteria. FEMS Microbiol Rev. 1994;15: 217–237.

162. LeBlanc DJ, Crow VL, Lee LN, Garon CF. Influence of the lactose plasmid on the metabolism of galactose by *Streptococcus lactis*. J Bacteriol. 1979;137: 878–884.
163. Zeng L, Das S, Burne RA. Utilization of lactose and galactose by *Streptococcus mutans*: transport, toxicity, and carbon catabolite repression. J Bacteriol. 2010;192: 2434–2444. doi:10.1128/JB.01624-09
164. Abranches J, Chen Y-YM, Burne RA. Galactose metabolism by *Streptococcus mutans*. Appl Env Microbiol. 2004;70: 6047–6052. doi:10.1128/AEM.70.10.6047-6052.2004
165. Neves AR, Pool WA, Solopova A, Kok J, Santos H, Kuipers OP. Towards enhanced galactose utilization by *Lactococcus lactis*. Appl Env Microbiol. 2010;76: 7048–7060. doi:10.1128/AEM.01195-10
166. Zeng L, Martino NC, Burne RA. Two gene clusters coordinate galactose and lactose metabolism in *Streptococcus gordonii*. Appl Env Microbiol. 2012;78: 5597–5605. doi:10.1128/AEM.01393-12
167. Kaufman GE, Yother J. CcpA-dependent and -independent control of beta-galactosidase expression in *Streptococcus pneumoniae* occurs via regulation of an upstream phosphotransferase system-encoding operon. J Bacteriol. 2007;189: 5183–5192. doi:10.1128/JB.00449-07
168. Chen Y-YM, Betzenhauser MJ, Snyder JA, Burne RA. Pathways for lactose/galactose catabolism by *Streptococcus salivarius*. FEMS Microbiol Lett. 2002;209: 75–79.
169. Vaillancourt K, LeMay J-D, Lamoureux M, Frenette M, Moineau S, Vadeboncoeur C. Characterization of a galactokinase-positive recombinant strain of *Streptococcus thermophilus*. Appl Environ Microbiol. 2004;70: 4596–4603. doi:10.1128/AEM.70.8.4596-4603.2004
170. Afzal M, Shafeeq S, Kuipers OP. LacR is a repressor of *lacABCD* and LacT an activator of *lacTFEG*, constituting the lac-gene cluster in *Streptococcus pneumoniae*. Appl Environ Microbiol. 2014; doi:10.1128/AEM.01370-14
171. Grossiord B, Vaughan EE, Luesink E, de Vos WM. Genetics of galactose utilisation via the Leloir pathway in lactic acid bacteria. Le Lait. 1998;78: 77–84. doi:10.1051/lait:1998110
172. Sharma V, Ichikawa M, Freeze HH. Mannose metabolism: More than meets the eye. Biochem Biophys Res Commun. 2014; doi:10.1016/j.bbrc.2014.06.021
173. Homer KA, Roberts G, Byers HL, Tarelli E, Whiley RA, Philpott-Howard J, et al. Mannosidase production by viridans group Streptococci. J Clin Microbiol. 2001;39: 995–1001. doi:10.1128/JCM.39.3.995-1001.2001
174. Sasaki M, Teramoto H, Inui M, Yukawa H. Identification of mannose uptake and catabolism genes in *Corynebacterium glutamicum* and genetic engineering for simultaneous utilization of mannose and glucose. Appl Microbiol Biotechnol. 2011;89: 1905–1916. doi:10.1007/s00253-010-3002-8
175. Darzins A, Nixon LL, Vanags RI, Chakrabarty AM. Cloning of *Escherichia coli* and *Pseudomonas aeruginosa* phosphomannose isomerase genes and their expression in alginate-negative mutants of *Pseudomonas aeruginosa*. J Bacteriol. 1985;161: 249–257.
176. Stolz B, Huber M, Marković-Housley Z, Erni B. The mannose transporter of Escherichia coli. Structure and function of the IIABMan subunit. J Biol Chem. 1993;268: 27094–27099.

177. Martin-Verstraete I, Michel V, Charbit A. The levanase operon of *Bacillus subtilis* expressed in *Escherichia coli* can substitute for the mannose permease in mannose uptake and bacteriophage lambda infection. J Bacteriol. 1996;178: 7112–7119.
178. Kornberg HL, Lambourne LTM. Role of the phosphoenolpyruvate-dependent fructose phosphotransferase system in the utilization of mannose by *Escherichia coli*. Proc Biol Sci. 1992;250: 51–55.
179. Pelletier G, Frenette M, Vadeboncoeur C. Transport of mannose by an inducible phosphoenolpyruvate:fructose phosphotransferase system in *Streptococcus salivarius*. Microbiol Read Engl. 1994;140 (Pt 9): 2433–2438.
180. Sun T, Altenbuchner J. Characterization of a mannose utilization system in *Bacillus subtilis*. J Bacteriol. 2010;192: 2128–2139. doi:10.1128/JB.01673-09
181. Köplin R, Arnold W, Hötte B, Simon R, Wang G, Pühler A. Genetics of xanthan production in *Xanthomonas campestris*: the *xanA* and *xanB* genes are involved in UDP-glucose and GDP-mannose biosynthesis. J Bacteriol. 1992;174: 191–199.
182. Schmidt M, Arnold W, Niemann A, Kleickmann A, Pühler A. The *Rhizobium meliloti pmi* gene encodes a new type of phosphomannose isomerase. Gene. 1992;122: 35–43. doi:10.1016/0378-1119(92)90029-O
183. Arias A, Gardiol A, Martínez-Drets G. Transport and catabolism of D-mannose in *Rhizobium meliloti*. J Bacteriol. 1982;151: 1069–1072.
184. Rodionov DA, Yang C, Li X, Rodionova IA, Wang Y, Obraztsova AY, et al. Genomic encyclopedia of sugar utilization pathways in the Shewanella genus. BMC Genomics. 2010;11: 494. doi:10.1186/1471-2164-11-494
185. Berry AM, Lock RA, Paton JC. Cloning and characterization of *nanB*, a second *Streptococcus pneumoniae* neuraminidase gene, and purification of the NanB enzyme from recombinant *Escherichia coli*. J Bacteriol. 1996;178: 4854–4860.
186. Cámara M, Boulnois GJ, Andrew PW, Mitchell TJ. A neuraminidase from *Streptococcus pneumoniae* has the features of a surface protein. Infect Immun. 1994;62: 3688–3695.
187. Clarke VA, Platt N, Butters TD. Cloning and expression of the beta-N-acetylglucosaminidase gene from *Streptococcus pneumoniae*. Generation of truncated enzymes with modified aglycon specificity. J Biol Chem. 1995;270: 8805–8814.
188. Severi E, Hood DW, Thomas GH. Sialic acid utilization by bacterial pathogens. Microbiology. 2007;153: 2817–2822. doi:10.1099/mic.0.2007/009480-0
189. Pezzicoli A, Ruggiero P, Amerighi F, Telford JL, Soriani M. Exogenous sialic acid transport contributes to group B streptococcus infection of mucosal surfaces. J Infect Dis. 2012;206: 924–931. doi:10.1093/infdis/jis451
190. Konopka JB. N-acetylglucosamine (GlcNAc) functions in cell signaling. Scientifica. 2012. doi:10.6064/2012/489208
191. Moye ZD, Burne RA, Zeng L. Uptake and metabolism of N-acetylglucosamine and glucosamine by *Streptococcus mutans*. Appl Env Microbiol. 2014; doi:10.1128/AEM.00820-14
192. Boulanger A, Dejean G, Lautier M, Glories M, Zischek C, Arlat M, et al. Identification and regulation of the N-acetylglucosamine utilization pathway of the plant pathogenic bacterium *Xanthomonas campestris* pv. *campestris*. J Bacteriol. 2010;192: 1487–1497. doi:10.1128/JB.01418-09

193. Takahashi Y, Ruhl S, Yoon J-W, Sandberg AL, Cisar JO. Adhesion of viridans group streptococci to sialic acid-, galactose- and N-acetylgalactosamine-containing receptors. Oral Microbiol Immunol. 2002;17: 257–262.
194. Bidart GN, Rodríguez-Díaz J, Monedero V, Yebra MJ. A unique gene cluster for the utilization of the mucosal and human milk-associated glycans galacto- *N* -biose and lacto- *N* -biose in *L actobacillus casei*: Galacto- and lacto- *N* -biose utilization in *Lactobacillus*. Mol Microbiol. 2014;93: 521–538. doi:10.1111/mmi.12678
195. Trappetti C, Kadioglu A, Carter M, Hayre J, Iannelli F, Pozzi G, et al. Sialic acid: a preventable signal for pneumococcal biofilm formation, colonization, and invasion of the host. J Infect Dis. 2009;199: 1497–1505. doi:10.1086/598483
196. Parker D, Soong G, Planet P, Brower J, Ratner AJ, Prince A. The NanA neuraminidase of *Streptococcus pneumoniae* is involved in biofilm formation. Infect Immun. 2009;77: 3722–3730. doi:10.1128/IAI.00228-09
197. Chang D-E, Smalley DJ, Tucker DL, Leatham MP, Norris WE, Stevenson SJ, et al. Carbon nutrition of *Escherichia coli* in the mouse intestine. Proc Natl Acad Sci U S A. 2004;101: 7427–7432. doi:10.1073/pnas.0307888101
198. Rigali S, Nothaft H, Noens EEE, Schlicht M, Colson S, Müller M, et al. The sugar phosphotransferase system of *Streptomyces coelicolor* is regulated by the GntR-family regulator DasR and links N-acetylglucosamine metabolism to the control of development. Mol Microbiol. 2006;61: 1237–1251. doi:10.1111/j.1365-2958.2006.05319.x
199. Rigali S, Titgemeyer F, Barends S, Mulder S, Thomae AW, Hopwood DA, et al. Feast or famine: the global regulator DasR links nutrient stress to antibiotic production by *Streptomyces*. EMBO Rep. 2008;9: 670–675. doi:10.1038/embor.2008.83
200. Swiatek MA, Tenconi E, Rigali S, van Wezel GP. Functional analysis of the N-acetylglucosamine metabolic genes of *Streptomyces coelicolor* and role in control of development and antibiotic production. J Bacteriol. 2012;194: 1136–1144. doi:10.1128/JB.06370-11
201. Barthelson R, Mobasseri A, Zopf D, Simon P. Adherence of *Streptococcus pneumoniae* to respiratory epithelial cells is inhibited by sialylated oligosaccharides. Infect Immun. 1998;66: 1439–1444.
202. Andersson B, Beachey EH, Tomasz A, Tuomanen E, Svanborg-Edén C. A sandwich adhesion on *Streptococcus pneumoniae* attaching to human oropharyngeal epithelial cells in vitro. Microb Pathog. 1988;4: 267–278.
203. Cundell DR, Tuomanen EI. Receptor specificity of adherence of *Streptococcus pneumoniae* to human type-II pneumocytes and vascular endothelial cells in vitro. Microb Pathog. 1994;17: 361–374. doi:10.1006/mpat.1994.1082
204. Krivan HC, Roberts DD, Ginsburg V. Many pulmonary pathogenic bacteria bind specifically to the carbohydrate sequence GalNAc beta 1-4Gal found in some glycolipids. Proc Natl Acad Sci U S A. 1988;85: 6157–6161.
205. Almagro-Moreno S, Boyd EF. Insights into the evolution of sialic acid catabolism among bacteria. BMC Evol Biol. 2009;9: 118. doi:10.1186/1471-2148-9-118
206. Vimr ER, Kalivoda KA, Deszo EL, Steenbergen SM. Diversity of microbial sialic acid metabolism. Microbiol Mol Biol Rev. 2004;68: 132–153. doi:10.1128/MMBR.68.1.132-153.2004
207. King SJ, Hippe KR, Gould JM, Bae D, Peterson S, Cline RT, et al. Phase variable desialylation of host proteins that bind to *Streptococcus pneumoniae* in vivo and

protect the airway: Pneumococcal desialylation of host proteins. Mol Microbiol. 2004;54: 159–171. doi:10.1111/j.1365-2958.2004.04252.x

208. Gualdi L, Hayre J, Gerlini A, Bidossi A, Colomba L, Trappetti C, et al. Regulation of neuraminidase expression in *Streptococcus pneumoniae*. BMC Microbiol. 2012;12: 200. doi:10.1186/1471-2180-12-200
209. Pettigrew MM, Fennie KP, York MP, Daniels J, Ghaffar F. Variation in the presence of neuraminidase genes among *Streptococcus pneumoniae* isolates with identical sequence types. Infect Immun. 2006;74: 3360–3365. doi:10.1128/IAI.01442-05
210. Vimr ER, Troy FA. Identification of an inducible catabolic system for sialic acids (nan) in Escherichia coli. J Bacteriol. 1985;164: 845–853.
211. Steenbergen SM, Lichtensteiger CA, Caughlan R, Garfinkle J, Fuller TE, Vimr ER. Sialic acid metabolism and systemic pasteurellosis. Infect Immun. 2005;73: 1284–1294. doi:10.1128/IAI.73.3.1284-1294.2005
212. Allen S, Zaleski A, Johnston JW, Gibson BW, Apicella MA. Novel sialic acid transporter of *Haemophilus influenzae*. Infect Immun. 2005;73: 5291–5300. doi:10.1128/IAI.73.9.5291-5300.2005
213. Severi E, Randle G, Kivlin P, Whitfield K, Young R, Moxon R, et al. Sialic acid transport in *Haemophilus influenzae* is essential for lipopolysaccharide sialylation and serum resistance and is dependent on a novel tripartite ATP-independent periplasmic transporter. Mol Microbiol. 2005;58: 1173–1185. doi:10.1111/j.1365-2958.2005.04901.x
214. Post DMB, Mungur R, Gibson BW, Munson RS. Identification of a novel sialic acid transporter in *Haemophilus ducreyi*. Infect Immun. 2005;73: 6727–6735. doi:10.1128/IAI.73.10.6727-6735.2005
215. Severi E, Hosie AHF, Hawkhead JA, Thomas GH. Characterization of a novel sialic acid transporter of the sodium solute symporter (SSS) family and in vivo comparison with known bacterial sialic acid transporters: An SSS transporter for sialic acid from *Salmonella*. FEMS Microbiol Lett. 2010;304: 47–54. doi:10.1111/j.1574-6968.2009.01881.x
216. Byers HL, Homer KA, Beighton D. Utilization of sialic acid by viridans streptococci. J Dent Res. 1996;75: 1564–1571. doi:10.1177/00220345960750080701
217. Brigham CJ, Malamy MH. Characterization of the RokA and HexA broad-substrate-specificity hexokinases from *Bacteroides fragilis* and their role in hexose and N-acetylglucosamine utilization. J Bacteriol. 2005;187: 890–901. doi:10.1128/JB.187.3.890-901.2005
218. Brigham C, Caughlan R, Gallegos R, Dallas MB, Godoy VG, Malamy MH. Sialic acid (N-acetyl neuraminic acid) utilization by *Bacteroides fragilis* requires a novel N-acetyl mannosamine epimerase. J Bacteriol. 2009;191: 3629–3638. doi:10.1128/JB.00811-08
219. Roy S, Douglas CWI, Stafford GP. A novel sialic acid utilization and uptake system in the periodontal pathogen *Tannerella forsythia*. J Bacteriol. 2010;192: 2285–2293. doi:10.1128/JB.00079-10
220. Rogers MJ, Ohgi T, Plumbridge J, Söll D. Nucleotide sequences of the *Escherichia coli nagE* and *nagB* genes: the structural genes for the N-acetylglucosamine transport protein of the bacterial phosphoenolpyruvate: sugar phosphotransferase system and for glucosamine-6-phosphate deaminase. Gene. 1988;62: 197–207.

221. Alvarez-Añorve LI, Calcagno ML, Plumbridge J. Why does *Escherichia coli* grow more slowly on glucosamine than on N-acetylglucosamine? Effects of enzyme levels and allosteric activation of GlcN6P deaminase (NagB) on growth rates. J Bacteriol. 2005;187: 2974–2982. doi:10.1128/JB.187.9.2974-2982.2005
222. Gaugué I, Oberto J, Putzer H, Plumbridge J. The use of amino sugars by *Bacillus subtilis*: presence of a unique operon for the catabolism of glucosamine. Uversky VN, editor. PLoS ONE. 2013;8: e63025. doi:10.1371/journal.pone.0063025
223. Xiao X, Wang F, Saito A, Majka J, Schlösser A, Schrempf H. The novel *Streptomyces olivaceoviridis* ABC transporter Ngc mediates uptake of N-acetylglucosamine and N,N'-diacetylchitobiose. Mol Genet Genomics. 2002;267: 429–439. doi:10.1007/s00438-002-0640-2
224. Yang C, Rodionov DA, Li X, Laikova ON, Gelfand MS, Zagnitko OP, et al. Comparative genomics and experimental characterization of N-acetylglucosamine utilization pathway of *Shewanella oneidensis*. J Biol Chem. 2006;281: 29872–29885. doi:10.1074/jbc.M605052200
225. Reizer J, Ramseier TM, Reizer A, Charbit A, Saier MH Jr. Novel phosphotransferase genes revealed by bacterial genome sequencing: a gene cluster encoding a putative N-acetylgalactosamine metabolic pathway in *Escherichia coli*. Microbiol Read Engl. 1996;142 (Pt 2): 231–250.
226. Brinkkötter A, Klöss H, Alpert C, Lengeler JW. Pathways for the utilization of N-acetyl-galactosamine and galactosamine in *Escherichia coli.* Mol Microbiol. 2000;37: 125–135.
227. Hu Z, Patel IR, Mukherjee A. Genetic analysis of the roles of *agaA*, *agaI*, and *agaS* genes in the N-acetyl-D-galactosamine and D-galactosamine catabolic pathways in *Escherichia coli* strains O157:H7 and C. BMC Microbiol. 2013;13: 94. doi:10.1186/1471-2180-13-94
228. Ezquerro-Sáenz C, Ferrero MA, Revilla-Nuin B, López Velasco FF, Martínez-Blanco H, Rodríguez-Aparicio LB. Transport of N-acetyl-D-galactosamine in *Escherichia coli* K92: effect on acetyl-amino sugar metabolism and polysialic acid production. Biochimie. 2006;88: 95–102. doi:10.1016/j.biochi.2005.06.011
229. Brinkkötter A, Shakeri-Garakani A, Lengeler JW. Two class II D-tagatose-bisphosphate aldolases from enteric bacteria. Arch Microbiol. 2002;177: 410–419. doi:10.1007/s00203-002-0406-6
230. Leyn SA, Gao F, Yang C, Rodionov DA. N-Acetylgalactosamine utilization pathway and regulon in proteobacteria: genomic reconstruction and experimental characterization in *Shewanella*. J Biol Chem. 2012;287: 28047–28056. doi:10.1074/jbc.M112.382333
231. Becker DJ, Lowe JB. Fucose: biosynthesis and biological function in mammals. Glycobiology. 2003;13: 41R–53R. doi:10.1093/glycob/cwg054
232. Hugdahl MB, Beery JT, Doyle MP. Chemotactic behavior of *Campylobacter jejuni*. Infect Immun. 1988;56: 1560–1566.
233. Higgins MA, Abbott DW, Boulanger MJ, Boraston AB. Blood group antigen recognition by a solute-binding protein from a serotype 3 strain of *Streptococcus pneumoniae*. J Mol Biol. 2009;388: 299–309. doi:10.1016/j.jmb.2009.03.012
234. Higgins MA, Suits MD, Marsters C, Boraston AB. Structural and functional analysis of fucose-processing enzymes from *Streptococcus pneumoniae*. J Mol Biol. 2014;426: 1469–1482. doi:10.1016/j.jmb.2013.12.006

235. Scott KP, Martin JC, Campbell G, Mayer C-D, Flint HJ. Whole-genome transcription profiling reveals genes up-regulated by growth on fucose in the human gut bacterium "Roseburia inulinivorans." J Bacteriol. 2006;188: 4340–4349. doi:10.1128/JB.00137-06
236. Yu Z-T, Chen C, Newburg DS. Utilization of major fucosylated and sialylated human milk oligosaccharides by isolated human gut microbes. Glycobiology. 2013;23: 1281–1292. doi:10.1093/glycob/cwt065
237. Coyne MJ, Reinap B, Lee MM, Comstock LE. Human symbionts use a host-like pathway for surface fucosylation. Science. 2005;307: 1778–1781. doi:10.1126/science.1106469
238. Hooper LV, Xu J, Falk PG, Midtvedt T, Gordon JI. A molecular sensor that allows a gut commensal to control its nutrient foundation in a competitive ecosystem. Proc Natl Acad Sci U S A. 1999;96: 9833–9838.
239. Badía J, Ros J, Aguilar J. Fermentation mechanism of fucose and rhamnose in *Salmonella typhimurium* and *Klebsiella pneumoniae*. J Bacteriol. 1985;161: 435–437.
240. Baldomà L, Aguilar J. Metabolism of L-fucose and L-rhamnose in *Escherichia coli*: aerobic-anaerobic regulation of L-lactaldehyde dissimilation. J Bacteriol. 1988;170: 416–421.
241. Embry A, Hinojosa E, Orihuela CJ. Regions of Diversity 8, 9 and 13 contribute to *Streptococcus pneumoniae* virulence. BMC Microbiol. 2007;7: 80. doi:10.1186/1471-2180-7-80
242. Higgins MA, Whitworth GE, El Warry N, Randriantsoa M, Samain E, Burke RD, et al. Differential recognition and hydrolysis of host carbohydrate antigens by *Streptococcus pneumoniae* family 98 glycoside hydrolases. J Biol Chem. 2009;284: 26161–26173. doi:10.1074/jbc.M109.024067
243. Pacheco AR, Curtis MM, Ritchie JM, Munera D, Waldor MK, Moreira CG, et al. Fucose sensing regulates bacterial intestinal colonization. Nature. 2012;492: 113–117. doi:10.1038/nature11623
244. Hooper LV, Gordon JI. Glycans as legislators of host-microbial interactions: spanning the spectrum from symbiosis to pathogenicity. Glycobiology. 2001;11: 1R–10R. doi:10.1093/glycob/11.2.1R
245. Ilver D, Arnqvist A, Ogren J, Frick IM, Kersulyte D, Incecik ET, et al. Helicobacter pylori adhesin binding fucosylated histo-blood group antigens revealed by retagging. Science. 1998;279: 373–377.
246. Cinco M, Banfi E, Ruaro E, Crevatin D, Crotti D. Evidence for l-fucose (6-deoxy-l-galactopyranose)-mediated adherence of *Campylobacter* spp. to epithelial cells. FEMS Microbiol Lett. 1984;21: 347–351.
247. Liu T-W, Ho C-W, Huang H-H, Chang S-M, Popat SD, Wang Y-T, et al. Role for alpha-L-fucosidase in the control of *Helicobacter pylori*-infected gastric cancer cells. Proc Natl Acad Sci U S A. 2009;106: 14581–14586. doi:10.1073/pnas.0903286106
248. Higgins MA, Boraston AB. Structure of the fucose mutarotase from *Streptococcus pneumoniae* in complex with L-fucose. Acta Crystallograph Sect F Struct Biol Cryst Commun. 2011;67: 1524–1530. doi:10.1107/S1744309111046343
249. Chen YM, Zhu Y, Lin EC. The organization of the fuc regulon specifying L-fucose dissimilation in *Escherichia coli* K12 as determined by gene cloning. Mol Gen Genet MGG. 1987;210: 331–337.

250. Chen YM, Zhu Y, Lin EC. NAD-linked aldehyde dehydrogenase for aerobic utilization of L-fucose and L-rhamnose by *Escherichia coli*. J Bacteriol. 1987;169: 3289–3294.
251. Lu Z, Lin EC. The nucleotide sequence of *Escherichia coli* genes for L-fucose dissimilation. Nucleic Acids Res. 1989;17: 4883–4884.
252. Sugihara J, Sun L, Yan N, Kaback HR. Dynamics of the L-fucose/H+ symporter revealed by fluorescence spectroscopy. Proc Natl Acad Sci. 2012;109: 14847–14851. doi:10.1073/pnas.1213445109
253. Muraoka WT, Zhang Q. Phenotypic and genotypic evidence for L-Fucose utilization by *Campylobacter jejuni*. J Bacteriol. 2011;193: 1065–1075. doi:10.1128/JB.01252-10
254. Stahl M, Friis LM, Nothaft H, Liu X, Li J, Szymanski CM, et al. L-Fucose utilization provides *Campylobacter jejuni* with a competitive advantage. Proc Natl Acad Sci. 2011;108: 7194–7199. doi:10.1073/pnas.1014125108
255. Hofreuter D. Defining the metabolic requirements for the growth and colonization capacity of *Campylobacter jejuni*. Front Cell Infect Microbiol. 2014;4. doi:10.3389/fcimb.2014.00137
256. Yew WS, Fedorov AA, Fedorov EV, Rakus JF, Pierce RW, Almo SC, et al. Evolution of enzymatic activities in the enolase superfamily: L-fuconate dehydratase from *Xanthomonas campestris*. Biochemistry (Mosc). 2006;45: 14582–14597. doi:10.1021/bi061687o
257. Petit E, LaTouf WG, Coppi MV, Warnick TA, Currie D, Romashko I, et al. Involvement of a bacterial microcompartment in the metabolism of fucose and rhamnose by *Clostridium phytofermentans*. de Crécy-Lagard V, editor. PLoS ONE. 2013;8: e54337. doi:10.1371/journal.pone.0054337
258. Havemann GD, Bobik TA. Protein content of polyhedral organelles involved in coenzyme B12-dependent degradation of 1,2-propanediol in *Salmonella enterica* serovar *Typhimurium LT2*. J Bacteriol. 2003;185: 5086–5095. doi:10.1128/JB.185.17.5086-5095.2003
259. Bobik TA, Xu Y, Jeter RM, Otto KE, Roth JR. Propanediol utilization genes (pdu) of *Salmonella typhimurium:* three genes for the propanediol dehydratase. J Bacteriol. 1997;179: 6633–6639.
260. Chen YM, Lu Z, Lin EC. Constitutive activation of the *fucAO* operon and silencing of the divergently transcribed *fucPIK* operon by an IS5 element in *Escherichia coli* mutants selected for growth on L-1,2-propanediol. J Bacteriol. 1989;171: 6097–6105.
261. Schwab C, Gänzle M. Lactic acid bacteria fermentation of human milk oligosaccharide components, human milk oligosaccharides and galactooligosaccharides: LAB fermentation of HMOs and GOSs. FEMS Microbiol Lett. 2011;315: 141–148. doi:10.1111/j.1574-6968.2010.02185.x
262. Rodriguez-Diaz J, Rubio-del-Campo A, Yebra MJ. *Lactobacillus casei* ferments the N-acetylglucosamine moiety of fucosyl-alpha -1,3-N-acetylglucosamine and excretes L-Fucose. Appl Environ Microbiol. 2012;78: 4613–4619. doi:10.1128/AEM.00474-12
263. Castro R, Neves AR, Fonseca LL, Pool WA, Kok J, Kuipers OP, et al. Characterization of the individual glucose uptake systems of *Lactococcus lactis*: mannose-PTS, cellobiose-PTS and the novel GlcU permease. Mol Microbiol. 2009;71: 795–806. doi:10.1111/j.1365-2958.2008.06564.x

264. Gosset G. Improvement of Escherichia coli production strains by modification of the phosphoenolpyruvate:sugar phosphotransferase system. Microb Cell Factories. 2005;4: 14. doi:10.1186/1475-2859-4-14
265. Paulsen IT, Chauvaux S, Choi P, Saier MH. Characterization of glucose-specific catabolite repression-resistant mutants of *Bacillus subtilis*: identification of a novel hexose:H^+ symporter. J Bacteriol. 1998;180: 498–504.
266. Neves AR, Ramos A, Shearman C, Gasson MJ, Almeida JS, Santos H. Metabolic characterization of *Lactococcus lactis* deficient in lactate dehydrogenase using *in vivo* 13C-NMR. Eur J Biochem FEBS. 2000;267: 3859–3868.
267. Gaspar P, Neves AR, Shearman CA, Gasson MJ, Baptista AM, Turner DL, et al. The lactate dehydrogenases encoded by the *ldh* and *ldhB* genes in *Lactococcus lactis* exhibit distinct regulation and catalytic properties − comparative modeling to probe the molecular basis: Lactacte dehydrogenases of *Lactococcus lactis*. FEBS J. 2007;274: 5924–5936. doi:10.1111/j.1742-4658.2007.06115.x
268. Gaspar P, Neves AR, Gasson MJ, Shearman CA, Santos H. High yields of 2,3-butanediol and mannitol in *Lactococcus lactis* through engineering of NAD^+ cofactor recycling. Appl Environ Microbiol. 2011;77: 6826–6835. doi:10.1128/AEM.05544-11
269. C. Garrigues, P. Loubiere, N. D. Lindley, M. Cocaign-Bousquet. Control of the shift from homolactic acid to mixed-acid fermentation in *Lactococcus lactis*: predominant role of the NADH/NAD^+ ratio. J Bacteriol. 1997;179: 5282–5287.
270. Melchiorsen CR, Jokumsen KV, Villadsen J, Israelsen H, Arnau J. The level of pyruvate-formate lyase controls the shift from homolactic to mixed-acid product formation in *Lactococcus lactis*. Appl Microbiol Biotechnol. 2002;58: 338–344. doi:10.1007/s00253-001-0892-5
271. Neves AR, Ventura R, Mansour N, Shearman C, Gasson MJ, Maycock C et al. Is the glycolytic flux in *Lactococcus lactis* primarily controlled by the redox charge? Kinetics of NAD+ and NADH pools determined *in vivo* by 13C NMR. J Biol Chem. 2002;277: 28088–28098. doi:10.1074/jbc.M202573200
272. Thomas TD, Ellwood DC, Longyear VM. Change from homo- to heterolactic fermentation by *Streptococcus lactis* resulting from glucose limitation in anaerobic chemostat cultures. J Bacteriol. 1979;138: 109–117.
273. Lanie JA, Ng W-L, Kazmierczak KM, Andrzejewski TM, Davidsen TM, Wayne KJ, et al. Genome sequence of Avery's virulent serotype 2 strain D39 of *Streptococcus pneumoniae* and comparison with that of unencapsulated laboratory strain R6. J Bacteriol. 2007;189: 38–51. doi:10.1128/JB.01148-06
274. Ramos-Montañez S, Kazmierczak KM, Hentchel KL, Winkler ME. Instability of ackA (acetate kinase) mutations and their effects on acetyl phosphate and ATP amounts in *Streptococcus pneumoniae* D39. J Bacteriol. 2010;192: 6390–6400. doi:10.1128/JB.00995-10

Chapter 2

Host glycan sugar-specific pathways in *Streptococcus pneumoniae*: galactose as a key sugar in colonisation and infection

The results of this chapter are published in:

Paixão, L, Oliveira, J, Veríssimo, A, Vinga, S, Lourenço, EC, Ventura, MR, Kjos, M, Veening, J-W, Fernandes, VE, Andrew, PW, Yesilkaya, H and Neves, AR (2015). Host glycan sugar-specific pathways in *Streptococcus pneumoniae*: galactose as a key sugar in colonisation and infection. Plos One. 2015. In press.

Chapter 2 – Contents

Abstract

The human pathogen *Streptococcus pneumoniae* is a strictly fermentative organism that relies on glycolytic metabolism to obtain energy. In the human nasopharynx *S. pneumoniae* encounters glycoconjugates composed of a variety of monosaccharides, which can potentially be used as nutrients once depolymerized by glycosidases. Therefore, it is reasonable to hypothesise that the pneumococcus would rely on these glycan-derived sugars to grow. Here, we identified the sugar-specific catabolic pathways used by *S. pneumoniae* during growth on mucin. Transcriptome analysis of cells grown on mucin showed specific upregulation of genes likely to be involved in deglycosylation, transport and catabolism of galactose, mannose and N-acetylglucosamine. In contrast to growth on mannose and N-acetylglucosamine, *S. pneumoniae* grown on galactose re-route their metabolic pathway from homolactic fermentation to a truly mixed acid fermentation regime. By measuring intracellular metabolites, enzymatic activities and mutant analysis, we provide an accurate map of the biochemical pathways for galactose, mannose and N-acetylglucosamine catabolism in *S. pneumoniae*. Intranasal mouse infection models of pneumococcal colonisation and disease showed that only mutants in galactose catabolic genes were attenuated. Our data pinpoint galactose as a key nutrient for growth in the respiratory tract and highlights the importance of central carbon metabolism for pneumococcal pathogenesis.

Introduction

Streptococcus pneumoniae is an important human pathogen responsible for high morbidity and mortality worldwide, mainly due to

community-acquired pneumonia, meningitis, bacteraemia and otitis media [1,2]. The pneumococcus is, however, also a transient commensal that asymptomatically resides and proliferates in the human nasopharynx [3]. Colonisation of the nasopharynx is of importance as it represents a reservoir from which bacteria can disseminate throughout the community [2,4]. Furthermore, the establishment of a carrier state is accepted to be a pre-requisite for disease [3,5]. Despite the significance of colonisation to the lifestyle of *S. pneumoniae*, little is known about the mechanisms employed by the bacterium to grow and proliferate in the human nasopharynx.

S. pneumoniae is a strictly fermentative bacterium that relies on glycolytic metabolism to obtain energy [6]. Therefore, the ability to acquire and metabolize sugars is of major importance for *in vivo* fitness of this microorganism. Indeed, the pneumococcus lacks a complete set of genes for respiratory proteins and is for this reason unable to generate energy by respiration [6,7]. The genomic abundance of genes involved in sugar transport further supports the significant role of carbohydrates in the lifestyle of *S. pneumoniae* [6,7]. Over 30% of the transporters in the *S. pneumoniae* genome were predicted to be involved in the uptake of carbohydrates [7], and these predictions were validated by a recent functional genomic approach targeting carbohydrate transport [8]. Furthermore, several putative carbohydrate degradation pathways have been annotated in the genome sequences of *S. pneumoniae* [6,7]. In summary, *S. pneumoniae* potentially harbours an incredible flexibility with respect to sugar consumption. Hexoses, and in particular glucose (Glc), are the preferred carbon and energy sources of *S. pneumoniae* [9]. However, in the human airway the abundance of free sugars is scarce, the concentration of Glc being below 1 mM [10,11]. In this case, *in vivo* growth must rely on alternative nutritional reservoirs. In the human nasopharynx, the glycoproteins lining the epithelial surfaces appear as

good candidates to serve as carbon and energy sources for pneumococcal growth. Importantly, *S. pneumoniae* is able to grow on mucin as a sole carbon source [12]. Mucins are major components of the mucus that cover the epithelial surfaces [13]. These structures are heavily O-glycosylated glycoproteins and despite their composition variability, mucins are generally composed of N-acetylglucosamine (GlcNAc), N-acetylgalactosamine (GalNAc), N-acetylneuraminic acid (NeuNAc), galactose (Gal), fucose (Fuc) and sulphated sugars linked to the protein core, most commonly via a N-acetylgalactosamine moiety [13,14]. Furthermore, *S. pneumoniae* can use other host glycans, such as N-glycans and glycosaminoglycans [15,16]. In fact, the pneumococcus is equipped with a high number of extracellular glycosidases covering a wide range of substrates specificities (reviewed in [17]). The action of these enzymes on host glycans generates a variety of free sugars that potentially can be used by the pneumococcus. The deglycosylation activity of both exo- and endoglycosidades has been previously demonstrated in *S. pneumoniae* [15,18–20]. Furthermore, the role of these enzymes in *in vivo* fitness is substantiated by the observations that glycosidase mutants show attenuated ability to colonise and to cause disease in mouse models [14,19–23].

In this study, we set out to identify the putative catabolic pathways important for growth on mucin. To this end, we used the well-established laboratorial model for pneumococcal studies *S. pneumoniae* D39 [24]. Subsequently, the predicted utilization routes of the glycan-derived sugars Gal, GlcNAc and Man were functionally established, by positive detection of phosphorylated metabolic intermediates and measurement of specific enzyme activities. Inactivation of a unique gene in each catabolic pathway rendered mutant strains unable or with impaired ability to grow in the presence of the corresponding sugar. Finally, the contribution of the sugar-specific catabolic pathways to colonisation and pneumococcal

disease was assessed in appropriate mouse models, demonstrating that mutants in Gal catabolic pathways were attenuated in their ability to colonise and had reduced virulence in respiratory infection models.

Overall, we experimentally validated the catabolic pathways of glycan-derived Gal, Man and GlcNAc and found Gal as a key nutrient during pneumococcal *in vivo* growth.

Materials and Methods

Bacterial strains and growth conditions

Streptococcus pneumoniae strain D39 (serotype 2) and its derivatives are listed in Table S2.1. The D39 isolate was obtained from the culture collection of the Department of Infection, Immunity and Inflammation, of the University of Leicester. Stocks and working stocks were prepared as described elsewhere [25] and stored in 25% (vol/vol) glycerol M17 medium (Difco) at -80°C.

Routinely, *S. pneumoniae* was grown statically in M17 broth containing 0.5% (wt/vol) glucose (Glc-M17) at 37°C. For physiological studies, bacteria were grown in static rubber-stoppered bottles (80 ml in 100 ml bottles) at 37ºC and without pH control (initial pH 6.5) in the chemically defined medium (CDM) described by Carvalho *et al.* [25]. For each sugar tested (Gal, GlcNAc, Man and Glc), growth was analysed under sugar excess (34±2 mM) and a lower concentration (13±1 mM). In sugar mixtures each carbohydrate (Gal, Man and GlcNAc) was added to an initial concentration of *circa* 6.5 mM. Cultures were started by inoculating fresh CDM, to an initial optical density at 600 nm (OD_{600}) of ~0.05, with a pre-culture grown until late-exponential phase of growth. Pre-cultures were performed as described previously [25]. Pre-cultures for growth on

sugar mixtures were grown in CDM containing 30 mM of each carbon source. Growth was monitored by measuring OD_{600} hourly. Maximum specific growth rates (μ_{max}) were calculated through linear regressions of the plots of $\ln(OD_{600})$ *versus* time during the exponential phase of growth. The values reported are averages of at least eight independent growths. Representative growth curves were selected based on the minimum value of the sum:

$$\left(\frac{OD_{\max}-\overline{OD}_{\max}}{SD_{OD\max}}\right)^2+\left(\frac{\mu_{\max}-\overline{\mu}_{\max}}{SD_{\mu\max}}\right)^2$$

Where, $\overline{OD}_{\max}$ and $\overline{\mu}_{\max}$ are the averages of the maximum optical density (OD_{max}) and μ_{max}, respectively; $SD_{OD\max}$ and $SD_{\mu\max}$ are the standard deviation of OD_{max} and μ_{max}, respectively.

Statistical analysis of the growth parameters

ANOVA was applied to test the hypothesis that μ_{max} values are independent of the sugar. Additionally, the differences across the two initial substrate conditions were also compared. The same ANOVA procedure was taken to assess if differences of OD_{max} values depended on the sugar and initial condition and assess if they were statistically significant.

The null hypothesis of equal values for the μ_{max} was tested for all possible pairwise combinations of initial conditions and sugars. This was accomplished by independent two-sample t-tests, whose results are summarized on Table S2.2. Likewise, similar tests were also performed for the OD_{max}. Results are presented in Table S2.2.

Multiple non-linear regression method for generating confidence interval bands

Multiple non-linear regressions were performed for all the combinations of experimental conditions (4 sugars and 2 initial concentrations) using the Gompertz model [26]:

$$f(t;\mu_{\max},\lambda,A) = A\cdot\exp\left(-\exp\left\{\frac{\mu_{\max}\cdot\exp(1)}{A}(\lambda-t)+1\right\}\right),$$

where $\mu_{\max}$ is the tangent in the inflection point (maximum growth rate), λ is the x-axis intercept of this tangent (lag) and A is the asymptote $A=\log\left(\frac{y_\infty}{y_0}\right)$. To obtain better fittings, the data were previously log-transformed as $y'=\log\left(\frac{y}{y_0}\right)$ and the parameters estimated directly with the BGFit web-application [27] using non-linear least squares.

After obtaining the estimates for each sugar and initial concentration condition, a 95% confidence interval for the data and bands for the predicted responses of the model were computed. These computations were performed in MATLAB and Statistics Toolbox R2013a using the function *nlpredci*.

General molecular techniques

Chromosomal DNA isolation was performed according to the procedure described by Johansen and Kibenich [28]. Pwo polymerase was used according to the supplier's instructions (Roche). PCRs were performed with a MyCycler thermal cycler (Bio-Rad). Purification of the PCR fragments was accomplished using the High Pure PCR product Purification Kit (Roche) according to the supplier's instructions. Plasmid isolation was done using a High Pure Plasmid Isolation Kit (Roche),

according to the manufacturer's protocol. Restriction enzymes were purchased from New England Biolabs.

Construction of loss-of-function mutants

Chromosomal DNA of *S. pneumoniae* D39 was used as template in the PCR amplifications. Oligonucleotide primers used for these constructs are listed in Table S2.3. *galK* (SPD_1634), *lacD* (SPD_1050), *manA* (SPD_0641), *nagA* (SPD_1866) and *galT-2* (SPD_1633) disruption was accomplished by allelic replacement mutagenesis, essentially as described by Song *et al.* [29]. The upstream and downstream flanking regions of the genes to be disrupted were amplified using the appropriate primers' combinations KO1_Fw/KO2_Rv_Spe and KO3_Fw_Spe/KO4_Rv, respectively (Table S2.3). Flanking fragments were fused to the spectinomycin resistance marker (Spe) (1032 bp, amplified with primers Spe_Fp and Spe_Rp from pORI38), by overlap extension PCR using the appropriate primers KO1_Fw and KO4_Rv. The resulting fused fragments were purified and transformed into D39 as described before [30]. Positive transformants were selected on Glc-M17 sheep blood (1% vol/vol) agar plates supplemented with 150 μg ml^{-1} of spectinomycin. The correct integration of the insert in the mutant clones was confirmed by PCR. Genomic DNA was used as template for PCR with primers designed to anneal around 100 bp upstream and downstream of the recombination site, as well as combinations of these primers with those used to construct the mutants (Table S2.3).

A double mutant, D39Δ*lacD*Δ*galK*, was constructed by allelic replacement of the *galK* gene in the D39Δ*lacD* mutant using trimethoprim (Tmp) selection. The up and downstream flanking regions of the *galK* gene were amplified using the appropriate primer combinations: GalK_KO1_Fw/GalK_KO2_Rv_Tmp and GalK_KO3_Fw_Tmp/GalK_KO4_Rv, respectively (Table S2.3). The

regions flanking *galK* were fused to the Tmp cassette in an overlap extension PCR reaction with the primer combination GalK_KO1_Fw/GalK_KO4_Rv, yielding Δ*galK::tmp*. The purified fused fragment was transformed into D39Δ*lacD* and positive clones were selected on Glc-M17 sheep blood (1% vol/vol) agar plates supplemented with 18 µg ml^{-1} of trimethoprim. Gene replacement was confirmed as described above, using the primers listed in Table S2.3.

Construction of the pKB01 derivatives for complementation studies

pKB01, containing a zinc-inducible P_{czcD} promoter (P_{Zn}), was used as a complementation system [31]. The target genes were amplified using chromosomal DNA from *S. pneumoniae* D39. For the construction of pKB01-*lacD*, pKB01-*galK* and pKB01-*manA, lacD, galK* and *manA* genes were amplified using LacD_Fw_EcoRI/LacD_Rv_BamHI, GalK_Fw_EcoRI/GalK_Rv_BamHI and ManA_Fw_EcoRI/ManA_Rv_BamHI, respectively. The PCR-amplified fragments and pKB01 were digested with EcoRI and BamHI and subsequently ligated. To generate pKB01-*nagA* the gene was amplified with its own promoter using primers NagA_Fw_NotI/NagA_Rv_BamHI. The digested fragment (NotI/BamHI) was cloned into pKB01 using the same restriction sites. pKB01-*galT-2* was made by amplifying *galT-2* with GalT-2_Fw_EcoRI/GalT-2_Rv_NotI. The PCR-fragment and PKB01 were cleaved using EcoRI/NotI enzymes and ligated. To construct PKB01-*galKgalT-2*, *galKgalT-2* was amplified using GalK_Fw_EcoRI_B/GalT-2_Rv_XbaI, digested with EcoRI and XbaI and ligated into pKB01 at the same restriction sites. The primers used are listed in Table S2.3.
All the generated constructs were transformed into *E. coli* DH5α [32]. *E. coli* was grown in Luria broth at 37ºC supplemented with 100 µg ml^{-1} ampicillin. The constructs were verified by sequencing at Macrogen.

Complementation of deletion strains

The pKB01-based plasmids were transformed into competent cells of *S. pneumoniae* D39 loss-of-function mutants. For transformation, 2 µl of the competence-stimulating peptide (CSP, 0.1 mg ml^{-1}) was added to pre-competent cells and activation achieved by 12 min at 37ºC. Plasmid DNA was added and transformation was accomplished by 20 min at 30ºC, followed by a phenotypic expression period of 90 min at 37ºC and overnight growth on Columbia blood agar plates supplemented with 1 µg ml^{-1} of tetracycline [33]. pKB01 constructs integrate by a double cross-over into the chromosomal *bgaA* locus. Correct integration was verified, in single colonies, by PCR. The constructed strains are listed in Table S2.1.

Growth of complemented strains

Growth experiments were performed in a 96 well microtiter plate reader (Tecan Genius) in a total volume of 200 µl C+Y medium [34], devoid of Glc and sucrose. The medium was supplemented with 55 mM of the desired carbon source in the presence or absence of 0.1 mM $ZnCl_2$. Cells were grown at 37ºC and OD_{595} was measured hourly.

Transcriptome analysis

For microarrays analysis, *S. pneumoniae* D39 was grown using Sicard's defined medium with or without modification [35]. Modification was done to include mucin as the sole carbon source, replacing Glc and bovine serum albumin. Porcine gastric mucin (Sigma) was dissolved in water at a concentration of 10 mg ml^{-1} and dialysed against water overnight at 4ºC using snake skin dialysis membrane (MWCO 10 kDa, Pierce). After freeze drying, the mucin was dissolved in 10 mM potassium phosphate buffer, pH 7.0, autoclaved at 121ºC for 15 min. This was then

briefly centrifuged to remove insoluble residues and mixed with 2X concentrated Sicard's medium. The extraction of RNA was done as described previously [36,37].

Microarray experiments

Microarray slides were purchased from the Bacterial Microarray Group at St. George's Hospital Medical School, University of London. The SPv1.1.0 array contained spotted PCR products that represent all of the genes in the *S. pneumoniae* TIGR4 and R6 genomes. The array design is available in BµG@Sbase (accession number: A-BUGS-14; http://bugs.sgul.ac.uk/A-BUGS-14) and also ArrayExpress (accession number: A-BUGS-14). The Materials and Methods for microarray analysis followed previously reported methodology [37].

Analysis of microarrays

The microarray slides were scanned using an Axon GenePix 4000A microarray scanner, which utilises GenePix 5.1 software (Molecular Devices Ltd) for identification and for a visual analysis of the quality of the spots. The raw intensity data obtained from four independent experiments were normalised and further analysed using GeneSpring 7.3 software (Agilent Technologies). Data were subjected to LOWESS intensity-dependent normalisation. Statistically significant changes in gene expression were determined as t-test p-values < 0.05 after Benjamini and Hochberg false discovery rate correction [38]. Genes of interest were further identified by requiring >2-fold differences in all four samples analysed. In addition, the microarray results for selected genes whose expression significantly altered in the presence of mucin were verified and confirmed by real time quantitative reverse transcription PCR (qRT-PCR), in order to ensure that dye affinity did not bias the results.

Fully annotated microarray data have been deposited in BμG@Sbase (accession number E-BUGS-159; http://bugs.sgul.ac.uk/E-BUGS-159) and also ArrayExpress (accession number E-BUGS-159).

Quantitative RT-PCR

To assess the expression of specific Gal catabolic genes (*galT-2, galT-1, galK, lacD*), by qRT-PCR, cells were grown in CDM supplemented with the appropriate carbohydrate, as previously described, and a 4 ml aliquot was collected (16,100 *x g*, 2 min at 27ºC) in mid-exponential phase of growth. The supernatant was discarded and the pellet suspended in 0.5 ml Trizol (Life Technologies). Samples were stored at -80ºC until further analysis. RNA extraction was performed as described previously [37].

To confirm the microarray results, two independent RNA preparations were used for qRT-PCR analysis. First strand cDNA synthesis was performed on approximately 1 μg DNase-treated total RNA, immediately after isolation, using 200 U of SuperScript II reverse transcriptase (Invitrogen) and random hexamers at 42ºC for 55 min [39]. cDNA (15 ng) was amplified in a 20 μl reaction volume that contained 1 x SYBR Green PCR master mix (Applied Biosystems) and 3 pmol of each primer (Table S2.3). The transcription level of genes was normalised to *gyrB* transcription, amplified in parallel with SPDRT0709F and SPDRT0709R primers. The reactions were performed in triplicate using the following cycling parameters with a Rotor Gene real time PCR cycler (Qiagen): 1 cycle of 10 min 95ºC followed by 40 cycles of 30 sec 95ºC, 1 min 55°C, and 30 sec 72°C. The results were interpreted using the comparative C_T method [40].

In silico analysis for catabolic pathway prediction

Potential catabolic pathways for the monosaccharides Gal, Man, GlcNAc, NeuNAc, GalNAc and Fuc were predicted *in silico* by combining

data obtained from the metabolic databases MetaCyc (http://metacyc.org/META/class-tree?object=Pathways) and Kegg (http://www.genome.jp/kegg/pathway.html), literature surveys and genome sequences. In addition, functionally characterized proteins from other microorganisms were used as query for BlastP searches of *S. pneumoniae* D39 genome deposited at NCBI (http://www.ncbi.nlm.nih.gov/genome/176?project_id=58581).

Growth assay for assessment of sugar utilization by *S. pneumoniae* D39

The ability of monosaccharides Glc, Gal, Man, GlcNAc, glucosamine (GlcN), galactosamine (GalN), and GalNAc to support growth of *S. pneumoniae* D39 was investigated using 96-well microtiter plates containing 250 µl CDM supplemented with 30 mM of each sugar. Cultures were started at an initial OD_{595} of ~0.05 by addition of an overnight Glc-grown pre-culture pelleted (6300 *x g*, 7 min, RT) and suspended in fresh CDM without sugar. Growth was monitored at 595 nm over 24 h at 37ºC. Readings were taken every 30 min, after 1 s shaking, using an ELx808 Absorbance Microplate Reader (BioTek Instruments, Inc.). The growth curves were generated by using Gen5™ (BioTek Instruments, Inc.). Each growth condition was done in triplicate using two independent pre-cultures.

Quantification of sugar consumption and fermentation products

Strains were grown in CDM supplemented with the appropriate sugar as described above. Culture samples (2 mL) were taken immediately after inoculation and at the onset of the stationary phase of growth, and centrifuged (16,100 *x g*, 3 min, 4ºC). For high performance liquid

chromatography (HPLC) analysis, samples were treated as described by Carvalho *et al*. [9]. Fermentation products and Glc were quantified by HPLC as before [9]. Gal, Man, GlcNAc and formate were quantified by ^{1}H-NMR and the spectra were acquired with a Bruker AMX300 spectrometer (Bruker BioSpin GmbH). To quantify Gal the temperature of the probe was set to 18ºC, whereas for Man and GlcNAc it was 37ºC. DSS (3-(trimethylsilyl) propionic acid sodium salt) was added to the samples as an internal concentration standard in ^{1}H-NMR quantifications.

Yields were calculated using the data from samples taken immediately after inoculation and at the onset of stationary phase of growth. A factor of 0.38, determined from a dry weight (DW) (mg ml^{-1}) *versus* OD_{600} curve, was used to convert OD_{600} into DW (mg biomass ml^{-1}). The yield in biomass was calculated as g of dry weight per mol of substrate consumed. The ATP yield was determined as the ratio of ATP produced to substrate consumed at the time of growth arrest assuming that all ATP was synthesized by substrate-level phosphorylation. The values reported are averages of at least two independent growths.

Cold ethanol extractions and determination of intracellular metabolites by ^{31}P-NMR

For ethanol extractions, the Na_2-β-glycerophosphate in the CDM growth medium was replaced by 15.4 g l^{-1} MES (2-(N-morpholino) ethanesulfonic acid), to avoid the intense buffer resonance in the phosphomonoester (PME) region. The ethanol extracts were prepared as described previously by Carvalho *et al.* [9]. Cells were harvested (20,980 *x g*, 4ºC, 5 min) during exponential growth and the pellet suspended in milliQ water, pH 6.5. Cell suspensions were transferred to the appropriate volume of cold ethanol 70% (vol/vol) in an ice bath, and extraction was performed for 30 min with vigorous agitation. Cell debris was removed by centrifugation (39,191 *x g*, 4ºC, 20 min). The ethanol in the supernatant

was removed via a rotavap and the extract frozen in liquid nitrogen, and lyophilized overnight. The dried extract was dissolved in 1 ml of deuterated water containing 5 mM EDTA. The pH was set to 6.5 and the extract was stored at -20ºC until analysis by ^{31}P-NMR. Resonances were assigned by addition of pure compounds to the extracts or on basis of comparison with previous studies [9]. ^{31}P-NMR spectra were recorded using a selective probe head (^{31}P-SEX) at 30ºC on a Bruker AVANCE II 500 MHz spectrometer (Bruker BioSpin GmbH) by using standard Bruker pulse programs. Spectra were referenced to the resonance of external 85% H_3PO_4, designated at 0 ppm.

Enzyme activity determination

For enzyme activity determination, cells of *S. pneumoniae* were grown, in CDM supplemented with 30 mM sugar (Gal, Man, GlcNAc or Glc), until late-exponential phase of growth, and harvested by centrifugation (7,519 *x g*, 7 min, 4ºC). The supernatant was removed, the pellet suspended in cold potassium phosphate buffer (KP_i) 10 mM, pH 7.0, and stored at -20ºC until further analysis. Dithiothreitol (1 mM) was added to the suspension and cell-free extracts prepared by mechanical disruption in a French Press (6.21 MPa). Cell debris was removed (16,100 *x g* for 15 min, at 4ºC) and the supernatant was used for enzyme activity measurements. Extracts were kept on ice during these measurements.

For measurement of galactokinase (GalK) activity, removal of low molecular weight substances from the cell-free extract was performed using a PD-10 desalting column equilibrated with KPi buffer 10 mM pH 7.0 according to the supplier's instructions (GE Healthcare Life Sciences). The GalK assay mixture contained 100 mM triethanolamine (TEA) buffer pH 7.6, 5 mM $MgCl_2$, 10 mM ATP and 10 mM galactose. The mixture was incubated at 37ºC, in a Thermomixer® comfort (Eppendorf) and the reaction started by the addition of the cell-free extract. The reaction was

stopped, at different time points, by incubating for 5 min at 85ºC and subsequently freezing in liquid nitrogen. Samples were stored at -20ºC until further analysis. Quantification of galactose 1-phosphate formed was accomplished by ^{1}H-NMR spectroscopy using a Brucker AMX300 spectrometer (Brucker BioSpin GmbH). DSS was added to the samples and used as an internal concentration standard. The slopes of the galactose 1-phosphate (Gal1P) formed *versus* time were determined using linear regression.

Tagatose 1,6-diphosphate aldolase (LacD) activity was determined essentially as described by Crow and Thomas [41]. The reaction mixture (1 ml) contained 50 mM TEA buffer pH 7.8, 0.25 mM NADH, 1.2 U α-glycerolphosphate dehydrogenase (Roche), 11.5 U triosephosphate isomerase from rabbit muscle (Sigma-Aldrich) and 0.16 mM tagatose 1,6-diphosphate (TBP). The oxidation of NADH was measured by the decrease in absorbance at 340 nm.

N-acetylglucosamine 6-phosphate deacetylase (NagA) activity was enzymatically assayed as described by Homer *et al.* [42]. The method couples this activity to the other GlcNAc-specific catabolic enzyme – glucosamine 6-phosphate isomerase (NagB). To ensure the applicability of this protocol, the specific activity of NagB was measured [43]. The specific activity of this enzyme was higher than that of NagA for all conditions assayed, thus showing that the glucosamine 6-phosphate isomerase activity was not a rate limiting step. The reaction mixture (1 ml) contained 40 mM sodium phosphate buffer pH 7.5, 1 mM N-acetylglucosamine 6-phosphate, 0.2 mM $NADP^{+}$, 4 U phosphoglucose isomerase (Sigma) and 1.5 U glucose 6-phosphate dehydrogenase (Roche). Glucosamine 6-phosphate isomerase was measured in an identical assay but N-acetylglucosamine 6-phosphate was replaced by glucosamine 6-phosphate. NADPH formation was monitored by measuring the increase in absorbance at 340 nm spectrophotometrically.

Mannose 6-phosphate isomerase (ManA) activity was measured essentially as described by Gracy and Noltmann [44], and modified as follows: the assay mixture contained 100 mM TEA pH 7.6, 10 mM mannose 6-phosphate, 2 mM $NADP^+$, 1 U of phosphoglucose isomerase (Sigma) and 1 U of glucose 6-phosphate dehydrogenase (Roche), in a total volume of 250 µl. The rate of change of absorbance at 340 nm (due to $NADP^+$ reduction), coupled to mannose 6-phosphate isomerization, was measured spectrophotometrically.

The coupled enzyme protocols were carried out at 25ºC. All the reactions were started by adding adequate amounts of freshly prepared cell-free extracts. The absorbance changes were recorded in a Shimadzu UV-1603 spectrophotometer (Shimadzu Corporation).

One unit (U) of GalK activity is defined as the amount of protein required for the formation of 1 µmol of Gal1P per minute. For the coupled enzyme protocols, the enzyme activity is given as the amount of protein required to catalyse the oxidation or reduction of 1 µmol of NADH or $NADP^+$, respectively, per minute. Specific activity was expressed as units (µmol min^{-1}) per milligram of protein (U mg $protein^{-1}$). Protein concentration in the cell-free extracts was determined by the Pierce BCA protein assay kit (Thermo Scientific). All the determinations were made at least in triplicate in two extracts obtained from independent cultures.

In vivo analysis of pneumococcal strains

Ten-week-old female MF1 outbred mice (Charles River) were used. Before use, a standard inoculum for each pneumococcal strain was prepared as described before [39].

To assess the virulence of pneumococcal strains, mice were lightly anesthetized with 3% (vol/vol) isoflurane over oxygen, and an inoculum of 50 µl containing approximately 1 X 10^6 CFU in PBS was given drop by drop into the nostrils. After infection, the inoculum dose was confirmed by

viable counting on blood agar plates. Animals were monitored for disease signs (progressively starry coat, hunched, and lethargic) every six hours in the first 24 h. After the onset of disease signs, which is after 24 h post-infection, the mice were monitored every 2 hours [39,45]. When the mice become lethargic, they were culled by cervical dislocation. Therefore, time to reach lethargic state was defined as the “survival time.” Mice that were alive 7 days after infection were deemed to have survived the infection.

Colonisation experiments were done essentially as described above except that mice were administered with 5 X 10^5 CFU of *S. pneumoniae* in 10 μl PBS. For intravenous infections, approximately 5 X 10^5 CFU of *S. pneumoniae* in 100 μl PBS (pH 7.0) were administered via a tail vein. The inoculum dose was confirmed by plating onto blood agar, as described above.

To monitor the development of bacteraemia, approximately 20 μl of venous blood was obtained from each mouse at predetermined time points after infection, and viable counts were determined, as described above. The growth of pneumococci in the nasopharynx was also determined, as described previously [39,45]. For this, at predetermined time intervals following intranasal infection, pre assigned groups of mice were deeply anesthetized with 5% (vol/vol) isoflurane over oxygen, and the mice were subsequently killed by cervical dislocation. Nasopharyngeal tissue was collected as described previously [39,45] and transferred into 10 ml of sterile PBS, weighed, and then homogenized with an Ultra Turrax blender (Ika-Werke). Viable counts in homogenates were determined as described above.

Survival times were calculated by using GraphPad Prism software and analysed by the Mann-Whitney U test. Data were analysed by an analysis of variance followed by the Bonferroni post-test. Statistical significance was considered to be a *p*-value of < 0.05.

Chemicals

N-acetylglucosamine 6-phosphate (GlcNAc6P) was obtained through a modification of established procedures [46,47] according to Fig. S2.1. The synthesis of tagatose 1,6-diphosphate (TBP) is described in Fig. S2.2. Modifications to the synthesis of TBP previously published [48] were made in order to optimize the process (see Text S2.1). The synthesized compounds were quantified by ^{1}H-NMR, using a Brucker AMX300 spectrometer (Brucker BioSpin GmbH). DSS, used as an internal concentration standard in ^{1}H-NMR quantifications, was purchased from Merck.

Galactose, mannose, and N-acetylneuraminic acid were purchased from Sigma-Aldrich. Glucose was supplied by Merck and N-acetyl-D-galactosamine, N-acetyl-D-glucosamine, glucosamine and galactosamine were purchased from Applichem. All other chemicals used were reagent grade.

Ethical disclaimer

Mouse experiments at the University of Leicester were performed under appropriate project (no. 60/4327) and personal (no. 80/10279) licenses according to the United Kingdom Home Office guidelines and local ethical approval. The animal work is approved by Animal Welfare and Ethical Review Body (AWERB) ethics committee. Where appropriate, the procedures were carried out under anaesthesia with isoflurane.

Results

Genomic potential for the utilization of host monosaccharides

Host glycans are rich in the carbohydrate monomers Gal, GalNAc, GlcNAc, NeuNAc, mannose (Man) and Fuc. We set out to uncover the genomic potential of *S. pneumoniae* D39 for utilization of these sugars and amino sugars by performing pathway reconstruction using data from the literature and deposited in metabolic databases (MetaCyc and Kegg), as well as by protein homology (BlastP) to functionally characterized enzymes (Fig. 2.1 and Table S2.4). In general, our systematic analysis confirmed genome annotations, and a schematic representation of the inferred sugar catabolic pathways is depicted in Fig. 2.1. A more detailed description is provided as supplemental material (Table S2.4 and Text S2.2).

Galactose can be metabolized via the Leloir or tagatose 6-phosphate (T6P) pathways (Fig. 2.1), and homologues of the genes involved in both pathways are present in the genome (Table S2.4). A duplication event of the Leloir genes, *galT* and *galE,* seems to have occurred (Table S2.4), but whether the proteins are functional is unknown. Mannose is, most likely, taken up via a PTS [8] and the phosphorylated product isomerised to fructose 6-phosphate (F6P) via mannose 6-phosphate isomerase. Complete pathways for utilization of GalNAc and Fuc could not be successfully reconstituted using the tools in this work. *S. pneumoniae* D39 also possesses homologues of all proteins involved in the bacterial superpathway for the dissimilation of the amino sugars N-acetylneuraminate and GlcNAc (Table S2.4 and Text S2.2) [49].

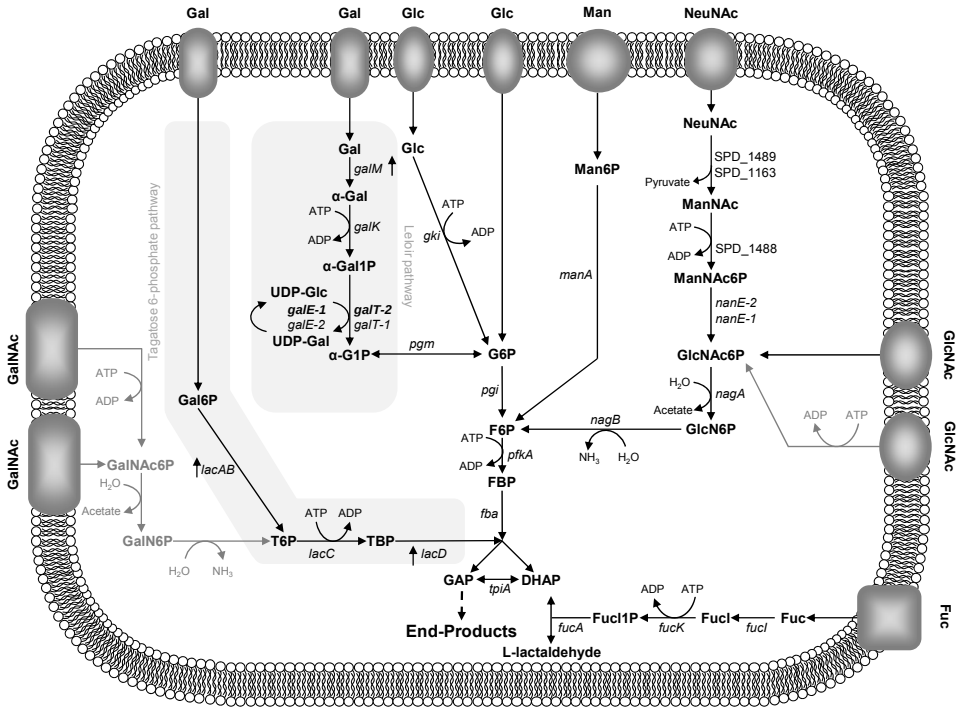

Figure 2.1. Schematic representation of the proposed pathways for the dissimilation of monosaccharides originating from deglycosylation of host glycans in *S. pneumoniae* D39.

Pathways were reconstructed resorting to metabolic databases (MetaCyc and KEGG), genome annotations at NCBI and literature. Genes and intermediates involved in the galactose (Gal), mannose (Man), N-acetylneuraminic acid (NeuNAc), N-acetylgalactosamine (GalNAc), N-acetylglucosamine (GlcNAc) and fucose (Fuc) catabolism are shown. Initial steps of glycolysis are depicted.

galM, aldolase 1-epimerase; *galK,* galactokinase; *galT-1*, *galT-2*, galactose 1-phosphate uridylyltransferase; *galE-1*, *galE-2*, UDP-glucose 4-epimerase; *pgm*, phosphoglucomutase/phosphomannomutase family protein; *lacA*, galactose 6-phosphate isomerase subunit LacA; *lacB*, galactose 6-phosphate isomerase subunit LacB ; *lacC*, tagatose 6-phosphate kinase; *lacD*, tagatose 1,6-diphosphate aldolase; *manA*, mannose 6-phosphate isomerase; SPD_1489, SPD_1163, N-acetylneuraminate lyase; SPD_1488, ROK family protein, *nanE-1*, *nanE-2*, N-acetylmannosamine 6-phosphate 2-epimerase; *nagA*, N-acetylglucosamine 6-phosphate deacetylase; *nagB*, glucosamine 6-phosphate isomerase; *fucI*, L-fucose isomerase; *fucK*, L-fuculose kinase; *fucA*, L-fuculose phosphate aldolase.

α-Gal, α-galactose; α-Gal1P, α-galactose 1-phosphate; α-G1P, α-glucose 1-phosphate; UDP-Glc, UDP-glucose; UDP-Gal, UDP-galactose; Gal6P, galactose 6-phosphate; T6P, tagatose 6-phosphate; TBP, tagatose 1,6-diphosphate; Man6P, mannose 6-phosphate; ManNAc, N-acetylmannosamine; ManNAc6P, N-acetylmannosamine 6-phosphate; GlcNAc6P, N-acetylglucosamine 6-phosphate; GlcN6P, glucosamine 6-phosphate; FucI,

fuculose; FucI1P, fuculose 1-phosphate; GalNAc6P, N-acetylgalactosamine 6-phosphate; GalN6P, galactosamine 6-phosphate.
The upper glycolytic intermediates and gene annotations are as follows: G6P, glucose 6-phosphate; F6P, fructose 6-phosphate; FBP, fructose 1,6-biphosphate; GAP, glyceraldehyde 3-phosphate; DHAP, dihydroxyacetone phosphate. *gki*, glucokinase; *pgi*, glucose 6-phosphate isomerase; *pfkA*, 6-phosphofructokinase; *fba*, fructose-biphosphate aldolase; *tpiA*, triosephosphate isomerase. The lower glycolytic pathway is represented by a dashed arrow. Pathways or steps present in other organisms but uncertain in D39 are represented in grey.
Vertical arrows near the gene name indicate the upregulation during growth on mucin as compared to Glc, in *S. pneumoniae* D39.

The ability of host glycan-derived sugars to support growth is sugar dependent

The presence of the genes for a full metabolic pathway in the genome does not confirm that the pathway is functional. Thus, we assessed the ability of monosaccharide constituents of host glycans to support growth of *S. pneumoniae* D39 in a chemically defined medium (Fig. 2.2). Of the monosaccharides tested, growth was observed on glucosamine, GlcNAc, Gal and Man. In contrast, *S. pneumoniae* was unable to use GalNAc, galactosamine (Fig. 2.2) and NeuNAc (data not shown) as single carbon sources for growth. Fucose was not tested, since inability to grow in this sugar has been previously documented [8,50–52]. The ability of each sugar to sustain growth was consistent with the conclusions from genome analysis.

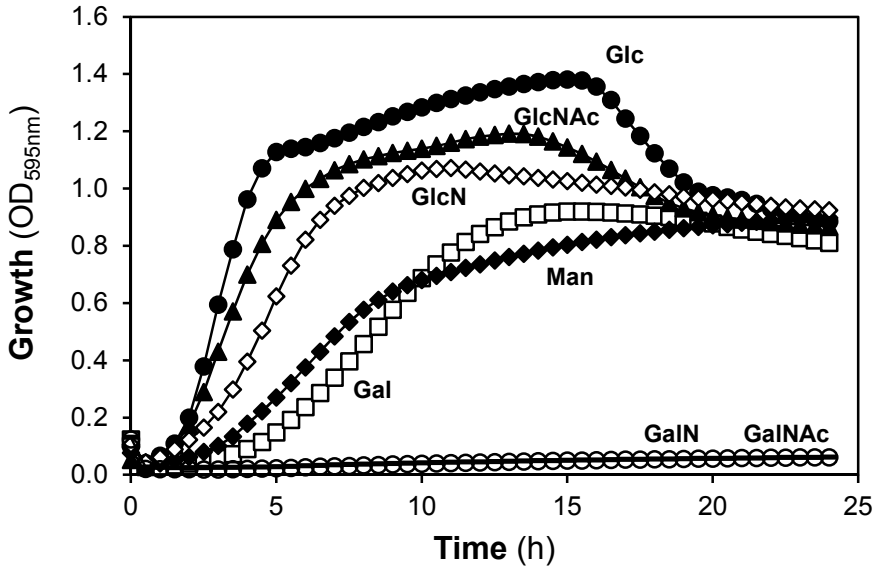

Figure 2.2. Growth of *S. pneumoniae* D39 in glycan-derived sugars.

Growth profiles of D39 grown in CDM supplemented with 30 mM of galactose (Gal), mannose (Man), N-acetylglucosamine (GlcNAc), glucosamine (GlcN), N-acetylgalactosamine (GalNAc), galactosamine (GalN) and glucose (Glc). Growth experiments were performed at 37ºC and at an initial of pH 6.5, using a 96-well microtiter plate reader.
Symbols: (●) Glc; (▲) GlcNAc; (◇) GlcN; (□) Gal; (◆) Man, (▬) GalNAc and (○) GalN. Growth curves are plotted in decimal scale to assess for significant differences in the growth profiles.

Mucin induces expression of genes involved in utilization of Gal, GlcNAc and Man

Mucins are the most abundant glycoproteins in the human respiratory tract, and *S. pneumoniae* is capable of growing on mucin as sole carbon source [12]. To reveal prevalent pathways during growth on mucin, we performed a whole transcriptome analysis comparing the mRNA levels of *S. pneumoniae* D39 cells grown on porcine gastric mucin to those of cells grown on glucose (Glc) (see Materials and Methods). The reasoning for this experimental design was that genes potentially involved in the utilization of sugar moieties in mucin would be upregulated. Accordingly,

39 out of 83 genes that were significantly differentially expressed (according to the established criterion) encode for proteins with predicted functions in sugar processing (modification, uptake and catabolism) (Table 2.1).

Seven of the upregulated genes were involved in the hydrolysis of sugars (Table 2.1). Of note, *bgaA* encoding a β-galactosidase, the activity of which results in free Gal, showed the highest differential expression value. *strH,* which codes for a *β-N*-acetylhexosaminidase, involved in the hydrolysis of terminal non-reducing *N*-acetyl-D-hexosamine residues, was the second most upregulated glycosidase (Table 2.1).

Among the genes implicated in sugar processing (Table 2.1), 49% encode components of PTS or ABC transporters. Three genes encoding a complete PTS in the galactitol family, and presumably involved in Gal uptake [8,53], showed a high positive response to mucin. In the genome of D39, this Gat-PTS transport system is located upstream of the *bgaA* locus. Also, highly overexpressed was the Man-PTS family transporter (SPD_0066-8-9) presumably involved in Gal and Man transport (Tables 2.1 and S2.4) [8]. In fact, genes putatively involved in Man uptake represented the highest fraction of transport systems upregulated in the presence of mucin (Tables 2.1 and S2.4). Moreover, a gene (SPD_1496) presumed to be involved in the translocation of GlcNAc was found differentially overexpressed (Tables 2.1 and S2.4), in accordance with the observed upregulation of *strH*. Mucin also induced the expression of genes potentially involved in NeuNAc uptake (Tables 2.1 and S2.4).

Finally, genes involved in both Gal catabolic routes, *lacAB* and *lacD* of T6P pathway and *galM* of the Leloir pathway were highly overexpressed during growth on mucin (Table 2.1 and Fig. 2.1). Expression levels of selected genes, obtained by qRT-PCR, confirmed the transcriptome results (Table S2.6).

Table 2.1. Expression levels of genes upregulated in *S. pneumoniae* D39 cells grown in mucin as compared to glucose-grown cells [a,b].

Locus-tag	Gene	Function	Overexpression fold
SPD_0562	*bgaA*	Beta-galactosidase	71.8
SPD_1057		PTS system transporter subunit IIB	61.3
SPD_0561		PTS system transporter subunit IIC	45.5
SPD_0068		PTS system transporter subunit IID	25.4
SPD_1053	*lacA*	Galactose 6-phosphate isomerase subunit LacA	24.5
SPD_0069		PTS system transporter subunit IIA	23.9
SPD_1052	*lacB*	Galactose 6-phosphate isomerase subunit LacB	21.7
SPD_0071	*galM*	Aldose 1-epimerase	19.4
SPD_1050	*lacD*	Tagatose 1,6-diphosphate aldolase	17.6
SPD_0559		PTS system transporter subunit IIA	15.1
SPD_0560		PTS system transporter subunit IIB	12.1
SPD_1494		Sugar ABC transporter permease	10.3
SPD_0070	*agaS*	Sugar isomerase	9.8
SPD_0063	*strH*	Beta-N-acetylhexosaminidase	8.7
SPD_1663	*treC*	Alpha,alpha-phosphotrehalase	8.0
SPD_0066		PTS system transporter subunit IIB	7.8
SPD_0287		Hyaluronate lyase	7.7
SPD_1495		Sugar ABC transporter sugar-binding protein	6.7
SPD_0293		PTS system transporter subunit IIA	6.5
SPD_1834		Bifunctional acetaldehyde-CoA/alcohol dehydrogenase	5.8
SPD_0292		Gluconate 5-dehydrogenase	5.3
SPD_1409		Sugar ABC transporter ATP-binding protein	4.8
SPD_1934	*malX*	Maltose/maltodextrin ABC transporter maltose/maltodextrin-binding protein	4.8
SPD_0297		PTS system transporter subunit IID	4.4
SPD_1496		PTS system transporter subunit IIBC	4.4
SPD_1006	*glgC*	Glucose 1-phosphate adenylyltransferase	4.4
SPD_0621	*lctO*	Lactate oxidase	4.0
SPD_1935	*malC*	Maltodextrin ABC transporter permease	3.9
SPD_0420	*pflB*	Formate acetyltransferase	3.7
SPD_1007	*glgD*	Glucose 1-phosphate adenylyltransferase, GlgD subunit	3.5
SPD_1005	*glgB*	Glycogen branching protein	2.9

Locus-tag	Gene	Function	Overexpression fold
SPD_1936	*malD*	Maltodextrin ABC transporter permease	2.9
SPD_0250		Pullulanase, extracellular	2.9
SPD_1989		PTS system transporter subunit IID	2.6
SPD_0427	*lacG-1*	6-phospho-beta-galactosidase	2.5
SPD_1675	*rafG*	Sugar ABC transporter permease	2.4
SPD_0925		Hydrolase	2.4
SPD_1937	*malA*	Maltodextrose utilization protein MalA	2.3
SPD_0424		PTS system cellobiose-specific transporter subunit IIC	2.2

[a] Only genes potentially involved in sugar hydrolysis, uptake and metabolism are shown. Hypothetical proteins have been omitted.

[b] For a complete appreciation a full list of the significantly differentially expressed genes is provided in Table S2.5.

In summary, our transcriptome analysis revealed that mucin induced the expression of genes required to benefit from Gal, GlcNAc and Man residues present in host glycans. Capitalizing on the growth and expression data, we surmised that these sugars are important carbon sources for D39 during colonisation of the nasopharynx. Hence, we set out to characterize growth and validate predicted metabolic pathways for utilization of Gal, GlcNAc and Man.

Growth properties on Gal, GlcNAc and Man or on a mixture thereof

Growth parameters and fermentation end-products were determined in batch cultures of *S. pneumoniae* D39 using chemically defined medium and two concentrations of Gal, GlcNAc or Man: 13±1 mM and a higher non-limiting 34±2 mM.

Growth profiles on Gal, Man and GlcNAc.

Representative growth profiles (experimental data) and model 95% confidence and prediction curves that best describe the growth data are

depicted in Fig. 2.3. In general, the model fits well with the experimental data. The 95% confidence curves (Fig. 2.3) reveal that the larger differences between biological growth replicas occur at the final stage of the growth, as shown by higher discrepancies in the final optical density (OD_{max}) rather than specific growth rate (μ_{max}). The parameters derived from the growth analysis are shown in Table 2.2. Analysis through ANOVA and pairwise t-tests allowed assessment of the statistical significance of the growth parameter differences across the experimental conditions (Table S2.2).

In medium containing the higher substrate concentration, GlcNAc supported a significantly faster growth than Gal and Man (Tables 2.2 and S2.2). However, no significant differences (p=0.15) were found between cells growing on higher concentrations of Gal or Man, with the specific growth rate similar in both conditions (Tables 2.2 and S2.2). In contrast, for the lower substrate concentration, the growth rate was sugar dependent with the amino sugar supporting a significantly higher growth rate than Man or Gal (Tables 2.2 and S2.2). The specific growth rate is independent of the initial substrate concentration (Table 2.2), except for Gal which supports higher growth rates when the substrate is in excess. The involvement of a low affinity transporter in the uptake of this sugar would explain this behaviour.

When the higher substrate concentration was used, Gal supported the highest final biomass, which was similar to that on Glc (p=0.06) (Tables 2.2 and S2.2). No significant differences in the final biomass (p=0.89) were observed between growths on GlcNAc and Man, which were lower than that on Gal (Tables 2.2 and S2.2). At the lower substrate concentration the biomass formed was similar for the glycan-derived sugars and Glc, and unsurprisingly lower than those obtained using non-limiting sugar concentrations (Fig. 2.3, Tables 2.2 and S2.2).

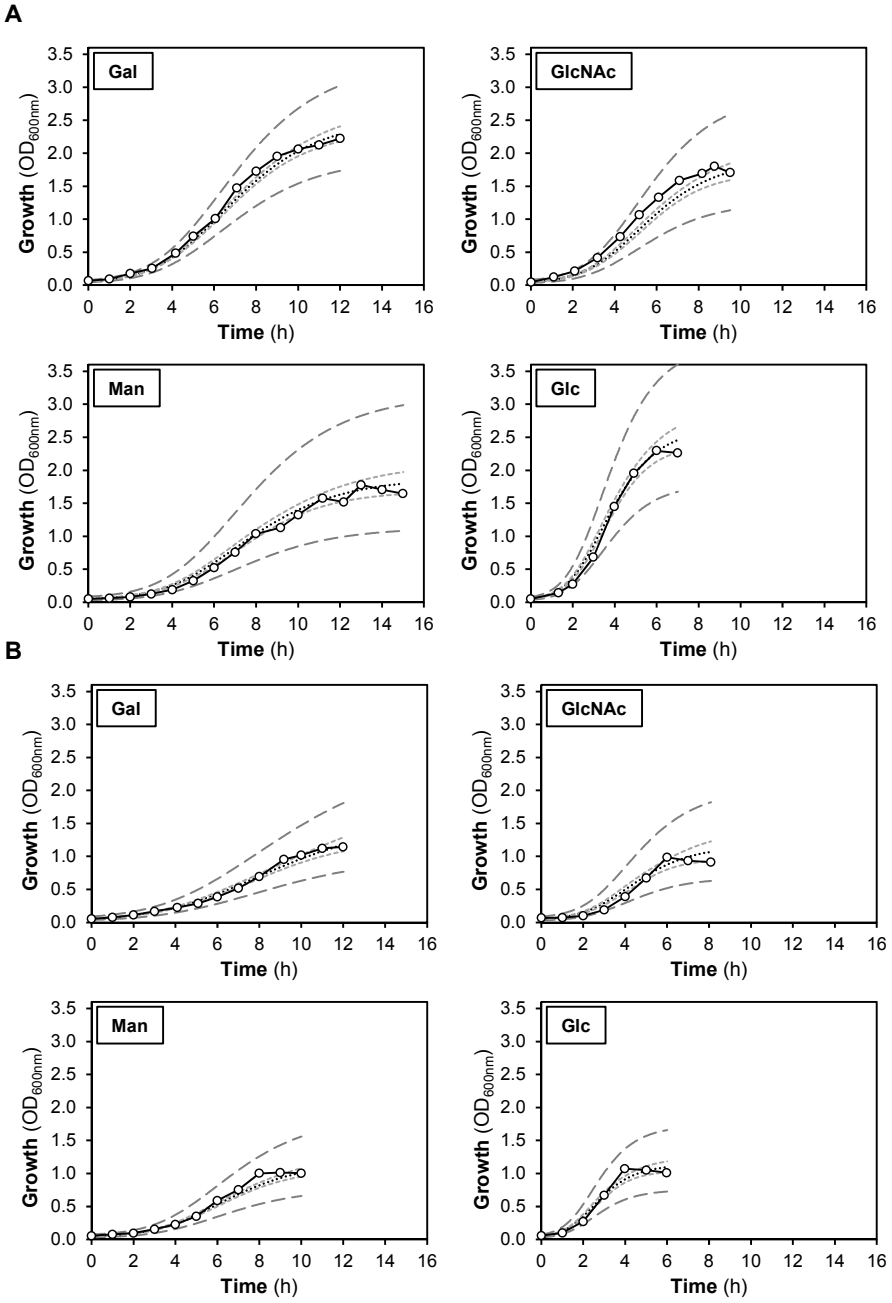

Figure 2.3. Representative growth profiles of *S. pneumoniae* D39 grown in CDM in the presence of two different concentrations of galactose (Gal), N-acetylglucosamine (GlcNAc), mannose (Man) or glucose (Glc).

Growth profiles in 80 ml batch cultures using (**A**) excess substrate concentration (34±2 mM) and (**B**) a 3-fold lower initial substrate concentration (13±1 mM).
Representative growth curves (empty dots) were selected based on the established criterion (see Materials and Methods). The experimental data was fitted using the Gompertz model with all replicates (estimated curve in black dashed line) and the 95% confidence bands (small dashed light grey lines) and 95% predicted bands (big dashed dark grey lines) were determined (see Materials and Methods).
Growth was performed at 37ºC, under semi-anaerobic conditions, without pH control (initial pH 6.5). Growth curves are plotted in decimal scale to allow the visual discernment between significantly differences in the growth parameters using the two initial substrate concentrations.

In medium with Gal, growth arrest occurred before substrate depletion, even for the low Gal concentration (Table 2.2). For the higher sugar concentrations, a pH decrease of about one unit was observed at the onset of stationary phase, which is consistent with growth arrest due to acidification. However, the observed change in pH of 0.5 units does not explain the arrest of growth in the lower Gal concentration. Even though a full explanation cannot be put forward, the possession of only low-affinity Gal importers can be proposed as a cause for growth slow-down with decreasing Gal concentrations.

Table 2.2. Growth and energetic parameters of *S. pneumoniae* D39 on sugars present in host glycans.

	GlcNAc		Gal		Man		Glc		Mix
[substrate]$_{initial}$ (mM)	**30.8±0.6**	**12.3±0.6**	**33.7±1.5**	**13.4±1.3**	**33.4±0.3**	**12.4±0.1**	**34.2±1.8**	**12.9±0.4**	**6.5±0.3[a]**
μmax (h^{-1})	0.55±0.06	0.54±0.08	0.48±0.04	0.32±0.03	0.45±0.04	0.44±0.04	0.93±0.07	0.93±0.09	0.61±0.05 0.07±0.01[b]
OD_{600max}	1.76±0.25	0.99±0.08	2.16±0.12	1.12±0.26	1.77±0.16	1.03±0.08	2.29±0.17	1.06±0.04	1.19±0.11
ΔpH	1.10±0.08	0.41±0.05	1.02±0.06	0.48±0.07	1.23±0.15	0.44±0.03	1.28±0.09	0.44±0.03	0.57±0.08
Substrate Consumed (%)	93±6	100±0	69±9	84±7	87±10	100±0	92±4	100±0	86±2
Substrate Recovery	87±5	84±3	72±1	76±9	85±9	89±3	86±5	84±2	79±3
Redox Balance	86±5	83±3	70±2	75±5	85±9	85±3	85±5	82±1	81±4
ATP yield (mol mol^{-1} substrate)	1.77±0.09	1.74±0.08	2.08±0.03	2.27±0.31	1.80±0.21	1.98±0.04	1.75±0.11	1.71±0.04	1.73±0.06
YATP (g biomass mol^{-1} ATP)	12.1±0.7	16.8±0.9	17.5±1.4	14.9±0.5	13.6±1.4	16.2±0.4	15.3±0.8	18.8±0.0	16.4±0.4
Ybiomass (g mol^{-1} substrate)	21.4±2.4	29.3±2.9	36.3±2.4	34.1±5.8	24.3±0.3	31.9±0.1	26.7±0.3	32.0±0.8	28.3±1.8

Growth rate, maximal biomass, yields, carbon and redox balances, substrate consumed and variation of pH were obtained for *S. pneumoniae* D39 grown in CDM in the presence of N-acetylglucosamine (GlcNAc), galactose (Gal), mannose (Man) and glucose (Glc) using two substrate concentrations or in a mixture of Gal, Man and GlcNAc (*circa* 6.5 mM each). Growth was performed at 37ºC without pH control (initial pH 6.5). Values represent the average and standard deviation of at least two independent growth experiments and are estimated at the time point of growth arrest (maximal biomass).

[a]The value represents the average ± standard deviation of the concentration of sugars present in the mixture. Individual values are: Gal, 6.4±0.7 mM; Man, 6.6±0.1 mM and GlcNAc, 6.7±0.2 mM.

[b]Second specific growth rate.

ΔpH is the difference between the initial pH and the pH at the time of growth arrest; **substrate recovery** is the percentage of carbon in metabolized sugar that is recovered in the fermentation products (lactate, ethanol, acetate, and formate); **redox balance** is the ratio between [lactate]+2×[ethanol] and 2×[substrate consumed] multiplied by 100.

Fermentation products.

End-products resulting from the fermentations of Gal, GlcNAc and Man are shown in Table 2.3. *S. pneumoniae* displayed a fully homolactic fermentation profile when GlcNAc was the sole carbon source, regardless of the initial concentration. In addition to lactate, acetate, ethanol and formate were produced as minor fermentation products (Table 2.3). On Man, the fermentation profile was still mainly homolactic. However, a shift towards mixed acid fermentation was evident, accounting for 9% and 17% of the substrate consumed in the higher and lower substrate concentrations, respectively. In contrast, cells grown on Gal showed a pronounced mixed acid fermentation (Table 2.3), independently of the initial concentration of sugar. Formate, ethanol and acetate were produced in the ratio 2:1:1, as expected from mixed acid fermentation under anaerobic conditions. Lactate was detected as a minor fermentation product, accounting for 8% and 2% of the consumed Gal, for the higher and lower substrate concentration, respectively (Table 2.3). The shift towards mixed acid fermentation profile was generally higher for the lower substrate concentrations.

The calculated values for substrate recovery are in good agreement with fermentative metabolism (above 80%). On Gal, carbon balances in the 70% range were determined, indicating an additional carbon sink (Table 2.2).

Table 2.3. End-products derived from the catabolism of N-acetylglucosamine (GlcNAc), galactose (Gal), mannose (Man) and glucose (Glc) by *S. pneumoniae* D39, using 34±2 mM or 13±1 mM initial substrate concentrations.

	Higher substrate concentration				**Lower substrate concentration**			
Sugar	GlcNAc	Man	Gal	Glc	GlcNAc	Man	Gal	Glc
[End-products] (mM)								
Lactate	49.02±8.19	43.80±0.11	3.88±0.54	53.10±1.59	19.42±0.35	17.27±1.63	0.50±0.00	20.93±0.29
Acetate	0.92±0.10	2.68±0.17	14.91±1.24	0.83±0.38	0.79±0.14	2.44±0.26	8.43±0.06	0.46±0.12
Ethanol	0.48±0.08	2.66±1.67	14.30±1.53	0.10±0.04	0.42±0.11	1.64±0.43	8.16±0.86	0.08±0.02
Formate	1.62±0.43	5.10±0.75	29.43±1.85	BDL	1.82±0.73	3.77±0.44	16.53±0.84	BDL

Growth was done in CDM supplemented with the appropriate sugar, at 37ºC, under semi-anaerobic conditions, without pH control (initial pH 6.5). The results represent averages of at least two experiments and the error bars the standard deviation.

BDL, below detection limit. In glucose grown cells, formate was produced, but in quantities below the limit of quantification.

Growth profiles, substrate consumption and end-products of fermentation in a mixture of Gal, GlcNAc and Man.

In its ecological niche, *S. pneumoniae* is exposed to a multiplicity of sugars. Thus, we set out to evaluate growth on a sugar mixture containing Gal, GlcNAc and Man. An initial concentration of approximately 6.5 mM for each carbohydrate, was tested (Fig. 2.4). On the sugar mixture, *S. pneumoniae* D39 displayed a biphasic growth profile. The maximal growth rate (μ_1) was observed within the first 4 h of growth and was about nine times higher than the second growth rate (μ_2) (Fig. 2.4A). Interestingly, μ_1 was similar to that determined in the presence of the lower concentration of GlcNAc alone (Table 2.2), suggesting that this sugar was consumed first.

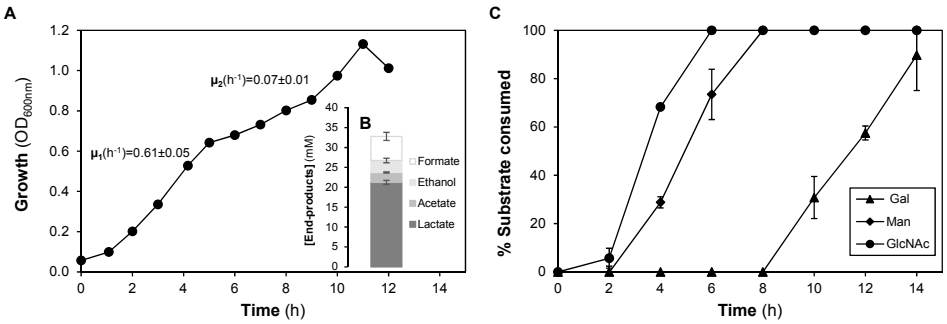

Figure 2.4. Growth profile of D39 in a mixture of galactose (Gal), mannose (Man) and N-acetylglucosamine (GlcNAc).

(**A**) Representative growth curve of *S. pneumoniae* D39 grown in CDM supplemented with a mixture of Gal, GlcNAc and Man (6.5 mM each), at 37ºC, under semi-anaerobic conditions, without pH control (initial pH 6.5). (**B**) End-products of fermentation derived from the catabolism of the sugars in the mixture (Gal, Man and GlcNAc), determined at the time of growth arrest (maximal biomass). (**C**) Gal, Man and GlcNAc consumption, over time, during the growth of *S. pneumoniae* D39 in CDM. The values are percentages of the initial sugar concentration for each sugar.
The representative growth curve was selected based on the established criterion (see Materials and Methods). The results represent averages of two independent growths and the error bars represent the standard deviation.

The profile of sugar utilization was determined by measuring the sugars in the culture medium using ^{1}H-NMR (Fig. 2.4C). We confirmed that GlcNAc was consumed first and was totally depleted after 6 h of growth. Consumption of Man started while GlcNAc was still available, and its depletion occurred 8 h after inoculation. Interestingly, Gal was only used after depletion of GlcNAc and Man. This is in good agreement with the two distinct growth rates found: the first is related to GlcNAc and Man consumption, whereas the second mostly reflects the utilization of Gal.

In the sugar mixture, the end-products profile was mainly homolactic, with lactate as the major product (21.2 ± 0.5 mM) (Fig. 2.4B). Minor quantities of formate, ethanol and acetate were formed in a proportion of 2:1:1. (Fig. 2.4B). Growth arrest was most likely not due to acidification, since only a modest change in pH (ΔpH) was registered (Table 2.2). On the other hand, Gal was not fully consumed, with approximately 40% remaining in the medium at the time of growth arrest (12 h after inoculation) (Table 2.2 and Fig. 2.4C). A similar behaviour was observed when Gal was used as single carbon source. These results demonstrated that *S. pneumoniae* D39 is able to metabolize different carbon sources simultaneously or sequentially. In a mixture consisting of 6.5 mM GlcNAc, Man and Gal, strain D39 had a preference for GlcNAc, but could use Man concurrently. Gal was the least preferred sugar, and was only consumed after exhaustion of the two other carbon sources.

Catabolic pathways for the utilization of Gal, GlcNAc and Man as assessed using biochemical and molecular tools

Experimental confirmation of the predicted metabolic routes for the catabolism of Gal, Man and GlcNAc was performed at the biochemical level through metabolite profiling by ^{31}P-NMR and enzyme activity measurements, and at the genetic level by mutating key genes in the pathways.

Intracellular metabolites during growth on glycan-derived sugars.

Ethanol extracts of growing cells were examined for phosphorylated intermediates of catabolic pathways by targeted metabolomics using ^{31}P-NMR. In extracts derived from *S. pneumoniae* D39 Gal-grown cells, phosphorylated intermediates of the Leloir pathway, α-galactose 1-phosphate (α-Gal1P) and α-glucose 1-phosphate (α-Glc1P), as well as phosphorylated metabolites involved in the T6P pathway: galactose 6-phosphate (Gal6P) and tagatose 1,6-diphosphate (TBP), were detected (Fig. 2.5), indicating the active presence of both catabolic routes for Gal catabolism. These data are in agreement with an earlier report for a different isolate of *S. pneumoniae* strain D39 [9]. The accumulation of mannose 6-phosphate (Man6P) during growth on Man is a strong indication of the functioning of the predicted catabolic route (Figs. 2.1 and 2.5). The intracellular intermediates predicted in the catabolic pathway of GlcNAc, N-acetylglucosamine 6-phosphate (GlcNAc6P) and glucosamine 6-phosphate (GlcN6P), were detected in the extracts of cells grown on this carbon source (Figs. 2.1 and 2.5). Surprisingly, fructose 6-phosphate (F6P) was highly accumulated under this condition.

Thus, the occurrence of specific phosphorylated metabolites in cell extracts correlated well with the predicted metabolic intermediates in the catabolism of each sugar.

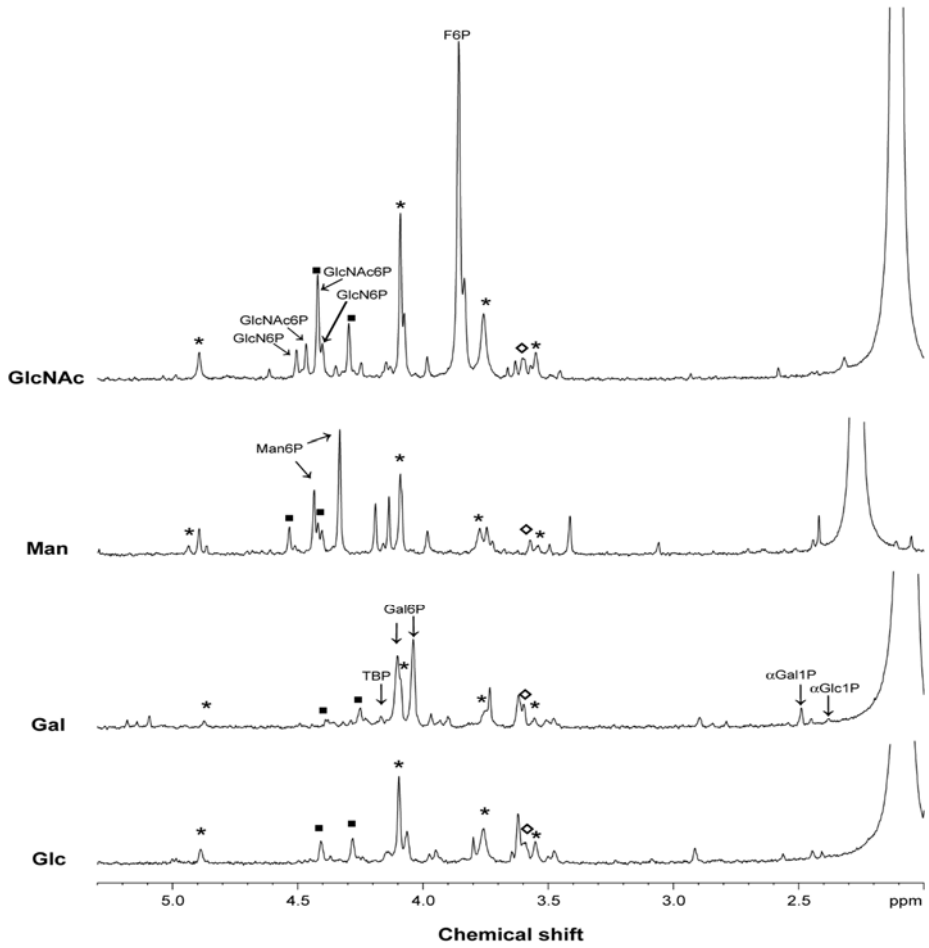

Figure 2.5. Phosphomonoester region of ^{31}P-NMR spectra of ethanol extracts obtained in late-exponential cells of *S. pneumoniae* D39 grown in CDM with galactose (Gal), mannose (Man) or N-acetylglucosamine (GlcNAc).

Ethanol extracts of glucose (Glc) grown cells were used as control. The glycolytic intermediates fructose 1,6-biphosphate (FBP), glucose 6-phosphate (G6P) and 3-phosphoglycerate (3-PGA) were firmly assigned.
Abbreviations: αGal1P, α-galactose 1-phosphate; αGlc1P, α-glucose 1-phosphate; TBP, tagatose 1,6-diphosphate; Gal6P, galactose 6-phosphate; Man6P, mannose 6-phosphate; GlcN6P, glucosamine 6-phosphate; GlcNAc6P, N-acetylglucosamine 6-phosphate and F6P, fructose 6-phosphate.
Identification of phosphorylated intermediates was performed by spiking the ethanol extracts with pure compounds. Symbols: (*) FBP, (■) G6P, (◇) 3-PGA.

Enzymatic activities of key enzymes involved in the catabolism of glycan-derived sugars.

To further substantiate the functioning of the predicted pathways, we selected enzymes presumed to be required for pathway activity, galactokinase (GalK, SPD_1634) and tagatose 1,6-diphosphate aldolase (LacD, SPD_1050) for Gal, mannose 6-phosphate isomerase (ManA, SPD_0641) for Man and N-acetylglucosamine 6-phosphate deacetylase (NagA, SPD_1866) for GlcNAc, and determined their specific activities using specific biochemical assays (see Materials and Methods).

On galactose, the specific activities of GalK and LacD in cell-free extracts of D39 were considerably higher than those measured on Glc-grown cells (Table 2.4), suggesting induction of the pathway on Gal. These data are consistent with the functioning of both pathways during growth on Gal. The GalK specific activity was higher than the LacD specific activity, under the conditions assayed (Table 2.4).

The specific activity of N-acetylglucosamine 6-phosphate deacetylase (NagA), the enzyme dedicated to GlcNAc catabolism, was 2-fold higher when grown on GlcNAc than in Glc-grown cells (Table 2.4). The method to assay NagA, couples its activity to that of glucosamine 6-phosphate isomerase (NagB). The latter was not limiting in the assay, since its specific activity was 4 times higher than that of NagA (data not shown).

Table 2.4. Enzyme specific activities determined in extracts of *S. pneumoniae* derived from cells grown to late-exponential phase of growth in CDM supplemented with different monosaccharides.

Strain	Growth condition (carbon source)	**Specific activities** (U mg protein^{-1}) GalK	LacD	NagA	ManA
D39	Gal	0.89 ± 0.11	0.08 ± 0.01	-	-
D39	GlcNAc	-	-	0.04 ± 0.00	-
D39	Man	-	-	-	0.10 ± 0.01
D39	Glc	BDL	BDL	0.02 ± 0.00	0.07 ± 0.01
D39Δ*galK*	Glc	BDL	-	-	-
D39Δ*lacD*	Gal	-	BDL	-	-
D39Δ*nagA*	Glc	-	-	BDL	-
D39Δ*manA*	Glc	-	-	-	0.04 ± 0.01

Specific activity is expressed as units (U) (µmol min^{-1}) per milligram of protein (U mg protein^{-1}).
GalK specific activity is defined as the amount of protein required for the formation of 1 µmol of Gal1P min^{-1} mg protein^{-1}. LacD specific activity is given as the amount of protein required to catalyse the oxidation of 1 µmol of NADH min^{-1} mg protein^{-1}. NagA and ManA specific activities are the amount of protein to reduce 1 µmol of NADP min^{-1} mg protein^{-1}. The values reported represent averages ± standard deviation obtained in cell-free extracts of at least two independent cultures.
-, not determined.
BDL, below detection limit.

The key enzyme of the Man catabolic pathway, ManA, was detected in Man-grown cells, but the level was only marginally reduced (30%) in Glc-grown cells (Table 2.4).

In summary, enzyme activities of dedicated sugar catabolic enzymes were detected for each metabolic pathway assayed, indicating the operability of the dissimilation routes proposed.

Genetic confirmation of pathway functionality.

The biochemical approach to investigate the Gal, Man and GlcNAc catabolic pathways was complemented by a genetic approach. Mutants in key enzymatic steps of each catabolic route were constructed by allelic replacement mutagenesis, yielding D39Δ*galK*, D39Δ*lacD*, D39Δ*manA* and D39Δ*nagA* (Fig. S2.3). The mutations were confirmed by growth profiles and enzyme activity measurement (Table 2.4 and Fig. 2.6). The deletion mutants lost the activity encoded by the inactivated gene, except for the D39Δ*manA* mutant (Table 2.4).

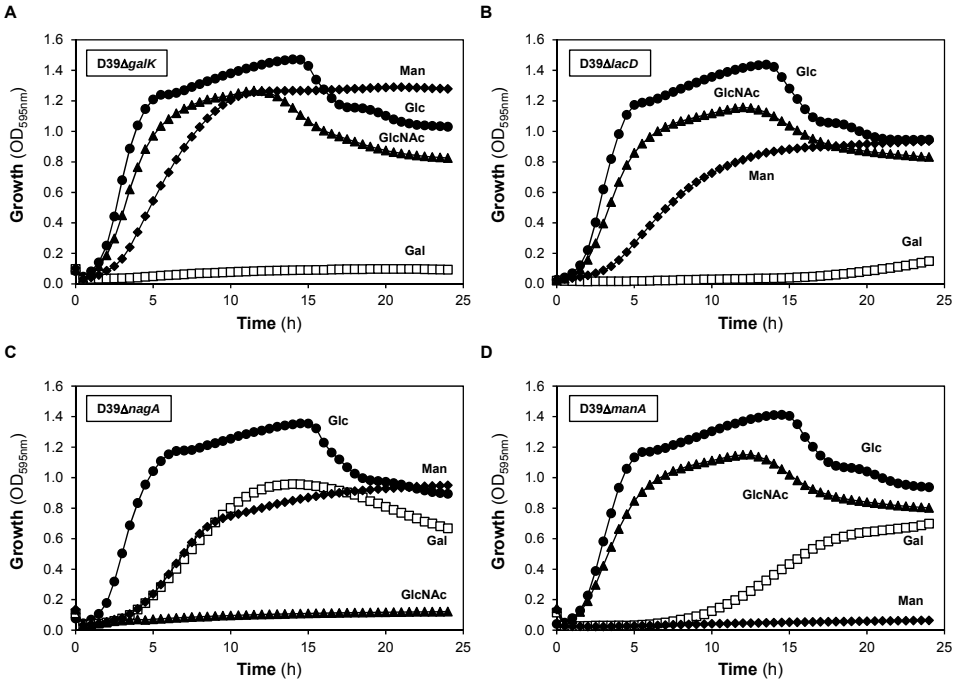

Figure 2.6. Growth profile of D39 sugar-specific mutants.

Growth phenotypes of (**A**) D39Δ*galK*, (**B**) D39Δ*lacD*, (**C**) D39Δ*nagA* and (**D**) D39Δ*manA*. Growth was performed in CDM supplemented with galactose (Gal), N-acetylglucosamine (GlcNAc), mannose (Man) or glucose (Glc), using the 96-well microplate reader. Symbols: (▲) GlcNAc; (♦) Man; (□) Gal and (●) Glc.

In Glc-grown D39Δ*manA*, the activity of mannose 6-phosphate isomerase showed a 43% and 60% reduction compared to that in Glc- or Man-grown wild type D39 cells, respectively (Table 2.4).

Importantly, the D39Δ*manA* or D39Δ*nagA* strains were unable to use Man or GlcNAc as sole carbon source, respectively (Fig. 2.6C and 6D). D39Δ*lacD* was able to grow on Gal, although only after a lag period of *circa* 20 h (Fig. 2.6B). A mutant in both Gal catabolic pathways was constructed, D39Δ*lacD*Δ*galK*, which lost the ability to grow on this monosaccharide. Unexpectedly, inactivation of *galK* alone resulted in a strain unable to grow on Gal, even though the T6P pathway was still intact (Fig. 2.6A). All pathway-specific mutants were able to grow on sugars other than the substrate of the targeted catabolic pathway (Fig. 2.6). To ensure that growth abrogation was unrelated to possible polar effects, complementation studies were conducted (see Materials and Methods, Fig. S2.4). D39Δ*manA and* D39Δ*lacD* complemented with *manA* and *lacD* under the Zn^{2+}-inducible promoter (P_{czcD}) [54], had fully restored growth on Man and Gal, respectively. It is worth noting that growth on Man was better in the complemented D39Δ*manA* as compared to wild type D39, suggesting that the ManA activity level might be a limiting factor for Man utilization (Fig. S4D). For the D39Δ*nagA*, the ability to grow on GlcNAc was recovered by expressing, in *trans*, *nagA* under its own promoter (Fig. S4C).

For D39Δ*galK*, the ability to grow on Gal was not recovered by complementation in *trans* with *galK*. RNA-Seq data [55] showed that *galK* is co-transcribed with the downstream gene *galT-2* and a polar effect of the *galK* deletion on *galT-2* is therefore possible (Fig. S2.3). Indeed, the growth phenotype on Gal could be restored by complementation in *trans* with *galKgalT-2* (Fig. S4A). Importantly, complementation with *galT-2* alone was not successful, suggesting that abrogation of growth on Gal is a consequence of *galK* inactivation.

To further analyse the effect of gene deletions in the Leloir pathway, a D39Δ*galT-2* mutant was constructed. The D39Δ*galT-2* grew on Gal, but the time to reach maximal biomass was 2.3-fold longer as compared to the wild type (data not shown). This result indicates the occurrence of an alternative galactose 1-phosphate activity, likely to be encoded by *galT-1*. On Gal, the expression level of *galT-1* in D39Δ*galT-2* was 49-fold higher than in D39, as shown by qRT-PCR (Table S2.7). Expression of *lacD* was 87-fold higher in Gal-grown D39Δ*galT-2* (Table S2.7) than in Gal-grown wild type, indicating that in the D39Δ*galT-2* mutant the *lac* operon is expressed and the T6P pathway is active.

Attenuated virulence in the absence of a functional Gal pathway

The contribution of genes encoding proteins involved in catabolism of host-derived glycans was tested in mouse models of colonisation, and of models of bronchopneumonia with bacteraemia that result from intranasal infection. While the bronchopneumonia model allows evaluation of factors that are important for acute infection and invasiveness, the colonisation model is ideal to evaluate the determinants of longer term pneumococcal survival *in vivo* [56].

Mice infected with the mutants in Gal catabolic pathways survived significantly longer than wild type D39 strain in the bronchopneumonia model (Fig. 2.7A) (average survival time of mice infected with: D39 44±30.7 h, n=20; D39Δ*galK* 60±36.3 h, n=10; D39Δ*lacD* 59±54.1 h, n=10 and D39Δ*lacD*Δ*galK* 123±55.8 h, n=10; $p<0.01$ for D39Δ*galK,* and $p<0.001$ for D39Δ*lacD* and D39Δ*lacD*Δ*galK*; Mann-Whitney U test). In addition, reintroduction of an intact copy of *galK* and *lacD* into D39Δ*galK* and D39Δ*lacD*, respectively, reconstituted the virulence of these strains with the median survival times of mice infected with D39Δ*galK*comp (44±40.3 h, n=10) and D39Δ*lacD*comp (51.2±40.3 h, n=10), not

significantly different from the wild type infected cohort (p>0.05). This shows that the observed reduction in virulence was not due to polar effect of mutations.

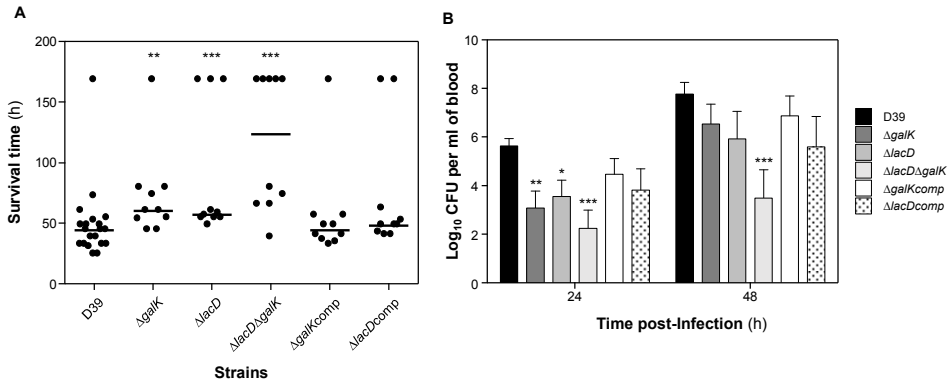

Figure 2.7. **Impaired virulence of pneumococcal strains defective in galactose catabolic pathways following intranasal infection.**

(**A**) Survival time of mice after infection with approximately 1 X 10^6 CFU pneumococci. Symbols show the times mice became severely lethargic. The horizontal bars mark the median times to the severely lethargic state. (**B**) Growth of bacteria in the blood. Each point is the mean of data from ten mice except for D39, which represents 20 mice. Error bars show the standard error of the mean.
Symbols: * p<0.05; ** p<0.01; *** p<0.001.

The progression of bacteraemia in animals infected with the pneumococcal strains was also determined. At 24 h post-infection mice infected either with D39Δ*galK* (log_{10} 3.10±0.7, n=10), D39Δ*lacD* (log_{10} 3.54±0.6, n=10), or D39Δ*lacD*Δ*galK* (log_{10} 2.23±0.75, n=10) had significantly lower mean CFU ml^{-1} of bacteria in the blood than that of the wild type infected cohort (log_{10} 5.21±0.4, n=20) (p<0.01 for D39Δ*galK,* p<0.05 for D39Δ*lacD*, and p<0.001 for D39Δ*lacD*Δ*galK*) (Fig. 2.7B). At 48 h post-infection, the blood bacterial counts recovered from D39Δ*lacD*Δ*galK* (log_{10} 3.48±1.16, n=10) infected cohort was still significantly lower than that of the wild type infected (log_{10} 7.76±0.48, n=20) (p<0.001), however, the numbers of D39Δ*galK* (log_{10} 6.53±0.81, n=10) and D39Δ*lacD* (log_{10} 5.92±1.13, n=10) were similar to the wild type

(p>0.05). Furthermore, no significant difference could be detected in the numbers of D39Δ*galK*comp (24 h: $\log_{10}$ 4.47±0.64 and 48 h: $\log_{10}$ 6.86±0.82 n=10), D39Δ*lacD*comp (24 h: $\log_{10}$ 3.81±0.86 and 48 h: $\log_{10}$ 5.59±1.24 n=10), and the wild type at 24 and 48 h post-infection (*p*>0.05). D39Δ*manA* and D39Δ*nagA* were also tested in bronchopneumonia model, however, the virulence properties of these strains were similar to the wild type (data not shown).

In the colonisation model, the counts for all the pneumococcal strains were determined in nasopharyngeal tissue at the time of infection, and at 3 and 7 days after infection (Fig. 2.8). The results show that at 3 and 7 days post-infection the numbers of D39Δ*galK* ($\log_{10}$ 1.75±0.14 and $\log_{10}$ 1.80±0.17 n=5), D39Δ*lacD* ($\log_{10}$ 1.72±0.2 and $\log_{10}$ 1.87±0.24, n=5), and D39Δ*lacD*Δ*galK* ($\log_{10}$ 1.08±0.33 and $\log_{10}$ 0.89±0.25, n=5) were significantly lower than the counts of wild type ($\log_{10}$ 2.82±0.02; and $\log_{10}$ 2.77±0.08, n=5, for days 3 and 7, respectively) (*p*<0.01 for D39Δ*galK,* *p*<0.0001 for D39Δ*lacD*Δ*galK,* and *p*<0.01 and *p*<0.05 for D39Δ*lacD* for 3 and 7 days post-infection, respectively).

Similar to the bronchopneumonia model, in the colonisation model no phenotypic differences were observed between the wild type and D39Δ*galK*comp, D39Δ*lacD*comp (Fig. 2.8) (*p*>0.05), and the wild type and D39Δ*manA* and D39Δ*nagA* (data not shown).

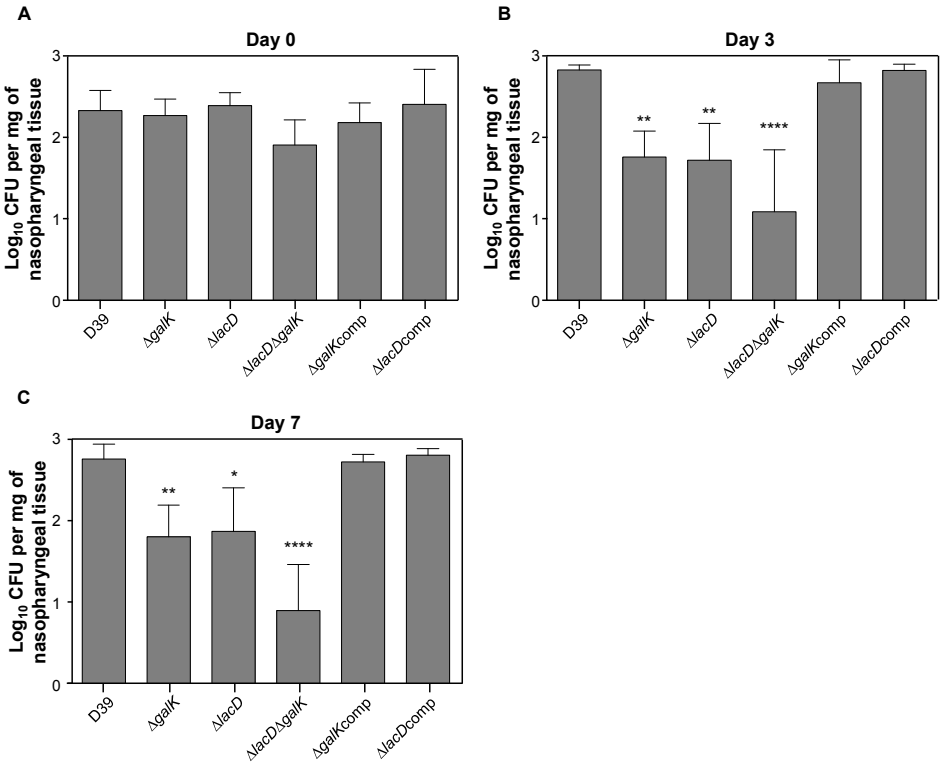

Figure 2.8. Pneumococcal strains defective in galactose catabolic pathways are less able to colonise nasopharynx.

Mice were infected with approximately 1 X 10^5 CFU pneumococci. At predetermined times, five mice were culled, and CFU mg^{-1} of bacteria were determined by serial dilutions of nasopharyngeal homogenates. Each column represents the mean of data from five mice. Error bars show the standard error of the mean. Symbols: * p<0.05; ** p<0.01, **** p<0.0001.

In addition to respiratory infection models, we also tested all the strains in a bacteraemia model through direct administration of bacteria through a tail vein in order to distinguish niche-specific contribution of individual pneumococcal proteins. There was no difference in the median survival times of cohorts (Fig. S5A) (p>0.05). In addition, the mutants had grown as well as the wild type strain in the blood at 24 and 48 h post-infection (Fig. S5B), showing that the observed reduction in virulence and

colonisation in D39Δ*galK,* D39Δ*lacD* and D39Δ*lacD*Δ*galK* was specific to the respiratory tract.

Overall, the results showed that Gal catabolic mutants, particularly D39Δ*lacD*Δ*galK,* were attenuated in the ability to colonise the nasopharynx and have reduced virulence in a respiratory infection mouse model.

Discussion and Conclusions

The study of *S. pneumoniae* has been heavily focused on factors that directly impinge on host-pathogen interactions, such as toxins, cell wall components, adhesins and capsule [3]. In contrast, investigation of pneumococcal physiology has only recently been addressed, in spite of it being a fundamental aspect of pneumococcal survival *in vivo*. This important pathogen is a strictly fermentative organism, which possesses one of the highest genomic abundances of genes encoding sugar transporters [6,7,24]. Thus, we surmised that the ability to take up and metabolize sugars is of key importance for the lifestyle of *S. pneumoniae*. Our view is strongly supported by previous studies consistently identifying genes involved in sugar catabolism as essential for virulence [11,57–61] as well as reports showing that sugar transporters contribute to *S. pneumoniae* colonisation and disease [16,62–64]. In the nasopharynx free sugars are scarce, but recent findings indicate that sugars derived from deglycosylation provide suitable carbon and energy sources for nasopharyngeal growth [12,14,15]. In order to understand the role of different host derived sugars in pneumococcal lifestyle and pathogenicity, we followed a top-down approach to identify, establish and validate functional sugar-specific catabolic pathways implicated in the utilization of

sugars that may originate from glycan deglycosylation and evaluated the impact of sugar-specific pathways on the ability to colonise and cause disease *in vivo.*

Despite the vast diversity of host glyconjugates, their glycan portions are often composed of the monosaccharides GalNAc, Gal, NeuNAc, GlcNAc, Fuc, Man, Glc and fructose. While the first five sugars are widespread in both N- and O-glycans (*e.g*. mucins), the other three are generally restricted to N-glycans. *S. pneumoniae* can grow on mucin as sole carbon source [12]. This ability is associated to a range of glycosidases that hydrolyse the mucins releasing to the medium neuraminic acids (NeuNAc and N-glycolylneuraminic acid), Gal and GalNAc, and to a less extent also GlcNAc and Fuc [14]. From our own analysis of the genomic content and the work of others [8,9,14,39,49,63], *S. pneumoniae* D39 harbours genes to potentially catabolise the glycan components Gal, GlcNAc, NeuNAc and Man. A bias towards utilization of the monosaccharide Gal and GlcNAc by *S. pneumoniae* D39 during growth on an O-glycan was hypothesised, since the monosaccharides account respectively for 14% and 30% (wt/vol) of the mucin [14]. Furthermore, *S. pneumoniae* is equipped with the machinery to utilize those constituents including glycosidases (at least two galactosidases, BgaA and BgaC, and a *N*-acetylglucosaminidase StrH [14,20,65,66]), putative transporters and catabolic genes (Table S2.4). This hypothesis was corroborated in a transcriptome analysis comparing gene expression of cells growing on porcine gastric mucin to Glc. Of the genes showing significant increased expression on mucin, the vast majority was implicated in the uptake and internal metabolism of Gal (25% of genes involved in sugar metabolism (Table 2.1)), and GlcNAc. Of note, mucin highly induced the expression of *bgaA* and *strH* encoding a β-galactosidase and a *β-N*-acetylglucosaminidase, whose activities result in free Gal and GlcNAc, respectively [18,65–68]. Growth of *S. pneumoniae*

on mucin was shown to reduce by 30% the content in Gal of the glycoprotein, while the content in GlcNAc was not altered. This was rationalized as resulting from the complex structure of mucin, in which GlcNAc residues might be masked by other sugars.

Genes associated with the transport of Man, a monosaccharide generally found in N-glycans, were also upregulated in mucin. Like Gal and GlcNAc, Man could sustain growth of *S. pneumoniae* D39 in a chemically defined medium (Fig. 2.2). Whether all the transporters upregulated show affinity for mannose remains to be investigated. Activity of α-mannosidase has been described for *S. pneumoniae* and homologues of previously characterized streptococcal mannosidase genes are found in the genome of D39 [69–71], but these genes were not differentially expressed in mucin-grown cells.

Previously, it was shown that growth on mucin required the activity of neuraminidase A (NanA) [12]. Initial removal of terminal NeuNAc seems to be essential for further breakdown by other glycosidases and subsequent utilization of the glycan-derived sugars [14,18,72]. In our study, neuraminidase A was not significantly induced in presence of mucin as compared to Glc, which leads us to propose that its constitutive expression is sufficient to ensure the activity level to remove terminal NeuNAc. Furthermore, we (and others) verified that NeuNAc cannot sustain growth of strain D39 in chemically defined medium, most likely due to a frame shift mutation in the N-acetylneuraminate lyase gene of the *nanAB* operon [8]. The mucin derivatives GalNAc and Fuc also failed to support growth of *S. pneumoniae*. For GalNAc we could not firmly identify genes encoding the activities converting N-acetylgalactosamine 6-phosphate to tagatose 6-phosphate, although genes with homology to *E. coli* counterparts are present in the genome (Text S2.2). Genes implicated in the downstream processing of L-lactaldehyde, the product of L-fuculose phosphate aldolase in the Fuc pathway, were not found (Text S2.2) [8].

This inability to identify the full catabolic pathways for Fuc and GalNAc is in good agreement with previous reports that *S. pneumoniae* is unable to grow on these sugars as sole carbon sources [8,50–52].

Overall, our integrated approach combining genomic, transcriptomic and growth data identified Gal, GlcNAc and Man as the glycan-originating monosaccharides more likely to be used as substrates for growth of *S. pneumoniae* D39 in the respiratory tract.

The predicted routes for Gal, GlcNAc and Man dissimilation in *S. pneumoniae* D39 (Fig. 2.1) were validated at the biochemical and genetic level in this study.

Mannose

The phosphorylated intermediate Man6P accumulated to high levels in exponential cells and the activity of Man6P isomerase (ManA) was induced by Man. A *manA* mutant was unable to grow on Man, even though mannose 6-phosphate isomerase activity was detected to a certain extent in the loss-of-function mutant. Homologues of genes coding for ManA or other known Man6P isomerases were not found in the genome of D39, suggesting that the residual isomerase activity is non-specific, and insufficient to support growth on Man, as shown in Fig. 2.6D. Of interest, a strain expressing *manA* in *trans* under the control of an inducible zinc promoter showed better growth than the wild type D39, suggesting a bottleneck at the level of ManA. This observation is further supported by the high accumulation of Man6P during growth on Man.

N-acetylglucosamine

Both intermediates for the catabolism of GlcNAc, GlcNAc6P and GlcN6P, were present in exponentially-growing cells. Furthermore, the activity of GlcNAc6P deacetylase was induced by GlcNAc. A *nagA* mutant lost the ability to grow on the amino sugar, and the growth could be restored by in *trans* complementation. In other bacteria GlcNAc can be taken up via PTS or non-PTS transporters [73–78]. A recent report

indicated that *S. pneumoniae* internalizes this amino sugar exclusively via PTS transporter(s) [8], and this has been confirmed for strain D39 (A. M. Cavaleiro, P. Gaspar, T. Kloosterman, O. P. Kuipers and A. R. Neves, unpublished data).

Galactose

In a previous study using a different isolate of *S. pneumoniae* D39, we reported activity of both the Leloir and the T6P pathways in the utilization of Gal, since intermediates of both pathways (α-Gal1P and α-Glc1P from the Leloir and TBP from the T6P pathway) were observed during growth on Gal [9], and this was confirmed with D39 isolate used in the present study. Specific activities of enzymes for the Leloir (galactokinase, GalK) or T6P (tagatose 1,6-diphosphate aldolase, LacD) pathways were detected during growth on Gal, but not on Glc. This result for GalK and LacD contrasts with the activities of the other enzymes tested (NagA and ManA), which showed activity also when grown on Glc and not only on their dedicated sugars (Table 2.4). These findings may be explained by the fact that both NagA and ManA are involved in cellular processes other than the catabolism of the monosaccharides, such as providing precursors for biosynthesis. Inactivation of both *galK* and *lacD* in D39 rendered the pneumococcus unable to grow on Gal. Surprisingly, inactivation of *galK* alone abolished growth on Gal, whereas exponential growth of a *lacD* mutant was observed although only after a long lag phase. The behavior of the *lacD* mutant can be partially explained in the context of carbon catabolite repression. The Leloir genes are under strong negative control by the carbon catabolite protein A, CcpA [9], thus alleviation of the repression is required before the pathway is activated. In line with this conclusion, in D39 Glc-grown cells the activity of galactokinase was undetectable. Catabolism via the Leloir pathway is normally associated with uptake of Gal via a non-PTS permease (secondary carriers or ABC transporters). Bidossi *et al*. [8], implicated the

ABC transporter SPD_0088-9-90 CUT1 in the uptake of Gal. On the other hand, a *Lactococcus lactis* strain exclusively harboring the Leloir pathway, inactivated for the Gal permease, translocates Gal by a PTS and the resulting Gal6P enters the Leloir pathway upon dephosphorylation by a phosphatase [79]. The same could be active in *S. pneumoniae*, however, exclusive transport via the PTS is not in agreement with the observations that *S. pneumoniae* G54 and DP1004 devoid of PTS activity (*ptsI* mutants) are capable of growing on Gal [8]. Interestingly, a D39 *ptsI* mutant shows good growth on Gal, but only after a lag phase of about 11 h (A. M. Cavaleiro, P. Gaspar, T. Kloosterman, O. P. Kuipers and A. R. Neves, unpublished data). In light of these results, we propose that induction of an adequate transport system, presumably a non-PTS type, and alleviation of the carbon catabolite repression exerted over the Leloir genes are strict requirements for Gal dissimilation via the Leloir pathway in *S. pneumoniae* D39. Our hypothesis is in agreement with the elimination of the lag phase upon subculturing of the *lacD* strain on Gal containing-medium (Fig. S2.6).

While the residual growth on Gal in the *lacD* mutant can be attributed to activation of the Leloir pathway, we do not know why growth on Gal is totally abolished in the *galK* mutant. A plausible explanation relies on the unintentional elimination of Gal1P uridylyltransferase (GalT) activity that provides essential precursors for the biosynthesis of structural polysaccharides. Indeed, inactivation of *galK* affected the expression of *galT-2*, and reversion of the *galK* mutant to the wild type phenotype on Gal required complementation with both *galK* and *galT-2*. However, inability to grow on Gal could be largely attributed to the *galK* mutation, since expression in *trans* of *galT-2* did not restore growth and a *galT-2* mutant was able to grow on Gal (data not shown). In the latter mutant, expression of *galT-1* was substantially increased, indicating that the product of the duplicated gene accounts for the lost GalT-2 activity, thus

restoring the Leloir pathway functionality. Based on our data, we therefore conclude that Gal metabolism in *S. pneumoniae* requires an operational Leloir pathway, or at least an active galactokinase.

In other streptococci, efficient dissimilation of Gal has been associated with the presence of a high affinity specific Gal transporter [80,81]. According to Bidossi *et al.* [8], the PTS transporters implicated in the import of Gal in *S. pneumoniae* are the mannose-family PTS (ManMNL), a galactitol-family PTS (SPD_0559-0-1) and probably a mannose-family PTS (SPD_0066-7-8-9). In addition, our team showed that *lacFE* genes are induced by Gal, suggesting a potential contribution of the lactose-PTS to the uptake of the sugar [9]. Interestingly, the galactitol-family PTS, which has previously been implicated in Gal uptake [8,53], is a homologue of the specific galactose-PTS identified in *Streptococcus gordonii*, *Streptococcus mutans* and *Streptococcus oligofermentans* [80–82]. However, the affinity of this putative galactose-specific PTS for Gal is seemingly not very high, as noted by markedly decreased growth rates at low Gal concentration and the inability to fully scavenge Gal from the culture medium (Fig. 2.3 and Table 2.2). The absence of high-affinity PTSs would certainly be a bottleneck for efficient functionality of the T6P pathway, but cannot fully explain the *galK* phenotype. Moreover, the uptake of Gal via a PTS system ensures a typical PTS-mediated signal transduction pathway for CcpA regulation and renders Gal an effective inducer of catabolite repression [9]. Of note, our team has previously reported that CcpA repression of key metabolic genes (Leloir pathway and fermentative pathways) is counterbalanced by a Gal-dependent activation [9]. In view of the results with the *galK* mutant we propose that galactokinase activity is essential for Gal catabolism, and that its product, α-Gal1P, is likely to be the inducer of gene expression. Collectively, our data provide evidence that utilization of Gal in *S. pneumoniae* is subject to complex regulation and of a subtle regulatory link between the Leloir

and the T6P pathways. Unravelling these regulatory mechanisms certainly deserves future investigations.

Growth in non-preferential sugars is usually associated with mixed acid fermentation profiles [83,84]. This is indeed the case for *S. pneumoniae* D39 growing on Gal as sole carbon source (Table 2.3; [9]). Unexpectedly, growth on the other slowly metabolizable monosaccharide, Man, resulted in only a modest shift towards mixed acid products suggesting a different regulation of the central carbon pathways in the presence of Man. The underlying mechanisms are, however, out of the scope of this work and will be further investigated in the future.

We hypothesised that the ability to efficiently use monosaccharides originating from mucins conferred on *S. pneumoniae* a metabolic advantage during colonisation and subsequent invasive states. *S. pneumoniae* strains defective in Gal catabolic genes, and in particular the double mutant, D39Δ*lacD*Δ*galK*, presented impaired ability to colonise the murine nasopharynx and had reduced virulence. Inactivation of *nagA* or *manA* had no significant effect in test mice. Importantly, direct administration of the Gal mutants into the bloodstream induced responses of the same magnitude (similar survival times and CFU per ml of blood) as the wild type D39 strain. In the bloodstream the main sugar present is Glc [10,11], and thus the Gal-deficient phenotype was not expected to have any impact. Furthermore, this finding adds to the importance of Gal metabolism in the airways, further supporting the view connecting Gal metabolism in *S. pneumoniae* to its virulence in this niche.

At first glance, the inefficient Gal metabolism and the observation that Gal is a less preferred sugar compared to Man and GlcNAc *in vitro*, seems to be in conflict with the role of Gal genes in colonisation and virulence. The lack of correlation between sugar preferences *in vitro* and the effect of mutations in specific sugar catabolic pathways *in vivo* has been reported before for *E. coli* [85]. This apparent inconsistency might arise

from the multifactorial milieu in host niches. Furthermore, we showed that Gal catabolic genes represent the largest fraction of genes induced by mucin and others had previously established that Gal is widespread and abundant in the airway glycoconjugates (*e.g.* mucins). The relevance of Gal acquisition and metabolism had been previously suggested. Indeed, loss of beta-galactosidase activity, resulted in attenuated pneumococcal growth in the nasopharynx [14], and mutants defective in pyruvate formate lyase, an enzyme essential for Gal fermentation, were attenuated in virulence [39]. Furthermore, using Tn-seq in *S. pneumoniae* TIGR4 van Opijnen *et al.* [86] identified *lacD* as relevant for pneumococcal fitness in the nasopharynx. In addition, they also showed that both *galK* and *lacD* played a critical role for fitness of TIGR4 during *in vitro* growth on Gal. In *S. pneumoniae* D39, *galK* is essential for growth on Gal, while loss of *lacD* causes a long lag phase prior to exponential growth. The different results in the two studies most likely derive from using different serotypes (D39 *vs.* TIGR4) or different experimental conditions for growth of *S. pneumoniae.* Nevertheless, both studies highlight the relevance of Gal and its catabolism in the airways.

In light of these results we propose that pneumococcal Gal metabolism is of key importance during colonisation and throughout the transition from carriage to an invasive state. The loss of fitness in the Gal mutants can be due to metabolic impairment and deficient expression of specific virulence traits induced by Gal. We have previously reported that Gal-grown cells produce twice as much capsule as Glc-grown cells [9], and it has been reported that a thicker capsule allows evasion from immune system and from initial mucociliary clearance *in vivo* [87]. On Gal, the carbon balance was lower than on other sugars, but no other end-products/metabolites were detected, thus we propose that Gal is directed to processes other than fermentation such as the polysaccharide synthesis [9]. Whether it is the capsule or other factors such as increased

carbon availability that determines the Gal-associated virulence remains to be investigated.

In summary, we followed a multidisciplinary approach to identify the monosaccharides in host glycoproteins that serve as carbon sources for growth of *S. pneumoniae* strain D39. Accumulating evidence connects pathogenesis to carbohydrate metabolism, and the findings herein presented further strengthen this view as we specifically show that mutants in Gal catabolic genes showed attenuated ability to colonise and reduced virulence following intranasal infection in mouse models. With widespread antibiotic resistance and re-emergence of non-type vaccine strains, it is urgent that new targets are found for the development of novel therapeutic and preventive drugs. One such opportunity is perhaps offered by the discovery of Gal as an “essential” nutrient for pneumococcal growth and persistence in the host. The Leloir and the tagatose 6-phosphate pathways are present and conserved across pneumococcal serogroups (Table S2.8) supporting our suggestion that Gal catabolism could be a potential target for novel therapeutics.

Acknowledgments

This work was supported by Fundação para a Ciência e a Tecnologia, Portugal (FCT) and FEDER, project PTDC/SAU-MII/100964/2008, and through grants PEst-OE/EQB/LA0004/2011 and IDMEC, under LAETA Pest-OE/EME/LA0022. L. Paixão, E. C. Lourenço and A. Veríssimo acknowledge FCT for the award of Ph.D. grants SFRH/BD/46997/2008, SFRH/47702/2008 and SFRH/BD/97415/2013, respectively. M. Kjos was supported by a FEBS Long-term fellowship. Work in the lab of J.-W. Veening was supported by European Research Council Starting grant

(337399-PneumoCell) and a Vidi fellowship (864.12.001) from the Netherlands Organisation for Scientific Research (NWO-ALW). S. Vinga acknowledges support by Program Investigator FCT (IF/00653/2012) from FCT, co-funded by the European Social Fund (ESF) through the Operational Program Human Potential (POPH). The NMR spectrometers are part of The National NMR Facility, supported by Fundação para a Ciência e a Tecnologia (RECI/BBB-BQB/0230/2012)

Ricardo Sequeira is acknowledged for his support with acquiring and analysing the ^{31}P-NMR spectra of cell-free extracts. Dr Adam Witney is acknowledged for his support with depositing microarray data. Anne de Jong is acknowledged for his support in the blast search of galactose pathways across pneumococcal genomes.

Author's contribution

L. Paixão contributed to the design of all the experiments. She performed and analysed experiments as follows:

Growth Experiments:

Performed: L. Paixão and J. Oliveira

Quantification of end-products formation and sugar consumption by HPLC and NMR: L. Paixão

Estimation of growth and energetic parameters: L. Paixão

Statistical Analysis:

Performed: L. Paixão and S. Vinga

Simulation analysis of the growth experiments:

Performed: A. Veríssimo and S. Vinga

Construction of loss-of-function mutants:

Performed: L. Paixão and J. Oliveira

Complementation studies:

Performed: L. Paixão and M. Kjos

Transcriptome Analysis:

Analysed: L. Paixão and H. Yesilkaya

qRT-PCR

Performed: H. Yesilkaya

Analysed: L. Paixão

***In silico* analysis:**

L. Paixão and A.R. Neves

Cold Ethanol extracts and intracellular metabolites determination:

Performed: R. Sequeira

Analysed: A.R. Neves

Enzyme Activities:

Designed and Performed: L. Paixão

***In vivo* analysis of pneumococcal strains:**

Performed: H. Yesilkaya, V.E. Fernandes

Analysis: H. Yesilkaya, V.E. Fernandes, L. Paixão

Chemical synthesis of phosphorylated metabolites TBP and GlcNAc6P:

Designed and Performed: E.C. Lourenço and M.R. Ventura

All authors contributed to the critical reading of this chapter.

References

1. Kadioglu A. Upper and lower respiratory tract infection by *Streptococcus pneumoniae* is affected by pneumolysin deficiency and differences in capsule type. Infect Immun. 2002;70: 2886–2890. doi:10.1128/IAI.70.6.2886-2890.2002
2. Hava DL, LeMieux J, Camilli A. From nose to lung: the regulation behind *Streptococcus pneumoniae* virulence factors: Virulence gene regulation in *S. pneumoniae*. Mol Microbiol. 2003;50: 1103–1110. doi:10.1046/j.1365-2958.2003.03764.x

3. Kadioglu A, Weiser JN, Paton JC, Andrew PW. The role of *Streptococcus pneumoniae* virulence factors in host respiratory colonization and disease. Nat Rev Microbiol. 2008;6: 288–301. doi:10.1038/nrmicro1871
4. Bogaert D, de Groot R, Hermans P. *Streptococcus pneumoniae* colonisation: the key to pneumococcal disease. Lancet Infect Dis. 2004;4: 144–154. doi:10.1016/S1473-3099(04)00938-7
5. Weiser JN. The pneumococcus: why a commensal misbehaves. J Mol Med (Berl). 2010;88: 97–102. doi:10.1007/s00109-009-0557-x
6. Hoskins J, Alborn WE, Arnold J, Blaszczak LC, Burgett S, DeHoff BS, et al. Genome of the bacterium *Streptococcus pneumoniae* strain R6. J Bacteriol. 2001;183: 5709–5717. doi:10.1128/JB.183.19.5709-5717.2001
7. Tettelin H, Nelson KE, Paulsen IT, Eisen JA, Read TD, Peterson S, et al. Complete genome sequence of a virulent isolate of *Streptococcus pneumoniae*. Science. 2001;293: 498–506. doi:10.1126/science.1061217
8. Bidossi A, Mulas L, Decorosi F, Colomba L, Ricci S, Pozzi G, et al. A functional genomics approach to establish the complement of carbohydrate transporters in *Streptococcus pneumoniae*. Miyaji EN, editor. PLoS ONE. 2012;7: e33320. doi:10.1371/journal.pone.0033320
9. Carvalho SM, Kloosterman TG, Kuipers OP, Neves AR. CcpA ensures optimal metabolic fitness of *Streptococcus pneumoniae*. Horsburgh MJ, editor. PLoS ONE. 2011;6: e26707. doi:10.1371/journal.pone.0026707
10. Philips BJ, Meguer J-X, Redman J, Baker EH. Factors determining the appearance of glucose in upper and lower respiratory tract secretions. Intensive Care Med. 2003;29: 2204–2210. doi:10.1007/s00134-003-1961-2
11. Shelburne SA, Davenport MT, Keith DB, Musser JM. The role of complex carbohydrate catabolism in the pathogenesis of invasive streptococci. Trends Microbiol. 2008;16: 318–325. doi:10.1016/j.tim.2008.04.002
12. Yesilkaya H, Manco S, Kadioglu A, Terra VS, Andrew PW. The ability to utilize mucin affects the regulation of virulence gene expression in *Streptococcus pneumoniae*. FEMS Microbiol Lett. 2008;278: 231–235. doi:10.1111/j.1574-6968.2007.01003.x
13. Rose MC, Voynow JA. Respiratory tract mucin genes and mucin glycoproteins in health and disease. Physiol Rev. 2006;86: 245–278. doi:10.1152/physrev.00010.2005
14. Terra VS, Homer KA, Rao SG, Andrew PW, Yesilkaya H. Characterization of novel β-galactosidase activity that contributes to glycoprotein degradation and virulence in *Streptococcus pneumoniae*. Infect Immun. 2010;78: 348–357. doi:10.1128/IAI.00721-09
15. Burnaugh AM, Frantz LJ, King SJ. Growth of *Streptococcus pneumoniae* on human glycoconjugates is dependent upon the sequential activity of bacterial exoglycosidases. J Bacteriol. 2008;190: 221–230. doi:10.1128/JB.01251-07
16. Marion C, Stewart JM, Tazi MF, Burnaugh AM, Linke CM, Woodiga SA, et al. *Streptococcus pneumoniae* can utilize multiple sources of hyaluronic acid for growth. Infect Immun. 2012;80: 1390–1398. doi:10.1128/IAI.05756-11
17. King SJ. Pneumococcal modification of host sugars: a major contributor to colonization of the human airway? Mol Oral Microbiol. 2010;25: 15–24. doi:10.1111/j.2041-1014.2009.00564.x

18. King SJ, Hippe KR, Weiser JN. Deglycosylation of human glycoconjugates by the sequential activities of exoglycosidases expressed by *Streptococcus pneumoniae*. Mol Microbiol. 2006;59: 961–974. doi:10.1111/j.1365-2958.2005.04984.x
19. Marion C, Limoli DH, Bobulsky GS, Abraham JL, Burnaugh AM, King SJ. Identification of a pneumococcal glycosidase that modifies O-linked glycans. Infect Immun. 2009;77: 1389–1396. doi:10.1128/IAI.01215-08
20. Jeong JK, Kwon O, Lee YM, Oh D-B, Lee JM, Kim S, et al. Characterization of the *Streptococcus pneumoniae* BgaC protein as a novel surface β-galactosidase with specific hydrolysis activity for the Galβ1-3GlcNAc moiety of oligosaccharides. J Bacteriol. 2009;191: 3011–3023. doi:10.1128/JB.01601-08
21. Brittan JL, Buckeridge TJ, Finn A, Kadioglu A, Jenkinson HF. Pneumococcal neuraminidase A: an essential upper airway colonization factor for *Streptococcus pneumoniae*: *Streptococcus pneumoniae* neuraminidase. Mol Oral Microbiol. 2012;27: 270–283. doi:10.1111/j.2041-1014.2012.00658.x
22. Tong HH, Blue LE, James MA, DeMaria TF. Evaluation of the virulence of a *Streptococcus pneumoniae* neuraminidase-deficient mutant in nasopharyngeal colonization and development of otitis media in the chinchilla model. Infect Immun. 2000;68: 921–924.
23. Manco S, Hernon F, Yesilkaya H, Paton JC, Andrew PW, Kadioglu A. Pneumococcal neuraminidases A and B both have essential roles during infection of the respiratory tract and sepsis. Infect Immun. 2006;74: 4014–4020. doi:10.1128/IAI.01237-05
24. Lanie JA, Ng W-L, Kazmierczak KM, Andrzejewski TM, Davidsen TM, Wayne KJ, et al. Genome sequence of Avery's virulent serotype 2 strain D39 of *Streptococcus pneumoniae* and comparison with that of unencapsulated laboratory strain R6. J Bacteriol. 2007;189: 38–51. doi:10.1128/JB.01148-06
25. Carvalho SM, Kuipers OP, Neves AR. Environmental and nutritional factors that affect growth and metabolism of the pneumococcal serotype 2 strain D39 and its nonencapsulated derivative strain R6. Horsburgh MJ, editor. PLoS ONE. 2013;8: e58492. doi:10.1371/journal.pone.0058492
26. Zwietering MH, Jongenburger I, Rombouts FM, van 't Riet K. Modeling of the bacterial growth curve. Appl Environ Microbiol. 1990;56: 1875–1881.
27. Veríssimo A, Paixão L, Neves A, Vinga S. BGFit: management and automated fitting of biological growth curves. BMC Bioinformatics. 2013;14: 283. doi:10.1186/1471-2105-14-283
28. Johansen E, Kibenich A. Isolation and characterization of IS1165, an insertion sequence of *Leuconostoc mesenteroides* subsp. *cremoris* and other lactic acid bacteria. Plasmid. 1992;27: 200–206.
29. Song J-H, Ko KS, Lee J-Y, Baek JY, Oh WS, Yoon HS, et al. Identification of essential genes in *Streptococcus pneumoniae* by allelic replacement mutagenesis. Mol Cells. 2005;19: 365–374.
30. Kloosterman TG. To have neighbour's fare: extending the molecular toolbox for *Streptococcus pneumoniae*. Microbiology. 2006;152: 351–359. doi:10.1099/mic.0.28521-0
31. Overkamp W, Beilharz K, Detert Oude Weme R, Solopova A, Karsens H, Kovacs AT, et al. Benchmarking various green fluorescent protein variants in *Bacillus subtilis*, *Streptococcus pneumoniae*, and *Lactococcus lactis* for live cell imaging. Appl Environ Microbiol. 2013;79: 6481–6490. doi:10.1128/AEM.02033-13

32. Sambrook J. Molecular cloning: a laboratory manual. 3rd ed. Cold Spring Harbor, N.Y: Cold Spring Harbor Laboratory Press; 2001.
33. Beilharz K, Nováková L, Fadda D, Branny P, Massidda O, Veening J-W. Control of cell division in *Streptococcus pneumoniae* by the conserved Ser/Thr protein kinase StkP. Proc Natl Acad Sci USA. 2012;109: E905–913. doi:10.1073/pnas.1119172109
34. Martin B, García P, Castanié MP, Claverys JP. The *recA* gene of *Streptococcus pneumoniae* is part of a competence-induced operon and controls lysogenic induction. Mol Microbiol. 1995;15: 367–379.
35. Sicard AM. A new synthetic medium for *Diplococcus pneumoniae*, and its use for the study of reciprocal transformations at the *amia* locus. Genetics. 1964;50: 31–44.
36. Stewart GR, Wernisch L, Stabler R, Mangan JA, Hinds J, Laing KG, et al. Dissection of the heat-shock response in *Mycobacterium tuberculosis* using mutants and microarrays. Microbiology (Reading, Engl). 2002;148: 3129–3138.
37. Bortoni ME, Terra VS, Hinds J, Andrew PW, Yesilkaya H. The pneumococcal response to oxidative stress includes a role for Rgg. Microbiology (Reading, Engl). 2009;155: 4123–4134. doi:10.1099/mic.0.028282-0
38. Green GH, Diggle PJ. On the operational characteristics of the Benjamini and Hochberg False Discovery Rate procedure. Stat Appl Genet Mol Biol. 2007;6: Article27. doi:10.2202/1544-6115.1302
39. Yesilkaya H, Spissu F, Carvalho SM, Terra VS, Homer KA, Benisty R, et al. Pyruvate formate lyase is required for pneumococcal fermentative metabolism and virulence. Infect Immun. 2009;77: 5418–5427. doi:10.1128/IAI.00178-09
40. Livak KJ, Schmittgen TD. Analysis of relative gene expression data using real-time quantitative PCR and the 2(-Delta Delta C(T)) Method. Methods. 2001;25: 402–408. doi:10.1006/meth.2001.1262
41. Crow VL, Thomas TD. D-tagatose 1,6-diphosphate aldolase from lactic streptococci: purification, properties, and use in measuring intracellular tagatose 1,6-diphosphate. J Bacteriol. 1982;151: 600–608.
42. Homer KA, Patel R, Beighton D. Effects of N-acetylglucosamine on carbohydrate fermentation by *Streptococcus mutans* NCTC 10449 and *Streptococcus sobrinus* SL-1. Infect Immun. 1993;61: 295–302.
43. White RJ, Pasternak CA. The purification and properties of N-acetylglucosamine 6-phosphate deacetylase from *Escherichia coli*. Biochem J. 1967;105: 121–125.
44. Gracy RW, Noltmann EA. Studies on phosphomannose isomerase. I. Isolation, homogeneity measurements and determination of some physical properties. J Biol Chem. 1968;243: 3161–3168.
45. Hajaj B, Yesilkaya H, Benisty R, David M, Andrew PW, Porat N. Thiol peroxidase is an important component of *Streptococcus pneumoniae* in oxygenated environments. Infect Immun. 2012;80: 4333–4343. doi:10.1128/IAI.00126-12
46. Szabó P. Phosphorylated sugars. Part 25. Synthesis and behaviour in acidic media of 2-acetamido-2-deoxy-D-glucose 4- and 6-phosphates and of a “Lipid A” analogue. J Chem Soc, Perkin Trans 1. 1989; 919–924. doi:10.1039/p19890000919
47. Yeager AR, Finney NS. Synthesis of fluorescently labeled UDP-GlcNAc analogues and their evaluation as chitin synthase substrates. J Org Chem. 2005;70: 1269–1275. doi:10.1021/jo0483670

48. Eyrisch O, Sinerius G, Fessner W-D. Facile enzymic de novo synthesis and NMR spectroscopy characterization of D-tagatose 1,6-biphosphate. Carbohyd Res. 1993;238: 287–306.
49. Gualdi L, Hayre J, Gerlini A, Bidossi A, Colomba L, Trappetti C, et al. Regulation of neuraminidase expression in *Streptococcus pneumoniae*. BMC Microbiol. 2012;12: 200. doi:10.1186/1471-2180-12-200
50. Chan PF, O'Dwyer KM, Palmer LM, Ambrad JD, Ingraham KA, So C, et al. Characterization of a novel fucose-regulated promoter (PfcsK) suitable for gene essentiality and antibacterial mode-of-action studies in *Streptococcus pneumoniae*. J Bacteriol. 2003;185: 2051–2058. doi:10.1128/JB.185.6.2051-2058.2003
51. Embry A, Hinojosa E, Orihuela CJ. Regions of Diversity 8, 9 and 13 contribute to *Streptococcus pneumoniae* virulence. BMC Microbiol. 2007;7: 80. doi:10.1186/1471-2180-7-80
52. Higgins MA, Suits MD, Marsters C, Boraston AB. Structural and functional analysis of fucose-processing enzymes from *Streptococcus pneumoniae*. J Mol Biol. 2014;426: 1469–1482. doi:10.1016/j.jmb.2013.12.006
53. Kaufman GE, Yother J. CcpA-dependent and -independent control of beta-galactosidase expression in *Streptococcus pneumoniae* occurs via regulation of an upstream phosphotransferase system-encoding operon. J Bacteriol. 2007;189: 5183–5192. doi:10.1128/JB.00449-07
54. Eberhardt A, Wu LJ, Errington J, Vollmer W, Veening J-W. Cellular localization of choline-utilization proteins in *Streptococcus pneumoniae* using novel fluorescent reporter systems. Mol Microbiol. 2009;74: 395–408. doi:10.1111/j.1365-2958.2009.06872.x
55. Slager J, Kjos M, Attaiech L, Veening J-W. Antibiotic-induced replication stress triggers bacterial competence by increasing gene dosage near the origin. Cell. 2014;157: 395–406. doi:10.1016/j.cell.2014.01.068
56. Richards L, Ferreira DM, Miyaji EN, Andrew PW, Kadioglu A. The immunising effect of pneumococcal nasopharyngeal colonisation; protection against future colonisation and fatal invasive disease. Immunobiology. 2010;215: 251–263. doi:10.1016/j.imbio.2009.12.004
57. Polissi A, Pontiggia A, Feger G, Altieri M, Mottl H, Ferrari L, et al. Large-scale identification of virulence genes from *Streptococcus pneumoniae*. Infect Immun. 1998;66: 5620–5629.
58. Lau GW, Haataja S, Lonetto M, Kensit SE, Marra A, Bryant AP, et al. A functional genomic analysis of type 3 *Streptococcus pneumoniae* virulence. Mol Microbiol. 2001;40: 555–571.
59. Hava DL, Camilli A. Large-scale identification of serotype 4 *Streptococcus pneumoniae* virulence factors. Mol Microbiol. 2002;45: 1389–1406.
60. Orihuela CJ, Radin JN, Sublett JE, Gao G, Kaushal D, Tuomanen EI. Microarray analysis of pneumococcal gene expression during invasive disease. Infect Immun. 2004;72: 5582–5596. doi:10.1128/IAI.72.10.5582-5596.2004
61. Song X-M, Connor W, Hokamp K, Babiuk LA, Potter AA. *Streptococcus pneumoniae* early response genes to human lung epithelial cells. BMC Research Notes. 2008;1: 64. doi:10.1186/1756-0500-1-64
62. Iyer R, Camilli A. Sucrose metabolism contributes to in vivo fitness of *Streptococcus pneumoniae*. Mol Microbiol. 2007;66: 1–13. doi:10.1111/j.1365-2958.2007.05878.x

63. Marion C, Burnaugh AM, Woodiga SA, King SJ. Sialic acid transport contributes to pneumococcal colonization. Infect Immun. 2011;79: 1262–1269. doi:10.1128/IAI.00832-10
64. Ogunniyi AD, Mahdi LK, Trappetti C, Verhoeven N, Mermans D, Van der Hoek MB, et al. Identification of genes that contribute to the pathogenesis of invasive pneumococcal disease by in vivo transcriptomic analysis. Infect Immun. 2012;80: 3268–3278. doi:10.1128/IAI.00295-12
65. Zähner D, Hakenbeck R. The *Streptococcus pneumoniae* beta-galactosidase is a surface protein. J Bacteriol. 2000;182: 5919–5921.
66. Clarke VA, Platt N, Butters TD. Cloning and expression of the β-N-acetylglucosaminidase gene from *Streptococcus pneumoniae*: generation of truncated enzymes with modified aglycon specificity. J Biol Chem. 1995;270: 8805–8814.
67. Pluvinage B, Higgins MA, Abbott DW, Robb C, Dalia AB, Deng L, et al. Inhibition of the pneumococcal virulence factor StrH and molecular insights into N-glycan recognition and hydrolysis. Structure. 2011;19: 1603–1614. doi:10.1016/j.str.2011.08.011
68. Jiang Y-L, Yu W-L, Zhang J-W, Frolet C, Di Guilmi A-M, Zhou C-Z, et al. Structural basis for the substrate specificity of a novel β-N-acetylhexosaminidase StrH protein from *Streptococcus pneumoniae* R6. J Biol Chem. 2011;286: 43004–43012. doi:10.1074/jbc.M111.256578
69. Homer KA, Roberts G, Byers HL, Tarelli E, Whiley RA, Philpott-Howard J, et al. Mannosidase production by viridans group Streptococci. J Clin Microbiol. 2001;39: 995–1001. doi:10.1128/JCM.39.3.995-1001.2001
70. Suits MDL, Zhu Y, Taylor EJ, Walton J, Zechel DL, Gilbert HJ, et al. Structure and kinetic investigation of *Streptococcus pyogenes* family GH38 α-mannosidase. Hofmann A, editor. PLoS ONE. 2010;5: e9006. doi:10.1371/journal.pone.0009006
71. Gregg KJ, Zandberg WF, Hehemann J-H, Whitworth GE, Deng L, Vocadlo DJ, et al. Analysis of a new family of widely distributed metal-independent alpha-mannosidases provides unique insight into the processing of N-linked glycans. J Biol Chem. 2011;286: 15586–15596. doi:10.1074/jbc.M111.223172
72. Corfield AP, Wagner SA, Clamp JR, Kriaris MS, Hoskins LC. Mucin degradation in the human colon: production of sialidase, sialate O-acetylesterase, N-acetylneuraminate lyase, arylesterase, and glycosulfatase activities by strains of fecal bacteria. Infect Immun. 1992;60: 3971–3978.
73. Plumbridge J, Vimr E. Convergent pathways for utilization of the amino sugars N-acetylglucosamine, N-acetylmannosamine, and N-acetylneuraminic acid by *Escherichia coli*. J Bacteriol. 1999;181: 47–54.
74. Moye ZD, Burne RA, Zeng L. Uptake and metabolism of N-acetylglucosamine and glucosamine by *Streptococcus mutans*. Appl Environ Microbiol. 2014; doi:10.1128/AEM.00820-14
75. Xiao X, Wang F, Saito A, Majka J, Schlösser A, Schrempf H. The novel *Streptomyces olivaceoviridis* ABC transporter Ngc mediates uptake of N-acetylglucosamine and N,N'-diacetylchitobiose. Mol Genet Genomics. 2002;267: 429–439. doi:10.1007/s00438-002-0640-2
76. Yang C, Rodionov DA, Li X, Laikova ON, Gelfand MS, Zagnitko OP, et al. Comparative genomics and experimental characterization of N-acetylglucosamine

utilization pathway of *Shewanella oneidensis*. J Biol Chem. 2006;281: 29872–29885. doi:10.1074/jbc.M605052200

77. Boulanger A, Dejean G, Lautier M, Glories M, Zischek C, Arlat M, et al. Identification and regulation of the N-acetylglucosamine utilization pathway of the plant pathogenic bacterium *Xanthomonas campestris* pv. *campestris*. J Bacteriol. 2010;192: 1487–1497. doi:10.1128/JB.01418-09
78. Swiatek MA, Tenconi E, Rigali S, van Wezel GP. Functional analysis of the N-acetylglucosamine metabolic genes of *Streptomyces coelicolor* and role in control of development and antibiotic production. J Bacteriol. 2012;194: 1136–1144. doi:10.1128/JB.06370-11
79. Neves AR, Pool WA, Solopova A, Kok J, Santos H, Kuipers OP. Towards enhanced galactose utilization by *Lactococcus lactis*. Appl Environ Microbiol. 2010;76: 7048–7060. doi:10.1128/AEM.01195-10
80. Zeng L, Xue P, Stanhope MJ, Burne RA. A galactose-specific sugar: phosphotransferase permease is prevalent in the non-core genome of *Streptococcus mutans*. Mol Oral Microbiol. 2013;28: 292–301. doi:10.1111/omi.12025
81. Zeng L, Martino NC, Burne RA. Two gene clusters coordinate galactose and lactose metabolism in *Streptococcus gordonii*. Appl Environ Microbiol. 2012;78: 5597–5605. doi:10.1128/AEM.01393-12
82. Cai J, Tong H, Qi F, Dong X. CcpA-dependent carbohydrate catabolite repression regulates galactose metabolism in *Streptococcus oligofermentans*. J Bacteriol. 2012;194: 3824–3832. doi:10.1128/JB.00156-12
83. Thomas TD, Turner KW, Crow VL. Galactose fermentation by *Streptococcus lactis* and *Streptococcus cremoris*: pathways, products, and regulation. J Bacteriol. 1980;144: 672–682.
84. Garrigues C, Loubiere P, Lindley ND, Cocaign-Bousquet M. Control of the shift from homolactic acid to mixed-acid fermentation in *Lactococcus lactis*: predominant role of the NADH/NAD+ ratio. J Bacteriol. 1997;179: 5282–5287.
85. Fabich AJ, Jones SA, Chowdhury FZ, Cernosek A, Anderson A, Smalley D, et al. Comparison of carbon nutrition for pathogenic and commensal *Escherichia coli* strains in the mouse intestine. Infect Immun. 2008;76: 1143–1152. doi:10.1128/IAI.01386-07
86. Van Opijnen T, Camilli A. A fine scale phenotype-genotype virulence map of a bacterial pathogen. Genome Research. 2012;22: 2541–2551. doi:10.1101/gr.137430.112
87. Nelson AL, Roche AM, Gould JM, Chim K, Ratner AJ, Weiser JN. Capsule enhances pneumococcal colonization by limiting mucus-mediated clearance. Infect Immun. 2007;75: 83–90. doi:10.1128/IAI.01475-06

Supporting Information_Chapter 2

Supporting Tables

Table S2.1. Bacterial strains and plasmids used in this study.

Strain	Relevant genotype	Reference/Source
S. pneumoniae		
D39	serotype 2 strain, *cps2*	(a)
D39Δ*galK*	D39 Δ*galK::spe*, Spe^R	This work
D39Δ*lacD*	D39 Δ*lacD::spe,* Spe^R	This work
D39Δ*manA*	D39 Δ*manA::spe,* Spe^R	This work
D39Δ*nagA*	D39 Δ*nagA::spe,* Spe^R	This work
D39Δ*lacD*Δ*galK*	D39 Δ*lacD::spe* Δ*galK::tmp,* Spe^R, Tmp^R	This work
D39Δ*galT-2*	D39 Δ*galT-2::spe*, Spe^R	This work
D39Δ*galK* + pKB01-*galK*	D39 Δ*galK::spc, bgaA*::P_{zn}-*galK-sfgfp(iGEM)*, Spe^R,Tet^R	This work
D39Δ*lacD* + pKB01-*lacD*	D39 Δ*lacD::spc, bgaA*::P_{zn}-*lacD-sfgfp(iGEM),* Spe^R,Tet^R	This work
D39Δ*manA* + pKB01-*manA*	D39 Δ*manA::spc, bgaA*::P_{zn}-*manA-sfgfp(iGEM)*,Spe^R,Tet^R	This work
D39Δ*nagA* + pKB01-*nagA*	D39 Δ*nagA::spc, bgaA*::$P_{ownnagA}$-*nagA-sfgfp(iGEM)*, Spe^R,Tet^R	This work
D39Δ*galK* + pKB01-*galT-2*	D39 Δ*galK::spc, bgaA*::P_{Zn}-*galT-2-sfgfp(iGEM)*, Spe^R,Tet^R	This work
D39Δ*galK* + pKB01-*galKgalT-2*	D39 Δ*galK::spc, bgaA*::P_{Zn}-*galKgalT-2-sfgfp(iGEM)*, Spe^R,Tet^R	This work
E. coli		
DH5α	*F– Φ80lacZΔM15 Δ(lacZYA-argF) U169 recA1 endA1 hsdR17 (rK–, mK+) phoA supE44 λ– thi-1 gyrA96 relA1*	Invitrogen (b)
DH5α + pKB01	Amp^R	(b)
Plasmids		
pORI138	Ori^+ $repA^-$, deletion derivative of pWV01; Spe^R	[1]
pKB01	*bgaA,* P_{zn}-*sfgfp(iGEM)*+, Amp^R, Tet^R	[2]
pKB01-*galK*	*bgaA,* P_{zn}-*galK-sfgfp(iGEM)*, Amp^R, Tet^R	This work
pKB01-*lacD*	*bgaA,* P_{zn}-*lacD-sfgfp(iGEM)*, Amp^R, Tet^R	This work
pKB01-*manA*	*bgaA,* P_{zn}-*manA-sfgfp(iGEM)*, Amp^R, Tet^R	This work
pKB01-*nagA*	*bgaA,* $P_{ownnagA}$-*nagA-sfgfp(iGEM)*, Amp^R, Tet^R	This work
pKB01-*galT-2*	*bgaA,* P_{zn}-*galT-2-sfgfp(iGEM)*, Amp^R, Tet^R	This work
pKB01-*galKgalT-2*	*bgaA,* P_{zn}-*galKgalT-2-sfgfp(iGEM)*, Amp^R, Tet^R	This work

Spe^R, spectinomycin resistance marker, Tmp^R, trimethoprim resistance marker, Amp^R, ampicillin resistance marker, Tet^R, tetracycline resistance marker.
(a) Laboratory stock obtained from the Department of Infection, Immunity & Inflammation, University of Leicester.
(b) Laboratory stock obtained from the Molecular Genetics Department, Groningen Biomolecular Sciences and Biotechnology Institute (GBB), Centre for Synthetic Biology, University of Groningen.
1. Leenhouts K, Buist G, Bolhuis A, ten Berge A, Kiel J, Mierau I, et al. A general system for generating unlabelled gene replacements in bacterial chromosomes. Mol Gen Genet MGG. 1996;253: 217–224.
2. Overkamp W, Beilharz K, Detert Oude Weme R, Solopova A, Karsens H, Kovacs AT, et al. Benchmarking various green fluorescent protein variants in *Bacillus subtilis*, *Streptococcus pneumoniae*, and *Lactococcus lactis* for live cell imaging. Appl Env Microbiol. 2013;79: 6481–6490. doi:10.1128/AEM.02033-13

Table S2.2. Pairwise comparisons, across combinations of different sugars and initial substrate concentrations, to test the null hypothesis of equal values for the μ_{max} and OD_{max}.

		Lower sugar concentration				Higher sugar concentration			
Sugar A	**Sugar B**	n_A	n_B	μ_{max}	OD_{max}	n_A	n_B	μ_{max}	OD_{max}
Glc	Gal	12	9	$< 10^{-7}$	NS	10	10	$< 10^{-7}$	NS
Glc	GlcNAc	12	8	$< 10^{-7}$	0.049621	10	8	$< 10^{-7}$	0.000041
Glc	Man	12	14	$< 10^{-7}$	NS	10	9	$< 10^{-7}$	0.000002
Gal	GlcNAc	9	8	0.000057	NS	10	8	0.009460	0.000329
Gal	Man	9	14	$< 10^{-7}$	NS	10	9	NS	0.000017
GlcNAc	Man	14	8	0.008151	NS	8	9	0.001814	NS

For each comparison, the *p-values* of the Student's t-test are reported. Statistically significant values (*p-value*<0.05) are shown. *P-values*>0.05 were considered non-significant (NS). The number of replicates for each condition is depicted (n).

Table S2.3. Oligonucleotide primers used in this study (from 5' to 3').

Primer	Sequence (from 5' to 3')	Description
Allelic replacement mutagenesis		
GalK_KO1_Fw	CTAGACGCTTGTCCTGAATG	
GalK_KO2_Rv_Spe	***TCCTCCTCACTATTTTGATTAG***GCGAAGAGTTTCAGCAGTAAGATG	***Overlap with* spe**
GalK_KO3_Fw_Spe	***CGTTTTAGCGTTTATTTCGTTTAGT***GTTGCAGGTGGCACTCGCGTC	***Overlap with* spe**
GalK_KO4_Rv	CGGCAGGTCGGCATTAGATCC	
LacD_KO1_Fw	CTCAATTCAGGGAGAAACTCG	
LacD_KO2_Rv_Spe	***TCCTCCTCACTATTTTGATTAG***GATGATACCATTTTCATCAGAAAG	***Overlap with* spe**
LacD_KO3_Fw_Spe	***CGTTTTAGCGTTTATTTCGTTTAGT***GCGACTTCATGGAAAGAACGTGTG	***Overlap with* spe**
LacD_KO4_Rv	CAATCGACTCCACAAGTTCCAC	
ManA_KO1_Fw	GACTTTCCTGATAGAGTTGTTC	
ManA_KO2_Rv_Spe	***TCCTCCTCACTATTTTGATTAG***GGTACCACCCCAGATTTTTTCTTGC	***Overlap with* spe**
ManA_KO3_Fw_Spe	***CGTTTTAGCGTTTATTTCGTTTAGT***TCTTGGACTCTAGAAGGGC	***Overlap with* spe**
ManA_KO4_Rv	GGTTCTTTACTTCCTCAAACCAG	
NagA_KO1_Fw	CTAAGACGGTGGTCATTGCGACTG	
NagA_KO2_Rv_Spe	***TCCTCCTCACTATTTTGATTAG***GTGTGGGTAGAAAAACTGATCCGC	***Overlap with* spe**
NagA_KO3_Fw_Spe	***CGTTTTAGCGTTTATTTCGTTTAGT***GATGGCGTAAAACGTTATCAAGCA	***Overlap with* spe**
NagA_KO4_Rv	CACGTAGATATTCAGCCTGCATACC	
Spe_Fp	CTAATCAAAATAGTGAGGAGG	
Spe_Rp	ACTAAACGAAATAAACGC	
GalK_KO2_Rv_Tmp	***TCCAAGCTCACAAAAATCC***GCGAAGAGTTTCAGCAGTAAGATG	***Overlap with* tmp**
GalK_KO3_Fw_Tmp	***CCGTCTATGCGCGTCGTAAC***GTTGCAGGTGGCACTCGCGTC	***Overlap with* tmp**
Tmp_ FW	GGATTTTTGTGAGCTTGGA	
Tmp_RV	GTTACGACGCGCATAGACGG	

Primer	Sequence (from 5' to 3')	Description
GalT-2_KO1_Fw	CTTCAGCATCCTTGGAGATCTTG	
GalT-2_KO2_Rv_Spe	***TCCTCCTCACTATTTTGATTAG***GACATGTGTTACAAATTTATCTACTAAGGTCAC	***Overlap with* spe**
GalT-2_KO3_FW_Spe	***CGTTTTAGCGTTTATTTCGTTTAGT***GGAATTTTACTAGACTAG	***Overlap with* spe**
GalT-2_KO4_Rv	CCCACAATTAGGGCAATAAGAC	
Confirmation of genotype by PCR		
GalK_S_Fw	CCGATAGCTAAACTATCGCTGGC	
GalK_S_Rv	GAAGTCAAGCGTAGGACAGACATTGG	
ManA_S_Fw	GGCGCTTCAACAGTTGATAG	
ManA_S_Rv	GCCATTGCTCTAGGAGCTCAAGCG	
LacD_S_Fw	CGGCTGGTGGTAAGGGACTCAATG	
LacD_S_Rv	CGTATGTTGCGTAATCACATCATAG	
NagA_S_Fw	GTGGGAGCGTTTGAGACAGAC	
NagA_S_Rv	CGCACCGAATGATAGGGCAG	
GalT-2_S_Fw	GGGGTTCTTCATTTCTTGCAAGAAGC	
GalT-2_S_Rv	TGCATAAGCACCATCATTGATTG	
Complementation of loss-of-function mutants		REnz
GalK_Fw_EcoRI	AATTGAATTCCAAAGGAGAAATCATATGACACAACATCTTACTGC	EcoRI
GalK_Rv_BamHI	GATCGGATCCCTAGTCAAGGACGCGAGTGCC	BamHI
GalK_Fw_EcoRI_B	AATTGAATTCTAAGGAGGCAAATATGACACAACATCTTACTGC	EcoRI
GalT-2_Rv_XbaI	ACGTCTAGATGTGCAAGGAGAAAGCTCCT	XbaI
LacD_Fw_EcoRI	AATTGAATTCTAAAAGAGGTATAAAATGGCTTTAACAGAAC	EcoRI
LacD_Rv_BamHI	GATCGGATCCTTACACACGTTCTTTCC	BamHI
NagA_Fw_NotI	AATTGCGGCCGCGAGTTGGAGAAATCCAGC	NotI
NagA_Rv_BamHI	GATCGGATCCTTATGCTTGATAACGTTTTACGC	BamHI

Primer	Sequence (from 5' to 3')	Description
ManA_Fw_EcoRI	AATTGAATTCAGACAGGAGATTAAGATGTCAGAACCATTATTTTTAC	EcoRI
ManA_Rv_BamHI	GATCGGATCCTTATGGATGACTAACAATTAATTC	BamHI
GalT-2_Fw_EcoRI	AATTGAATTCAGGAGGCTCTATAGTGACCTTAGTAGATAAATTTG	EcoRI
GalT-2_Rv_NotI	GGCCGCGGCCGCCTAGTCTAGTAAAATTCCGACC	NotI
Confirmation of integration in the *bgaA* locus of the pneumococcal chromosome		
Integration 1	CTTGATGAAACCTACATTTG	
Integration 2	GCTTCCATTAAGGATAGTTC	
Integration 5	GCTATCGCTGAGCGCCGG	
Integration 6	AGCTAGAGTTCCGCAATTGG	
P up gatC Fw	ATGGATGCAATCTTTGACCTAATCGG	
P Tet Rv	CACATCGAAGTGCCGCCAAATCC	
Primers used for qRT-PCR		
GALT1RTF	CTCGTAAAGTGGACGGGAGA	
GALT1RTR	GCAAGTCCCATCACTTCGAT	
GALT2RTF	TCACACCAATAGCGCGTAAG	
GALT2RTR	AGCCCATGACCTCAATCAAG	
SPD1050F	GCCAGACTGCTTGGATGTTT	
SPD1050R	TCAGCCACACACTCAGAACC	
SPD1634F	TCTCGGTGCTCGTATGACAG	
SPD1634R	CACCTGCAACTTCAGCGATA	
SP0645RTF	GCTTAGAAGCGGATAGTCAAG	
SP0645RTR	GTGAGGAATCGCTACATTTGG	
SP0647RTF	TTGCCACTTGCAGGTATCATC	
SP0647RTR	TTCTGGGAAGGCACCTACAC	

Primer	Sequence (from 5’ to 3’)	Description
SP1197RTF	CTGGTTCAAAACCAAGGTCTG	
SP1197RTR	GCGGTGCAGGTGTTAACTC	
SP1682RTF	TGATGGGCTGACCAACTG	
SP1682RTR	GTGTTGCCGTGACAGTTG	
SP2184RTF	ACCTGTTGTCCCACCTAGTG	
SP2184RTR	TACTGGACCAGCCATCAAGG	
SP703RTF	TAGCGCCTATAGTGGGTCAG	
SP703RTR	CTGGATTCCAAGAACCTGAAG	
SP1507RTF	ATCGGTTCGAACTCTGGATG	
SP1507RTR	ATAACGCCACCGTTTACTGC	
SP1615RTF	AAAATGTTCGCGTCCGTTAC	
SP1615RTR	GGGTGAGCCGTAACCAATTA	
SP2126RTF	TCATGCCACTTGAAAATCCA	
SP2126RTR	GCCTGAATCGCATCTTCTTC	
SPDRT0709F	AAGGAGACTCAGCTGGTGGA	
SPDRT0709R	CCCATGGCTGTGAAAAGACT	

Abbreviations: Spe, spectinomycin; Tmp, trimethoprim. REnz, restriction enzyme. Restriction enzyme sites are underlined.

Table S2.4. Genes proposed to be involved in the uptake and dedicated catabolism of galactose (Gal), mannose (Man), N-acetylneuraminic acid (NeuNAc), N-acetylglucosamine (GlcNAc), fucose (Fuc), and glucose (Glc) in *S. pneumoniae* D39.

Locus_Tag	Gene	Description	Identification Method or Ref.
Galactose			
Gal transport			
SPD_0263	*manM*	PTS system mannose-specific transporter subunit IIC	[1]
SPD_0067[a]	-	PTS system transporter subunit IIC	[1–3]
SPD_0561	-	PTS system transporter subunit IIC	[1,4]
SPD_0090	-	ABC transporter substrate-binding protein	[1]
Gal catabolism			
SPD_0071	*galM*	Aldose 1-epimerase	Genome annotation at NCBI
SPD_1634	*galK*	Galactokinase	Genome annotation at NCBI
SPD_1613	*galT-1*	Galactose 1-phosphate uridylyltransferase	Genome annotation at NCBI
SPD_1633	*galT-2*	Galactose 1-phosphate uridylyltransferase	Genome annotation at NCBI
SPD_1432	*galE-1*	UDP-glucose 4-epimerase	Genome annotation at NCBI
SPD_1612	*galE-2*	UDP-glucose 4-epimerase	Genome annotation at NCBI
SPD_1326	*pgm*	Phosphoglucomutase/phosphomannomutase family protein	Genome annotation at NCBI
SPD_1053	*lacA*	Galactose 6-phosphate isomerase subunit LacA	Genome annotation at NCBI
SPD_1052	*lacB*	Galactose 6-phosphate isomerase subunit LacB	Genome annotation at NCBI
SPD_1051	*lacC*	Tagatose 6-phosphate kinase	Genome annotation at NCBI
SPD_1050	*lacD*	Tagatose 1,6-diphosphate aldolase	Genome annotation at NCBI
Mannose			
Man transport			
SPD_0263	*manM*	PTS system, mannose-specific transporter subunit IIC	[1]
SPD_0428	*lacE-1*	PTS system, lactose-specific transporter subunit IIBC	[1]
SPD_0090	-	ABC transporter, substrate-binding protein	[1]
SPD_0067	-	PTS system transporter subunit IIC	Database annotation[b]
SPD_0296	-	PTS system transporter subunit IIC	Database annotation[b]
SPD_1990	-	PTS system transporter subunit IIC	Database annotation[b]
Man catabolism			

Locus_Tag	Gene	Description	Identification Method or Ref.
SPD_0641	*manA*	Mannose 6-phosphate isomerase	Genome annotation at NCBI
N-acetylneuraminac acid and N-acetylglucosamine			
NeuNAc transport			
SPD_1495	-	Sugar ABC transporter, sugar-binding protein	[1,5–7]
SPD_1502	-	ABC transporter, substrate-binding protein	[1,6,7]
SPD_1170[c]	-	Oligopeptide ABC transporter, oligopeptide-binding protein	[1,7]
GlcNAc transport			
SPD_0263	*manM*	PTS system, mannose specific transporter subunit IIC	[1]
SPD_0661	*exp5*	PTS system transporter subunit IIABC	Database annotation[b]
SPD_1496	-	PTS system transporter subunit IIBC	Database annotation[b]
SPD_1532	-	PTS system IIABC components	Database annotation[b]
SPD_1664	-	PTS system, trehalose-specific IIABC components	Database annotation[b]
NeuNAc & GlcNAc catabolism			
SPD_1489	-	N-acetylneuraminate lyase	Genome annotation at NCBI BlastP search[d]
SPD_1163	-	N-acetylneuraminate lyase	Genome annotation at NCBI BlastP search[d]
SPD_1488	-	ROK family protein	BlastP search[d]
SPD_1497	*nanE-1*	N-acetylmannosamine 6-phosphate 2-epimerase	Genome annotation at NCBI
SPD_1172	*nanE-2*	N-acetylmannosamine 6-phosphate 2-epimerase	Genome annotation at NCBI
SPD_1171[e]	-	Hypothetical protein	BlastP search[d]
SPD_1866	*nagA*	N-acetylglucosamine 6-phosphate deacetylase	Genome annotation at NCBI
SPD_1246	*nagB*	Glucosamine 6-phosphate isomerase	Genome annotation at NCBI
Fucose			
Fuc transport			
SPD_1990[f]	-	PTS system, transporter subunit IIC	[1,8]
Fuc catabolism			
SPD_1995	*fucK*	L-fuculose kinase	[8]
SPD_1994	*fucA*	L-fuculose phosphate aldolase	[8]
SPD_1986	*fucI*	L-fucose isomerase	[8]
SPD_1993	*fucU*	RbsD/FucU transport protein family protein	Genome annotation at NCBI
Glucose			
Glc transport			
SPD_0263[g]	*manM*	PTS system, mannose-specific transporter subunit IIC	[1]
Glycolysis			

Locus_Tag	Gene	Description	Identification Method or Ref.
SPD_0580	*gki*	Glucokinase	Genome annotation at NCBI
SPD_1897	*pgi*	Glucose 6-phosphate isomerase	Genome annotation at NCBI
SPD_0789	*pfkA*	6-phosphofructokinase	Genome annotation at NCBI
SPD_0526	*fba*	Fructose-bisphosphate aldolase	Genome annotation at NCBI
SPD_1404	*tpiA*	Triosephosphate isomerase	Genome annotation at NCBI
SPD_1823	*gap*	Glyceraldehyde 3-phosphate dehydrogenase	Genome annotation at NCBI
SPD_0445	*pgk*	Phosphoglycerate kinase	Genome annotation at NCBI
SPD_1468	*gpmA*	Phosphoglyceromutase	Genome annotation at NCBI
SPD_1012	*eno*	Phosphopyruvate hydratase	Genome annotation at NCBI
SPD_0790	*pyk*	Pyruvate kinase	Genome annotation at NCBI

[a]Theoretical Gal transporter. Inferred from genomic context.
[b]According to http://www.membranetransport.org/. For the sake of simplicity, only the genes encoding the EIIC component of the PTS system and the substrate binding protein in case of ABC transporters are shown.
[c]Allelic variation of SP1328 of *S. pneumoniae* TIGR4 [1].
[d]For BlastP searches functionally characterized *E. coli* proteins were used as query.
[e]Homology (22% identity; 39% positives) with YjhT from *E. coli* K-12 MG1655. A recently characterized sialic acid mutarotase [9].
[f]Putative transporter. Fucose transport by this PTS is not yet fully disclosed [1,8,10].
[g]Due to the high multiplicity of glucose transporters of *S. pneumoniae,* only the main glucose uptake system identified in D39 is shown [1].

References

1. Bidossi A, Mulas L, Decorosi F, Colomba L, Ricci S, Pozzi G, et al. A functional genomics approach to establish the complement of carbohydrate transporters in *Streptococcus pneumoniae*. Miyaji EN, editor. PLoS ONE. 2012;7: e33320. doi:10.1371/journal.pone.0033320
2. Terra VS, Homer KA, Rao SG, Andrew PW, Yesilkaya H. Characterization of novel β-galactosidase activity that contributes to glycoprotein degradation and virulence in *Streptococcus pneumoniae*. Infect Immun. 2010;78: 348–357. doi:10.1128/IAI.00721-09
3. Jeong JK, Kwon O, Lee YM, Oh D-B, Lee JM, Kim S, et al. Characterization of the *Streptococcus pneumoniae* BgaC protein as a novel surface β-galactosidase with specific hydrolysis activity for the Galβ1-3GlcNAc moiety of oligosaccharides. J Bacteriol. 2009;191: 3011–3023. doi:10.1128/JB.01601-08
4. Kaufman GE, Yother J. CcpA-dependent and -independent control of beta-galactosidase expression in *Streptococcus pneumoniae* occurs via regulation of an

upstream phosphotransferase system-encoding operon. J Bacteriol. 2007;189: 5183–5192. doi:10.1128/JB.00449-07
5. Marion C, Burnaugh AM, Woodiga SA, King SJ. Sialic acid transport contributes to pneumococcal colonization. Infect Immun. 2011;79: 1262–1269. doi:10.1128/IAI.00832-10
6. King SJ, Hippe KR, Gould JM, Bae D, Peterson S, Cline RT, et al. Phase variable desialylation of host proteins that bind to *Streptococcus pneumoniae* in vivo and protect the airway: Pneumococcal desialylation of host proteins. Mol Microbiol. 2004;54: 159–171. doi:10.1111/j.1365-2958.2004.04252.x
7. Almagro-Moreno S, Boyd EF. Insights into the evolution of sialic acid catabolism among bacteria. BMC Evol Biol. 2009;9: 118. doi:10.1186/1471-2148-9-118
8. Higgins MA, Suits MD, Marsters C, Boraston AB. Structural and functional analysis of fucose-processing enzymes from *Streptococcus pneumoniae*. J Mol Biol. 2014;426: 1469–1482. doi:10.1016/j.jmb.2013.12.006
9. Severi E, Muller A, Potts JR, Leech A, Williamson D, Wilson KS, et al. Sialic acid mutarotation is catalyzed by the *Escherichia coli* beta-propeller protein YjhT. J Biol Chem. 2008;283: 4841–4849. doi:10.1074/jbc.M707822200
10. Higgins MA, Whitworth GE, El Warry N, Randriantsoa M, Samain E, Burke RD, et al. Differential recognition and hydrolysis of host carbohydrate antigens by *Streptococcus pneumoniae* family 98 glycoside hydrolases. J Biol Chem. 2009;284: 26161–26173. doi:10.1074/jbc.M109.024067

Table S2.5. Expression levels of genes upregulated in *S. pneumoniae* D39 cells grown in mucin as compared to glucose-grown cells, according to the established criterion (see Materials and Methods).

Gene	Fold	P-value	Description
SPD_0562	71.8	0.0062	beta-galactosidase
SPD_1057	61.3	0.0085	PTS system transporter subunit IIB
SPD_0561	45.5	0.0478	PTS system transporter subunit IIC
SPD_0068	25.4	0.0206	PTS system transporter subunit IID
SPD_1053	24.5	0.0201	galactose-6-phosphate isomerase subunit LacA
SPD_0069	23.9	0.0185	PTS system transporter subunit IIA
SPD_1052	21.7	0.0307	galactose-6-phosphate isomerase subunit LacB
SPD_2013	20.8	0.0074	glycerol kinase
SPD_0071	19.4	0.0281	aldose 1-epimerase
SPD_1050	17.6	0.0411	tagatose 1,6-diphosphate aldolase
SPD_0559	15.1	0.0041	PTS system transporter subunit IIA
SPD_0560	12.1	0.0127	PTS system transporter subunit IIB
SPD_2011	10.3	0.0031	glycerol uptake facilitator protein
SPD_1494	10.3	0.0197	sugar ABC transporter permease
SPD_0070	9.8	0.0393	sugar isomerase
SPD_0610	8.9	0.0096	hypothetical protein

Gene	Fold	P-value	Description
SPD_0063	8.7	0.0335	beta-N-acetylhexosaminidase
SPD_1590	8.6	0.0463	general stress protein 24
SPD_1663	8.0	0.0191	alpha,alpha-phosphotrehalase
SPD_0066	7.8	0.0255	PTS system transporter subunit IIB
SPD_0287	7.7	0.0017	hyaluronate lyase
SPD_1495	6.7	0.0252	sugar ABC transporter sugar-binding protein
SPD_0293	6.5	0.0292	PTS system transporter subunit IIA
SPD_1834	5.8	0.0216	bifunctional acetaldehyde-CoA/alcohol dehydrogenase
SPD_1977	5.6	0.0114	carbamate kinase
SPD_0613	5.5	0.0091	hypothetical protein
SPD_0292	5.3	0.0093	gluconate 5-dehydrogenase
SPD_0259	5.3	0.0398	hypothetical protein
SPD_1976	5.2	0.0018	ornithine carbamoyltransferase
SPD_0337	5.2	0.0425	Holliday junction-specific endonuclease
SPD_1979	5.1	0.0009	hypothetical protein
SPD_1652	4.9	0.038	iron-compound ABC transporter iron-compound-binding protein
SPD_1978	4.9	0.0063	hypothetical protein
SPD_1409	4.8	0.0271	sugar ABC transporter ATP-binding protein
SPD_1934	4.8	0.0048	maltose/maltodextrin ABC transporter maltose/maltodextrin-binding protein
SPD_1975	4.7	0.0083	pseudo
SPD_0619	4.5	0.0175	hypothetical protein
SPD_0297	4.4	0.0419	PTS system transporter subunit IID
SPD_1496	4.4	0.0193	PTS system transporter subunit IIBC
SPD_1006	4.4	0.0092	glucose-1-phosphate adenylyltransferase
SPD_0308	4.4	0.0101	ATP-dependent Clp protease, ATP-binding subunit
SPD_0336	4.0	0.0238	penicillin-binding protein 1A
SPD_0621	4.0	0.0104	lactate oxidase
SPD_1935	3.9	0.0058	maltodextrin ABC transporter permease
SPD_1651	3.8	0.0115	iron-compound ABC transporter ATP-binding protein
SPD_0420	3.7	0.021	formate acetyltransferase
SPD_0093	3.6	0.0308	hypothetical protein
SPD_0095	3.6	0.0036	hypothetical protein
SPD_0094	3.6	0.001	hypothetical protein
SPD_1007	3.5	0.0081	glucose-1-phosphate adenylyltransferase, GlgD subunit
SPD_2012	3.4	0.0029	alpha-glycerophosphate oxidase
SPD_1408	3.3	0.0317	hypothetical protein

Gene	Fold	P-value	Description
SPD_1566	3.2	0.0015	hypothetical protein
SPD_1567	3.1	0.0153	thioredoxin
SPD_1005	2.9	0.0272	glycogen branching protein
SPD_1936	2.9	0.0286	maltodextrin ABC transporter permease
SPD_0250	2.9	0.038	pullulanase, extracellular
SPD_0086	2.8	0.0004	hypothetical protein
SPD_0692	2.7	0.0207	hypothetical protein
SPD_1709	2.6	0.0298	chaperonin GroEL
SPD_0691	2.6	0.019	hypothetical protein
SPD_1989	2.6	0.0438	PTS system transporter subunit IID
SPD_0628	2.6	0.0281	transcriptional activator TenA, TENA/THI-4 family protein
SPD_0616	2.5	0.0251	amino acid ABC transporter ATP-binding protein
SPD_0427	2.5	0.0268	6-phospho-beta-galactosidase
SPD_1675	2.4	0.0355	sugar ABC transporter permease
SPD_0925	2.4	0.0443	hydrolase
SPD_0440	2.4	0.0139	hypothetical protein
SPD_1789	2.4	0.0194	cell wall surface anchor family protein
SPD_1937	2.3	0.0231	maltodextrose utilization protein MalA
SPD_0627	2.3	0.0275	hypothetical protein
SPD_1554	2.2	0.0428	iojap-like protein
SPD_0626	2.2	0.023	ABC transporter ATP-binding protein
SPD_1282	2.2	0.0192	hypothetical protein
SPD_0424	2.2	0.0259	PTS system cellobiose-specific transporter subunit IIC
SPD_0814	2.2	0.004	agmatine iminohydrolase
SPD_1944	2.1	0.0112	hypothetical protein
SPD_0008	2.1	0.0103	hypothetical protein
SPD_1557	2.1	0.0109	nicotinic acid mononucleotide adenylyltransferase
SPD_1558	2.1	0.0391	hypothetical protein
SPD_0439	2.1	0.042	hypothetical protein
SPD_1655	2.1	0.003	segregation and condensation protein B
SPD_0863	2.0	0.0488	SsrA-binding protein

Table S2.6. Expression ratio as determined by qRT-PCR of genes selected from the microarray experiment comparing mRNA levels in mucin-grown to glucose-grown *S. pneumoniae* D39 cells.

Targets		Relative fold increase	SD
SPD_0559	PTS system transporter subunit IIA	32.9	5.0
SPD_0561	PTS system transporter subunit IIC	31.4	3.1
SPD_0610	Hypothetical protein	2.4	0.5
SPD_1057	PTS system transporter subunit IIB	38.2	6.3
SPD_1494	Sugar ABC transporter permease	67.0	16.9
SPD_2011	Glycerol uptake facilitator protein	16.0	1.1
SPD_1334	F0F1 ATP synthase subunit epsilon (EC:3.6.3.14)	0.3	0.1
SPD_1839	Transketolase (EC:2.2.1.1)	0.2	0.0
SPD_1956	Dihydroxy-acid dehydratase	0.2	0.1

SD, standard deviation.

Table S2.7. Expression ratio of genes involved in galactose catabolism in exponentially growing *S. pneumoniae* D39 cells disrupted in *galK* or *galT-2* genes.

	Carbon source - strain		
Gene	**Glc-Δ*galK* / Glc-D39**	**Glc-Δ*galK* / Gal-D39**	**Gal-Δ*galT-2* / Gal-D39**
galT-2	0.54 ± 0.24	0.51 ± 0.22	-
galT-1	ND	ND	49.41 ± 3.55
lacD	0.81 ± 0.03	0.0044 ± 0.0002	87.42 ± 5.41
galK	-	-	19.29 ± 0.74

Values represent the fold difference ± standard deviation transcript levels in the mutant strain as compared to the wild type. Cells were grown in CDM supplemented with glucose or galactose. In the qRT-PCR experiments, the expression values were normalized relative to the housekeeping gene *gyrB*.
ND, not determined.

Table S2.8. Conservation of Gal metabolic genes in different *S. pneumoniae* strains[1].

Strains/ Genes	*lacA*	*lacB*	*lacC*	*lacD*	*galE-1*	*galE-2*	*galT-1*	*galT-2*	*galK*	*galM*	*pgm*
D39	SPD_1053	SPD_1052	SPD_1051	SPD_1050	SPD_1432	SPD_1612	SPD_1613	SPD_1633	SPD_1634	SPD_0071	SPD_1326
TIGR4	SP_0066|SP_0066|NP_344615.1|GeneID:929828|0.0|1	SP_1190|SP_1190|NP_345659.1|GeneID:931704|0.0|1	SP_1191|SP_1191|NP_345660.1|GeneID:931705|0.0|1	SP_1192|SP_1192|NP_345661.1|GeneID:931706|9e-127|1	SP_1193|SP_1193|NP_345662.1|GeneID:931707|1e-99|1	SP_1498|SP_1498|NP_345949.1|GeneID:931340|0.0|1	SP_1607|SP_1607|NP_346051.1|GeneID:931229|0.0|2	SP_1828|SP_1828|NP_346261.1|GeneID:931007|0.0|2	SP_1829|SP_1829|NP_346262.1|GeneID:931006|0.0|2	SP_1852|SP_1852|NP_346284.1|GeneID:930983|0.0|2	SP_1853|SP_1853|NP_346285.1|GeneID:930981|0.0|1
R6	spr0065|galM|NP_357659.1|GeneID:932955|0.0|1	spr1073|lacD|NP_358666.1|GeneID:933800|0.0|1	spr1074|lacC|NP_358667.1|GeneID:933209|0.0|1	spr1075|lacB|NP_358668.1|GeneID:933958|9e-128|1	spr1076|lacA|NP_358669.1|GeneID:933185|3e-100|1	spr1351|pgm|NP_358944.1|GeneID:934575|0.0|1	spr1460|galE|NP_359053.1|GeneID:933804|0.0|2	spr1647|galE|NP_359239.1|GeneID:933268|0.0|2	spr1648|galT|NP_359240.1|GeneID:932967|0.0|2	spr1667|galT|NP_359259.1|GeneID:933029|0.0|2	spr1668|galK|NP_359260.1|GeneID:933086|0.0|1
G54	SPG_0070|SPG_0070|YP_002036785.1|GeneID:6480193|0.0|1	SPG_1085|lacD|YP_002037795.1|GeneID:6479088|0.0|1	SPG_1086|lacC|YP_002037796.1|GeneID:6478686|0.0|1	SPG_1087|lacB|YP_002037797.1|GeneID:6480347|9e-127|1	SPG_1088|lacA|YP_002037798.1|GeneID:6480700|4e-100|1	SPG_1421|SPG_1421|YP_002038128.1|GeneID:6480668|0.0|1	SPG_1531|SPG_1531|YP_002038236.1|GeneID:6479373|0.0|2	SPG_1531|SPG_1531|YP_002038236.1|GeneID:6479373|3e-137|2	SPG_1737|SPG_1737|YP_002038441.1|GeneID:6478868|0.0|1	SPG_1737|SPG_1737|YP_002038441.1|GeneID:6478868|0.0|1	SPG_1738|SPG_1738|YP_002038442.1|GeneID:6480580|0.0|1
670_6B	SP670_0143|SP670_0143|YP_003878325.1|GeneID:9728873|0.0|1	SP670_1086|lacD|YP_003879249.1|GeneID:9729805|0.0|1	SP670_1085|lacC|YP_003879248.1|GeneID:9729804|0.0|1	SP670_1084|lacB|YP_003879247.1|GeneID:9729803|1e-127|1	SP670_1083|lacA|YP_003879246.1|GeneID:9729802|4e-100|1	SP670_0799|SP670_0799|YP_003878966.1|GeneID:9729520|0.0|1	SP670_1691|SP670_1691|YP_003879847.1|GeneID:9730406|0.0|2	SP670_1903|SP670_1903|YP_003880055.1|GeneID:9730616|0.0|2	SP670_1904|SP670_1904|YP_003880056.1|GeneID:9730617|0.0|2	SP670_1927|SP670_1927|YP_003880079.1|GeneID:9730640|0.0|2	SP670_1928|galK|YP_003880080.1|GeneID:9730641|0.0|1
70585	SP70585_0132|SP70585_0132|YP_002739444.1|GeneID:7683722|0.0|1	SP70585_1240|lacD|YP_002740485.1|GeneID:7684238|0.0|1	SP70585_1241|lacC|YP_002740486.1|GeneID:7683262|0.0|1	SP70585_1242|lacB|YP_002740487.1|GeneID:7683690|1e-127|1	SP70585_1243|lacA|YP_002740488.1|GeneID:7682913|2e-99|1	SP70585_1536|SP70585_1536|YP_002740766.1|GeneID:7683612|0.0|1	SP70585_1647|galE|YP_002740872.1|GeneID:7684655|0.0|1	SP70585_1647|galE|YP_002740872.1|GeneID:7684655|2e-137|1	SP70585_1907|galT|YP_002741124.1|GeneID:7683577|0.0|1	SP70585_1907|galT|YP_002741124.1|GeneID:7683577|0.0|1	SP70585_1908|galK|YP_002741125.1|GeneID:7683539|0.0|1
A026	T308_00260|T308_00260|REF_PRJNA22282:T308_00260|GeneID:17438499|0.0|1	T308_04815|T308_04815|REF_PRJNA22282:T308_04815|GeneID:17439402|0.0|1	T308_04810|T308_04810|REF_PRJNA22282:T308_04810|GeneID:17439401|0.0|1	T308_04805|T308_04805|REF_PRJNA22282:T308_04805|GeneID:17439400|9e-127|1	T308_04800|T308_04800|REF_PRJNA22282:T308_04800|GeneID:17439399|7e-99|1	T308_06785|T308_06785|REF_PRJNA22282:T308_06785|GeneID:17439792|0.0|1	T308_07310|T308_07310|REF_PRJNA22282:T308_07310|GeneID:17439896|0.0|2	T308_08295|T308_08295|REF_PRJNA22282:T308_08295|GeneID:17440090|0.0|2	T308_08300|T308_08300|REF_PRJNA22282:T308_08300|GeneID:17440091|0.0|2	T308_08395|T308_08395|REF_PRJNA22282:T308_08395|GeneID:17440110|0.0|2	T308_08400|T308_08400|REF_PRJNA22282:T308_08400|GeneID:17440111|0.0|1
AP200	SPAP_0114|SPAP_0114|YP_003875710.1|GeneID:9726131|0.0|1	SPAP_1217|SPAP_1217|YP_003876807.1|GeneID:9727232|0.0|1	SPAP_1218|SPAP_1218|YP_003876808.1|GeneID:9727233|0.0|1	SPAP_1219|SPAP_1219|YP_003876809.1|GeneID:9727234|2e-126|1	SPAP_1220|SPAP_1220|YP_003876810.1|GeneID:9727235|4e-100|1	SPAP_1521|SPAP_1521|YP_003877109.1|GeneID:9727536|0.0|1	SPAP_1628|SPAP_1628|YP_003877214.1|GeneID:9727642|0.0|3	SPAP_1824|SPAP_1824|YP_003877409.1|GeneID:9727838|0.0|2	SPAP_1825|SPAP_1825|YP_003877410.1|GeneID:9727839|0.0|2	SPAP_1848|SPAP_1848|YP_003877433.1|GeneID:9727862|0.0|2	SPAP_1849|SPAP_1849|YP_003877434.1|GeneID:9727863|0.0|1
ATCC_700669	SPN23F_00810|SPN23F_00810|YP_002510165.1|GeneID:7328641|0.0|1	SPN23F_10890|lacD2|YP_002511048.1|GeneID:7328099|0.0|1	SPN23F_10900|lacC2|YP_002511049.1|GeneID:7328094|0.0|1	SPN23F_10910|lacB1|YP_002511050.1|GeneID:7328093|9e-128|1	SPN23F_10920|lacA|YP_002511051.1|GeneID:7328092|6e-99|1	SPN23F_14630|pgmA|YP_002511364.1|GeneID:7328703|0.0|1	SPN23F_16210|galE|YP_002511515.1|GeneID:7328817|0.0|2	SPN23F_18460|galE|YP_002511723.1|GeneID:7329376|0.0|2	SPN23F_18470|SPN23F_18470|YP_002511724.1|GeneID:7328581|0.0|2	SPN23F_18670|galT|YP_002511743.1|GeneID:7329392|0.0|2	SPN23F_18680|galK|YP_002511744.1|GeneID:7328584|0.0|1
CGSP14	SPCG_0067|galM|YP_001834784.1|GeneID:6218128|0.0|1	SPCG_1108|lacD|YP_001835825.1|GeneID:6217572|0.0|1	SPCG_1107|lacC|YP_001835824.1|GeneID:6217879|0.0|1	SPCG_1106|lacB|YP_001835823.1|GeneID:6217990|1e-127|1	SPCG_1105|lacA|YP_001835822.1|GeneID:6217984|4e-100|1	SPCG_1481|pgm|YP_001836198.1|GeneID:6217664|0.0|1	SPCG_1588|galE|YP_001836305.1|GeneID:6217784|0.0|1	SPCG_1588|galE|YP_001836305.1|GeneID:6217784|2e-137|1	SPCG_1826|galT|YP_001836543.1|GeneID:6217075|0.0|1	SPCG_1826|galT|YP_001836543.1|GeneID:6217075|0.0|1	SPCG_1827|galK|YP_001836544.1|GeneID:6217626|0.0|1
gamPNI0373	HMPREF1038_00130|galM|YP_006742338.1|GeneID:	HMPREF1038_01197|HMPREF1038_01197|YP_006743360.1|Ge	HMPREF1038_01198|HMPREF1038_01198|YP_006743361.1|Ge	HMPREF1038_01199|HMPREF1038_01199|YP_006743362.1|Ge	HMPREF1038_01200|HMPREF1038_01200|YP_006743363.1|Ge	HMPREF1038_01481|HMPREF1038_01481|YP_006743634.1|Ge	HMPREF1038_01592|galE|YP_006743742.1|GeneID:1	HMPREF1038_01592|galE|YP_006743742.1|GeneID:1	HMPREF1038_01821|HMPREF1038_01821|YP_006743965.1|Ge	HMPREF1038_01821|HMPREF1038_01821|YP_006743965.1|Ge	HMPREF1038_01822|HMPREF1038_01822|YP_006743966.1|Ge

Strains/ Genes	*lacA*	*lacB*	*lacC*	*lacD*	*galE-1*	*galE-2*	*galT-1*	*galT-2*	*galK*	*galM*	*pgm*
	13695663|0.0|1	neID:1369 4484|0.0|1	neID:1369 4485|0.0|1	neID:1369 4486|9e-128|1	neID:1369 4487|2e-99|1	neID:1369 4764|0.0|1	3694904|0.0|2	3694904|2e-137|2	neID:1369 5131|0.0|1	neID:1369 5131|0.0|1	neID:1369 5132|0.0|1
Hungary 19A_6	SPH_0172|SPH_0172|YP_00169 3594.1|GeneID:6028868|0.0|1	SPH_1308|lacD|YP_0 01694629. 1|GeneID:6 029119|0.0 |1	SPH_1309|lacC|YP_0 01694630. 1|GeneID:6 028693|0.0 |1	SPH_1310|lacB|YP_0 01694631. 1|GeneID:6 028237|1e-127|1	SPH_1311|lacA|YP_0 01694632. 1|GeneID:6 028658|4e-100|1	SPH_1610|SPH_1610|YP_00169 4905.1|GeneID:6029914|0.0|1	SPH_1720|galE|YP_0 01695005. 1|GeneID:6 029325|0.0 |1	SPH_1720|galE|YP_0 01695005. 1|GeneID:6 029325|3e-137|1	SPH_1968|galT|YP_0 01695219. 1|GeneID:6 028304|0.0 |1	SPH_1968|galT|YP_0 01695219. 1|GeneID:6 028304|0.0 |1	SPH_1969|galK|YP_0 01695220. 1|GeneID:6 027916|0.0 |1
INV104	INV104_00 560|INV10 4_00560|Y P_0060617 66.1|GeneI D:1289033 4|0.0|1	INV104_10 250|lacD2| YP_00606 2675.1|Ge neID:1288 9297|0.0|1	INV104_10 260|lacC2| YP_00606 2676.1|Ge neID:1288 9298|0.0|1	INV104_10 270|lacB1| YP_00606 2677.1|Ge neID:1288 9299|9e-128|1	INV104_10 280|lacA|Y P_0060626 78.1|GeneI D:1288930 0|3e-100|1	INV104_12 720|pgmA| YP_00606 2901.1|Ge neID:1288 9544|0.0|1	INV104_13 750|galE|Y P_0060630 00.1|GeneI D:1288964 7|0.0|1	INV104_13 750|galE|Y P_0060630 00.1|GeneI D:1288964 7|1e-136|1	INV104_15 910|galT|Y P_0060632 06.1|GeneI D:1288986 3|0.0|1	INV104_15 910|galT|Y P_0060632 06.1|GeneI D:1288986 3|0.0|1	INV104_15 920|galK|Y P_0060632 07.1|GeneI D:1288986 4|0.0|1
INV200	SPNINV20 0_00640|S PNINV200 _00640|YP _00606542 1.1|GeneID :12892837| 0.0|1	SPNINV20 0_10400|la cD2|YP_00 6066334.1| GeneID:12 893843|0.0 |1	SPNINV20 0_10390|la cC2|YP_00 6066333.1| GeneID:12 893842|0.0 |1	SPNINV20 0_10380|la cB1|YP_00 6066332.1| GeneID:12 893841|9e-128|1	SPNINV20 0_10370|la cA|YP_006 066331.1| GeneID:12 893840|4e-100|1	SPNINV20 0_13340|p gmA|YP_0 06066606. 1|GeneID:1 2894137|0. 0|1	SPNINV20 0_14390|g alE|YP_00 6066707.1| GeneID:12 894242|0.0 |1	SPNINV20 0_14390|g alE|YP_00 6066707.1| GeneID:12 894242|2e-137|1	SPNINV20 0_16720|g alT|YP_00 6066933.1| GeneID:12 894475|0.0 |1	SPNINV20 0_16720|g alT|YP_00 6066933.1| GeneID:12 894475|0.0 |1	SPNINV20 0_16730|g alK|YP_00 6066934.1| GeneID:12 894476|0.0 |1
JJA	SPJ_0096| SPJ_0096| YP_00273 5212.1|Ge neID:7679 307|0.0|1	SPJ_1106|l acD|YP_00 2736172.1| GeneID:76 78952|0.0| 1	SPJ_1107|l acC|YP_00 2736173.1| GeneID:76 79693|0.0| 1	SPJ_1108|l acB|YP_00 2736174.1| GeneID:76 78624|9e-127|1	SPJ_1109|l acA|YP_00 2736175.1| GeneID:76 79099|4e-100|1	SPJ_1399| SPJ_1399| YP_00273 6453.1|Ge neID:7678 642|0.0|1	SPJ_1513| galE1|YP_ 002736560 .1|GeneID: 7679002|0. 0|2	SPJ_1735| galE2|YP_ 002736778 .1|GeneID: 7679225|0. 0|2	SPJ_1736| galT1|YP_ 002736779 .1|GeneID: 7679139|0. 0|2	SPJ_1757| galT2|YP_ 002736798 .1|GeneID: 7679807|0. 0|2	SPJ_1758| galK|YP_0 02736799. 1|GeneID:7 679467|0.0 |1
OXC141	SPNOXC_ 01030|SPN OXC_0103 0|YP_0060 63636.1|G eneID:128 92523|0.0| 1	SPNOXC_ 10670|lacD 2|YP_0060 64512.1|G eneID:128 92053|0.0| 1	SPNOXC_ 10680|lacC 2|YP_0060 64513.1|G eneID:128 92054|0.0| 1	SPNOXC_ 10690|lacB 1|YP_0060 64514.1|G eneID:128 92055|8e-127|1	SPNOXC_ 10700|lacA |YP_00606 4515.1|Ge neID:1289 2056|3e-100|1	SPNOXC_ 13110|pgm A|YP_0060 64725.1|G eneID:128 92294|0.0| 2	SPNOXC_ 14110|galE |YP_00606 4821.1|Ge neID:1289 2394|0.0|1	SPNOXC_ 14110|galE |YP_00606 4821.1|Ge neID:1289 2394|2e-137|1	SPNOXC_ 16250|galT |YP_00606 5024.1|Ge neID:1289 1359|0.0|1	SPNOXC_ 16250|galT |YP_00606 5024.1|Ge neID:1289 1359|0.0|1	SPNOXC_ 16260|galK |YP_00606 5025.1|Ge neID:1289 1360|0.0|1
P1031	SPP_0130| SPP_0130| YP_00273 7365.1|Ge neID:7681 722|0.0|1	SPP_1231|lacD|YP_0 02738374. 1|GeneID:7 682622|0.0 |1	SPP_1232|lacC|YP_0 02738375. 1|GeneID:7 680790|0.0 |1	SPP_1233|lacB|YP_0 02738376. 1|GeneID:7 682869|9e-128|1	SPP_1234|lacA|YP_0 02738377. 1|GeneID:7 682635|2e-99|1	SPP_1518| SPP_1518| YP_00273 8635.1|Ge neID:7682 217|0.0|1	SPP_1628| galE2|YP_ 002738740 .1|GeneID: 7681911|0. 0|2	SPP_1628| galE2|YP_ 002738740 .1|GeneID: 7681911|4 e-137|2	SPP_1852| galT1|YP_0 02738951. 1|GeneID:7 681641|0.0 |1	SPP_1852| galT1|YP_0 02738951. 1|GeneID:7 681641|0.0 |1	SPP_1853| galK1|YP_0 02738952. 1|GeneID:7 681858|0.0 |1
SPN034 156	SPN03415 6_11710|S PN034156 _11710|YP _00776545 3.1|GeneID :15313175| 0.0|1	SPN03415 6_01550|la cD2|YP_00 7764514.1| GeneID:15 314122|0.0 |1	SPN03415 6_01560|la cC2|YP_00 7764515.1| GeneID:15 312766|0.0 |1	SPN03415 6_01570|la cB1|YP_00 7764516.1| GeneID:15 313128|8e-127|1	SPN03415 6_01580|la cA|YP_007 764517.1| GeneID:15 314298|3e-100|1	SPN03415 6_03990|p gmA|YP_0 07764726. 1|GeneID:1 5314080|0. 0|2	SPN03415 6_04980|g alE|YP_00 7764821.1| GeneID:15 313158|0.0 |1	SPN03415 6_04980|g alE|YP_00 7764821.1| GeneID:15 313158|2e-137|1	SPN03415 6_06980|g alT|YP_00 7765009.1| GeneID:15 313148|0.0 |1	SPN03415 6_06980|g alT|YP_00 7765009.1| GeneID:15 313148|0.0 |1	SPN03415 6_06990|g alK|YP_00 7765010.1| GeneID:15 313130|0.0 |1
SPN034 183	SPN03418 3_01090|S PN034183 _01090|YP _00781380 0.1|GeneID :15316268| 0.0|1	SPN03418 3_10670|la cD2|YP_00 7814667.1| GeneID:15 315196|0.0 |1	SPN03418 3_10680|la cC2|YP_00 7814668.1| GeneID:15 315524|0.0 |1	SPN03418 3_10690|la cB1|YP_00 7814669.1| GeneID:15 315420|8e-127|1	SPN03418 3_10700|la cA|YP_007 814670.1| GeneID:15 314679|3e-100|1	SPN03418 3_13100|p gmA|YP_0 07814881. 1|GeneID:1 5315744|0. 0|2	SPN03418 3_14090|g alE|YP_00 7814975.1| GeneID:15 315756|0.0 |1	SPN03418 3_14090|g alE|YP_00 7814975.1| GeneID:15 315756|2e-137|1	SPN03418 3_16280|g alT|YP_00 7815179.1| GeneID:15 314538|0.0 |1	SPN03418 3_16280|g alT|YP_00 7815179.1| GeneID:15 314538|0.0 |1	SPN03418 3_16290|g alK|YP_00 7815180.1| GeneID:15 315034|0.0 |1
SPN994 038	SPN99403 8_01090|S PN994038 _01090|YP _00781198 2.1|GeneID :15317785| 0.0|1	SPN99403 8_10560|la cD2|YP_00 7812845.1| GeneID:15 317750|0.0 |1	SPN99403 8_10570|la cC2|YP_00 7812846.1| GeneID:15 316890|0.0 |1	SPN99403 8_10580|la cB1|YP_00 7812847.1| GeneID:15 317206|8e-127|1	SPN99403 8_10590|la cA|YP_007 812848.1| GeneID:15 317776|3e-100|1	SPN99403 8_12990|p gmA|YP_0 07813058. 1|GeneID:1 5316697|0. 0|2	SPN99403 8_13980|g alE|YP_00 7813153.1| GeneID:15 317358|0.0 |1	SPN99403 8_13980|g alE|YP_00 7813153.1| GeneID:15 317358|2e-137|1	SPN99403 8_16170|g alT|YP_00 7813359.1| GeneID:15 317536|0.0 |1	SPN99403 8_16170|g alT|YP_00 7813359.1| GeneID:15 317536|0.0 |1	SPN99403 8_16180|g alK|YP_00 7813360.1| GeneID:15 317211|0.0 |1
SPN994 039	SPN99403 9_01090|S PN994039 _01090|YP _00776265 6.1|GeneID :15319150| 0.0|1	SPN99403 9_10570|la cD2|YP_00 7763519.1| GeneID:15 319663|0.0 |1	SPN99403 9_10580|la cC2|YP_00 7763520.1| GeneID:15 319825|0.0 |1	SPN99403 9_10590|la cB1|YP_00 7763521.1| GeneID:15 318841|8e-127|1	SPN99403 9_10600|la cA|YP_007 763522.1| GeneID:15 318803|3e-100|1	SPN99403 9_13000|p gmA|YP_0 07763732. 1|GeneID:1 5318850|0. 0|2	SPN99403 9_13990|g alE|YP_00 7763826.1| GeneID:15 319503|0.0 |1	SPN99403 9_13990|g alE|YP_00 7763826.1| GeneID:15 319503|2e-137|1	SPN99403 9_16180|g alT|YP_00 7764033.1| GeneID:15 318996|0.0 |1	SPN99403 9_16180|g alT|YP_00 7764033.1| GeneID:15 318996|0.0 |1	SPN99403 9_16190|g alK|YP_00 7764034.1| GeneID:15 319135|0.0 |1

Strains/ Genes	*lacA*	*lacB*	*lacC*	*lacD*	*galE-1*	*galE-2*	*galT-1*	*galT-2*	*galK*	*galM*	*pgm*
SPNA45	SPNA45_01963|SPNA45_01963|YP_006702322.1|GeneID:13653306|0.0|1	SPNA45_01452|SPNA45_01452|YP_006701858.1|GeneID:13652797|0.0|1	SPNA45_01453|SPNA45_01453|YP_006701859.1|GeneID:13652798|0.0|1	SPNA45_01454|SPNA45_01454|YP_006701860.1|GeneID:13652799|2e-127|1	SPNA45_01455|SPNA45_01455|YP_006701861.1|GeneID:13652800|3e-100|1	SPNA45_00722|pgmA|YP_006701190.1|GeneID:13652070|0.0|2	SPNA45_00620|galE|YP_006701097.1|GeneID:13651968|0.0|2	SPNA45_00418|SPNA45_00418|YP_006700907.1|GeneID:13651768|0.0|2	SPNA45_00417|SPNA45_00417|YP_006700906.1|GeneID:13651767|0.0|2	SPNA45_00399|galT|YP_006700891.1|GeneID:13651749|0.0|2	SPNA45_00398|galK|YP_006700890.1|GeneID:13651748|0.0|1
ST556	MYY_01400|MYY_01400|YP_006252338.1|GeneID:12900678|0.0|1	MYY_1045|MYY_1045|YP_006253238.1|GeneID:12900478|0.0|1	MYY_1044|MYY_1044|YP_006253237.1|GeneID:12900477|0.0|1	MYY_1043|MYY_1043|YP_006253236.1|GeneID:12900476|9e-127|1	MYY_1042|MYY_1042|YP_006253235.1|GeneID:12900475|7e-99|1	MYY_1427|MYY_1427|YP_006253619.1|GeneID:12901770|0.0|1	MYY_1537|MYY_1537|YP_006253729.1|GeneID:12901881|0.0|2	MYY_1727|MYY_1727|YP_006253917.1|GeneID:12902071|0.0|2	MYY_1728|MYY_1728|YP_006253918.1|GeneID:12902072|0.0|2	MYY_1747|MYY_1747|YP_006253937.1|GeneID:12902091|0.0|2	MYY_1748|MYY_1748|YP_006253938.1|GeneID:12902092|0.0|1
Taiwan19F_14	SPT_0103|SPT_0103|YP_002741615.1|GeneID:7685477|0.0|1	SPT_1036|lacD|YP_002742479.1|GeneID:7686698|0.0|1	SPT_1035|lacC|YP_002742478.1|GeneID:7685228|0.0|1	SPT_1034|lacB|YP_002742477.1|GeneID:7686601|9e-127|1	SPT_1033|lacA|YP_002742476.1|GeneID:7685628|7e-99|1	SPT_1435|SPT_1435|YP_002742841.1|GeneID:7685433|0.0|1	SPT_1547|galE1|YP_002742948.1|GeneID:7685643|0.0|2	SPT_1748|galE2|YP_002743136.1|GeneID:7685733|0.0|2	SPT_1749|galT1|YP_002743137.1|GeneID:7685524|0.0|2	SPT_1769|galT2|YP_002743155.1|GeneID:7686614|0.0|2	SPT_1770|galK|YP_002743156.1|GeneID:7685612|0.0|1
TCH8431_19A	HMPREF0837_10354|HMPREF0837_10354|YP_003723796.1|GeneID:9343608|0.0|1	HMPREF0837_11310|lacD|YP_003724752.1|GeneID:9344568|0.0|1	HMPREF0837_11309|lacC|YP_003724751.1|GeneID:9344567|0.0|1	HMPREF0837_11308|lacB|YP_003724750.1|GeneID:9344566|9e-127|1	HMPREF0837_11307|lacA|YP_003724749.1|GeneID:9344565|7e-99|1	HMPREF0837_11732|pgcA|YP_003725174.1|GeneID:9344995|0.0|1	HMPREF0837_11843|galE|YP_003725285.1|GeneID:9345107|0.0|2	HMPREF0837_12053|galE2|YP_003725495.1|GeneID:9345319|0.0|2	HMPREF0837_12054|galT1|YP_003725496.1|GeneID:9345320|0.0|2	HMPREF0837_12075|galT2|YP_003725517.1|GeneID:9345341|0.0|2	HMPREF0837_12076|galK|YP_003725518.1|GeneID:9345342|0.0|1

[1] The table was obtained by a unidirectional Blast search, where the genes of S. pneumoniae D39 was used a query to find homologs in the 25 other genomes. Only the best hit in each genome is shown. Each cell contains the locus tag, e-value and the number of blast hits. The e-value is reflected in the blue colour code. The darker the blue colour, the lower the e-value (and more significant hit).
This table is also available on the CD.

Supporting Figures

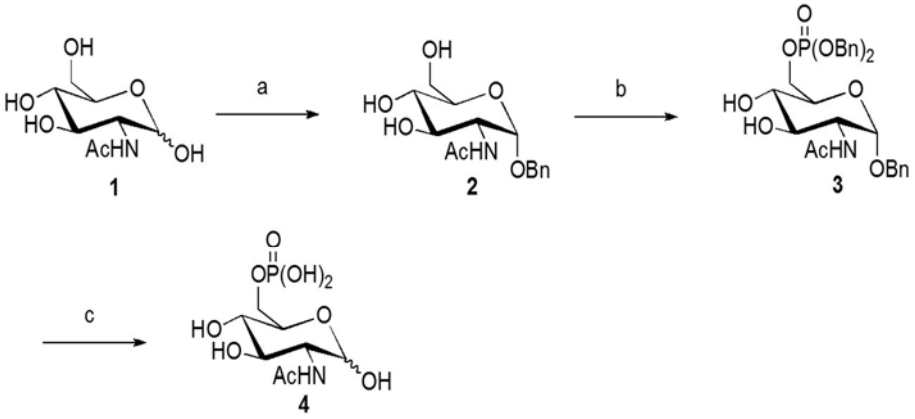

a) BnOH, HCl, 90 ºC, 70%. b) i. $(BnO)_2PN(iPr)_2$, pyr.HCl, CH_2Cl_2, rt; ii. cumene hydroperoxide, 0 ºC. 65%. c) Pd/C 10%, EtOH/H_2O 1:1, 70 psi, 99%.

Figure S2.1. Schematic representation of N-acetylglucosamine 6-phosphate synthesis.

N-acetylglucosamine 6-phosphate **4** was obtained through a modification of established procedures [1,2].
Benzylation of the anomeric hydroxyl group afforded compound **2** [2]**,** which was selectively phosphorylated at the primary hydroxyl group using dibenzyldiisopropyl phosphoramidite and pyridinium hydrochloride followed by oxidation of the resulting phosphite, with cumene hydroperoxide, to the corresponding phosphate **3**. Hydrogenolysis of **3** with H_2/Pd/C (10%) in ethanol/water afforded N-acetylglucosamine 6-phosphate **4** quantitatively. Interestingly, when the hydrogenation was performed under anhydrous conditions it was not possible to remove the benzyl protecting group at the anomeric position.

References

1. Szabó P. Phosphorylated sugars. Part 25. Synthesis and behaviour in acidic media of 2-acetamido-2-deoxy-D-glucose 4- and 6-phosphates and of a “Lipid A” analogue. J Chem Soc Perkin Trans 1. 1989; 919–924. doi:10.1039/p19890000919
2. Yeager AR, Finney NS. Synthesis of fluorescently labeled UDP-GlcNAc analogues and their evaluation as chitin synthase substrates. J Org Chem. 2005;70: 1269–1275. doi:10.1021/jo0483670

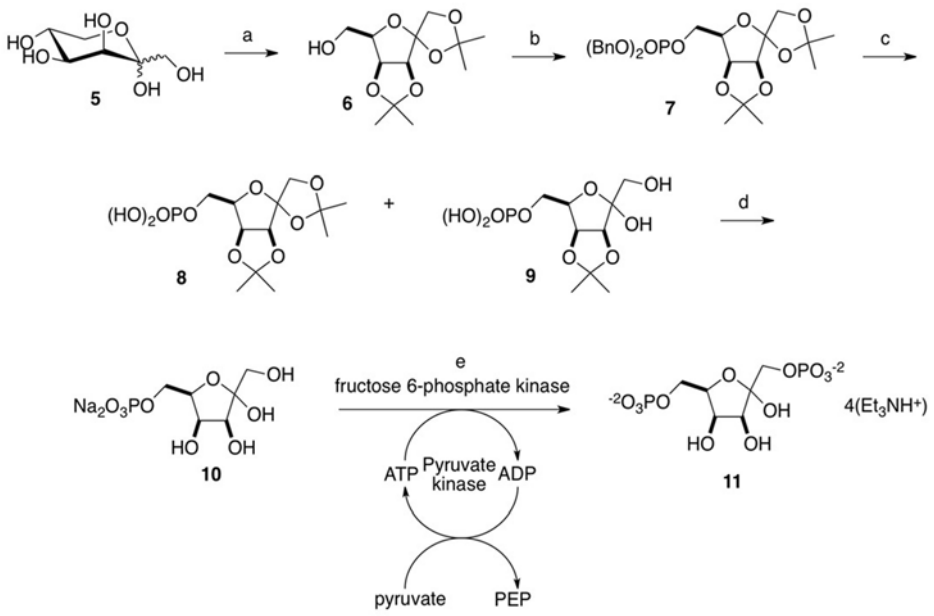

a) H_2SO_4, $Cu(SO_4)$, acetone, rt, 18h, 78%. b) i. $(BnO)_2PN(i\text{-}Pr)_2$, pyr.HCl, CH_2Cl_2, rt; ii. cumene hydroperoxide, -60ºC-rt, 94%. c) H_2, Pd/C, EtOH, 50 psi, **8** (40%), **9** (30%). d) TFA/H_2O, 73%. e) 66%.

Figure S2.2. Schematic representation of tagatose 1,6-biphosphate 11 synthesis.

Modifications to the synthesis previously published [1] were made in order to optimize the process (details in Text S2.1). 1,2:3,4-di-*O*-isopropylidene-α-D-tagatofuranose **6** was obtained in one step (78%) from D-tagatopyranose [2], instead of the 4 steps required when starting from D-galacturonic acid. Phosphorylation of **6**, under the same reaction conditions used for the synthesis of 3 (Fig. S2.1), afforded protected tagatose 6-phosphate **7** in 94% yield. Hydrogenolysis of the benzyl protecting groups of the phosphate afforded phosphate **8** and partially hydrolysed compound **9**, which was probably catalysed by the acidic hydrogen phosphate group. However, this was not a problem, since the next step was the removal of the isopropylidene acetals to afford tagatose 6-phosphate **10**. The enzymatic phosphorylation [2] of the primary alcohol at C-1 of **10** afforded tagatose 1,6-bisphosphate in 66% yield, as the salt of triethylammonium. All attempts to chemically phosphorylate the C-1 primary alcohol failed.

References

1. Eyrisch O, Sinerius G, Fessner W-D. Facile enzymic de novo synthesis and NMR spectroscopy characterization of D-tagatose 1,6-biphosphate. Carbohyd Res. 1993;238: 287–306.
2. Jenkinson SF, Fleet GWJ, Nash RJ, Koike Y, Adachi I, Yoshihara A, et al. Looking-glass synergistic pharmacological chaperones: DGJ and L-DGJ from the enantiomers of tagatose. Org Lett. 2011;13: 4064–4067. doi:10.1021/ol201552q

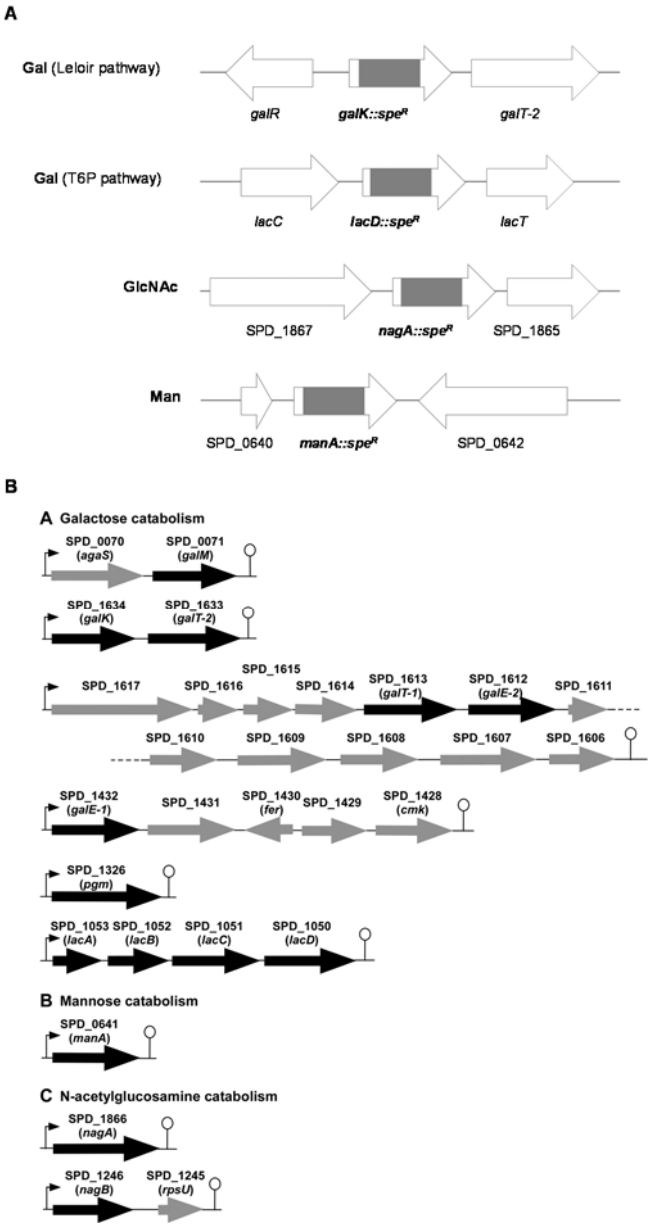

Figure S2.3. Genomic environment of the target genes.

(**A**) Schematic representation of the genomic context of sugar pathway mutant strains generated in this study. Mutants were constructed by allelic replacement mutagenesis. (**B**) Organization of genes involved in the catabolism of galactose (A), mannose (B) and N-acetylglucosamine (C). Genes are represented by large arrows. Genes known to be involved in the catabolic reactions (Table S2.4) are shown in black, while other genes in

the same operons are shown in grey. Promoters (arrows) and terminators (lollipops) were determined by RNA-seq [1].
Gene annotations (as from NCBI): *galR*, galactose operon repressor; g*alK,* galactokinase; *galT-2*, galactose 1-phosphate uridylyltransferase; *lacC*, tagatose 6-phosphate kinase; *lacD,* tagatose 1,6-diphosphate aldolase; *lacT*, transcription antiterminator LacT; SPD_1867*,* hypothetical protein*; nagA*, N-acetylglucosamine 6-phosphate deacetylase; SPD_1865, zinc-containing alcohol dehydrogenase; SPD_0640, pseudo; *manA*, mannose 6-phosphate isomerase; SPD_0642, sodium-dependent transporter; *agaS*, sugar isomerase; *galM*, aldose 1-epimerase; SDP_1617, cell wall surface anchor family protein; SPD_1616, hypothetical protein; SPD_1615, hypothetical protein; SPD_1614, phosphate transport system regulatory protein PhoU; *galT-1*, galactose 1-phosphate uridylyltransferase; *galE-2*, UDP-glucose 4-epimerase; SPD_1611, hypothetical protein; SPD_1610, hypothetical protein; SPD_1609, ABC transporter substrate-binding protein; SPD_1608, ABC transporter ATP-binding protein; SPD_1607, ABC transporter permease; SPD_1606, MgtC/SapB family protein; *galE-1*, UDP-glucose 4-epimerase; SPD_1431, glycosyl transferase family protein; *fer*, ferredoxin; SPD_1429, hypothetical protein; *cmk*, cytidylate kinase; *pgm*, phosphoglucomutase/phosphomannomutase family protein; *lacA*, galactose 6-phosphate isomerase subunit LacA; *lacB*, galactose 6-phosphate isomerase subunit LacB; *nagB*, glucosamine 6-phosphate isomerase; *rpsU*, 30S ribosomal protein S21. Spe^R spectinomycin resistance marker.

References

1. Yuzenkova Y, Gamba P, Herber M, Attaiech L, Shafeeq S, Kuipers OP, et al. Control of transcription elongation by GreA determines rate of gene expression in *Streptococcus pneumoniae*. Nucleic Acids Res. 2014;42: 10987–10999. doi:10.1093/nar/gku790

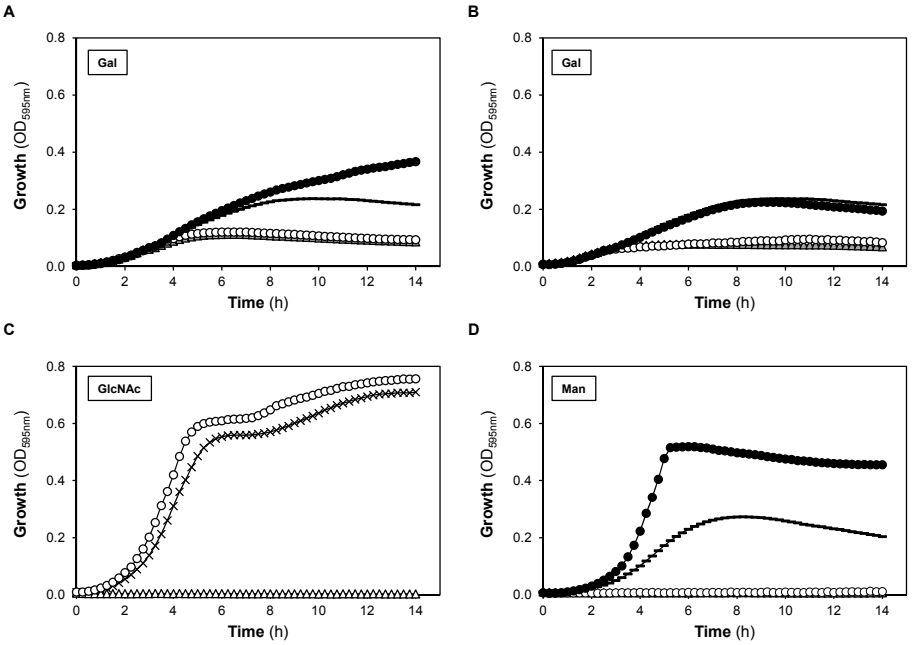

Figure S2.4. Growth profiles of the sugar specific deletion mutants and their complemented derivatives in C+Y medium.

(**A**) Growth on galactose (Gal) of D39Δ*galK* complemented with pKB01-*galKgalT-2*. (**B**) Growth on galactose (Gal) of D39Δ*lacD* complemented with pKB01-*lacD*. (**C**) Growth on N-acetylglucosamine (GlcNAc) of D39Δ*nagA* complemented with pKB01-*nagA*. (**D**) Growth on mannose (Man) of D39Δ*manA* complemented with pKB01-*manA*.
Growths were made in C+Y (without sucrose and glucose) with or without 0.1 mM $ZnCl_2$, at 37ºC.
Symbols: (▬) D39 grown in presence of zinc; (▲) D39 loss-of-function mutants grown in presence of zinc; (●) complemented strains grown in presence of zinc; (○) complemented strains grown without Zn; (✕) D39 grown without Zn; (Δ) D39Δ*nagA* grown without Zn.

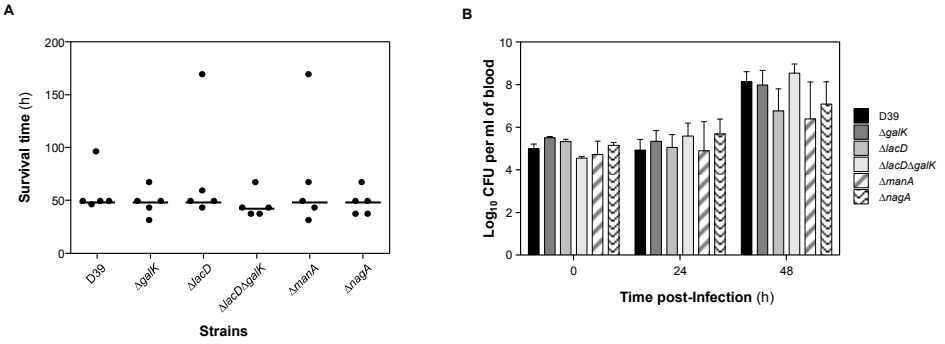

Figure S2.5. Analysis of pneumococcal strains in bacteremia model.

Mice were infected intravenously with 100 µl PBS containing approximately 5 X10^5 CFU through dorsal tail vein. (**A**) The animals were monitored over 168 h. Symbols show the times when individual mice became severely lethargic, the point when the animals were culled. The horizontal bars mark the median times to the severely lethargic state. (**B**) Growth of bacteria in the blood. Each point is the mean of data from five mice. Error bars show the standard error of the mean.

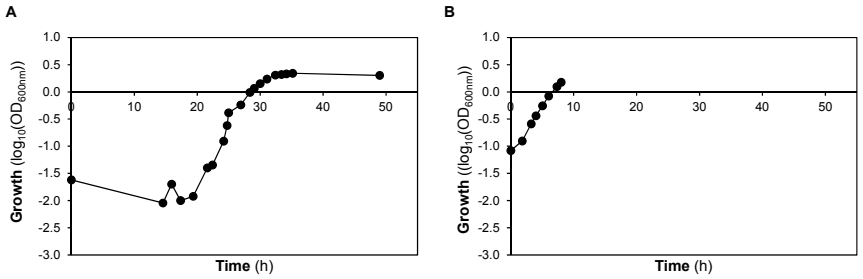

Figure S2.6. Subculturing of *S. pneumoniae* D39Δ*lacD* in chemically defined medium (CDM) supplemented with galactose (Gal).

(A) Pre-culture of *S. pneumoniae* D39Δ*lacD* in CDM-Gal (55 mM). 1 ml glycerol stock inoculated in 80 ml CDM-Gal (see Materials and Methods). (B) Subculturing of *S. pneumoniae* D39Δ*lacD*. Inoculation of fresh CDM-Gal (30 mM), to an initial optical density at 600 nm (OD_{600}) of ~ 0.05, with a pre-culture grown in the same sugar (Gal) until late-exponential phase of growth.
Growth was performed at 37ºC, under semi-anaerobic conditions, without pH control (initial pH 6.5).

Supporting Texts

Text S2.1. Modifications to the previously published synthesis of tagatose 1,6-biphosphate.

Modifications to the synthesis previously published [1] were made in order to optimize the process.

General.

1H NMR spectra were obtained at 400MHz in $CDCl_3$, with chemical shift values (δ) in ppm downfield from tetramethylsilane, DMSO-d_6 and in D_2O, 13C NMR spectra were obtained at 100.61 MHz, 31P NMR spectra were obtained at 161.97 MHz. Assignments are supported by 2D correlation NMR studies. Medium pressure preparative column chromatography: Silica Gel Merck 60 H. Analytical TLC: Aluminium-backed Silica Gel Merck 60 F254. Reagents and solvents were purified and dried according to Armarego and Chai [2]. All the reactions were carried out under an inert atmosphere (argon).

6-*O*-diBenzylphospho-(1,2:3,4)-di-*O*-isopropylidene-α-D-tagatofuranose 7. To a stirred solution of **6** (0.53 g, 2.01 mmol) in THF (10 mL) at r.t. was added dibenzyl *N,N*-diisopropylphosphoramidite (1.33 mL, 4.02 mmol) and tetrazole (0.28 g, 4.02 mmol). After 24 hours and complete conversion of the starting material, the reaction was cooled down to -78ºC and mCPBA (0.69 g, 4.02 mmol) was added. The temperature was allowed to rise to r.t., and after 90 minutes the reaction mixture was evaporated. Purification by flash column chromatography on silica gel (20:80, EtOAc/hexane) afforded the product **6** as a viscous colourless foam (0.98 g, 94%). ^{1}H NMR ($CDCl_3$): δ 7.37-7.31 (m, 10H, $CH_2\underline{Ph}$), 5.08-5.05 (m, 4H, $C\underline{H}_2Ph$), 4.73 (dd, 1H, J=3.5 Hz, J=5.8 Hz, H-4), 4.58 (d, 1H, J=5.8 Hz, H-3), 4.32-4.12 (m, 3H, H-5, 2xH-6), 4.24 (d,

1H, J=9.7 Hz, H-1), 4.01 (d, 1H, J=9.7 Hz, H-1), 1.42 (s, 3H, OMe), 1.38 (s, 3H, OMe), 1.35 (s, 3H, OMe), 1.26 (s, 3H, OMe). ^{13}C NMR ($CDCl_3$): δ 135.8, 135.7, 128.7, 128.6, 128.5, 128.0, 127.9 ($CH_2\underline{Ph}$), 112.9 (C-2), 111.9 ($\underline{C}(CH_3)_2$), 111.8 ($\underline{C}(CH_3)_2$), 85.0 (C-3), 79.6 (C-4), 77.7 (d, $J_{C,P}$=8.0 Hz, C-5), 69.3 (d, J_{C-P}=3.2 Hz, $\underline{C}H_2Ph$), 69.2 (d, J_{C-P} =2.9 Hz, $\underline{C}H_2Ph$), 67.3 (d, J_{C-P}=5.7 Hz, C-1), 65.5 (d, J_{C-P}=5.4 Hz, C-6) 26.4 (OMe), 26.3 (OMe), 25.9 (OMe), 24.8 (OMe). ^{31}P NMR ($CDCl_3$): δ -1.15 (s).

(1,2:3,4)-di-*O*-isopropylidene-α-D-tagatofuranose 6-(dihydrogen phosphate) 8. Dibenzyl phosphate **7** (0.98 g, 1.88 mmol) was hydrogenated at 50 psi in the presence of Pd/C 10% (0.19 g, 0.18 mmol) in EtOH (12 mL), for 20 hours at r.t. The reaction mixture was then filtered through celite, washed with EtOH and evaporated. Purification by column chromatography on silica gel (60:40, MeOH/CH_2Cl_2) afforded phosphate diacetal **8** (0.36 g, 56%) and phosphate monoacetal **9** (α/β 1:8.7, 0.23 g, 41%) as colourless viscous foams. The characterisation data for **8** was identical to the literature [3].

3,4-*O*-isopropylidene-α/β-D-tagatofuranose 6-(dihydrogen phosphate) 9. ^{1}H NMR (D_2O) : δ 4.95 (dd, J=3.8 Hz, J=5.9 Hz, H-4 β), 4.91 (dd, J=4.0 Hz, J=6.1 Hz, H-4 α) 4.59 (d, J=5.9 Hz, H-3 β), 4.54 (d, J=5.9 Hz, H-3 α), 4.36-4.32 (m, H-5 β), 4.30-4.27 (m, H-5 α), 4.10-4.04 (m, H-6 β), 3.96-3.90 (m, H-6 β), 3.74 (d, J=11.6 Hz, H-1 β), 3.60 (d, J=11.6 Hz, H-1 β), 1.49 (s, OMe α), 1.41 (s, OMe β), 1.32 (s, OMe α), 1.28 (s, OMe β). ^{31}P NMR (D_2O): δ -0.32 (s).

D-Tagatose 6-(dihydrogen phosphate). The product was obtained following the procedure described in the literature [3]. ^{1}H NMR (D_2O): δ 4.29-4.25 (m), 4.23-4.20 (m), 4.11-4.06 (m), 4.04-3.82 (m), 3.51 (dd, J=12.0 Hz, J=16.6 Hz, H-1 α), 3.42 (dd, J=12.0 Hz, J=16.6 Hz, H-1 β). ^{13}C NMR (D_2O): δ 102.7 (C-2), 79.2 (d, $J_{C,P}$=7.9 Hz, C-5), 70.9, 70.7, 64.6 (d, $J_{C,P}$=4.7 Hz, C-6), 62.9 (C-1). ^{31}P NMR (D_2O): δ -0.01 (s).

D-Tagatose 6-phosphate, disodium salt 10. The product was obtained following the procedure described in the literature [3]. Yield 73%. ^{1}H NMR (D_2O): δ 4.35-4.32 (m), 4.30-4.28 (m), 4.19-4.11 (m), 4.09-4.00 (m), 3.59 (dd, J=12.0 Hz, J=19.0 Hz, H-1 α), 3.50 (dd, J=12.0 Hz, J=16.4 Hz, H-1 β).

D-Tagatose 1,6-bisphosphate, tetrakis(triethylammonium) salt 11. The enzymatic phosphorylation of **10** was accomplished following the procedure described in the literature [3]. The tetrakis(triethylammonium) salt of **11** was prepared instead of the tetrakis(cyclohexylammonium) salt. Anomers α:β 1:4, yield 66%. ^{1}H NMR (D_2O): δ 4.54 (t, 1H, J=5.1 Hz, H-4 α), 4.45-4.42 (m, 1H, H-5 α), 4.38 (dd, 1H, J=4.8, J=4.0 Hz, H-4 β), 2.28 (d, 1H, J=4.9 Hz, H-3 β), 4.25-4.20 (m, 1H, H-5 β), 4.17-4.11 (m, 1H, H-6 β), 4.04-4.00 (m, 1H, H-6 β), 3.88 (dd, 1H, J=10.8, J=5.8 Hz, H-1 β), 3.82 (dd, 1H, J=10.8, J=5.08 Hz, H-1 β), 3.19 (q, 24H, J=7.3 Hz, $CH_3C\underline{H}_2N$), 1.27 (t, 36H, J=7.3 Hz, $C\underline{H}_3CH_2N$). ^{13}C NMR (D_2O), Anomer β: δ 101.8 (C-2), 79.04 (d, J=8.1 Hz, C-5), 70.78 and 70.73 (C-3 and C-4), 65.6 (d, J=4.99 Hz, C-1), 64.3 (d, J=5.0 Hz, C-6), 46.6 ($CH_3\underline{C}H_2N$), 8.2 ($\underline{C}H_3CH_2N$). ^{31}P NMR (D_2O), Anomer β: δ 0.66 (s), 0.29 (s).

References

1. Eyrisch O, Sinerius G, Fessner W-D. Facile enzymic de novo synthesis and NMR spectroscopy characterization of D-tagatose 1,6-biphosphate. Carbohyd Res. 1993;238: 287–306.
2. Armarego WLF, Chai CLL. Purification of laboratory chemicals. 5th ed. Amsterdam ; Boston: Butterworth-Heinemann; 2003.
3. Jenkinson SF, Fleet GWJ, Nash RJ, Koike Y, Adachi I, Yoshihara A, et al. Looking-glass synergistic pharmacological chaperones: DGJ and L-DGJ from the enantiomers of tagatose. Org Lett. 2011;13: 4064–4067. doi:10.1021/ol201552q

Text S2.2. Genomic potential for the utilization of host monosaccharides.

Fucose metabolism

Homologues of genes encoding the *E. coli* Fuc degradation pathway were found in the D39 genome (Fig. 1 and S4 Table) [1–3]. To further metabolize anaerobically the final product of Fuc metabolism, L-lactaldehyde, an L-1,2-propanediol oxidoreductase (FucO) gene is present in some operons [4]. A BlastP search using as query FucO from *E. coli* K-12 MG1655 showed homology (42% identity; 60% positives) to an iron-containing alcohol dehydrogenase (SPD_1985) of D39, but whether this protein is functionally active remains to be elucidated. However, the downstream steps of L-lactaldehyde aerobic degradation seem to be missing in *S. pneumoniae*. A PTS system is present in the Fuc operon of D39, but the implication of this transporter in the uptake of Fuc is not yet proven. It has been proposed to transport Fuc-containing oligosaccharides that would subsequently be processed by intracellular glycoside hydrolases releasing Fuc [2–4].

N-acetylgalactosamine metabolism

Genes involved in the initial steps for the intracellular catabolism of GalNAc [5–7] remain elusive in the pneumococcus (Fig. 1). However, the N-acetylgalactosamine 6-phosphate deacetylase (coded by *agaA*) for conversion of GalNAc6P to GalN6P in *E. coli C* str. ATCC 8739, shares 37% amino acid sequence identity with N-acetylglucosamine 6-phosphate deacetylase (coded by *nagA*) of D39. Recently, it was shown that NagA can substitute the activity of AgaA, in *E. coli* [7,8]. Moreover, in this microorganism, it was proposed that the isomeration/deamination of GalN6P to T6P was accomplished by galactosamine 6-phosphate isomerase (coded by *agaS*) and not by *agaI* [7]. The first is annotated in the genome of D39 and encodes a sugar isomerase (45% amino acid

sequence identity with the one present in *E. coli C* str. ATCC 8739). A putative GalNAc transporter (SPD_0293-5-6-7) is annotated in the D39 genome [3] and shares 33% amino acid sequence identity with the GalNAc transporter subunit EIIC (EcolC_0566) of *E. coli* C str. ATCC 8739. Additionally, the latter shares 32% amino acid sequence identity with SPD_1990, which is annotated as being potentially involved in amino sugar metabolism in D39.

Very recently, the GalNAc pathway was established for *Lactobacillus casei* and is encoded in the *gnb* gene cluster [9]. This route includes a PTS^{Gnb} that transports and phosphorylates the substrate to GalNAc6P and is subsequently processed through GnbF and GnbE, which encode for the activities of GalNAc6P deacetylase and GalN6P deaminase/isomerase, respectively. Moreover, it was found that conversion of GalNAc6P to GalN6P could also be accomplished by NagA, as full growth on GalNAc requires both activities.

The PTS^{Gnb} shares high amino acid sequence homology with the pneumococcal mannose-family PTS SPD_0066-7-8-9. In particular the PTS transport system subunit IIC (LCABL_02930) shares 50% identity and 65% positives with the *S. pneumoniae* D39 protein encoded by SPD_0067. The degradation enzymes GnbF and GnbE share 54% and 48% amino acid sequence identity with NagA (SPD_1866) and AgaS (SPD_0070) of S*. pneumoniae* D39, respectively.

In summary, GalNAc catabolic pathways were established in *E. coli* and *L. casei* and according to our analysis *S. pneumoniae* possesses gene products showing considerable homology to the proteins in these organisms. Therefore, it is tempting to suggest that GalNAc is processed through the combined action of *nagA* and *agaS* in *S. pneumoniae* D39. However, how to reconcile this hypothesis with the inability to grow on GalNAc still remains to be investigated.

N-acetylneuraminic acid metabolism

The NeuNAc utilization has been recently studied [3,10,11].

A duplication event might have occurred for the N-acetylneuraminate lyase gene (SPD_1489 and SPD_1163). N-acetylmannosamine kinase is annotated in the metabolic database MetaCyc as a glucokinase (*gki*). However, a BlastP search led us to suggest that this function is most likely performed by the ROK family protein (SPD_1488) as this locus is part of the *nanAB* operon.

References

1. Chan PF, O'Dwyer KM, Palmer LM, Ambrad JD, Ingraham KA, So C, et al. Characterization of a novel fucose-regulated promoter (PfcsK) suitable for gene essentiality and antibacterial mode-of-action studies in *Streptococcus pneumoniae*. J Bacteriol. 2003;185: 2051–2058. doi:10.1128/JB.185.6.2051-2058.2003
2. Higgins MA, Whitworth GE, El Warry N, Randriantsoa M, Samain E, Burke RD, et al. Differential recognition and hydrolysis of host carbohydrate antigens by *Streptococcus pneumoniae* family 98 glycoside hydrolases. J Biol Chem. 2009;284: 26161–26173. doi:10.1074/jbc.M109.024067
3. Bidossi A, Mulas L, Decorosi F, Colomba L, Ricci S, Pozzi G, et al. A functional genomics approach to establish the complement of carbohydrate transporters in *Streptococcus pneumoniae*. Miyaji EN, editor. PLoS ONE. 2012;7: e33320. doi:10.1371/journal.pone.0033320
4. Higgins MA, Suits MD, Marsters C, Boraston AB. Structural and functional analysis of fucose-processing enzymes from *Streptococcus pneumoniae*. J Mol Biol. 2014;426: 1469–1482. doi:10.1016/j.jmb.2013.12.006
5. Reizer J, Ramseier TM, Reizer A, Charbit A, Saier MH Jr. Novel phosphotransferase genes revealed by bacterial genome sequencing: a gene cluster encoding a putative N-acetylgalactosamine metabolic pathway in *Escherichia coli*. Microbiol Read Engl. 1996;142 (Pt 2): 231–250.
6. Brinkkötter A, Klöss H, Alpert C, Lengeler JW. Pathways for the utilization of N-acetyl-galactosamine and galactosamine in *Escherichia coli*. Mol Microbiol. 2000;37: 125–135.
7. Hu Z, Patel IR, Mukherjee A. Genetic analysis of the roles of *agaA*, *agaI*, and *agaS* genes in the N-acetyl-D-galactosamine and D-galactosamine catabolic pathways in *Escherichia coli* strains O157:H7 and C. BMC Microbiol. 2013;13: 94. doi:10.1186/1471-2180-13-94
8. Leyn SA, Gao F, Yang C, Rodionov DA. N-Acetylgalactosamine utilization pathway and regulon in proteobacteria: genomic reconstruction and experimental characterization in *Shewanella*. J Biol Chem. 2012;287: 28047–28056. doi:10.1074/jbc.M112.382333
9. Bidart GN, Rodríguez-Díaz J, Monedero V, Yebra MJ. A unique gene cluster for the utilization of the mucosal and human milk-associated glycans galacto- *N* -biose and

lacto- *N* -biose in *L actobacillus casei*: Galacto- and lacto- *N* -biose utilization in *Lactobacillus*. Mol Microbiol. 2014;93: 521–538. doi:10.1111/mmi.12678

10. Gualdi L, Hayre J, Gerlini A, Bidossi A, Colomba L, Trappetti C, et al. Regulation of neuraminidase expression in *Streptococcus pneumoniae*. BMC Microbiol. 2012;12: 200. doi:10.1186/1471-2180-12-200
11. Marion C, Burnaugh AM, Woodiga SA, King SJ. Sialic acid transport contributes to pneumococcal colonization. Infect Immun. 2011;79: 1262–1269. doi:10.1128/IAI.00832-10

Chapter 3

Transcriptional and metabolic effects of glucose on *S. pneumoniae* utilizing glycan-derived sugars

The results of this chapter will be submitted for publication:

Paixão L, Caldas J, Kloosterman TG, Kuipers OP, Vinga S and Neves AR (2015). Transcriptional and metabolic effects of glucose on *S. pneumoniae* utilizing glycan-derived sugars. Manuscript in preparation.

Chapter 3 – Contents

Abstract

During the progression from colonisation to disease *S. pneumoniae* has to cope with changes in the availability of nutrients, namely glucose (Glc) a prevailing sugar in blood and inflamed tissues is scarce in the nasopharynx. We assessed the pneumococcus response to galactose (Gal), N-acetylglucosamine (GlcNAc) and mannose (Man), which are present in glycans and support growth of *S. pneumoniae* D39. The gene expression and metabolic profiles on glycan-derived sugars were compared to those on Glc. Gal, GlcNAc and Man affected respectively the expression of 8.4%, 11.4%, and 14.2% of the genome, covering cellular functions including central carbon metabolism and virulence. Glycolytic dynamics were monitored in resting cells using *in vivo* ^{13}C-NMR. GlcNAc (and Glc) rendered homolactic fermentation, while Gal and Man generated mixed-acid profiles. The glycolytic metabolite fructose 1,6-bisphosphate accumulated, but the pool size was considerably higher (*circa* 2.5 times) on GlcNAc (and Glc) than on Man or Gal, consistent with the homolactic profile. On Gal and Man, the accumulation of specific metabolic intermediates (α-galactose 6-phosphate and mannose 6-phosphate) indicated catabolic bottlenecks possibly causing growth retardation.

S. pneumoniae growing on glycan-derived sugars was challenged with Glc, and the response to this stimulus was evaluated at transcriptional, physiological and metabolic levels. Glc was readily consumed (preferred sugar) and elicited a metabolic shift towards a homolactic profile. On Gal, this was accompanied by a transient increase of fructose 1,6-bisphosphate. The transcriptional response to Glc was large (over 5% of the genome). In central carbon metabolism (most represented category), Glc exerted mostly negative regulation. Interestingly, the smallest response was observed on a sugar mix, suggesting that exposure to

varied sugars improves the fitness of *S. pneumoniae*. The expression of classical virulence factors was negatively controlled by Glc in a sugar-dependent manner. Overall, our results strengthen the link between carbohydrate metabolism, adaptation to host niches and virulence.

Introduction

Streptococcus pneumoniae is a common asymptomatic commensal of the human nasopharynx, but also a life-threatening pathogen responsible for severe illnesses such as bacterial meningitis, pneumonia, septicaemia, as well as milder respiratory infections [1,2]. The establishment of a carrier state (colonisation) is a precursor for pneumococcal disease and an important feature for dissemination through the community [2–4]. Indeed, from the microbe's fitness perspective, the success of pneumococcal infections relies on colonisation, multiplication and transmission to a new host [5]. Consequently, the factors required for its commensal lifestyle might also be considered virulence factors [5,6]. The mechanisms underlying the progression from a carrier state to invasive disease are complex, probably multifactorial and are still poorly understood [7,8]. Notwithstanding, several studies based on different techniques to evaluate pneumococcal gene expression, revealed that pneumococcal virulence genes were differentially expressed in different host niches [7,9–14]. Therefore, we hypothesise that transition from carriage to disease involves modulation of pneumococcal gene expression in response to environmental changes. Indeed, it was shown that changes in the concentrations of metal ions in different host sites, contributes to virulence in *S. pneumoniae* (reviewed in [15,16]).

To a large extent the pneumococcal pathogenesis relies on efficient acquisition and metabolism of carbohydrates required for growth and survival, but the knowledge of pneumococcal physiology and pathogenesis is still limited. *S. pneumoniae* is a strictly fermentative bacterium relying exclusively on carbohydrates to obtain energy for growth (Fig. 3.1). Compared to other colonisers of its ecological niche like *Haemophilus influenzae* and *Neisseria meningitidis*, *S. pneumoniae* displays the broadest sugar utilization range [17]. Analysis of the genome suggested the existence of pathways for catabolism of a wide diversity of carbohydrates [17] and a recent study showed that *S. pneumoniae* is able to use at least 32 substrates [18]. In particular, the bacterium has catabolic pathways for the utilization of galactose (Gal), mannose (Man) and N-acetylglucosamine (GlcNAc) ([17,18]; Chapter 2). The pneumococcus possesses at least ten extracellular glycosidases, which enable the modification and breakdown of host glycans generating free sugars that can potentially be used for growth (reviewed in King *et al.* [4]). Furthermore, over 30% of all the transporters in the genome are presumably involved in sugar uptake [17,18], a by far larger proportion than that found in the other microorganisms occupying the same niche [17,19].

However, to thrive in diverse host environments, the bacterium has to cope with fluctuations in nature and availability of carbon sources. In the nasopharynx free sugars are scarce, but glycans are plentiful both in secretions and on the surface of epithelial cells. In contrast to the airways, the generally preferred sugar in *Streptococcaceae*, glucose (Glc), is present in comparatively higher concentrations in the bloodstream and during infection [20,21]. We hypothesise that this metabolic flexibility is important during the transition from colonisation to invasive disease in *S. pneumoniae*. To adapt to host environments, the pneumococcus has developed sophisticated and complex mechanisms.

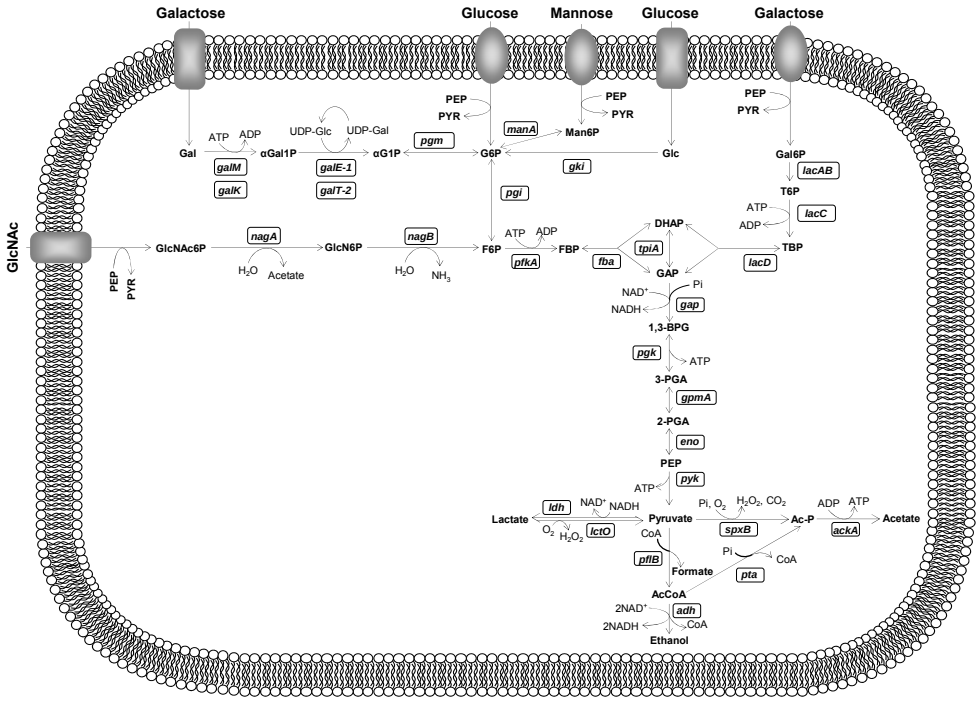

Figure 3.1. Schematic representation of Gal, Man, GlcNAc and Glc metabolism in *S. pneumoniae* D39.

Sugar-specific steps, glycolysis and fermentative metabolism are depicted. Putative and functional characterized genes encoding depicted metabolic steps are shown in white boxes. Proposed pathways were reconstructed based on genome information (http://www.ncbi.nlm.nih.gov/genomes/lproks.cgi), literature and database surveys (KEGG, MetaCyc). Gene annotation downloaded from NCBI: *gki*, glucokinase; *pgi*, glucose 6-phosphate isomerase; *pfkA*, 6-phosphofructokinase; *fba*, fructose bisphosphate aldolase; *tpiA*, triosephosphate isomerase; *gap*, glyceraldehyde-3-phosphate dehydrogenase; *pgk*, phosphogltcerate kinase; *gpmA*, phosphoglyceromutase; *eno*, phosphopyruvate hydratase (enolase); *pyk*, pyruvate kinase; *ldh*, L-lactate dehydrogenase; *lctO*, lactate oxidase; *spxB*, pyruvate oxidase; *ackA*, acetate kinase; *pta*, phosphotransacetylase; *pflB*, pyruvate formate-lyase; *adh* (spd_1834), bifunctional acetaldehyde-CoA/alcohol dehydrogenase; *galM*, aldose 1-epimerase; *galK*, galactokinase; *galE-1*, UDP-glucose 4-epimerase; *galT-2*, galactose 1-phosphate uridylyltransferase; *pgm*, phosphoglucomutase/phosphomannomutase family protein; *lacA*, galactose 6-phosphate isomerase subunit LacA; *lacB*, galactose 6-phosphate isomerase subunit LacB; *lacC*, tagatose 6-phosphate kinase; *lacD*, tagatose 1,6-diphosphate aldolase; *manA*, mannose 6-phosphate isomerase; *nagA*, N-acetylglucosamine 6-phosphate deacetylase; *nagB,* glucosamine 6-phosphate isomerase. Intermediates: G6P, glucose 6-phosphate; F6P, fructose 6-phosphate; FBP, fructose 1,6-biphosphate; GAP, glyceraldehyde 3-phosphate; DHAP, dihydroxyacetone phosphate;

1,3-BPG, 1,3-biphosphoglycerate; 3-PGA, 3-phosphoglycerate; 2-PGA, 2-phosphoglycerate; PEP, phospho*enol*pyruvate; GlcNAc6P, N-acetylglucosamine 6-phosphate; GlcN6P, glucosamine 6-phosphate; Man6P, mannose 6-phosphate; Gal, galactose; α-Gal, α-galactose; αGal1P, α-galactose 1-phosphate; αG1P, α-glucose 1-phosphate; UDP-Glc, UDP-glucose; UDP-Gal, UDP-galactose; Gal6P, galactose 6-phosphate; T6P, tagatose 6-phosphate; TBP, tagatose 1,6-diphosphate.
Sugar transporters depicted as rectangles and ovoids generically represent phosphoenolpyruvate phosphotransferase systems or ABC transporters, respectively.

It has been proposed that exchanging genetic material (genetic transformation) provides a selective advantage in the adaptation of the pneumococcus to distinct environmental conditions [22,23]. Moreover, when exposed to a mixture of substrates bacteria can sense the nutritional environment and adjust its catabolic capabilities, in a process termed as carbon catabolite repression (CCR) [24]. CCR is a regulatory process that enables bacteria to utilize preferred carbon sources in detriment of others, by downregulating the expression of genes and inhibiting enzyme activities involved in the use of secondary carbon sources [25,26]. The molecular mechanisms mediating CCR are diverse (reviewed in [24–26]) and act at different regulatory layers: gene expression (transcription activation and gene repression), protein activities (control of translation, post-translational modification) and metabolites (allosteric regulation) [26,27]. In the Firmicutes, CCR typically comprises the general phospho*enol*pyruvate phosphotransferase system component HPr, the bifunctional HPr kinase/phosphorylase (HPrK) and the transcription factor catabolite control protein A (CcpA). The latter binds to catabolite response elements (CRE) in promoter regions of CCR-sensitive genes [26]. Hence, a global understanding of the physiological response of *S. pneumoniae* to shifts in substrate availability requires the integration of diverse data sets collected at distinct “omic” levels.

With the aim to study the response of *S. pneumoniae* to the monosaccharides present in host glycans we have collected transcript and time series metabolic data during growth on Gal, Man and GlcNAc as

single carbon sources and compared to the profiles on Glc. Previously, we have shown that Glc supported the fastest growth followed by GlcNAc which was a better substrate than Gal or Man (Paixão *et al*., 2015, Chapter 2). The markedly different growth profiles led us to surmise that growth on these sugars is differently regulated. Furthermore, we investigated the effect of adding the fast metabolizable sugar (Glc) to *S. pneumoniae* cells actively growing on Gal, Man, GlcNAc or in a mixture thereof on the growth physiology and at the transcriptional and metabolic levels (by *in vivo* ^{13}C-NMR, for Gal-adapted cells). Finally, we evaluated the impact of the substrate for growth on the expression of virulence factors.

In this work we have generated data at transcript, metabolic and physiological levels, in respect to *S. pneumoniae*' response to sugar availability. These data can in the future be used as input for predictive multi-level mathematical models of the pneumococcus metabolic networks. It is expected that such tools will facilitate our understanding of complex phenomena and enable the identification of novel targets for the development of therapeutics.

Materials and Methods

Bacterial strains and growth conditions

Streptococcus pneumoniae strain D39 (serotype 2) and its derivative D39Δ*cps* (A. M. Cavaleiro, P. Gaspar, T. Kloosterman, O. P. Kuipers and A. R. Neves., unpublished) were used throughout this study. The D39 isolate was obtained from the culture collection of the Department of Infection, Immunity and Inflammation, of the University of Leicester. Stocks were prepared as described elsewhere [28] and stored in glycerol

(25% vol/vol) at -80°C. Working stocks were done by transferring 1 ml of the frozen stock to 25 ml Glc-M17 medium (Difco), followed by incubation at 37ºC until late exponential phase (OD_{600} ~0.8). Cultures were centrifuged (6300 *x g*, 7min, 4ºC), the supernatant discarded and the pellet suspended in 20 ml 25% (vol/vol) glycerol-M17. 1 ml aliquots were stored at -80ºC until further use.

Routinely, *S. pneumoniae* was grown statically in M17 broth (Difco) containing 0.5% (wt/vol) glucose (Glc-M17) at 37°C. For physiological studies and transcriptome analysis, *S. pneumoniae* D39 was grown in static rubber stoppered bottles at 37ºC and without pH control (initial pH 6.5) in the chemically defined medium (CDM) described by Carvalho *et al.* [28]. Growth was performed as reported before (Paixão *et al*. 2015, Chapter 2). Cells actively metabolizing single sugars Gal, GlcNAc and Man (12-15 mM) or a sugar mixture (approximately 6 mM each, herein denominated sugar mix) were challenged or not with a 10 mM pulse of Glc at mid-exponential phase of growth. In the case of Glc challenge, cells metabolizing other sugars were herein denominated “sugar”-adapted cells. Cultures were started by inoculating fresh CDM, to an initial optical density at 600 nm (OD_{600}) of ~ 0.05, with a pre-culture grown until late exponential phase of growth. Pre-cultures were performed as described by Carvalho *et al.* [28], except pre-cultures for growth on sugar mix, which were grown in CDM containing 30 mM of each carbon source. Growth was monitored by measuring OD_{600} hourly. Maximum specific growth rates (μ_{max}) were calculated through linear regressions of the plots of $\ln(OD_{600})$ *versus* time during the exponential phase of growth after the Glc pulse. The values reported are averages of two independent growths.

Quantification of substrate consumption and fermentation products

Strains were grown in CDM supplemented with the appropriate sugar as described above. Culture samples (2 mL) were taken at inoculation, immediately and 1 h after the Glc pulse, and at the onset of the stationary phase of growth, and centrifuged (16,100 *x g*, 3 min, 4ºC). The supernatants were filtered (Q-Max® RR NY syringe 0.22 µm filters) and stored at - 20ºC until further analysis. Fermentation products, Glc and GlcNAc were quantified by high performance liquid chromatography (HPLC) equipped with a refractive index detector (Shodex RI-101, Showa Denko K. K., Japan) using an HPX-87H anion exchange column (Bio-Rad Laboratories Inc., California, USA) at 60ºC, with 5 mM H_2SO_4 as the elution fluid and a flow rate of 0.5 ml min^{-1}. Gal and Man were quantified by ^{1}H-NMR and the spectra were acquired in a Bruker AMX300 spectrometer (Bruker BioSpin GmbH). To quantify Gal and Man the temperature of the probe was set to 18ºC and to 37ºC, respectively. DSS (3-(trimethylsilyl) propionic acid sodium salt) was added to the samples and used as an internal concentration standard in ^{1}H-NMR quantifications.

Yields were calculated using the data from samples taken immediately after inoculation and at the onset of stationary phase of growth. A factor of 0.38, determined from a dry weight (DW) (mg ml^{-1}) *versus* OD_{600} curve, was used to convert OD_{600} into DW (mg biomass ml^{-1}). The yield in biomass was calculated as g of dry weight per mol of substrate consumed. The ATP yield was determined as the ratio of ATP produced to substrate consumed at the time of growth arrest assuming that all ATP was synthesized by substrate-level phosphorylation. The values reported are averages of two independent growths.

Transcriptome analysis

The transcript levels of *S. pneumoniae* D39 growing in CDM supplemented with Gal, Man or GlcNAc were compared by transcriptome analysis to Glc-grown cells. Additionally, cells of D39 grown on a single sugar (Gal, Man or GlcNAc) or in their mixture challenged with a Glc pulse (10 mM) were compared to unchallenged cells using whole-genome *S. pneumoniae* DNA microarrays [29]. Cells were harvested by centrifugation (7197 *x g*, 2.5 min, at room temperature) at exponential phase of growth 1 h after the pulse challenge that was given at mid-exponential growth. Cell pellets were suspended in the remaining medium, frozen in liquid nitrogen and stored at -80 °C. mRNA isolation, synthesis and labelling of cDNA and hybridization were performed as described before [29]. RNA extraction was performed from three independent cultures. Microarray experiments and analysis were done essentially as described elsewhere [29,30].

In all cases, genes were considered significantly differentially expressed when the Bayesian *p-value* was < *0.05 / n.* The Bonferroni correction factor *n = 1769 x 7* corresponds to the total number of differential expression significance tests performed and thus accounts for multiple hypothesis testing. Overrepresentation of COG categories and Metacyc pathways (with more than five genes) among significant genes was assessed via hypergeometric tests with a *p-value* threshold of p < *0.05 / n*, with the Bonferroni correction factor *n = 63 x 7* corresponding to the total number of overrepresentation tests performed.

Heatmap were generated by taking into account the genes that were differentially expressed in each sample subset (single sugars *vs.* Glc and Glc challenged experiments *vs.* unchallenged cells), and intersecting those genes with the annotated subset categories: sugar transporters and sugar catabolic genes (reviewed in Chapter 2, Paixão *et al.*, 2015),

glycolytic genes and genes devoted to pyruvate metabolism (according to NCBI annotation) and virulence factors (Table S3.1).

Venn diagrams were generated with the Venny tool: http://bioinfogp.cnb.csic.es/tools/venny/. When creating the gene lists, we consider D39 genes that are differentially expressed in each conditions, regardless of the direction of differential expression.

In vivo ^{13}C-NMR experiments with resting cells

Cells of *S. pneumoniae* D39Δ*cps* were grown under anaerobic conditions, in a 2-L bioreactor (Sartorius Biostat® B plus) in CDM supplemented with 55 mM of Gal or GlcNAc. On Man, the biomass generated was insufficient for NMR studies, thus the cells were grown in presence of 55 mM of Glc supplemented with 0.5 mM of Man. Growth was performed with controlled pH (6.5) and temperature (37ºC), under anaerobic conditions essentially as described before [28]. The medium was aseptically degassed with argon during 60 min before inoculation. Cultures were kept homogenized by using an agitation speed of 50 rpm. Cells were harvested (5750 *x g*, 7min, 4ºC) in the late-exponential phase of growth and suspensions prepared essentially as described elsewhere [31]. In brief, cells were washed twice (5750 *x g*, 5min, 4ºC) with 50 mM KPi buffer (pH 6.5) supplemented with 1% (wt/vol) choline and suspended in 35 ml of the same buffer with 6% (vol/vol) of deuterium oxide.

In vivo ^{13}C-NMR experiments were performed online under controlled conditions of pH (6.5), temperature (37ºC) and atmosphere (anaerobic conditions, argon atmosphere), using the circulating system as described by Neves *et al.* [31]. Substrates specifically labelled with ^{13}C at carbon one (20 mM) were added to the cell suspension at time zero and spectra (30 s) acquired sequentially. For the two pulse substrate experiment, cells of D39Δ*cps* actively metabolizing 20 mM of [1-^{13}C]Gal were challenged with a 10 mM pulse of [2-^{13}C]Glc. ^{13}C enrichment in different carbons allows

traceability of the substrates in deriving intracellular metabolites and end-products. After substrate depletion and when no changes in the resonances due to end-products and intracellular metabolites were observed, the NMR experiment was stopped and a total cell extract was prepared by passing the cell suspension three times through the French press (6.21 MPa); the resulting total extract was incubated 15 min at 80-90ºC and cooled down on ice. Cell debris and denaturated macromolecules were removed by centrifugation (45696 *x g*, 10 min, 4ºC), and the supernatant (herein designated as NMR cell extract) was used for metabolite quantification of end-products and minor metabolites that remained inside the cells, which was accomplished in fully relaxed ^{13}C-spectra, at 30ºC. The lactic acid and acetate produced were quantified in the NMR cell extract by ^{1}H-NMR on a Bruker AMX300 spectrometer (Bruker Biospin GmbH), using formic acid (sodium salt) as an internal concentration standard [31].

Due to fast pulsing conditions during *in vivo* ^{13}C-spectra acquisition, correction factors were determined allowing the conversion of peak intensities into concentration of intracellular metabolites. Correction factors for resonances due to C1 and C6 of FBP were determined (0.73±0.07) to convert peak intensities to concentrations as described by Neves *et al.* [32], but the temperature was kept at 37ºC. Resonances due to C1 α-mannose 6-phosphate (α-Man6P) and C1 β-mannose 6-phosphate (β-Man6P) were determined (0.33 and 0.51, respectively), at 37ºC. A value of 3 µl (mg protein)$^{-1}$ of intracellular volume of *S. pneumoniae* was used to determine the intracellular concentrations of metabolites [33]. The concentration limit for detection of intracellular metabolites under the conditions employed was 3-4 mM. For dry mass determination, 1 ml of cell suspension obtained after *in vivo* ^{13}C NMR experiment was filtered through 0.22 µm pore size membranes, dried at 100ºC and desiccated for 45 min prior weighing. This was done in

duplicates for each experiment. The quantitative kinetic data for intracellular metabolites were determined as described elsewhere [31]. The values presented are averages of at least two independent assays.

Identification of transient resonances

Transient resonances observed during *in vivo* NMR experiments were assigned by spiking pure compound to NMR extracts obtained from actively metabolizing cell suspensions. In brief, during the metabolism of the labelled substrate, 1 ml aliquot was withdrawn and perchloric acid (0.6 M, final concentration) was added. After 20 min stirring on ice the pH was set neutral with 2M KOH, and the cell extract was centrifuged (60 min, 4ºC, 16100 *x g*). The supernatant was frozen with liquid nitrogen, lyophilized and suspended in bi-distilled water.

NMR spectroscopy

^{13}C spectra were acquired at 125.77 MHz using a quadruple nuclei probe head on a Bruker AVANCE II 500 MH spectrometer (Bruker Biospin GmbH, Karlsruhe, Germany), as described before [31].

Determination of the correction factors was accomplished by acquisition of ^{13}C-NMR spectra with a 60º flip angle and a recycle delay of 1.5 s, for saturating conditions or 60.5 s (relaxed conditions). For assignment of unknown compounds, carbon NMR spectra were recorded using a selective de carbon probe head (^{13}C-Dual).

Carbon chemical shifts are referenced to the resonances of external methanol, designated at 49.3 ppm.

Chemicals

Galactose and mannose were purchased from Sigma-Aldrich. Glucose was supplied by Merck and N-acetylglucosamine was purchased from

Applichem. [1-^{13}C] labelled compounds (galactose, glucose, mannose and N–acetylglucosamine) and [2-^{13}C]glucose, 99% isotopic enrichment, were obtained from Cortecnet. DSS and formic acid (sodium salt) were purchased from Merck. All other chemicals used were reagent grade.

Results and Discussion

Carbon and energy metabolism transcriptome of glycan-derived sugars

Mucins and other host glycans are composed of a variety of monosaccharides. We have previously shown the aptitude of *S. pneumoniae* D39 to use GlcNAc, Gal and Man as sole carbon sources for growth (Paixão *et al.*, 2015, Chapter 2). The growth profiles sustained by these sugars are markedly different, which indicates differential gene expression. Thus, to investigate the effect of the glycan-derived monosaccharides on gene expression, a whole-genome transcriptome analysis was conducted, in which the transcript levels of cells grown on Gal, Man or GlcNAc were compared to those of Glc-grown cells (Tables S3.2, S3.3 and S3.4, all provided on the CD). The results are summarized in Table 3.1.

Table 3.1. Significantly differentially expressed genes (up- or downregulated) in cells of *S. pneumoniae* D39 grown in CDM supplemented with N-acetylglucosamine (GlcNAc), mannose (Man) or galactose (Gal) as compared to glucose (Glc), determined by DNA microarrays[a].

			Up- or downregulation[b]		
Locus_tag	**Gene**	**Product**	**GlcNAc**	**Man**	**Gal**
Sugar-specific catabolism[c]					
SPD_0071	***galM***	**aldose 1-epimerase**			**0.58**
SPD_1050	***lacD***	**tagatose 1,6-diphosphate aldolase**			**3.00**
SPD_1051	***lacC***	**tagatose-6-phosphate kinase**			**2.87**
SPD_1052	***lacB***	**galactose-6-phosphate isomerase subunit LacB**			**3.05**
SPD_1163		N-acetylneuraminate lyase, putative	1.39	0.75	
SPD_1246	***nagB***	**glucosamine-6-phosphate isomerase**		0.46	
SPD_1432	***galE-1***	**UDP-glucose 4-epimerase**			**0.77**
SPD_1488		ROK family protein	1.58	0.83	
SPD_1612	***galE-2***	**UDP-glucose 4-epimerase**			**-0.57**
SPD_1633	**galT-2**	**galactose-1-phosphate uridylyltransferase**			**3.11**
SPD_1634	***galK***	**galactokinase**		0.64	**3.30**
SPD_1866	***nagA***	**N-acetylglucosamine-6-phosphate deacetylase**			0.47
SPD_1993	*fucU*	RbsD/FucU transport protein family protein		-0.98	
SPD_1994	*fucA*	L-fuculose phosphate aldolase		-0.82	
SPD_1995	*fucK*	L-fuculose kinase FucK, putative		-1.25	
Glycolysis					
SPD_0445	*pgk*	phosphoglycerate kinase		0.46	
SPD_0526	*fba*	fructose-bisphosphate aldolase		0.45	
SPD_0790	*pyk*	pyruvate kinase		0.57	
SPD_1012	*eno*	enolase		0.61	
SPD_1823	*gap*	glyceraldehyde-3-phosphate dehydrogenase		0.53	
Downstream pyruvate					
SPD_0420	*pflB*	pyruvate formate-lyase		1.25	
SPD_0621	*lcto*	lactate oxidase		0.38	
SPD_0985	*pta*	phosphotransacetylase			0.64
SPD_1834	*adh*	bifunctional acetaldehyde-CoA/alcohol dehydrogenase		1.00	
Sugar-specific transporters[c]					

SPD_0088		**ABC transporter, permease protein**			**-0.73**
SPD_0089		**ABC transporter, permease protein**			**-0.80**
SPD_0279	*celB*	cellobiose phosphotransferase system IIB component	-2.13	-1.80	-2.41
SPD_0281	*celC*	cellobiose phosphotransferase system IIA component	-2.30	-1.98	-2.29
SPD_0283	*celD*	cellobiose phosphotransferase system IIC component	-1.91	-2.24	-1.61
SPD_0360	*mtlA*	PTS system, mannitol-specific IIBC components			0.62
SPD_0502		PTS system, beta-glucosides-specific IIABC components	-0.65	-0.47	-0.73
SPD_0559		**PTS system IIA component, putative**			**1.26**
SPD_0560		**PTS system, IIB component, putative**			**1.21**
SPD_0561		**PTS system, IIC component, putative**			**1.55**
SPD_0661	***exp5***	**PTS system, IIABC components**	**-0.61**		
SPD_0773		PTS system, fructose specific IIABC components		0.36	
SPD_1039	*ptsI*	phosphoenolpyruvate-protein phosphotransferase		0.49	
SPD_1040	*ptsH*	phosphocarrier protein HPr		0.56	
SPD_1047	*lacE-2*	PTS system, lactose-specific IIBC components			0.78
SPD_1057		PTS system, IIB component, putative			1.48
SPD_1409		sugar ABC transporter, ATP-binding protein			-0.52
SPD_1493		sugar ABC transporter, permease protein		0.61	
SPD_1494		sugar ABC transporter, permease protein		0.54	
SPD_1495		sugar ABC transporter, sugar-binding protein		0.56	
SPD_1496		PTS system, IIBC components		-0.48	-0.72
SPD_1832		PTS system, IIB component		-0.54	
SPD_1833		PTS system, IIA component		-0.57	
SPD_1959	*ulaA*	ascorbate-specific PTS system enzyme IIC			-0.51
SPD_1989		**PTS system, IID component**		**-0.63**	
SPD_1991		**PTS system, IIB component**		**-0.78**	
SPD_1992		**PTS system, IIA component**		**-0.76**	

[a] Subtable of Tables S3.2, S3.3 and S3.4, all provided on the CD.
[b] Values of ln-ratio. Positive values indicate upregulation and negative values indicate downregulation.
[c] As reviewed by Paixão *et al*, 2015 (Chapter 2).
In bold are depicted the transporters and sugar-specific catabolic genes known or putatively involved in the metabolism of GlcNAc, Man or Gal, as reviewed by Paixão *et al*, 2015 (Chapter 2).

The number of genes significantly differentially expressed was sugar specific. Mannose elicited the largest transcriptional response, with a total of 247 genes out of 1738 (about 14.2%) showing altered mRNA levels as compared to Glc. In opposition, Gal-grown cells displayed the lowest percentage of significantly differentially expressed genes (8.4%) in comparison with Glc. A total of 198 genes were significantly differentially expressed in cells grown in GlcNAc-containing medium (11.4%). Interestingly, only a small percentage (1.8%) of genes significantly differentially expressed was common to the three carbon sources (Fig. 3.2A and Table S3.5).

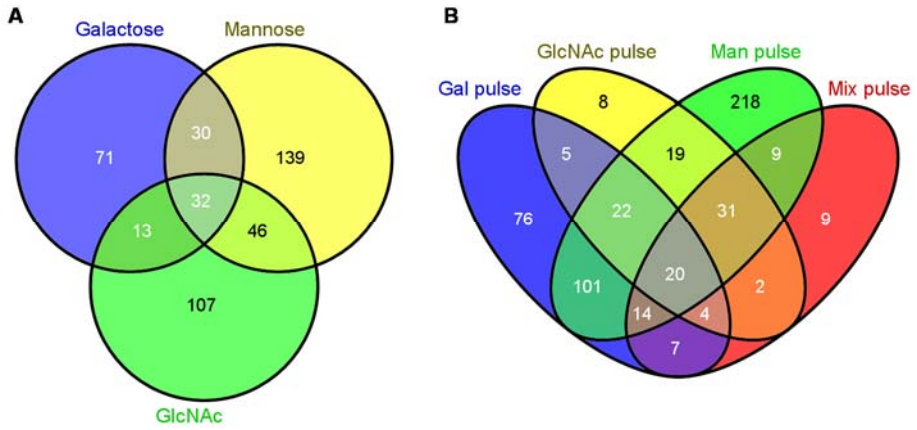

Figure 3.2. Comparison of the genome-wide transcriptional response to different carbohydrate availabilities.

Venn diagrams of the significantly differentially expressed genes during growth on (**A**) galactose (Gal), mannose (Man) and N-acetylglucosamine (GlcNAc) and (**B**) adapted to grow on galactose, mannose, N-acetylglucosamine or in a mixture thereof (Mix) and submitted to a pulse of Glc. Figures were generated using VENNY (http://bioinfogp.cnb.csic.es/tools/venny/index.html).

Of these, 12% were upregulated in the presence of the glycan-derived sugar, whereas the majority was seemingly activated by Glc. These was indeed the case for the SPD_0277-8-9-0-1-2-3 locus comprising the Lac-

PTS transporter *celBCD*, a 6-phospho-beta-glucosidase *celA*, a transcriptional regulator and two hypothetical proteins, which was downregulated on all conditions tested. Also downregulated was SPD_0502, which encodes the IIABC components of a Glc-family PTS system (Table S3.5). Thus, expression of two sugar transporters, SPD_0502 and CelBCD, supposedly involved in the translocation of beta-glucosides [18,34,35] is induced by Glc, suggesting a possible role of these transporters on Glc internalization. The involvement of transporters other than the PTS-Man (ManLMN) on Glc transport has been postulated, but not proven to date [18].

Among the three sugars, GlcNAc and Man showed the highest number of differentially expressed genes in common (46 genes), while Gal and GlcNAc had the least number of common differentially expressed genes (only 13 genes) (Fig. 3.2A). In conclusion, growth on Man and GlcNAc showed the lowest differentially regulation at the transcriptional level, thus the simultaneous utilization of GlcNAc and Man is likely more favourable than of one of the previous together with Gal.

Overrepresentation of COG categories among the significantly differentially expressed genes displayed a sugar dependency (Table S3.6 on the CD). In Gal-grown cells the COG category of “carbohydrate metabolism and transport” (G) was overrepresented (28 genes out of 146, fifteen of which were induced) (Tables S3.4 and S3.6, all provided on the CD). On GlcNAc, the “amino acid metabolism and transport” (E) and the “translation, ribosomal structure and biogenesis” (J) categories showed the highest number of genes significantly, differentially expressed (18.7% and 14.6%, respectively). While in the E category 8 genes out of 37 were induced, only one gene belonging to the J category was upregulated (Tables S3.2 and S3.6, all provided on the CD). In Man-grown cells no differential COG categories were overrepresented, according to the criterion established (Tables S3.3 and S3.6, all provided on the CD). In

accordance, Man-grown cells displayed the highest percentage (26.3%) of genes encoding hypothetical proteins differentially expressed.

N-acetylglucosamine

During exponential growth, 198 transcripts were differentially expressed on GlcNAc as compared to Glc (Bayesian *p-value* < 0.05 / n). Of these, only 5.6% belong to the COG category of "carbohydrate metabolism and transport" (G). Surprisingly, neither GlcNAc specific transporters nor the dedicated catabolic genes (*nagA* and *nagB*) were altered, except for gene *exp5*, a putative GlcNAc PTS transporter, which is downregulated (Tables 3.1 and S3.2 on the CD). This pattern suggests that Exp5 is not involved in the translocation of the amino sugar, but further experimental validation is required. In other bacteria, such as *Streptococcus mutans* or the model organisms *Bacillus subtilis* and *Escherichia coli*, GlcNAc induced the expression of genes encoding the specific catabolic pathway [36]. In a previous study, we showed that the activity of glucosamine 6-phosphate isomerase (NagB) was 4 times higher than that of N-acetylglucosamine 6-phosphate deacetylase (NagA) in GlcNAc-grown cells (Paixão *et al.* 2015, Chapter 2). Re-evaluation of the microarray data using a less restrictive criterion (Bayesian *p-value* < 0.001) showed that *nagB* was slightly induced by GlcNAc (1.40 times), but the expression of *nagA* was not altered. In *S. mutans,* the levels of *nagB* and *nagA* transcripts also differ (mRNA *nagB* > *nagA*) [36], and this profile was interpreted as a mechanism to ensure a response to sugar variations while keeping the pools of GlcN6P to optimize growth. GlcN6P was identified as an allosteric effector that alleviates the repression of *nagA* and *nagB* mediated by the transcriptional regulator NagR.

Genes encoding activities in the central carbon pathways, glycolysis and fermentation (pyruvate conversion) were not significantly differentially expressed (Table 3.1). The expression data are in good agreement with our earlier observations showing that fermentation of GlcNAc is

essentially homolactic, but fails to explain the lower growth rates on the amino sugar (about 1.7 times lower than on Glc) (Paixão *et al*., 2015, Chapter 2). Growth rate is by far a more complex property, which cannot be fully explained by differences in the glycolytic flux that might (or not) arise from differentially expression of genes. A limiting step, however, can be the uptake of GlcNAc as induction of specific transporters was not observed.

Of importance, also induced by GlcNAc is the N-acetylglucosaminidase encoded by *strH*. This surface-associated exoglycosidase is involved in the breakdown of GlcNAc residues from glycans [37,38]. Hence, sensing of free GlcNAc presumably enables *S. pneumoniae* to hydrolyse GlcNAc containing glycans.

Mannose

Mannose elicits a global effect and alters considerably the expression of genes in glycolysis and pyruvate metabolism, as opposed to GlcNAc (and Gal, see below). Of all the transporters previously postulated as potentially involved on Man uptake (Paixão *et al*., 2015, Chapter 2), only the putative Man-PTS system SPD_1989-1-2 was differentially expressed on Man. The genes were downregulated, suggesting that their product might not be involved in Man uptake. Mannose induced a CUT1 ATP-Binding Cassete (ABC) family transporter (SPD_1493-4-5) and a PTS system (SPD_0773) (Tables 3.1 and S3.3 on the CD). The first is present in the sialic acid operon and has been related to sialic acid and N-acetylmannosamine transport [18,39], whereas the second was assigned as a fructose transporter [18]. Whether these transporters are involved on mannose uptake remains to be investigated. Interestingly, the general components of the PTS systems, phosphocarrier protein HPr (*ptsH*) and phosphoenolpyruvate-protein phosphotransferase, Enzyme I (*ptsI*), were induced during growth on Man (Table 3.1), indicating that Man translocation is primarily mediated by a PTS system. In agreement, a *ptsI*

mutant of strain D39 showed practically no growth on Man, while inactivation of the PTS-Man (*manLMN*) dramatically reduced the ability of strain D39 to grow on mannose (A. M. Cavaleiro, P. Gaspar, T. Kloosterman, O. P. Kuipers and A. R. Neves, unpublished data). In strain DP1004, a rough derivative of D39, mutation of *ptsI* partially reduced the growth on Man, but non-PTS systems for Man uptake were not ruled out [18].

The dedicated Man catabolic gene mannose 6-phosphate isomerase (*manA*) was not differentially expressed (even using a less restrictive criterion). The absence of significantly differentially expressed sugar-specific catabolic genes in the presence of Man and GlcNAc might reflect the constitutive expression of these genes, as their activities provide precursors for biosynthesis. In accordance, we have shown activity of ManA and NagA in Glc-grown cells (Paixão *et al*., 2015, Chapter 2). However, we have also reported that in presence of the inducing sugar their activities were considerable higher (Paixão *et al*., 2015, Chapter 2). The lack of correlation between the transcript levels and biochemical data (enzyme activities) is a recurrent observation in biological systems and might reflect other layers of regulation [40].

Man induced the expression of glycolytic genes, namely those encoding fructose-bisphosphate aldolase (*fba*), glyceraldehyde-3-phosphate dehydrogenase (*gap*), phosphoglycerate kinase (*pgk*), enolase (*eno*) and pyruvate kinase (*pyk*) (Table 3.1). We have proposed ManA as a metabolic bottleneck in strain D39, since Man-grown cells accumulate high amounts of mannose 6-phosphate and expression in trans of *manA* improves the growth on mannose (Paixão *et al*., 2015, Chapter 2). Induction of the glycolytic genes could thereby be a cellular response to alleviate the burden associated with the accumulation of the phosphorylated intermediate. Indeed, toxicity ascribed to sugar-

phosphate accumulation has often been associated with defects or arrest of growth [41,42].

Downstream of the pyruvate node, genes encoding the pyruvate formate-lyase (*pflB*, SPD_0420*)*, the bifunctional acetaldehyde-CoA/alcohol dehydrogenase (SPD_1834, *adh*), and lactate oxidase (*lcto*) also showed altered transcription in response to Man (Tables 3.1 and S3.3 on the CD). *pflB* was among the most upregulated genes in Man-grown cells. The induction of pyruvate formate-lyase and alcohol dehydrogenase is in good agreement with the production of formate and ethanol during growth on the Man (Paixão *et al*., 2015, Chapter 2).

Galactose

Gal influenced differentially the expression of 146 genes, of which 44.5% were upregulated. On GlcNAc and Man, the fraction of induced genes was 37.4% and 40.9%, respectively, lower values than on Gal. In addition, the expression ratios were largest on Gal (Tables S3.2, S3.3 and S3.4, all provided on the CD), suggesting that Glc is a stronger repressor of Gal metabolism than of Man or GlcNAc.

Differently from Man and GlcNAc, Gal induced the expression of putative transporters and specific Gal catabolic genes (Table 3.1). The galactitol-family PTS, SPD_0559-0-1, was induced (3.4- to 4.7-fold) in comparison to Glc-grown cells (Tables 3.1 and S3.4 on the CD). Previously, we reported high upregulation of this operon in mucin-grown cells (Paixão *et al*., 2015, Chapter 2, Table 3.1). Our results corroborate earlier evidence pinpointing SPD_0559-0-1 as a Gal-transporter [18,43]. Additionally, Gal induced the expression of SPD_1057, codifying the EIIB subunit of a Gat-PTS, and of SPD_1047 (*lacE-2*) encoding the lactose-specific IIBC components of a Lac-family PTS. Upregulation of LacFE was also observed for a different isolate of *S. pneumoniae* D39 on Gal [27]. The positive effect suggests an involvement of the systems in the uptake of Gal (Table 3.1). Of note, this Lac-PTS has been implicated in Gal

transport in the closely related organisms *S. mutans* and *L. lactis* [44,45]. Induction of *mtlA* was observed, but this system is specific for mannitol transport, and the increase expression is most likely due to relief of Glc-mediated catabolite repression [18]. In contrast, the genes SPD_0088-9, which encode the permease proteins of a CUT1 ABC transporter proposed to take up Gal [18], were downregulated (Tables 3.1 and S3.4 on the CD). Whether this finding rules out the involvement of the ABC transporter in Gal uptake needs experimental confirmation. It should be noted however, that the evidence previously presented was relatively weak, since inactivation of the transporter resulted only in a mild reduction of Gal utilization [18]. A possible explanation is that the inactivation of the ABC is masked by the activity of other Gal transporters.

As expected, Gal induces both the Leloir and tagatose 6-phosphate (T6P) pathways (Table 3.1). The Leloir genes *galk* and *galT-2* were among the most upregulated genes (Table S3.4 on the CD), while UDP-glucose 4-epimerase (*galE-1*) and aldolase 1-epimerase (*galM*) were induced by 2.2- and 1.8-fold, respectively (Table 3.1). The duplicated gene *galE-2* was downregulated, underpinning the role of *galE-1* as the functional UDP-glucose 4-epimerase in strain D39. The duplicated gene *galT-1* was not differentially expressed, strongly pointing to *galT-2* as the Leloir catabolic gene. Interestingly, we have shown that deletion of *galT-2* resulted in *circa* 50 times increased expression of *galT-1,* indicating *galT-1* as a surrogate of *galT-2* (Paixão, *et al*., 2015, Chapter 2). The T6P pathway genes *lacB*, *lacD* and *lacC*, which codify for galactose 6-phosphate isomerase subunit LacB, tagatose 1,6-diphosphate aldolase and tagatose 6-phosphate kinase, respectively, were also highly up-regulated (Table 3.1). Induction of both pathways in response to Gal is a recurrent observation in previous studies from our laboratory (Paixão *et al*., 2015, Chapter 2, [27]). Curiously, Afzal *et al*. [46] observed only increased expression of the T6P pathway genes in response to Gal in *S.*

pneumoniae D39. The different results in the two studies most likely derive from differences in cultivation medium and/or other experimental conditions. While we have gathered strong evidence that both pathways are functional, determining the relative contribution of each pathway to the metabolism of Gal is, however, not trivial and would require estimating the flux partitioning between the two routes.

In addition, Gal induced expression of *galR*, a transcriptional regulator localized upstream of *galK-galT-2* and oriented in the opposite direction. In other streptococci *galR* acts as a transcriptional regulator of the Leloir pathway (*gal* operon) [47–49]. In *S. mutans*, GalR represses the *gal* operon in the absence of Gal, but intracellular Gal acts as an effective inducer of the Leloir genes, abolishing the binding of GalR to the intergenic region of *galR-galK* [49]. Contradictory studies were reported for the role of *galR* in *S. thermophillus* [50,51]. In *S. pneumoniae* the role of *galR* on Gal metabolism remains to be determined. Gal also induced the expression of a lactose phosphotransferase system repressor (*lacR2*), which recently was identified as a transcriptional repressor of the T6P pathway in the presence of Glc (and absence of Gal and lactose) [46]. The duplicated gene *lacR1* (SPD_0771) was downregulated in presence of Gal (Table S3.4 on the CD).

Regarding the fermentative genes, only the phosphotransacetylase gene (SPD_0985, *pta*), involved in the conversion of acetyl-CoA into acetyl-phosphate was induced by Gal (Table 3.1). The transcript levels of *ackA*, encoding acetate kinase, were unaltered, in agreement with *in silico* DNA microarray predictions [27]. This behaviour is however surprising, considering the remarkable increase (18-fold) in acetate production from Gal as compared to Glc (Paixão *et al*., 2015, Chapter 2). Moreover, genes encoding pyruvate formate-lyase (*pflB*), pyruvate formate-lyase activating enzyme (*pflA*), and the bifunctional acetaldehyde-CoA/alcohol dehydrogenase were not significantly differentially expressed. This profile

was unexpected, since a pronounced shift to mixed acid fermentation occurs on Gal (Paixão *et al*., 2015, Chapter 2, [27]), and induction of the mixed-acid pathways by Gal was reported before [27]. Also, Gal reportedly enhances the activity of pyruvate formate-lyase in *S. mutans* and *L. lactis* [52,53]. However, *pflB* appeared as induced by Gal (ratio ~1.90) in *S. pneumoniae* D39 when less restrictive significance criterion (*p-value* < 0.001 as compared to 0.05 / n) was used as in the study by Carvalho *et al*. [27] .

As for many other studies, we also fail to observe a complete correlation between expression profiles and pneumococcal phenotypic traits, which ultimately denotes regulation at other cellular layers, such as post-transcriptional and/or metabolic levels. Thus, in the next section the glycolytic dynamics of *S. pneumoniae* D39 during catabolism of the glycan-derived sugars are investigated.

Glycolytic and end-product profiles on glycan-derived monosaccharides

Catabolism of GlcNAc, Man and Gal was investigated by *in vivo* ^{13}C-NMR in non-growing suspensions of cells grown on the specific sugar under study. As described, a non-encapsulated derivative of strain D39 was used, D39Δ*cps*. The kinetics of sugar consumption and end-products formation during the catabolism of [1-^{13}C]GlcNAc, Man and Gal are shown on Fig. 3.3. Glucose catabolism is shown for comparison on Fig. 3.3D.

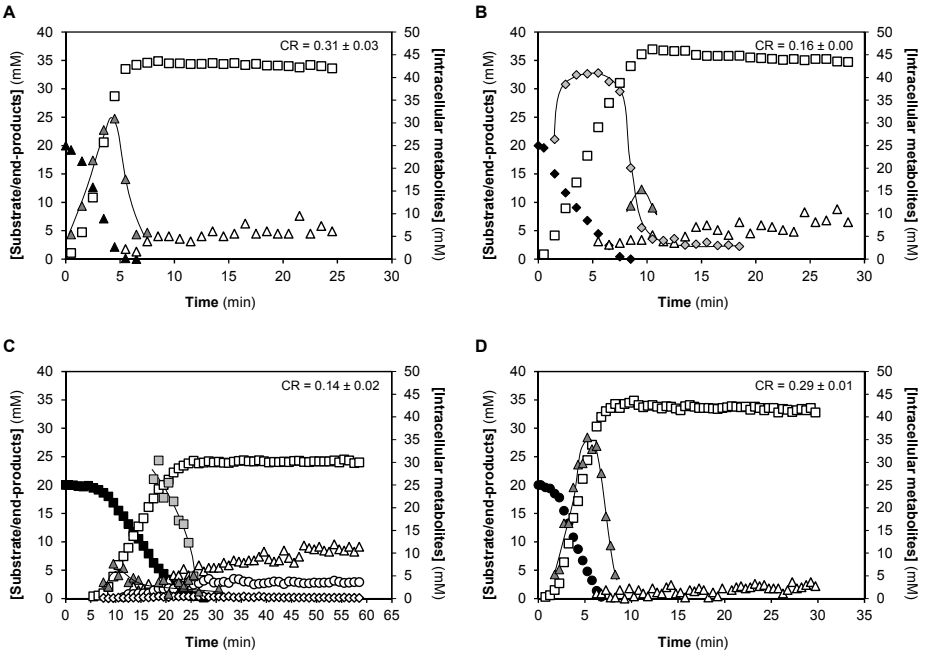

Figure 3.3. Kinetics of 20 mM [1-^{13}C]-sugar consumption, end-products formation and metabolic intermediates derived from the catabolism of different carbon sources by non-growing cells of *S. pneumoniae* D39Δ*cps*.

(**A**) N-acetylglucosamine (GlcNAc), (**B**) mannose (Man), (**C**) galactose (Gal) and (**D**) glucose (Glc). The metabolism was monitored online by *in vivo* ^{13}C-NMR. Experiments were carried out at 37ºC, under anaerobic conditions and pH control (6.5). Figures are from representative experiments from at least 2 replicates. The pyruvate concentration is depicted as extracellular concentration. Lines associated to intracellular metabolite time courses are simple interpolations. CR, maximal substrate consumption rate; FBP, fructose 1,6-biphosphate; Man6P, mannose 6-posphate; α-Gal6P, α-galactose 6-phosphate. Symbols: (▲), GlcNAc; (◆), Man; (■), Gal; (●), Glc; (□), lactate; (△) acetate; (○), ethanol; (◇), pyruvate; (▲), FBP; (◇), Man6P; (□), α-Gal6P.

The metabolism of GlcNAc was essentially homolactic. Lactate (33.6±1.1 mM), the main end-product from the fermentation of the amino sugar (20 mM), accounted for 84% of the substrate consumed. Acetate was also produced (4.0±0.9 mM) as a catabolic product of GlcNAc. Pyruvate was detected *in vivo*, but in quantities that did not allow its reliable quantification. The maximal substrate consumption rate was

0.31±0.03 µmol min^{-1} mg^{-1} of protein (Fig. 3.3A), a value higher than on Gal or Man, but similar to that on Glc (Fig. 3.3). The fermentation profile in non-growing suspensions is homolactic as previously shown for growing cells (Paixão *et al*., 2015, Chapter 2). In fermentative lactic acid bacteria, homolactic metabolism has generally been associated with fast metabolizable sugars [54]. GlcNAc fermentation in *S. pneumoniae* seems to be no exception, but the molecular mechanisms underlying this behaviour have yet to be disclosed (Fig. 3.3).

The glycolytic intermediate fructose 1,6-biphosphate (FBP), was the only intracellular metabolite detected in non-growing cells by *in vivo* NMR (Fig. 3.3A). The FBP pool increased immediately after substrate addition, reached the maximal concentration at the onset of GlcNAc exhaustion, and subsequently decreased to undetectable levels (Table 3.2, Fig. 3.3A). This profile resembles closely the accumulation of FBP during Glc metabolism (Fig. 3.3D), suggesting that regulation of glycolysis is similar for both sugars. In agreement, no changes in the transcript levels of glycolytic and fermentative genes were observed when comparing expression on GlcNAc to Glc (Tables 3.1 and S3.2 on the CD). Indeed, it is well documented that FBP accumulates to higher amounts during the catabolism of fast metabolizable sugars as Glc than less preferred carbohydrates. The reasons for the accumulation of this metabolite are diverse [31,54–56] and still matter of debate (reviewed in [57]).

In addition to FBP, the phosphorylated metabolites fructose 6-phosphate, N-acetylglucosamine 6-phosphate and glucosamine 6-phosphate were also detected in extracts of cells growing on GlcNAc (Paixão *et al*., 2015, Chapter 2, Table S3.7). While the amount of phosphorylated amino sugars was low, fructose 6-phosphate accumulated substantially, and thus it is surprising that this metabolite was not observed in resting cell suspensions (non-growing).

Table 3.2. Maximal concentrations of glycolytic and sugar-specific intermediates during the metabolism of N-acetylglucosamine (GlcNAc), mannose (Man), galactose (Gal) and glucose (Glc), by non-growing cells of *S. pneumoniae* D39Δ*Cps*, determined by *in vivo* ^{13}C NMR.

Sugar	GlcNAc	Man	Gal	Glc[a]	Gal pulse Glc
FBP_{max} (mM)	28.6±2.2	11.7±5.1	12.2±6.4	35.0±2.0	10.1±4.1[b]/3.8±0.5[c] 8.0±1.2[d]
$Man6P_{max}$ (mM)	ND	37.1±5.4	ND	ND	ND
α-$Gal6P_{max}$ (mM)	ND	ND	36.1±8.1	ND	39.0±0.4/19.1±3.4[e]

Values determined by ^{13}C-NMR in the NMR cell extracts from the cell suspensions used in the *in vivo* NMR. ND, not detected *in vivo* or in the NMR cell extract. The values are averages of at least two independent experiments.
[a] Values reported by (A. M. Cavaleiro, P. Gaspar, T. Kloosterman, O. P. Kuipers and A. R. Neves., unpublished data).
[b] Maximal FBP accumulation, derived from Gal metabolism.
[c] Maximal FBP accumulation, derived from Glc metabolism.
[d] Second FBP accumulation, derived from Gal metabolism.
[e] Second α-Gal6P accumulation, derived from Gal metabolism.
FBP, fructose 1,6-biphosphate; Man6P, mannose 6-phosphate; α-Gal6P, α-galactose 6-phosphate.

Consumption of GlcNAc and Glc was identical in resting cells (Fig. 3.3), but Glc supported much faster growth than GlcNAc (Paixão *et al*., 2015, Chapter 2). The poor performance of GlcNAc in supporting growth combined with larger accumulation of phosphorylated metabolites in growing cells indicate a metabolic bottleneck in anabolic processes, whereas catabolic processes are identical for GlcNAc and Glc as evidenced from the *in vivo* ^{13}C-NMR data. In agreement, glycolytic genes were not differentially expressed when comparing GlcNAc to Glc (Table S3.2 on the CD).

In Man metabolizing cells, lactate was the major end-product (30.4±6.1 mM), accounting for 76% of the Man consumed. The acetate produced (9.0±3.5 mM) was 4-fold higher than in Glc. Pyruvate was detected *in viv*o, but the low amounts hampered reliable quantification. The deviation

towards mixed acid fermentation is consistent with the profile observed in Man-grown cells (Paixão *et al*., 2015, Chapter 2). The upregulation of fermentative genes SPD_1834 (*adh*) and *pflB* (Table 3.1) is in accordance with this shift. However, a more pronounced shift could be expected, as fermentation of non-preferential sugars is generally associated with mixed acid profiles [54]. Earlier, we reported Man as a non-preferential sugar for growth and that it supported the lowest growth rates (Paixão *et al*., 2015, Chapter 2), and now we show that catabolism of Man (consumption rate 0.16±0.00 μmol min^{-1} $mg^{-}1$ of protein) is 2-times slower than that of Glc. What renders Man such a poor substrate is not clear, but the upregulation of glycolytic genes during growth on Man can be surmised as cellular response to overcome Man-associated metabolic limitations (Tables 3.1 and S3.3 on the CD).

The pools of FBP and mannose 6-phosphate (Man6P) accumulated during the catabolism of Man (Fig. 3.3B). The Man6P pool increased sharply to a steady concentration, which swiftly dropped to concentrations below 5 mM at the onset of Man depletion (Table 3.2 and Fig. 3.3B). In contrast, FBP became detectable after Man depletion and when the pool of Man6P was decreasing (Table 3.2 and Fig. 3.3B). Man6P is also the predominant phosphorylated metabolite in Man-grown cells (Table S3.7, Paixão *et al*., 2015, Chapter 2). High concentrations of phosphorylated metabolites have often been associated with metabolic toxicity [41,58], and accumulation to high-levels of non-glycolytic phosphorylated metabolites is a recurrent observation during the metabolism of less preferred substrates [59,60]. Thus, it is tempting to suggest that Man6P toxicity results in lower glycolytic and growth rates. In line, a strain displaying higher Man6P isomerase (ManA) activity grew faster (1.6-fold) on Man than strain D39 (Paixão *et al*. 2015, Chapter 2). In fungi (*Saccharomyces cerevisiae* and *Aspergillus fumigatus*) deletion of phosphomannose isomerase gene led to accumulation of Man6P, which

decreased the glycolytic flux [61,62]. In *Corynebacterium glutamicum*, overexpression of *manA* alleviated the accumulation of Man6P (and F6P) and improved Man catabolism [63].

In this context, induction of glycolytic genes (*fba*, *gap*, *pgk*, *eno* and *pyk*) as observed in presence of Man (Table 3.1), was most likely to alleviate the stress elicited by the accumulation of Man6P, allowing a more rapid flow through the central metabolism. On the other hand, we can speculate that Man6P might exert repression over Man transporters, thus slowing down the uptake of this sugar and subsequent metabolism.

The profile of Gal consumption was characterized by a plateau (concentration approx 20 mM), which preceded efficient conversion of Gal to fermentation end-products. This pattern has been described for *L. lactis* when the sugar uptake was exclusively mediated by non-PTS transporters, such as Glc catabolism in a PTS-mutant or Gal catabolism [44,64]. Transport systems for Gal in *S. pneumoniae* D39 have not been firmly identified, and thus the *in vivo* NMR data is an additional pointer for the involvement of non-PTS systems in Gal uptake. A plateau was also observed for Glc, but the length was smaller. Interestingly, GlcNAc and Man were used instantly by resting D39 cells, in line with the hypothesis that uptake of these sugars is exclusively mediated by PTS transporters [18]. The Gal consumption rate was 0.14±0.02 μmol min^{-1} mg^{-1} of protein, a value similar to the one found on Man, and 2-fold lower than the Glc consumption rate (Fig. 3.3C). A similar fold reduction was observed when comparing growth rates on Gal and Man with Glc (Paixão *et al*., 2015, Chapter 2), suggesting that for these two sugars catabolism is major in the multitude of factors determining growth rates. As in growing cells (Paixão *et al*., 2015, Chapter 2), catabolism of Gal in resting cell suspensions showed a pronounced shift to mixed acid fermentation (Fig. 3.3C), with about 35% of the Gal generating acetate (9.8±0.9 mM), ethanol (3.3±0.6mM) and pyruvate (0.6±0.1 mM), while lactate (24.1±0.2

mM) was lower than in the other sugars. (Fig. 3.3C) A similar profile was observed in *L. lactis* cells metabolizing Gal [60], but in the pneumococcus the deviation towards acetate and ethanol was 4.1- and 1.5-fold higher, respectively.

Yesilkaya *et al.* [65] attributed the mixed acid profile of Gal-grown cells of *S. pneumoniae* D39 to the activity of pyruvate formate-lyase (PFL) (encoded by SPD_0420, *pflB*) and pyruvate formate-lyase activating enzyme (encoded by SPD_1774, *pflA*). In presence of slow metabolizable sugars and anaerobic conditions PFL competes more efficiently with LDH for pyruvate. In consequence, one more molecule of ATP is generated (via acetate kinase activity), which is certainly an advantage during the metabolism of non-preferential sugars (slow metabolizable). The metabolic shift to mixed-acid fermentation has been the subject of intense research, and the underlying regulatory mechanisms are still under debate. Gal-dependent activation of the genes codifying for enzymes involved in the mixed-acid branch has been reported [27]. In this study, we observed a modest induction of the *pflB* gene, which is in accordance with regulation at the transcriptional level.

Resting D39 cells accumulated during the metabolism of [1-^{13}C]Gal FBP and the specific intermediate of the T6P pathway, α-galactose 6-phosphate (α-Gal6P) (Fig. 3.3C). A minor resonance due to 3-PGA, was observed but reliable quantification was hampered by the strong resonance of choline. Also, UDP-Glc was detected in very low concentration during Gal catabolism. In contrast to growing cells, accumulation of the Leloir intermediates galactose 1-phosphate and glucose 1-phosphate was not observed (Table S3.7). It is likely that the concentration of these metabolites is below the detection limit of *in vivo* ^{13}C-NMR technique. Indeed, the ^{31}P-NMR resonances in spectra of Gal-grown cell extracts were relatively weak (Paixão *et al*., 2015, Chapter 2). The pool of FBP accumulated once Gal started to decline, but the maximal

concentration was relatively low (approximately 12 mM) (Fig. 3.3C). Reduced FBP levels might derive from the slow flux through glycolysis, and correlate well with the metabolic shift towards mixed-acid fermentation. It is well established that FBP is an activator of LDH, whereas trioses-phosphate (DHAP and GAP), inhibit PFL [57]. Due to the reversibility of the reactions catalysed by FBP aldolase and triose 3-phosphate isomerase, low trioses-phosphate concentrations are to be expected when FBP is low. Thus, the activation of LDH and the inhibition of PFL are relieved and a mixed acid profile emerges. As for other fermentative organisms, the shift towards mixed acid fermentation is multifactorial and involves regulation at the different cellular layers.

α-Gal6P was detected after Gal addition, but overlap with the strong α-Gal resonance hampered reliable quantification during the first 17 min of Gal metabolism. Once the Gal resonances subsided, integration of the α-Gal6P resonance was possible: while Gal was abundant, the α-Gal6P concentration remained high (above 25 mM), declining rapidly to undetectable levels as Gal was nearing depletion (Fig. 3.3C). The high accumulation of Gal6P in resting cells, also observed in growing cells (Table S3.7, Paixão *et al*., 2015, Chapter 2), suggests a metabolic constraint in Gal processing through the tagatose 6-phosphate pathway. In addition, the accumulation of Gal6P is solid evidence for the functionally of a PTS system, since to our knowledge this is the only reaction capable of generating Gal6P in living cells [44].

Catabolism of Glc in galactose-adapted cells

Of the three monosaccharides studied, Gal showed the strongest effect on glycolytic dynamics and end-products profile (Fig. 3.3C). Thus, we asked whether Gal-adapted cells would be able to efficiently catabolise the preferred sugar Glc. To test this hypothesis, cells actively metabolizing 20 mM of [1-^{13}C]Gal where challenged with a 10 mM labelled Glc pulse,

[2-^{13}C]Glc. The kinetics of sugar consumption, end-products and metabolic intermediates is depicted in Fig. 3.4, as monitored by *in vivo* ^{13}C-NMR.

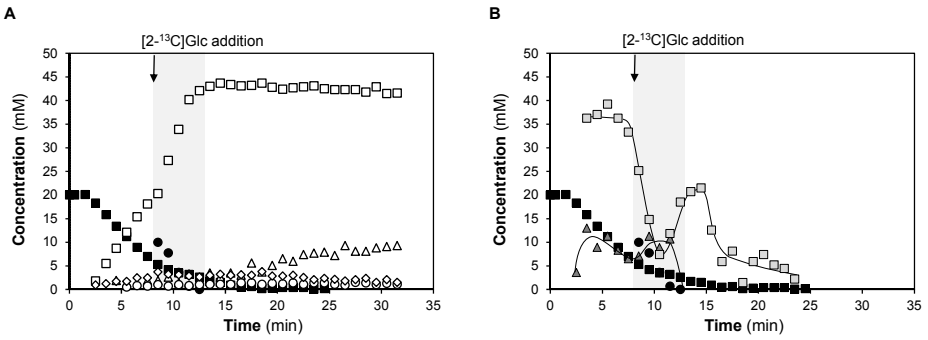

Figure 3.4. Metabolism of galactose (Gal), challenged with a pulse of glucose (Glc), using non-growing cells of *S. pneumoniae* D39Δ*cps*, monitored by *in vivo* NMR.

Kinetics of (**A**) sugar consumption and end-products formation and (**B**) pools of intracellular metabolites. Cells metabolizing a 20 mM pulse of [1-^{13}C]Gal where challenged with a 10 mM pulse of [2-^{13}C]Glc during the maximal consumption rate of Gal. Time course kinetics were obtained online by *in vivo* ^{13}C-NMR. Experiments were carried out at 37ºC, under anaerobic conditions and pH control (6.5). Figures are from representative experiments of at least 2 replicates. Lines associated with intracellular metabolite time courses are simple interpolations. The shaded area represents the time spam for which Glc was available, and the arrow the time-point of addition. Symbols: (■), [1-13C]Gal; (●), [2-13C]Glc; (□), total lactate; (Δ), acetate (derived from Gal catabolism); (○), ethanol (derived from Gal catabolism); (◇), pyruvate (derived from Gal catabolism); (▲), FBP, total fructose 1,6-biphosphate; (▢) α-Gal6P, α-galactose 6-phosphate derived from Gal catabolism.
In this experiment cells were suspended to 24 mg cell dried weight ml^{-1}. As compared to the cell suspension in Fig. 3.3C, the biomass is increased by a factor of 1.2, which most likely leads to the reduced Gal plateau in the current situation.

The addition of Glc decreased the rate of Gal utilization 3.5-fold in comparison with the initial Gal consumption rate (0.14±0.02 µmol min^{-1} mg^{-}1 of protein), showing a preference for Glc over Gal. Although Gal consumption was hindered by the presence of Glc, *S. pneumoniae* was able to catabolise both substrates simultaneously.

Glc was readily consumed as soon as it became available, at a consumption rate (0.27±0.01 µmol min^{-1} mg^{-1} of protein) similar to that of

Glc as a sole substrate (Fig. 3.3D). This behaviour shows that Gal-adapted cells are apt to efficiently metabolize Glc. Indeed, no major changes in transcription of glycolytic genes or *manLMN* (PTS-Man) were observed on Gal as compared to Glc.

The rate of lactate production doubled immediately after the pulse of Glc, shifting the metabolism to a more homolactic profile (Fig. 3.4A). Lactate (43±1.8 mM) accounted for 71% of the total substrate (Glc and Gal) consumed, as compared to 60% on Gal alone. This value is in good agreement with the estimated (68.2%) from a 2:1 Gal to Glc ratio and the 60% and 85% sole conversions of Gal and Glc, respectively. Of the total lactate, about 37% was labelled on C_2, and thereby derived from [2-^{13}C]Glc. Other products from this substrate were acetate (2.6±0.4 mM) and pyruvate (0.8±0.3 mM). The mixed acid products (acetate and ethanol) decreased from 33% (Gal alone) to 18% of the total substrate. Moreover, pyruvate accumulated to a maximal concentrations 5.5-fold higher than those on Gal alone. This behaviour suggests a bottleneck downstream of pyruvate. Curiously, the negative effect of Glc on mixed acid products was more pronounced on ethanol than acetate.

Addition of Glc, caused a sudden drop on the pool of α-Gal6P and rise of the FBP level, a trend that favours lactate production (Fig. 3.4B). All in all, these results show that Glc exerts a negative effect (metabolic inhibition) on the mixed acid fermentation profile.

Effect of glucose on the growth of *S. pneumoniae*

The significant impact of Glc over Gal catabolism at the metabolic level was evident on resting cells of *S. pneumoniae*. Thus, we deemed important to assess the impact Glc during growth of pneumococcus on the three glycan-derived monosaccharides. To this end, Glc was added to exponential cells growing on Gal, Man, GlcNAc or a mixture thereof (Fig. 3.5).

For all the conditions tested, an increase of growth rate was observed upon Glc addition sugar mix (Fig. 3.5 and Table 3.3). This positive effect was more pronounced in Gal-adapted cells (Fig. 3.5A and Table 3.3), for which the final biomass and the maximal specific growth rates were increased by 74% and 172%, respectively. Furthermore, Glc induced biphasic growth, with a phase displaying a maximal growth rate of 0.87±0.07 h^{-1}), followed by slower growth (0.14 ±0.01 h^{-1}). In the sugar mix, the final biomass increased by 30%, while the time to reach these maximal values was shortened by 43% (Fig. 3.5D).

Independently of the carbon source in the medium, growing *S. pneumoniae* cells consumed Glc at once after addition (Fig. 3.5). A similar behaviour was described for the resting cells (Fig. 3.4). A lag phase, typical of the diauxic behaviour associated with adaptation to the additional substrate, was not observed for any of the conditions tested. The rate of Glc utilization was higher than that of the other sugars, as evidenced by the higher quantity of Glc processed over a defined period of time. In summary, *S. pneumoniae* is well equipped to use its preferred substrate Glc, regardless of pre-conditioning to other sugars. However, utilization of Glc does not exclude co-metabolism of the other sugars.

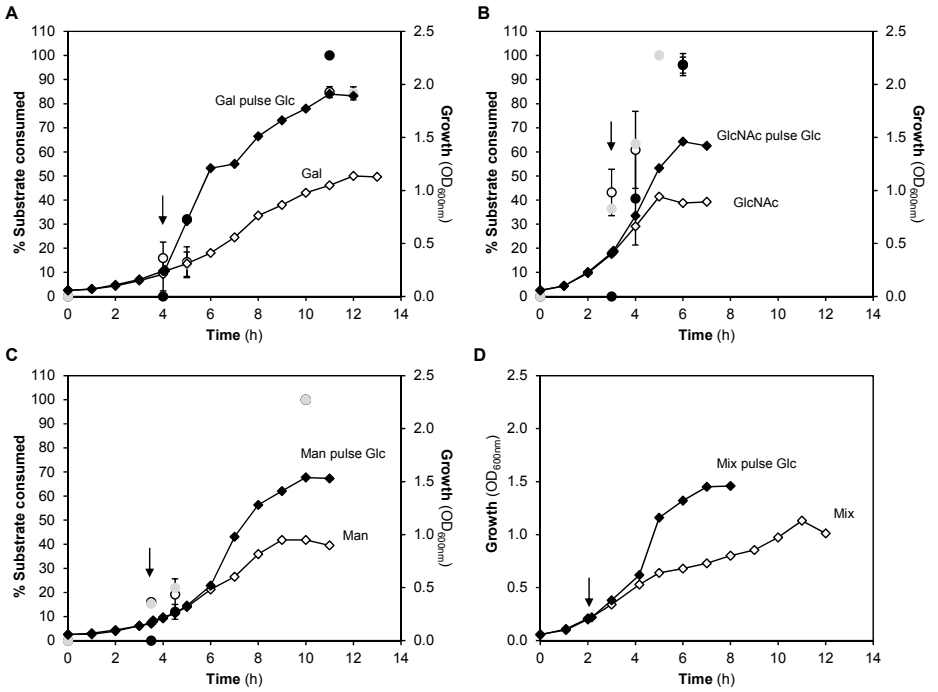

Figure 3.5. Representative growth profiles of *S. pneumoniae* D39 in presence of different carbon sources challenged or unchallenged with a pulse of glucose (Glc) and percentage of substrate consumed.

Growths were conducted in CDM supplemented with: (**A**) galactose (Gal); (**B**) N-aceylglucosamine (GlcNAc); (**C**) mannose (Man) and (**D**) a mixture of Gal, Man and GlcNAc, challenged or unchallenged with a 10 mM Glc pulse given at mid-exponential phase of growth. Cells were grown at 37ºC, under semi-anaerobic conditions, without pH control (initial pH 6.5). The black arrow indicates the time of the Glc pulse. The profiles are averages of two independent growths (unless stated otherwise) and standard deviation is depicted. The percentages of GlcNAc and Man consumed without the Glc challenge correspond to only one representative growth. Symbols: (●), percentage of Glc consumed in pulse chase experiments; (●), percentage of Gal, GlcNAc or Man consumed in unchallenged cells; (○), percentage of Gal, GlcNAc or Man consumed in Glc challenged cells.

Table 3.3. Growth and energetic parameters, carbon and redox balances and substrate consumed, obtained for *S. pneumoniae* D39 grown on CDM in the presence of N-acetylglucosamine (GlcNAc), galactose (Gal), mannose (Man) or in a mixture of sugar (GlcNAc, Man and Gal) challenged or not with a 10 mM glucose (Glc) pulse given at mid-exponential phase of growth.

	GlcNAc[a]	**GlcNAc pulse Glc**	**Gal[a]**	**Gal pulse Glc**	**Man[a]**	**Man pulse Glc**	**Mix[a]**	**Mix pulse Glc**
[substrate]$_{initial}$ (mM)	12.3±0.6	11.7±0.0	13.4±1.3	12.0±0.0	12.4±0.1	14.1±0.4	6.5±0.3[e]	6.1±0.8[e]
Product yields								
Lactate	1.58±0.04	1.66±0.01	0.04±0.01	1.14±0.07	1.43±0.12	1.42±0.06	1.25±0.02	1.81[c]
Formate	0.15±0.07	0.05±0.01	1.47±0.18	0.50±0.01	0.31±0.04	0.15±0.01	0.36±0.06	0.09[c]
Acetate	0.06±0.01	ND	0.75±0.13	0.27±0.05	0.20±0.02	0.08±0.00	0.15±0.01	0.03[c]
Ethanol	0.03±0.01	0.01±0.01	0.72±0.05	0.24±0.04	0.14±0.04	0.06±0.00	0.18±0.03	0.02[c]
μmax (h^{-1})[b]	0.40±0.04	0.44±0.13	0.32±0.04	0.87±0.07[d]	0.37±0.06	0.46±0.06	0.54±0.15	0.67±0.19
OD_{600max}	0.99±0.08	1.35±0.17	1.12±0.26	1.95±0.07	1.03±0.08	1.59±0.07	1.19±0.11	1.55±0.09
Substrate Consumed (%)	100±0	96±4	84±7	92±1	100±0	100±0	86±2	79[c]
Substrate Recovery	84±3	86±0	76±9	83±4	89±3	78±3	79±3	95[c]
Redox Balance	83±3	84±1	75±5	82±1	85±3	77±2	81±4	93[c]
ATP yield (mol mol^{-1} substrate)	1.74±0.08	1.67±0.01	2.27±0.31	1.93±0.14	1.98±0.04	1.65±0.06	1.73±0.06	1.89[c]
YATP (g biomass mol^{-1}ATP)	16.8±0.9	16.7±0.3	14.9±0.5	18.7±0.5	16.2±0.4	14.6±0.2	16.4±0.4	14.7[c]
Ybiomass (g mol^{-1} substrate)	29.3±2.9	27.9±0.7	34.1±5.8	36.0±1.6	31.9±0.1	24.0±0.6	28.3±1.8	27.7[c]

The controls (unchallenged cells) are displayed as reported (Paixão *et al*, 2015, Chapter 2). Growth experiments were made at 37ºC without pH control (initial pH 6.5). Values represent the average and standard deviation of at least two independent growth experiments and were estimated at the time point of growth arrest (maximal biomass).

[a] Values as reported in Paixão *et al*, 2015, Chapter 2, except growth rate.

[b] Maximal specific growth rate determined in the time range after the Glc pulse.
[c] Values of a representative experiment.
[d] Maximal specific growth rate. μ_2=0.14±0.01 h^{-1}.
[e] The value represents the average ± standard deviation of the concentration for all the sugars separately. Individual averages for sugar mixes are: Gal, 6.4±0.7 mM; Man, 6.6±0.1 mM and GlcNAc, 6.7±0.2 mM.
Individual averages for sugar mixes with pulse of Glc are: Gal, 5.7±0.1 mM; Man, 5.9±1.4 mM and GlcNAc, 6.5±0.4 mM.
ND – Not detected as product of pyruvate metabolism.
Substrate recovery is the percentage of carbon in metabolized sugar that is recovered in the fermentation products (lactate, ethanol, acetate and formate).
Redox balance is the ratio between [lactate]+2×[ethanol] and 2×[substrate consumed] multiplied by 100.

Glucose addition represses mixed acid fermentation profile

In resting cells actively metabolizing Gal, Glc promoted a more homolactic fermentation profile. The effects of Glc addition to the end-products formed during growth are shown on Table 3.3. Cells exponentially growing on Gal, GlcNAc or the sugar mix, when challenged with Glc displayed increased lactate yield, which was condition dependent (Table 3.3). Curiously, this pattern was not observed for Man-adapted cells (Table 3.3). Gal-adapted cells showed the largest change in lactate yield, even though no induction of *ldh* was observed (Table S3.8).

Furthermore, Glc addition repressed the formation of mixed acid fermentation products (acetate, ethanol and formate) to a larger extent (except for Gal) than the positive effect on lactate production in all the conditions tested (Table 3.3). Generally, Glc repressed the expression of genes involved in mixed acid fermentation (SPD_1834, *pflB*, *pta*) (Table S3.8), and the reduced transcription positively correlates with the reduced levels of mixed-acid products (Table 3.3). On Man, however, the addition of Glc resulted in elevated levels of *pflB*, *pta* and SPD_1834 transcripts, but still the mixed acid products were lessened (Tables 3.3 and S3.8). These results suggest that under this condition, regulatory mechanisms other than transcription are present.

Based on the results with resting cells we proposed that the partitioning between lactate and mixed acid products is largely regulated at the metabolic level. Overall, the results with growing cells further strengthen this view, without ruling out regulation at the transcriptional level.

Effect of glucose on the expression of genes involved in sugar metabolism

The effect of a Glc challenge to cells growing on the glycan-derived sugars was assessed at the transcriptional level (Table S3.8). The

number of genes significantly differentially expressed in response to Glc was dependent on the sugar (Tables S3.9, S3.10, S3.11 and S3.12, all provided on the CD). The largest transcriptional response was observed in Man-adapted cells (434 genes out of 1738) and the smallest in cells adapted to a sugar mixture (5.5% of the total transcripts) (Fig. 3.2B). In Gal-adapted cells, 249 genes were regulated by Glc, whereas in GlcNAc-adapted cultures 111 genes were differentially expressed after the Glc pulse (Fig. 3.2B). The transcriptional response of Gal and Man-adapted cells to Glc included altered expression of 157 shared genes, of which 101 were exclusive of these conditions. Despite the large number of common genes in the two conditions, the direction of regulation (upregulation *vs*. downregulation) of these genes was not necessarily the same. Indeed, Glc exerted positive (upregulation) and negative (downregulation) regulation in all conditions tested. Gal-adapted cells showed the highest number of upregulated genes (53% of the total), whereas GlcNAc-adapted cells showed the lowest (22.5% of the total) (Tables S3.9 and S3.10, all provided on the CD), an indication that Glc is a mightier repressor of Gal catabolism than of the catabolism of the other sugars. Interestingly, the lesser response in the sugar mix denotes better capacity of these cells to cope with a Glc stimulus, which can be perceived as improved metabolic fitness.

The results presented in Fig. 3.2B and Table S3.8 clearly show sugar-dependent responses to a Glc stimulus. Progression from colonisation to invasive disease is presumably associated with a change from an environment nearly devoid of Glc (nasopharynx) to niches rich in this sugar (blood, inflamed lung). Thus, determination of the transcriptional responses to Glc in clinical serotypes of *S. pneumoniae* should be pursued in the future.

For all the conditions tested, the COG category of “carbohydrate metabolism and transport” (G) was overrepresented (Table S3.6 on the

CD), with the proportion of genes showing altered expression in response to Glc as follows: 32.4%, 28.1%, 16.9% and 12.4% of the total transcripts on GlcNAc, sugar mix, Gal and Man, respectively. Also, most of the genes belonging to category G were downregulated by Glc, except for Man-adapted cultures in which a higher number was induced.

Glucose addition in GlcNAc-adapted cells repressed the expression of putative and proven transporters of this amino sugar (Paixão *et al*., 2015, Chapter 2, Table S3.8), among which the PTS-Man SPD_0262-3-4 (*manLMN*) was downregulated. This system is most likely the major GlcNAc transporter in *S. pneumoniae* D39 [18]. In addition, is also the principal Glc uptake transporter in *S. pneumoniae* [18]. Downregulation of glucose transport proteins in response to Glc is not without precedent, and in *E. coli* is one of the molecular mechanisms in the cellular response to prevent phosphosugar stress [66].

Genes involved in glycolysis were not differentially expressed upon Glc addition. Interestingly, Glc repressed the expression of the dedicated GlcNAc-specific catabolic gene *nagB,* but not *nagA* in the same transcriptional unit. Furthermore, only *nagB* was found upregulated in GlcNAc-growth medium (using a Bayesian *p-value* < 0.001) as compared to Glc. Thus, each gene in the *nagAB* operon is subjected to specific regulation.

The direction of the regulation elicited by Glc on Man-adapted cells was in most opposite to that observed in the other conditions studied (Table S3.8). Glc induced the expression of transporters presumably involved in Man uptake (Table S3.8), namely the permeases of the CUT1 ABC transporter SPD_0088-9, the subunits *manLM* of PTS-Man and the subunits IIABD of the mannose-type PTS encoded by SPD_0293-5-7, as well as other sugar transporters (Table S3.8). In addition, Glc induced the expression of the glycolytic genes *gap* and *eno* (Table S3.8). The

expression of the Man-specific catabolic gene, *manA,* was not affected by the Glc stimulus.

Furthermore, a large set of genes which was found upregulated when comparing Man to Glc (*eg*. glycolytic, fermentative and sugar-specific catabolic genes), showed increased fold upregulation in response to the Glc stimulus in Man-adapted cells.

We have shown that Glc hinders the use of Gal (Fig. 3.4) and this observation is fully substantiated by the transcriptional response to Glc in Gal-adapted cells. In Gal-adapted cells Glc downregulated the transporter genes SPD_0559-0-1 and *lacEF-2* (Lac-family PTS) (Table S3.8), which together with the observed upregulation on Gal as compared to Glc-grown cells (Tables 3.1 and S3.8), point towards their involvement on Gal uptake. The latter transporter is found in operon-II of the *lac* gene cluster, which comprises also a 6-phospho β-galactosidase, *lacG-2* (SPD_1046), and the transcriptional activator *lacT* (SPD_ 1049) [46]. While *lacG-2* was not differentially expressed, *lacT* was downregulated by Glc (Table S3.10 on the CD), and so was operon-I encoding the T6P pathway (*lacABCD*). Moreover, Glc downregulated the Leloir genes *galk* and *galT-2,* as well as the transcriptional regulator *galR* (Table S3.8). Our results provide strong evidence supporting the repressing effect of Glc over the catabolism of Gal. Previously, Carvalho *et al*. [27] showed that while CcpA repressed the Leloir genes independently of the carbon source, Gal was an effective inducer of this pathway. On the other hand the T6P pathway was weakly repressed by CcpA on Glc and activated on Gal. In line, Afzal *et al*. [46] could not observe a regulatory effect of CcpA on the *lac* gene cluster. Instead, LacR was the transcriptional repressor of the *lac* operon-I (T6P pathway) on Glc, but not of operon-II, which was under the control of LacT.

For the sugar mix, a negative effect over genes encoding sugar transporters was observed (Table S3.8). The Gal uptake system SPD_0559-0-1 [18,43], the permease proteins of the ABC transporter

SPD_0088-9 (involved in Man and Gal uptake) [18] and the IIBC components of the PTS system (SPD_1496) putatively involved in GlcNAc uptake (Chapter 2) showed altered expression. Furthermore, Glc downregulated genes in Gal catabolic pathways (*lacAB, galk and galT-2*), but had no impact on the expression of genes devoted to the catabolism of GlcNAc and Man. A clustering analysis revealed that Glc had a consistent impact on the N-acetylneuraminic acid processing enzymes: N-acetylmannosamine 6-phosphate 2-epimerase (*nanE-1*) and N-acetylneuraminate lyase, putative (SPD_1163), which were downregulated in all growth conditions except for Man-adapted cells (Table S3.13 and Fig. S3.1). Furthermore, Glc affected the expression of three sugar transporters: the fructose-PTS (SPD_0773) was upregulated in Man and Gal cells, but downregulated in GlcNAc and in the sugar mix, and the PTS proteins SPD_1496 (IIBC components) and SPD_0561 (IIC component) were upregulated on Man, but downregulated on all the other conditions (Table S3.13 and Fig. S3.1). The physiological interpretation of these observations requires further experimentation. Also intriguing is the opposite direction in regulation observed in the presence of Man as compared to the other sugars. While an explanation cannot be put forward, one can speculate that the Man signalling cascade is heavily intertwined with that of Glc, as both sugars are taken up by the Glc/Man-PTS, a well-recognized major player in catabolite control in low-GC Gram-positive bacteria. How the cell discriminates between the two sugars is unknown. From our studies it is clear that the cellular responses to Man (transcriptional and physiological/metabolic) are large and unique, but the underlying molecular mechanisms remain to be elucidated.

The expression profile of classical virulence factors displays a sugar dependency

It is now well accepted that sugar metabolism and virulence are strongly connected, thus contributing in different ways to the pathogenesis of the pneumococcus [20,67]. Therefore, we investigated the influence of the carbohydrates GlcNAc, Man and Gal on the expression of known virulence factors (Tables S3.1 and 3.4). How the ditto virulence factors responded to a Glc stimulus during growth on the different sugars or a sugar mix was also examined (Table 3.4).

A clustering analysis identified only two classical virulence genes as differentially regulated in the three sugars tested, showing that induction of virulence determinants is sugar dependent (Table 3.4 and Fig. S3.2). The immunoglobulin A1 protease precursor (SPD_1018, *iga*) [68] was upregulated in Gal- and Man-containing medium and downregulated in presence of GlcNAc, whereas the serine protease (SPD_2068) [69] gene was upregulated in all growth conditions. Interestingly, Man also induced the expression of DNA-binding response regulator *ciaR*, which was shown to regulate the serine protease. Mutants in both genes show reduced virulence, but in the Δ*ciaR* is most likely due to downregulation of the serine protease [70]. The effect of Glc on the expression of virulence genes was also sugar dependent (Table 3.4). A clustering analysis showed that a single virulence gene was regulated by Glc in all the conditions studied (Table S3.13 and Fig. S3.1). This gene, SPD_0373, which is found in an operon associated to virulence in bacteraemia and pneumonia [71] was downregulated by Glc, except for Man-adapted cells.

Galactose influenced the expression of the largest pool of virulence genes (8.2% of the significantly differential expressed genes), of which 5.5% were upregulated in this sugar (Table 3.4). Of note, the classical virulence factor β-galactosidase (*bgaA*) was highly induced (Table 3.4). Growing evidence supports the role of this gene in early stages of host-

pathogen interactions [72,73]. Moreover, the catabolic genes *lacD* and *galK* were upregulated. We have shown that *lacD* and *galK* mutants are impaired in their ability to colonise the nasopharynx and display attenuated virulence in a respiratory infection murine model, after intranasal challenge (Paixão *et al*., 2015, Chapter 2). Our earlier assumption that Gal metabolism is linked to virulence (Paixão *et al*., 2015, Chapter 2) is further strengthened by the transcriptome data. Interestingly, the expression of *bgaA*, *lacD* and *galK* was downregulated in Gal-adapted cells by Glc (Table 3.4). Other virulence factor genes also negatively regulated by Glc in Gal-adapted cells were *tpx* (thiol peroxidase), and *iga* (immunoglobulin A1 protease precursor). Glc induced the expression of the choline binding protein (*pcpA*), a protein involved in the adherence to nasopharyngeal and lung epithelial cells [74], and virulence determinant in mouse models of pneumonia and sepsis [75,76].

In GlcNAc-grown cells there was upregulation of *strH*, encoding the N-acetylglucosaminidase (Table 3.4). The removal of terminal GlcNAc by StrH from human N-glycans has been implicated in pneumococcal colonisation and pathogenesis, since it can facilitate sugars (GlcNAc) for growth, but it might also promote resistance to opsonophagocytic killing by avoiding complement deposition [37,38,77]. Interestingly, the gene was not downregulated in Glc challenged GlcNAc-adapted cells. In this sugar, all virulence genes responding to the Glc stimulus were downregulated (Table 3.4). Curiously, Glc stimulus repressed genes common to two sugar-adapted conditions (*bgaC, bgaA, pflB, pflA, galK*) (Table 3.4). This observation could indicate that while expressed in colonisation states (glycans as carbon sources), these genes are negatively regulated in conditions where Glc is the predominant sugar, like the blood or inflamed lungs. Thus it is tempting to suggest that while important for colonisation, those functions are not required in invasive disease.

Table 3.4. Significantly differentially expressed virulence factors (up- or downregulated) of cells of *S. pneumoniae* D39 grown in CDM supplemented with N-acetylglucosamine (GlcNAc), mannose (Man) or galactose (Gal) as compared to glucose (Glc) grown cells, or adapted to these single sugars or to a mixture thereof challenged with a Glc pulse and compared to unchallenged cells, determined by DNA microarrays.[a,b]

			Up- or downregulation[c]						
Locus_tag	**Gene**	**Product**	**GlcNAc**		**Man**		**Gal**		**Mix[d]**
			without Glc	with Glc	without Glc	with Glc	without Glc	with Glc	with Glc
SPD_0063	*strH*	beta-N-acetylhexosaminidase	0.43		0.90	1.11			-0.48
SPD_0065	*bgaC*	Beta-galactosidase 3		-0.81		0.64			-1.38
SPD_0126	*pspA*	pneumococcal surface protein A			0.68		0.76	-0.79	-0.50
SPD_0250		pullulanase, extracellular			0.47	1.00	-0.70		
SPD_0373		hypothetical protein SPD_0373		-1.10		0.76	1.43	-1.50	-1.30
SPD_0420	*pflB*	pyruvate formate-lyase		-0.53	1.25	0.70			-0.99
SPD_0558	*prtA*	cell wall-associated serine protease PrtA				0.47	-0.41		
SPD_0562	*bgaA*	beta-galactosidase precursor, putative		-0.33		0.71	1.61	-0.82	
SPD_0634		hypothetical protein SPD_0634	-0.89		-1.24				
SPD_0635		cation-transporting ATPase, E1-E2 family protein			-1.23				
SPD_0667	*sodA*	superoxide dismutase, manganese-dependent						-0.47	
SPD_0701	*ciaR*	DNA-binding response regulator CiaR	0.82		0.57	-0.53			
SPD_0729		hemolysin-related protein			0.44	0.48			
SPD_0853	*lytB*	endo-beta-N-acetylglucosaminidase precursor, putative	0.82						
SPD_0889	*phtD*	pneumococcal histidine triad protein D precursor				0.40			

SPD_1012	*eno*	enolase			0.61	0.33			
SPD_1018	*iga*	immunoglobulin A1 protease precursor	-0.30		0.49	0.48	0.72	-0.63	
SPD_1050	*lacD*	tagatose 1,6-diphosphate aldolase					3.00	-2.02	
SPD_1384		cation efflux family protein				-0.58		0.44	
SPD_1409		sugar ABC transporter, ATP-binding protein		-0.81		0.86	-0.52		-0.68
SPD_1464	*tpx*	thiol peroxidase					0.80	-0.64	-0.47
SPD_1634	*galK*	galactokinase			0.64	0.77	3.30	-1.69	-0.89
SPD_1636		alcohol dehydrogenase, zinc-containing			-0.62				0.69
SPD_1652		iron-compound ABC transporter, iron-compound-binding protein	-0.47			-0.58	-1.16	0.97	
SPD_1726	*ply*	pneumolysin	-0.36		-0.56				
SPD_1774	*pflA*	pyruvate formate-lyase activating enzyme		-0.67		0.73			-0.48
SPD_1797	*ccpA*	catabolite control protein A		-0.60		0.56			
SPD_1823	*gap*	glyceraldehyde-3-phosphate dehydrogenase			0.53	0.39			
SPD_1965	*pcpA*	choline binding protein PcpA				0.28		0.50	
SPD_2068		serine protease	1.06		0.73	-0.92	0.68		

[a] Subset table of Tables S3.2, S3.3, S3.4, S3.9, S3.10, S3.11 and S3.12, all provided on the CD.
[b] As reviewed in Table S3.1.
[c] Values of ln-ratio. Positive values indicate upregulation and negative values indicate downregulation.
[d] Mixture of Gal, Man and GlcNAc.

Induction of *pflB* and the glycolytic genes *eno* and *gap* during growth on Man (Table 3.4) is consistent with their roles in early phases of infection, since Man exists in gycoconjugates. *pflB*, was recently found to contribute to attenuated colonisation of the nasopharynx and lungs and delayed bacteraemia in mice infected intranasally [65], whereas *eno* and *gap* were shown to bind to plasminogen and plasmin, and hence can be of importance for the dissemination of the pathogen through host tissues [78,79]. These genes were still upregulated when Man-adapted cells were spiked with Glc, but the fold-expression values were smaller. Furthermore, expression of the choline binding protein (*pcpA*), of the cell wall-associated serine protease (*prtA*) of several glycosidase genes (*strH*, *bgaC*, *bgaA*) as well as *pflA* and *pflB* were induced by Glc in Man-adapted cells.

In *S. pneumoniae* cells growing on a sugar mix, Glc exerted mainly negative regulation. In addition to the genes mentioned above, the thiol peroxidase (*tpx*) and the pneumococcal surface protein A (p*spA*) were also downregulated. The gene encoding the zinc-containing alcohol dehydrogenase (SPD_1636) was, however, upregulated (Table 3.4). Virulence studies revealed that this gene is implied in survival in the bloodstream [80].

Of all the conditions tested, the smallest transcriptional response elicited by Glc was for cells adapted to the sugar mix (Tables S3.9, S3.10, S3.11 and S3.12, all provided on the CD). Curiously, it was in this condition that the highest fraction of virulence genes influenced by Glc was found (10.4% of the significantly differentially expressed genes) in comparison to 6.3%, 4.8% and 4.4% in GlcNAc-, Man- and Gal-adapted cells, respectively. This result strengthens our hypothesis that cells growing on the sugar mix are better equipped to cope with ever-changing environments. In these cells, a major adaptation is apparently the downregulation of virulence factors important in colonisation niches. Of

note, most of the virulence genes were negatively regulated by a Glc stimulus except in Man-adapted cells for which a significant number of virulence genes were upregulated. The *S. pneumoniae* physiological responses to Man are far from being understood and should be the focus of future research. In light of the transcriptional response to a Glc stimulus during growth on Gal, GlcNAc and the sugar mix, we can speculate that the development of pneumococcal virulence traits occurs in the ecological niche (nasopharynx), during colonisation, where Gal, Man and GlcNAc are prevalent in comparison to free Glc. Disease, on the other hand is accidental, as it culminates in a dead-end for the colonising microorganism, and likely occurs from an imbalance between the host and the microbe. In the disease state, the bacterium represses functions essential for colonisation, but no longer needed when Glc is the predominant substrate for growth. In accordance with this hypothesis, we have shown that pneumococcal mutants in the Gal catabolic genes administrated intravenously were not attenuated in murine models of disease (Paixão *et al.*, 2015, Chapter 2).

Overall, our results show that sugars influence the virulence potential of *S. pneumoniae* D39 both by modulating the expression of specific catabolic pathways (*in vivo* fitness) as well as the expression of classical virulence factors (Table 3.4). Similar findings have been reported for other *Streptococcaceae*, such as *S. mutans* and *S. suis* [81,82]. Indeed, successful infections rely on colonisation, multiplication and transmission to a new host, and therefore the line between factors required for growth and virulence determinants is blurred [5,6].

Conclusions

In this work we have conducted a systems approach to evaluate the *S. pneumoniae* response to sugar availability. The combined transcriptional, physiological and metabolic data collected revealed a strong carbohydrate-dependency on the phenotypic traits of *S. pneumoniae*. Despite the relatively simple metabolism of *S. pneumoniae*, which processes sugars through the Embden-Meyerhof-Parnas pathway to pyruvate, the transcriptional and metabolic responses elicited by each monosaccharide are remarkable and specific. This is especially relevant considering that generally this bacterium resides in the human nasopharynx, an environment poor in Glc, but rich in glycans. But during progression to disease and in disease states *S. pneumoniae* is subjected to changing environments that presumably are enriched in Glc. Our results firmly show that Glc is a preferential substrate for growth of *S. pneumoniae* and while growing on other sugars the bacterium avidly uses Glc when available. The specific response to the Glc stimulus results in changes both at the metabolic level (Figs. 3.4 and 3.5) and in gene regulation (Table S3.8), which allow for short and long term adaptation. Interestingly, cells adapted for growth on a sugar mixture displayed the smallest transcriptional response to Glc, suggesting improved metabolic resilience of *S. pneumoniae* when exposed to a multitude of sugars. In the human nasopharynx, *S. pneumoniae* is exposed to a fluctuating nutritional milieu that results from a fragile balance between varied factors (host, microbiota, environmental stimulus). In addition, deglycosylation of human glycans by bacterial glycosidases generates a varied sugar mixture. In the context of our observations, exposure to such a diverse environment improves the fitness of *S. pneumoniae*.

Carbohydrates specifically modulate the expression of virulence genes, thus influencing the virulence potential of the pneumococcus. We

suggest that the nasopharynx is the reservoir for the development of niche-specific virulence traits, essential for successful colonisation of the niche. Most of these virulence factors are downregulated by a Glc stimulus, and are therefore not required in disease. Collectively, our data strengthens the link between sugar metabolism and virulence. Indeed, effective infections rely on colonisation, multiplication and transmission to a new host, and therefore factors required for growth are also virulence determinants.

The “omic” data collected at different regulatory layers can in the future be used to fuel multi-scale mathematical models. Such mathematical representation of metabolism hopefully will contribute to deepen our understanding of how a functional state arises from the components, and ultimately will facilitate the identification of novel targets for alternative therapeutic and preventive drugs.

Acknowledgements

This work was supported by Fundação para a Ciência e a Tecnologia, Portugal (FCT) and FEDER, project PTDC/SAU-MII/100964/2008, and through grants PEst-OE/EQB/LA0004/2011. L. Paixão acknowledges FCT for the award of Ph.D. grant SFRH/BD/46997/2008. The NMR spectrometers are part of The National NMR Facility, supported by Fundação para a Ciência e a Tecnologia (RECI/BBB-BQB/0230/2012). Ana Lúcia Carvalho is acknowledged for assistance with *in vivo* NMR experiments. Joana Oliveira is acknowledged for her contribution with the the growth experiments.

Author's contribution

L. Paixão contributed to the design of all the experiments. She performed and analysed experiments as follows:

Growth Experiments:

Performed: L. Paixão

Quantification of end-products formation and sugar consumption by HPLC and NMR: L. Paixão

Estimation of growth and energetic parameters: L. Paixão

Transcriptome analysis:

Performed the growth experiments and harvested samples: L. Paixão

Performed the microarrays: T.G. Kloosterman

Analysed: T.G. Kloosterman, J. Caldas, L. Paixão

***In vivo* ^{13}C- NMR:**

Performed: L. Paixão

Analysed: L. Paixão

All authors contributed to the critical reading of this Chapter.

References

1. Giammarinaro P, Paton JC. Role of RegM, a homologue of the catabolite repressor protein CcpA, in the virulence of *Streptococcus pneumoniae*. Infect Immun. 2002;70: 5454–5461.
2. Bogaert D, de Groot R, Hermans P. *Streptococcus pneumoniae* colonisation: the key to pneumococcal disease. Lancet Infect Dis. 2004;4: 144–154. doi:10.1016/S1473-3099(04)00938-7
3. Kadioglu A, Weiser JN, Paton JC, Andrew PW. The role of *Streptococcus pneumoniae* virulence factors in host respiratory colonization and disease. Nat Rev Microbiol. 2008;6: 288–301. doi:10.1038/nrmicro1871
4. King SJ. Pneumococcal modification of host sugars: a major contributor to colonization of the human airway? Mol Oral Microbiol. 2010;25: 15–24. doi:10.1111/j.2041-1014.2009.00564.x
5. Hava DL, LeMieux J, Camilli A. From nose to lung: the regulation behind *Streptococcus pneumoniae* virulence factors: Virulence gene regulation in *S.*

pneumoniae. Mol Microbiol. 2003;50: 1103–1110. doi:10.1046/j.1365-2958.2003.03764.x
6. Weiser JN. The pneumococcus: why a commensal misbehaves. J Mol Med Berl. 2010;88: 97–102. doi:10.1007/s00109-009-0557-x
7. Ogunniyi AD, Mahdi LK, Trappetti C, Verhoeven N, Mermans D, Van der Hoek MB, et al. Identification of genes that contribute to the pathogenesis of invasive pneumococcal disease by in vivo transcriptomic analysis. Infect Immun. 2012;80: 3268–3278. doi:10.1128/IAI.00295-12
8. Obaro S, Adegbola R. The pneumococcus: carriage, disease and conjugate vaccines. J Med Microbiol. 2002;51: 98–104.
9. Orihuela CJ, Radin JN, Sublett JE, Gao G, Kaushal D, Tuomanen EI. Microarray analysis of pneumococcal gene expression during invasive disease. Infect Immun. 2004;72: 5582–5596. doi:10.1128/IAI.72.10.5582-5596.2004
10. Orihuela CJ, Janssen R, Robb CW, Watson DA, Niesel DW. Peritoneal culture alters *Streptococcus pneumoniae* protein profiles and virulence properties. Infect Immun. 2000;68: 6082–6086.
11. Mahdi LK, Ogunniyi AD, LeMessurier KS, Paton JC. Pneumococcal virulence gene expression and host cytokine profiles during pathogenesis of invasive disease. Infect Immun. 2008;76: 646–657. doi:10.1128/IAI.01161-07
12. LeMessurier KS. Differential expression of key pneumococcal virulence genes in vivo. Microbiology. 2006;152: 305–311. doi:10.1099/mic.0.28438-0
13. Ogunniyi AD, Grabowicz M, Mahdi LK, Cook J, Gordon DL, Sadlon TA, et al. Pneumococcal histidine triad proteins are regulated by the Zn^{2+}-dependent repressor AdcR and inhibit complement deposition through the recruitment of complement factor H. FASEB J. 2009;23: 731–738. doi:10.1096/fj.08-119537
14. Ogunniyi AD, Giammarinaro P, Paton JC. The genes encoding virulence-associated proteins and the capsule of *Streptococcus pneumoniae* are upregulated and differentially expressed in vivo. Microbiology. 2002;148: 2045–2053.
15. Shafeeq S, Kuipers OP, Kloosterman TG. The role of zinc in the interplay between pathogenic streptococci and their hosts: Zinc homeostasis in pathogenic streptococci. Mol Microbiol. 2013;88: 1047–1057. doi:10.1111/mmi.12256
16. Honsa ES, Johnson MDL, Rosch JW. The roles of transition metals in the physiology and pathogenesis of *Streptococcus pneumoniae*. Front Cell Infect Microbiol. 2013;3: 92. doi:10.3389/fcimb.2013.00092
17. Tettelin H, Nelson KE, Paulsen IT, Eisen JA, Read TD, Peterson S, et al. Complete genome sequence of a virulent isolate of *Streptococcus pneumoniae*. Science. 2001;293: 498–506. doi:10.1126/science.1061217
18. Bidossi A, Mulas L, Decorosi F, Colomba L, Ricci S, Pozzi G, et al. A functional genomics approach to establish the complement of carbohydrate transporters in *Streptococcus pneumoniae*. Miyaji EN, editor. PLoS ONE. 2012;7: e33320. doi:10.1371/journal.pone.0033320
19. Paulsen IT, Nguyen L, Sliwinski MK, Rabus R, Saier MH. Microbial genome analyses: comparative transport capabilities in eighteen prokaryotes. J Mol Biol. 2000;301: 75–100. doi:10.1006/jmbi.2000.3961
20. Shelburne SA, Davenport MT, Keith DB, Musser JM. The role of complex carbohydrate catabolism in the pathogenesis of invasive streptococci. Trends Microbiol. 2008;16: 318–325. doi:10.1016/j.tim.2008.04.002

21. Philips BJ, Meguer J-X, Redman J, Baker EH. Factors determining the appearance of glucose in upper and lower respiratory tract secretions. Intensive Care Med. 2003;29: 2204–2210. doi:10.1007/s00134-003-1961-2
22. Claverys JP, Prudhomme M, Mortier-Barrière I, Martin B. Adaptation to the environment: *Streptococcus pneumoniae*, a paradigm for recombination-mediated genetic plasticity? Mol Microbiol. 2000;35: 251–259.
23. Donati C, Hiller NL, Tettelin H, Muzzi A, Croucher NJ, Angiuoli SV, et al. Structure and dynamics of the pan-genome of *Streptococcus pneumoniae* and closely related species. Genome Biol. 2010;11: R107. doi:10.1186/gb-2010-11-10-r107
24. Titgemeyer F, Hillen W. Global control of sugar metabolism: a gram-positive solution. Antonie Van Leeuwenhoek. 2002;82: 59–71.
25. Deutscher J. The mechanisms of carbon catabolite repression in bacteria. Curr Opin Microbiol. 2008;11: 87–93. doi:10.1016/j.mib.2008.02.007
26. Görke B, Stülke J. Carbon catabolite repression in bacteria: many ways to make the most out of nutrients. Nat Rev Microbiol. 2008;6: 613–624. doi:10.1038/nrmicro1932
27. Carvalho SM, Kloosterman TG, Kuipers OP, Neves AR. CcpA ensures optimal metabolic fitness of *Streptococcus pneumoniae*. Horsburgh MJ, editor. PLoS ONE. 2011;6: e26707. doi:10.1371/journal.pone.0026707
28. Carvalho SM, Kuipers OP, Neves AR. Environmental and nutritional factors that affect growth and metabolism of the pneumococcal serotype 2 strain D39 and its nonencapsulated derivative strain R6. Horsburgh MJ, editor. PLoS ONE. 2013;8: e58492. doi:10.1371/journal.pone.0058492
29. Kloosterman TG, Hendriksen WT, Bijlsma JJE, Bootsma HJ, van Hijum SAFT, Kok J, et al. Regulation of glutamine and glutamate metabolism by GlnR and GlnA in *Streptococcus pneumoniae*. J Biol Chem. 2006;281: 25097–25109. doi:10.1074/jbc.M601661200
30. Van Hijum SAFT, de Jong A, Baerends RJS, Karsens HA, Kramer NE, Larsen R, et al. A generally applicable validation scheme for the assessment of factors involved in reproducibility and quality of DNA-microarray data. BMC Genomics. 2005;6: 77. doi:10.1186/1471-2164-6-77
31. Neves AR, Ramos A, Nunes MC, Kleerebezem M, Hugenholtz J, de Vos WM, et al. In vivo nuclear magnetic resonance studies of glycolytic kinetics in *Lactococcus lactis*. Biotechnol Bioeng. 1999;64: 200–212.
32. Neves AR. Is the Glycolytic Flux in Lactococcus lactis Primarily Controlled by the Redox Charge? kinetics of NAD^+ and NADH pools determined in vivo by ^{13}C NMR. J Biol Chem. 2002;277: 28088–28098. doi:10.1074/jbc.M202573200
33. Ramos-Montañez S, Kazmierczak KM, Hentchel KL, Winkler ME. Instability of ackA (acetate kinase) mutations and their effects on acetyl phosphate and ATP amounts in *Streptococcus pneumoniae* D39. J Bacteriol. 2010;192: 6390–6400. doi:10.1128/JB.00995-10
34. Cote CK, Cvitkovitch D, Bleiweis AS, Honeyman AL. A novel beta-glucoside-specific PTS locus from *Streptococcus mutans* that is not inhibited by glucose. Microbiol Read Engl. 2000;146 (Pt 7): 1555–1563.
35. McKessar SJ, Hakenbeck R. The two-component regulatory system TCS08 is involved in cellobiose metabolism of *Streptococcus pneumoniae* R6. J Bacteriol. 2007;189: 1342–1350. doi:10.1128/JB.01170-06

36. Moye ZD, Burne RA, Zeng L. Uptake and metabolism of N-acetylglucosamine and glucosamine by *Streptococcus mutans*. Appl Env Microbiol. 2014; doi:10.1128/AEM.00820-14
37. Burnaugh AM, Frantz LJ, King SJ. Growth of *Streptococcus pneumoniae* on human glycoconjugates is dependent upon the sequential activity of bacterial exoglycosidases. J Bacteriol. 2008;190: 221–230. doi:10.1128/JB.01251-07
38. King SJ, Hippe KR, Weiser JN. Deglycosylation of human glycoconjugates by the sequential activities of exoglycosidases expressed by *Streptococcus pneumoniae*. Mol Microbiol. 2006;59: 961–974. doi:10.1111/j.1365-2958.2005.04984.x
39. Marion C, Burnaugh AM, Woodiga SA, King SJ. Sialic acid transport contributes to pneumococcal colonization. Infect Immun. 2011;79: 1262–1269. doi:10.1128/IAI.00832-10
40. Heinemann M, Sauer U. Systems biology of microbial metabolism. Curr Opin Microbiol. 2010;13: 337–343. doi:10.1016/j.mib.2010.02.005
41. Andersen HW, Solem C, Hammer K, Jensen PR. Twofold reduction of phosphofructokinase activity in *Lactococcus lactis* results in strong decreases in growth rate and in glycolytic flux. J Bacteriol. 2001;183: 3458–3467. doi:10.1128/JB.183.11.3458-3467.2001
42. Vanderpool CK, Gottesman S. The novel transcription factor SgrR coordinates the response to glucose-phosphate stress. J Bacteriol. 2007;189: 2238–2248. doi:10.1128/JB.01689-06
43. Kaufman GE, Yother J. CcpA-dependent and -independent control of beta-galactosidase expression in *Streptococcus pneumoniae* occurs via regulation of an upstream phosphotransferase system-encoding operon. J Bacteriol. 2007;189: 5183–5192. doi:10.1128/JB.00449-07
44. Neves AR, Pool WA, Solopova A, Kok J, Santos H, Kuipers OP. Towards enhanced galactose utilization by *Lactococcus lactis*. Appl Env Microbiol. 2010;76: 7048–7060. doi:10.1128/AEM.01195-10
45. Zeng L, Das S, Burne RA. Utilization of lactose and galactose by *Streptococcus mutans*: transport, toxicity, and carbon catabolite repression. J Bacteriol. 2010;192: 2434–2444. doi:10.1128/JB.01624-09
46. Afzal M, Shafeeq S, Kuipers OP. LacR is a repressor of *lacABCD* and LacT an activator of *lacTFEG*, constituting the lac-gene cluster in *Streptococcus pneumoniae*. Appl Environ Microbiol. 2014; doi:10.1128/AEM.01370-14
47. De Vin F, Radstrom P, Herman L, De Vuyst L. Molecular and biochemical analysis of the galactose phenotype of dairy *Streptococcus thermophilus* strains reveals four different fermentation profiles. Appl Environ Microbiol. 2005;71: 3659–3667. doi:10.1128/AEM.71.7.3659-3667.2005
48. Vaillancourt K, Moineau S, Frenette M, Lessard C, Vadeboncoeur C. Galactose and lactose genes from the galactose-positive bacterium *Streptococcus salivarius* and the phylogenetically related galactose-negative bacterium *Streptococcus thermophilus*: organization, sequence, transcription, and activity of the gal gene products. J Bacteriol. 2002;184: 785–793. doi:10.1128/JB.184.3.785-793.2002
49. Ajdić D, Ferretti JJ. Transcriptional regulation of the *Streptococcus mutans* gal operon by the GalR repressor. J Bacteriol. 1998;180: 5727–5732.

50. Vaughan EE, van den Bogaard PTC, Catzeddu P, Kuipers OP, de Vos WM. Activation of silent gal genes in the lac-gal regulon of *Streptococcus thermophilus*. J Bacteriol. 2001;183: 1184–1194. doi:10.1128/JB.183.4.1184-1194.2001
51. Vaillancourt K, LeMay J-D, Lamoureux M, Frenette M, Moineau S, Vadeboncoeur C. Characterization of a galactokinase-positive recombinant strain of *Streptococcus thermophilus*. Appl Environ Microbiol. 2004;70: 4596–4603. doi:10.1128/AEM.70.8.4596-4603.2004
52. Abranches J, Nascimento MM, Zeng L, Browngardt CM, Wen ZT, Rivera MF, et al. CcpA regulates central metabolism and virulence gene expression in *Streptococcus mutans*. J Bacteriol. 2008;190: 2340–2349. doi:10.1128/JB.01237-07
53. Melchiorsen CR, Jokumsen KV, Villadsen J, Johnsen MG, Israelsen H, Arnau J. Synthesis and posttranslational regulation of pyruvate formate-lyase in *Lactococcus lactis*. J Bacteriol. 2000;182: 4783–4788. doi:10.1128/JB.182.17.4783-4788.2000
54. Garrigues C, Loubiere P, Lindley ND, Cocaign-Bousquet M. Control of the shift from homolactic acid to mixed-acid fermentation in *Lactococcus lactis*: predominant role of the NADH/NAD+ ratio. J Bacteriol. 1997;179: 5282–5287.
55. Neves AR, Ramos A, Costa H, van Swam II, Hugenholtz J, Kleerebezem M, et al. Effect of different NADH oxidase levels on glucose metabolism by *Lactococcus lactis*: kinetics of intracellular metabolite pools determined by In vivo nuclear magnetic resonance. Appl Environ Microbiol. 2002;68: 6332–6342. doi:10.1128/AEM.68.12.6332-6342.2002
56. Ramos A, Neves AR, Ventura R, Maycock C, López P, Santos H. Effect of pyruvate kinase overproduction on glucose metabolism of *Lactococcus lactis*. Microbiol Read Engl. 2004;150: 1103–1111.
57. Neves A, Pool W, Kok J, Kuipers O, Santos H. Overview on sugar metabolism and its control in – The input from in vivo NMR. FEMS Microbiol Rev. 2005;29: 531–554. doi:10.1016/j.femsre.2005.04.005
58. Carvalho AL, Cardoso FS, Bohn A, Neves AR, Santos H. Engineering trehalose synthesis in *Lactococcus lactis* for improved stress tolerance. Appl Environ Microbiol. 2011;77: 4189–4199. doi:10.1128/AEM.02922-10
59. Neves AR, Ramos A, Shearman C, Gasson MJ, Santos H. Catabolism of mannitol in *Lactococcus lactis* MG1363 and a mutant defective in lactate dehydrogenase. Microbiol Read Engl. 2002;148: 3467–3476.
60. Neves AR, Pool WA, Castro R, Mingote A, Santos F, Kok J, et al. The alpha-phosphoglucomutase of *Lactococcus lactis* is unrelated to the alpha-D-phosphohexomutase superfamily and is encoded by the essential gene *pgmH*. J Biol Chem. 2006;281: 36864–36873. doi:10.1074/jbc.M607044200
61. Fang W, Yu X, Wang B, Zhou H, Ouyang H, Ming J, et al. Characterization of the *Aspergillus fumigatus* phosphomannose isomerase Pmi1 and its impact on cell wall synthesis and morphogenesis. Microbiol Read Engl. 2009;155: 3281–3293. doi:10.1099/mic.0.029975-0
62. Pitkänen J-P, Törmä A, Alff S, Huopaniemi L, Mattila P, Renkonen R. Excess mannose limits the growth of phosphomannose isomerase PMI40 deletion strain of *Saccharomyces cerevisiae*. J Biol Chem. 2004;279: 55737–55743. doi:10.1074/jbc.M410619200
63. Sasaki M, Teramoto H, Inui M, Yukawa H. Identification of mannose uptake and catabolism genes in *Corynebacterium glutamicum* and genetic engineering for

simultaneous utilization of mannose and glucose. Appl Microbiol Biotechnol. 2011;89: 1905–1916. doi:10.1007/s00253-010-3002-8

64. Castro R, Neves AR, Fonseca LL, Pool WA, Kok J, Kuipers OP, et al. Characterization of the individual glucose uptake systems of *Lactococcus lactis*: mannose-PTS, cellobiose-PTS and the novel GlcU permease. Mol Microbiol. 2009;71: 795–806. doi:10.1111/j.1365-2958.2008.06564.x
65. Yesilkaya H, Spissu F, Carvalho SM, Terra VS, Homer KA, Benisty R, et al. Pyruvate formate lyase is required for pneumococcal fermentative metabolism and virulence. Infect Immun. 2009;77: 5418–5427. doi:10.1128/IAI.00178-09
66. Vanderpool CK. Physiological consequences of small RNA-mediated regulation of glucose-phosphate stress. Curr Opin Microbiol. 2007;10: 146–151. doi:10.1016/j.mib.2007.03.011
67. Iyer R, Camilli A. Sucrose metabolism contributes to in vivo fitness of *Streptococcus pneumoniae*. Mol Microbiol. 2007;66: 1–13. doi:10.1111/j.1365-2958.2007.05878.x
68. Poulsen K, Reinholdt J, Kilian M. Characterization of the *Streptococcus pneumoniae* immunoglobulin A1 protease gene (iga) and its translation product. Infect Immun. 1996;64: 3957–3966.
69. Sebert ME, Palmer LM, Rosenberg M, Weiser JN. Microarray-based identification of *htrA*, a *Streptococcus pneumoniae* gene that is regulated by the CiaRH two-component system and contributes to nasopharyngeal colonization. Infect Immun. 2002;70: 4059–4067. doi:10.1128/IAI.70.8.4059-4067.2002
70. Ibrahim YM, Kerr AR, McCluskey J, Mitchell TJ. Control of virulence by the two-component system CiaR/H is mediated via HtrA, a major virulence factor of *Streptococcus pneumoniae*. J Bacteriol. 2004;186: 5258–5266. doi:10.1128/JB.186.16.5258-5266.2004
71. Paterson GK, Blue CE, Mitchell TJ. An operon in *Streptococcus pneumoniae* containing a putative alkylhydroperoxidase D homologue contributes to virulence and the response to oxidative stress. Microb Pathog. 2006;40: 152–160. doi:10.1016/j.micpath.2005.12.003
72. Limoli DH, Sladek JA, Fuller LA, Singh AK, King SJ. BgaA acts as an adhesin to mediate attachment of some pneumococcal strains to human epithelial cells. Microbiology. 2011;157: 2369–2381. doi:10.1099/mic.0.045609-0
73. Song X-M, Connor W, Hokamp K, Babiuk LA, Potter AA. *Streptococcus pneumoniae* early response genes to human lung epithelial cells. BMC Res Notes. 2008;1: 64. doi:10.1186/1756-0500-1-64
74. Khan MN, Sharma SK, Filkins LM, Pichichero ME. PcpA of *Streptococcus pneumoniae* mediates adherence to nasopharyngeal and lung epithelial cells and elicits functional antibodies in humans. Microbes Infect Inst Pasteur. 2012;14: 1102–1110. doi:10.1016/j.micinf.2012.06.007
75. Johnston JW, Briles DE, Myers LE, Hollingshead SK. Mn^{2+}-dependent regulation of multiple genes in *Streptococcus pneumoniae* through PsaR and the resultant impact on virulence. Infect Immun. 2006;74: 1171–1180. doi:10.1128/IAI.74.2.1171-1180.2006
76. Glover DT, Hollingshead SK, Briles DE. *Streptococcus pneumoniae* surface protein PcpA elicits protection against lung infection and fatal sepsis. Infect Immun. 2008;76: 2767–2776. doi:10.1128/IAI.01126-07

77. Dalia AB, Standish AJ, Weiser JN. Three surface exoglycosidases from *Streptococcus pneumoniae*, NanA, BgaA, and StrH, promote resistance to opsonophagocytic killing by human neutrophils. Infect Immun. 2010;78: 2108–2116. doi:10.1128/IAI.01125-09
78. Bergmann S, Rohde M, Chhatwal GS, Hammerschmidt S. alpha-enolase of *Streptococcus pneumoniae* is a plasmin(ogen)-binding protein displayed on the bacterial cell surface. Mol Microbiol. 2001;40: 1273–1287.
79. Bergmann S, Rohde M, Hammerschmidt S. Glyceraldehyde-3-phosphate dehydrogenase of *Streptococcus pneumoniae* is a surface-displayed plasminogen-binding protein. Infect Immun. 2004;72: 2416–2419. doi:10.1128/IAI.72.4.2416-2419.2004
80. Stroeher UH, Kidd SP, Stafford SL, Jennings MP, Paton JC, McEwan AG. A pneumococcal MerR-like regulator and S-nitrosoglutathione reductase are required for systemic virulence. J Infect Dis. 2007;196: 1820–1826. doi:10.1086/523107
81. Moye ZD, Zeng L, Burne RA. Modification of gene expression and virulence traits in *Streptococcus mutans* in response to carbohydrate availability. Appl Environ Microbiol. 2014;80: 972–985. doi:10.1128/AEM.03579-13
82. Ferrando ML, van Baarlen P, Orrù G, Piga R, Bongers RS, Wels M, et al. Carbohydrate availability regulates virulence gene expression in *Streptococcus suis*. Kreth J, editor. PLoS ONE. 2014;9: e89334. doi:10.1371/journal.pone.0089334

Supporting Information_Chapter 3

Supporting Tables

Table S3.1. Virulence factors of *Streptococcus pneumoniae*.

TIGR4 locus_tag	D39 locus_tag	Gene name	Gene annotation_D39 (as described in NCBI)	References
SP2190	SPD_2017	*cbpA*	choline binding protein A	[1–3]
SP1693	SPD_1504	*nanA*	sialidase A	[1–4]
SP0648	SPD_0562	*bgaA*	beta-galactosidase	[1]
SP0057	SPD_0063	*strH*	beta-N-acetylhexosaminidase	[1]
SP0314	SPD_0287		hyaluronate lyase	[1–3]
SP0966	SPD_0854	*pavA*	adherence and virulence protein A	[1–3,5]
SP1128	SPD_1012	*eno*	phosphopyruvate hydratase (enolase)	[1,6]
SP1923	SPD_1726	*ply*	pneumolysin	[1–3,7]
SP0117	SPD_0126	*pspA*	surface protein A	[1–3,8]
SP1937	SPD_1737	*lytA*	autolysin/N-acetylmuramoyl-L-alanine amidase	[1–3,8,9]
SP1650	SPD_1463		ABC transporter substrate-binding protein	[1,3,10–12]
SP1032	SPD_0915		iron-compound ABC transporter iron compound-binding protein	[1,10,13,14]
SP1872	SPD_1652		iron-compound ABC transporter,iron-compound-binding protein	[1,10,13,14]
SP1687	SPD_1499	*nanB*	neuraminidase B	[1,4]
SP1154	SPD_1018	*iga*	immunoglobulin A1 protease precursor	[1,15]
SP0641	SPD_0558	*prtA*	cell wall-associated serine protease PrtA	[2,3,16]
SP1638	SPD_1450		iron-dependent transcriptional regulator	[10,17]
SP0766	SPD_0667	*sodA*	superoxide dismutase, manganese-dependent	[10,18]
SP1552	SPD_1384		cation efflux family protein	[10,19]
SP0240	SPD_0222		phosphoglycerate mutase family protein	[10,13]
SP0376	SPD_0344		DNA-binding response regulator	[10,20,21]
SP0728	SPD_0634		conserved hypothetical protein	[10,22]
SP0729	SPD_0635		cation-transporting ATPase, E1-E2 family protein	[10,22]
SP2170	SPD_1998	*adcB*	zinc ABC transporter, permease	[10,23]
SP1853	SPD_1634	*galk*	galactokinase	Chapter 2, Paixão *et al*., 2015
SP1190	SPD_1050	*lacD*	tagatose 1,6-diphosphate aldolase	Chapter 2, Paixão *et al*., 2015
SP1651	SPD_1464	*tpx*	thiol peroxidase	[24]
SP0746	SPD_0650	*clpP*	ATP-dependent Clp protease, proteolytic subunit ClpP	[25–27]

TIGR4 locus_tag	D39 locus_tag	Gene name	Gene annotation_D39 (as described in NCBI)	References
SP0060	SPD_0065	*bgaC*	Beta-galactosidase 3	[28]
SP0082	SPD_0080		cell wall surface anchor family protein	[29]
SP0340	SPD_0309	*luxS*	S-ribosylhomocysteinase	[30]
SP0409	SPD_0373		hypothetical protein	[31]
SP0459	SPD_0420	*pflB*	formate acetyltransferase	[32]
SP0834	SPD_0729		hemolysin-related protein	[33]
SP0908	SPD_0802		S1 RNA-binding domain-containing protein	[34]
SP1161	SPD_1025	*lpdA*	dihydrolipoamide dehydrogenase	[35]
SP1241	SPD_1098		amino acid ABC transporter amino acid-binding protein/permease	[36,37]
SP1795	SPD_1582		sucrose-6-phosphate hydrolase	[38]
SP1999	SPD_1797	*ccpA*	catabolite control protein A	[38,39]
SP2136	SPD_1965	*pcpA*	choline binding protein PcpA	[17,40,41]
SP0268	SPD_0250		pullulanase, extracellular	[42,43]
SP0927	SPD_0818		transcriptional regulator, LysR family protein	[25,44]
SP0390	SPD_0356	*cbpG*	pseudo	[45]
SP0730	SPD_0636	*spxB*	pyruvate oxidase	[46,47]
SP0965	SPD_0853	*lytB*	endo-beta-N-acetylglucosaminidase	[2,45]
SP1573	SPD_1403	*lytC*	1,4-beta-N-acetylmuramidase	[2,45]
SP0930	SPD_0821	*cbpE*	choline binding protein E	[2,45]
SP2201	SPD_2028	*cbpD*	choline binding protein D	[2,45]
Sp1175	SPD_1038	*phpA*	histidine triad protein A	[40,48,49]
Sp1174	SPD_1037		histidine triad protein	[40,48,49]
sp1003	SPD_0889	*phtD*	histidine triad protein D	[40,48,49]
SP0664	SPD_0577	*zmpB*	zinc metalloprotease Zmp	[50]
SP0330	SPD_0301	*regR*	sugar binding transcriptional regulator RegR	[51]
SP2236	SPD_2064	*comD*	sensor histidine kinase ComD	[44,52]
SP0798	SPD_0701	*ciaR*	DNA-binding response regulator CiaR	[53,54]
SP1855	SPD_1636		zinc-containing alcohol dehydrogenase	[55]
SP1976	SPD_1774	*pflA*	pyruvate formate-lyase activating enzyme	[32]
sp2239	SPD_2068		serine protease	[40,56]
SP1580	SPD_1409		sugar ABC transporter ATP-binding protein	[57,58]
SP2012	SPD_1823	*gap*	glyceraldehyde 3-phosphate dehydrogenase	[2,59]

References

1. Kadioglu A, Weiser JN, Paton JC, Andrew PW (2008) The role of *Streptococcus pneumoniae* virulence factors in host respiratory colonization and disease. Nat Rev Microbiol 6: 288–301.
2. Mitchell AM, Mitchell TJ (2010) *Streptococcus pneumoniae*: virulence factors and variation. Clin Microbiol Infect 16: 411–418.
3. Nieto PA, Riquelme SA, Riedel CA, Kalergis AM, Bueno SM (2013) Gene elements that regulate *Streptococcus pneumoniae* virulence and immunity evasion. Curr Gene Ther 13: 51–64.
4. Manco S, Hernon F, Yesilkaya H, Paton JC, Andrew PW, et al. (2006) Pneumococcal neuraminidases A and B both have essential roles during infection of the Rrespiratory tract and sepsis. Infect Immun 74: 4014–4020.
5. Holmes AR, McNab R, Millsap KW, Rohde M, Hammerschmidt S, et al. (2001) The pavA gene of *Streptococcus pneumoniae* encodes a fibronectin-binding protein that is essential for virulence. Mol Microbiol 41: 1395–1408.
6. Bergmann S, Rohde M, Chhatwal GS, Hammerschmidt S (2001) alpha-enolase of *Streptococcus pneumoniae* is a plasmin(ogen)-binding protein displayed on the bacterial cell surface. Mol Microbiol 40: 1273–1287.
7. Berry AM, Yother J, Briles DE, Hansman D, Paton JC (1989) Reduced virulence of a defined pneumolysin-negative mutant of *Streptococcus pneumoniae.* Infect Immun 57: 2037–2042.
8. Berry AM, Paton JC (2000) Additive attenuation of virulence of *Streptococcus pneumoniae* by mutation of the genes encoding pneumolysin and other putative pneumococcal virulence proteins. Infect Immun 68: 133–140.
9. Orihuela CJ, Gao G, Francis KP, Yu J, Tuomanen EI (2004) Tissue-specific contributions of pneumococcal virulence factors to pathogenesis. J Infect Dis 190: 1661–1669.
10. Honsa ES, Johnson MDL, Rosch JW (2013) The roles of transition metals in the physiology and pathogenesis of *Streptococcus pneumoniae*. Front Cell Infect Microbiol 3: 92.
11. Berry AM, Paton JC (1996) Sequence heterogeneity of PsaA, a 37-kilodalton putative adhesin essential for virulence of *Streptococcus pneumoniae*. Infect Immun 64: 5255–5262.
12. Marra A, Lawson S, Asundi JS, Brigham D, Hromockyj AE (2002) In vivo characterization of the psa genes from *Streptococcus pneumoniae* in multiple models of infection. Microbiology 148: 1483–1491.
13. Brown JS, Gilliland SM, Ruiz-Albert J, Holden DW (2002) Characterization of Pit, a *Streptococcus pneumoniae* iron uptake ABC transporter. Infect Immun 70: 4389–4398.
14. Brown JS, Gilliland SM, Holden DW (2001) A *Streptococcus pneumoniae* pathogenicity island encoding an ABC transporter involved in iron uptake and virulence. Mol Microbiol 40: 572–585.
15. Poulsen K, Reinholdt J, Kilian M (1996) Characterization of the *Streptococcus pneumoniae* immunoglobulin A1 protease gene (iga) and its translation product. Infect Immun 64: 3957–3966.

16. Bethe G, Nau R, Wellmer A, Hakenbeck R, Reinert RR, et al. (2001) The cell wall-associated serine protease PrtA: a highly conserved virulence factor of Streptococcus pneumoniae. FEMS Microbiol Lett 205: 99–104.
17. Johnston JW, Briles DE, Myers LE, Hollingshead SK (2006) Mn2+-dependent regulation of multiple genes in *Streptococcus pneumoniae* through PsaR and the resultant impact on virulence. Infect Immun 74: 1171–1180.
18. Yesilkaya H, Kadioglu A, Gingles N, Alexander JE, Mitchell TJ, et al. (2000) Role of manganese-containing superoxide dismutase in oxidative stress and virulence of *Streptococcus pneumoniae*. Infect Immun 68: 2819–2826.
19. Rosch JW, Gao G, Ridout G, Wang Y-D, Tuomanen EI (2009) Role of the manganese efflux system mntE for signalling and pathogenesis in *Streptococcus pneumoniae*: Role of the manganese efflux system mntE. Mol Microbiol 72: 12–25.
20. Ulijasz AT, Andes DR, Glasner JD, Weisblum B (2004) Regulation of iron transport in *Streptococcus pneumoniae* by RitR, an orphan response regulator. J Bacteriol 186: 8123–8136.
21. Throup JP, Koretke KK, Bryant AP, Ingraham KA, Chalker AF, et al. (2000) A genomic analysis of two-component signal transduction in *Streptococcus pneumoniae*. Mol Microbiol 35: 566–576.
22. Shafeeq S, Yesilkaya H, Kloosterman TG, Narayanan G, Wandel M, et al. (2011) The cop operon is required for copper homeostasis and contributes to virulence in *Streptococcus pneumoniae*. Mol Microbiol 81: 1255–1270.
23. McDevitt CA, Ogunniyi AD, Valkov E, Lawrence MC, Kobe B, et al. (2011) A Molecular mechanism for bacterial susceptibility to zinc. PLoS Pathog 7: e1002357.
24. Hajaj B, Yesilkaya H, Benisty R, David M, Andrew PW, et al. (2012) Thiol peroxidase is an important component of *Streptococcus pneumoniae* in oxygenated environments. Infect Immun 80: 4333–4343.
25. Mahdi LK, Ebrahimie E, Adelson DL, Paton JC, Ogunniyi AD (2013) A transcription factor contributes to pathogenesis and virulence in *Streptococcus pneumoniae*. PLoS ONE 8: e70862.
26. Robertson GT, Ng W-L, Foley J, Gilmour R, Winkler ME (2002) Global transcriptional analysis of clpP mutations of type 2 *Streptococcus pneumoniae* and their effects on physiology and virulence. J Bacteriol 184: 3508–3520.
27. Park C-Y, Kim E-H, Choi S-Y, Tran TD-H, Kim I-H, et al. (2010) Virulence attenuation of *Streptococcus pneumoniae* clpP mutant by sensitivity to oxidative stress in macrophages via an NO-mediated pathway. J Microbiol Seoul Korea 48: 229–235.
28. Terra VS, Homer KA, Rao SG, Andrew PW, Yesilkaya H (2010) Characterization of Novel β-galactosidase activity that contributes to glycoprotein degradation and virulence in *Streptococcus pneumoniae*. Infect Immun 78: 348–357.
29. Jensch I, Gámez G, Rothe M, Ebert S, Fulde M, et al. (2010) PavB is a surface-exposed adhesin of *Streptococcus pneumoniae* contributing to nasopharyngeal colonization and airways infections. Mol Microbiol 77: 22–43.
30. Joyce EA, Kawale A, Censini S, Kim CC, Covacci A, et al. (2004) LuxS is required for persistent pneumococcal carriage and expression of virulence and biosynthesis genes. Infect Immun 72: 2964–2975.

31. Paterson GK, Blue CE, Mitchell TJ (2006) An operon in *Streptococcus pneumoniae* containing a putative alkylhydroperoxidase D homologue contributes to virulence and the response to oxidative stress. Microb Pathog 40: 152–160.
32. Yesilkaya H, Spissu F, Carvalho SM, Terra VS, Homer KA, et al. (2009) Pyruvate formate lyase is required for pneumococcal fermentative metabolism and virulence. Infect Immun 77: 5418–5427.
33. Yamaguchi M, Minamide Y, Terao Y, Isoda R, Ogawa T, et al. (2009) Nrc of *Streptococcus pneumoniae* suppresses capsule expression and enhances anti-phagocytosis. Biochem Biophys Res Commun 390: 155–160.
34. He X, Thornton J, Carmicle-Davis S, McDaniel LS (2006) Tex, a putative transcriptional accessory factor, is involved in pathogen fitness in *Streptococcus pneumoniae*. Microb Pathog 41: 199–206.
35. Smith AW, Roche H, Trombe M-C, Briles DE, Håkansson A (2002) Characterization of the dihydrolipoamide dehydrogenase from *Streptococcus pneumoniae* and its role in pneumococcal infection. Mol Microbiol 44: 431–448.
36. Hendriksen WT, Kloosterman TG, Bootsma HJ, Estevão S, de Groot R, et al. (2008) Site-specific contributions of glutamine-dependent regulator GlnR and GlnR-regulated genes to virulence of *Streptococcus pneumoniae*. Infect Immun 76: 1230–1238.
37. Härtel T, Klein M, Koedel U, Rohde M, Petruschka L, et al. (2011) Impact of glutamine transporters on pneumococcal fitness under infection-related conditions. Infect Immun 79: 44–58.
38. Iyer R, Camilli A (2007) Sucrose metabolism contributes to in vivo fitness of *Streptococcus pneumoniae*. Mol Microbiol 66: 1–13.
39. Giammarinaro P, Paton JC (2002) Role of RegM, a homologue of the catabolite repressor protein CcpA, in the virulence of *Streptococcus pneumoniae*. Infect Immun 70: 5454–5461.
40. Hava DL, Camilli A (2002) Large-scale identification of serotype 4 Streptococcus pneumoniae virulence factors. Mol Microbiol 45: 1389–1406.
41. Glover DT, Hollingshead SK, Briles DE (2008) *Streptococcus pneumoniae* surface protein PcpA elicits protection against lung infection and fatal sepsis. Infect Immun 76: 2767–2776.
42. Bongaerts RJM, Heinz H-P, Hadding U, Zysk G (2000) Antigenicity, expression, and molecular characterization of surface-located pullulanase of *Streptococcus pneumoniae*. Infect Immun 68: 7141–7143.
43. Lammerts van Bueren A, Ficko-Blean E, Pluvinage B, Hehemann J-H, Higgins MA, et al. (2011) The conformation and function of a multimodular glycogen-degrading pneumococcal virulence factor. Struct Lond Engl 1993 19: 640–651.
44. Lau GW, Haataja S, Lonetto M, Kensit SE, Marra A, et al. (2001) A functional genomic analysis of type 3 *Streptococcus pneumoniae* virulence. Mol Microbiol 40: 555–571.
45. Gosink KK, Mann ER, Guglielmo C, Tuomanen EI, Masure HR (2000) Role of novel choline binding proteins in virulence of *Streptococcus pneumoniae*. Infect Immun 68: 5690–5695.
46. LeMessurier KS (2006) Differential expression of key pneumococcal virulence genes in vivo. Microbiology 152: 305–311.

47. Spellerberg B, Cundell DR, Sandros J, Pearce BJ, Idanpaan-Heikkila I, et al. (1996) Pyruvate oxidase, as a determinant of virulence in *Streptococcus pneumoniae*. Mol Microbiol 19: 803–813.
48. Ogunniyi AD, Grabowicz M, Mahdi LK, Cook J, Gordon DL, et al. (2009) Pneumococcal histidine triad proteins are regulated by the Zn2+-dependent repressor AdcR and inhibit complement deposition through the recruitment of complement factor H. FASEB J Off Publ Fed Am Soc Exp Biol 23: 731–738.
49. Adamou JE, Heinrichs JH, Erwin AL, Walsh W, Gayle T, et al. (2001) Identification and characterization of a novel family of pneumococcal proteins that are protective against sepsis. Infect Immun 69: 949–958.
50. Blue CE, Paterson GK, Kerr AR, Berge M, Claverys JP, et al. (2003) ZmpB, a novel virulence factor of *Streptococcus pneumoniae* that induces tumor necrosis factor alpha production in the respiratory tract. Infect Immun 71: 4925–4935.
51. Chapuy-Regaud S, Ogunniyi AD, Diallo N, Huet Y, Desnottes J-F, et al. (2003) RegR, a global LacI/GalR family regulator, modulates virulence and competence in *Streptococcus pneumoniae*. Infect Immun 71: 2615–2625.
52. Bartilson M, Marra A, Christine J, Asundi JS, Schneider WP, et al. (2001) Differential fluorescence induction reveals *Streptococcus pneumoniae* loci regulated by competence stimulatory peptide. Mol Microbiol 39: 126–135.
53. Ibrahim YM, Kerr AR, McCluskey J, Mitchell TJ (2004) Control of virulence by the two-component system CiaR/H is mediated via HtrA, a major virulence factor of *Streptococcus pneumoniae*. J Bacteriol 186: 5258–5266.
54. Trihn M, Ge X, Dobson A, Kitten T, Munro CL, et al. (2013) Two-component system response regulators involved in virulence of *Streptococcus pneumoniae* TIGR4 in infective endocarditis. PLoS ONE 8: e54320. doi:10.1371/journal.pone.0054320.
55. Stroeher UH, Kidd SP, Stafford SL, Jennings MP, Paton JC, et al. (2007) A pneumococcal MerR-like regulator and S-nitrosoglutathione reductase are required for systemic virulence. J Infect Dis 196: 1820–1826.
56. Ibrahim YM, Kerr AR, McCluskey J, Mitchell TJ (2004) Role of HtrA in the virulence and competence of *Streptococcus pneumoniae*. Infect Immun 72: 3584–3591.
57. Polissi A, Pontiggia A, Feger G, Altieri M, Mottl H, et al. (1998) Large-scale identification of virulence genes from *Streptococcus pneumoniae*. Infect Immun 66: 5620–5629.
58. Marion C, Burnaugh AM, Woodiga SA, King SJ (2011) Sialic acid transport contributes to pneumococcal colonization. Infect Immun 79: 1262–1269.
59. Bergmann S, Rohde M, Hammerschmidt S (2004) Glyceraldehyde-3-phosphate dehydrogenase of *Streptococcus pneumoniae* is a surface-displayed plasminogen-binding protein. Infect Immun 72: 2416–2419.

Table S3.5. Clustering of genes significantly, differentially expressed in the microarrays analysis of *S. pneumoniae* D39 grown in galactose, mannose or N-acetylglucosamine *versus* glucose.

D39 locus_Tag	Annotation_D39	Man vs Glc	Gal vs Glc	GlcNAc vs Glc
SPD_0249	hypothetical protein SPD_0249	DOWN	DOWN	UP
SPD_0277	6-phospho-beta-glucosidase	DOWN	DOWN	DOWN
SPD_0278	hypothetical protein SPD_0278	DOWN	DOWN	DOWN
SPD_0279	cellobiose phosphotransferase system IIB component	DOWN	DOWN	DOWN
SPD_0280	transcriptional regulator, putative	DOWN	DOWN	DOWN
SPD_0281	cellobiose phosphotransferase system IIA component	DOWN	DOWN	DOWN
SPD_0282	hypothetical protein SPD_0282	DOWN	DOWN	DOWN
SPD_0283	cellobiose phosphotransferase system IIC component	DOWN	DOWN	DOWN
SPD_0334	oligopeptide ABC transporter, oligopeptide-binding protein AliA	DOWN	DOWN	DOWN
SPD_0404	acetolactate synthase catalytic subunit	DOWN	DOWN	DOWN
SPD_0405	acetolactate synthase 3 regulatory subunit	DOWN	DOWN	DOWN
SPD_0407	hypothetical protein SPD_0407	DOWN	DOWN	DOWN
SPD_0409	threonine dehydratase	DOWN	DOWN	DOWN
SPD_0473	immunity protein BlpY	UP	UP	UP
SPD_0502	PTS system, beta-glucosides-specific IIABC components	DOWN	DOWN	DOWN
SPD_0954	hypothetical protein SPD_0954	DOWN	DOWN	DOWN
SPD_0955	amino acid or sugar ABC transport systems, permease protein	DOWN	DOWN	DOWN
SPD_1004	glyceraldehyde-3-phosphate dehydrogenase, NADP-dependent	DOWN	DOWN	DOWN
SPD_1018	immunoglobulin A1 protease precursor	UP	UP	DOWN
SPD_1176	ABC transporter, ATP-binding protein	UP	UP	UP
SPD_1179	hypothetical protein SPD_1179	UP	UP	UP
SPD_1569	aquaporin	DOWN	DOWN	DOWN
SPD_1596	tryptophan synthase subunit alpha	DOWN	DOWN	DOWN
SPD_1598	N-(5'-phosphoribosyl)anthranilate isomerase	DOWN	DOWN	DOWN
SPD_1600	anthranilate phosphoribosyltransferase	DOWN	DOWN	DOWN
SPD_1601	anthranilate synthase component II	DOWN	DOWN	DOWN
SPD_1602	anthranilate synthase component I	DOWN	DOWN	DOWN
SPD_1606	MgtC/SapB family protein	DOWN	DOWN	DOWN
SPD_1607	ABC transporter, permease protein	DOWN	DOWN	DOWN
SPD_1608	ABC transporter ATP-binding protein	DOWN	DOWN	DOWN
SPD_2052	hypothetical protein SPD_2052	DOWN	DOWN	DOWN
SPD_2068	serine protease	UP	UP	UP

Table S3.7. Intracellular intermediates of sugar-specific catabolic patways of *S. pneumoniae* determined in resting cells (by in vivo NMR) or in growing cells (ethanol extracts), metabolizing N-acetylglucosamine (GlcNAc), mannose (Man) or galactose (Gal).

Sugar	Intermediates	Resting cells	Growing cells[a]
GlcNAc			
	GlcNAc6P	-	+
	GlcN6P	-	+
	F6P	-	+
	FBP	+	+
	G6P	-	+
	3-PGA	-	+
Man			
	Man6P	+	+
	FBP	+	+
	3-PGA	-	+
	G6P	-	+
Gal			
	Gal6P	+	+
	TPB	-	+
	FBP	+	+
	α-Gal1P	-	+
	α-G1P	-	+
	G6P	-	+
	3-PGA	-	+

[a] as determined by Paixão *et al*., 2015 (Chapter 2).

Abbreviations:
+, presence; -, absence; GlcNAc6P, N-acetylglucosamine 6-phosphate; GlcN6P, glucosamine 6-phosphate; F6P, fructose 6-phosphate; FBP, fructose 1,6-biphosphate; G6P, glucose 6-phosphate; 3-PGA, 3-phosphoglycerato; Man6P, mannose 6-phosphate; Gal6P, galactose 6-phosphate; TPB, tagatose 1,6-biphosphate; α-Gal1P, α-galactose 1-phosphate; α-G1P, α-glucose 1-phosphate.

Table S3.8. Summary of the significantly differentially expressed genes (up- or downregulated) of cells of *S. pneumoniae* D39 grown in CDM supplemented with N-acetylglucosamine (GlcNAc), mannose (Man), galactose (Gal) or in a mixture thereof challenged with a glucose (Glc) pulse and compared to unchallenged cells, determined by DNA microarrays.

Locus_tag	Gene	Product	GlcNAc	Man	Gal	Mix [c]
Sugar-specific catabolism[d]						
SPD_1050	***lacD***	**tagatose 1,6-diphosphate aldolase**			**-2.02**	
SPD_1051	***lacC***	**tagatose-6-phosphate kinase**			**-1.76**	
SPD_1052	***lacB***	**galactose-6-phosphate isomerase subunit LacB**		0.32	**-2.10**	**-1.05**
SPD_1053	***lacA***	**galactose-6-phosphate isomerase subunit LacA**			**-1.95**	**-1.41**
SPD_1163		N-acetylneuraminate lyase, putative	-0.55	0.85	-0.82	-0.65
SPD_1246	***nagB***	**glucosamine-6-phosphate isomerase**	**-0.53**	0.66		
SPD_1488		ROK family protein		0.83	-0.71	-0.68
SPD_1497	*nanE-1*	N-acetylmannosamine-6-phosphate 2-epimerase	-0.63	0.88	-0.73	-0.54
SPD_1633	***gaT-2***	**galactose-1-phosphate uridylyltransferase**		0.45	**-1.78**	**-0.50**
SPD_1634	***galK***	**galactokinase**		0.77	**-1.69**	**-0.89**
SPD_1993	*fucU*	RbsD/FucU transport protein family protein	-0.70		-0.65	
SPD_1994	*fucA*	L-fuculose phosphate aldolase	-0.80		-0.90	-0.40
SPD_1995	*fucK*	L-fuculose kinase FucK, putative	-1.38			-0.71
Glycolysis						
SPD_1012	*eno*	enolase		0.33		
SPD_1823	*gap*	glyceraldehyde-3-phosphate dehydrogenase		0.39		
Pyruvate metabolism						
SPD_0420	*pflB*	pyruvate formate-lyase	-0.53	0.70		-0.99
SPD_0621	*lctO*	lactate oxidase	-0.93	0.98		-0.63
SPD_0985	*pta*	phosphotransacetylase	-0.34	0.56	-0.80	
SPD_1834	*adh*	bifunctional acetaldehyde-CoA/alcohol dehydrogenase	-0.95	0.53		-1.63
Sugar-specific transporters[d]						
SPD_0066		**PTS system, IIB component**				**-0.54**
SPD_0088		**ABC transporter, permease protein**	-1.49	**1.83**		**-1.66**
SPD_0089		**ABC transporter, permease protein**	-1.32	**1.60**		**-0.85**
SPD_0090		ABC transporter, substrate-binding protein	-0.60			

Locus_tag	Gene	Product	GlcNAc	Man	Gal	Mix [c]
SPD_0262		**PTS system, mannose/fructose/sorbose family protein, IID component**	**-0.50**		**-0.51**	
SPD_0263	***manM***	**PTS system, mannose-specific IIC component**	**-0.53**	**0.41**		
SPD_0264	***manL***	**PTS system, mannose-specific IIAB components**	**-0.61**	**0.55**		
SPD_0279	*celB*	cellobiose phosphotransferase system IIB component	-0.91		1.20	-1.06
SPD_0281	*celC*	cellobiose phosphotransferase system IIA component		-0.63	1.12	
SPD_0283	*celD*	cellobiose phosphotransferase system IIC component		-1.27	0.88	
SPD_0293		**PTS system, IIA component**		**0.48**		
SPD_0295		**PTS system, IIB component**		**0.44**		
SPD_0297		**PTS system, IID component**		**0.58**		
SPD_0559		**PTS system IIA component, putative**		1.11	**-0.67**	**-1.69**
SPD_0560		**PTS system, IIB component, putative**		1.31	**-0.89**	**-1.70**
SPD_0561		**PTS system, IIC component, putative**	-0.67	1.10	**-0.82**	**-1.15**
SPD_0661	*exp5*	PTS system, IIABC components			0.54	
SPD_0739		membrane lipoprotein TmpC precursor				-0.39
SPD_0773		PTS system, fructose specific IIABC components	-0.52	0.60	0.45	-0.51
SPD_1040	*ptsH*	phosphocarrier protein HPr			-0.43	
SPD_1047	*lacE-2*	PTS system, lactose-specific IIBC components			-0.79	
SPD_1048	*lacF-2*	PTS system, lactose-specific IIA component			-0.64	
SPD_1057		PTS system, IIB component, putative	-0.70	1.14		-1.79
SPD_1409		sugar ABC transporter, ATP-binding protein	-0.81	0.86		-0.68
SPD_1493		sugar ABC transporter, permease protein		1.09	-0.76	
SPD_1494		sugar ABC transporter, permease protein		1.04	-0.58	
SPD_1495		sugar ABC transporter, sugar-binding protein	-0.72	1.62	-0.55	
SPD_1496		**PTS system, IIBC components**	**-0.96**	1.36	-0.72	**-0.91**
SPD_1664		**PTS system, trehalose-specific IIABC components**	**-0.50**			
SPD_1934	*malX*	maltose/maltodextrin ABC transporter, maltose/maltodextrin-binding protein	-0.83	0.94		-0.64
SPD_1935	*malC*	maltodextrin ABC transporter, permease protein		0.48		
SPD_1991		PTS system, IIB component			-0.78	
SPD_1992		PTS system, IIA component			-0.71	

[a] Subtable of Tables S3.9, S3.10, S3.11 and S3.12 provided on the CD.
[b] Values of ln-ratio. Positive values indicate upregulation and negative values indicate downregulation.
[c] Mixture of Gal, Man and GlcNAc.
[d] As reviewed by Paixão *et al.* 2015 (Chapter 2).
In bold are depicted the transporters and sugar-specific catabolic genes known or putatively involved in the metabolism of GlcNAc, Man or Gal, as reviewed by Paixão *et al.* 2015 (Chapter 2).

Table S3.13. Clustering of genes significantly, differentially expressed in the microarrays analysis of *S. pneumoniae* D39 grown in galactose, mannose, N-acetylglucosamine or in a mixture thereof challenged with glucose *versus* unchallenged cells.

D39 locus_Tag	MixPulseGlc vs Mix	GlcNAcPulseGlc vs GlcNAc	ManPulseGlc vs Man	GalPulseGlc vs Gal	Annotation_D39
SPD_0277	DOWN	DOWN	DOWN	UP	6-phospho-beta-glucosidase
SPD_0373	DOWN	DOWN	UP	DOWN	hypothetical protein SPD_0373
SPD_0476	UP	UP	DOWN	UP	hypothetical protein SPD_0476
SPD_0561	DOWN	DOWN	UP	DOWN	PTS system, IIC component, putative
SPD_0724	DOWN	DOWN	UP	DOWN	phosphopentomutase
SPD_0725	DOWN	DOWN	UP	DOWN	pseudo
SPD_0771	DOWN	DOWN	UP	UP	lactose phosphotransferase system repressor
SPD_0772	DOWN	DOWN	UP	UP	1-phosphofructokinase, putative
SPD_0773	DOWN	DOWN	UP	UP	PTS system, fructose specific IIABC components
SPD_1163	DOWN	DOWN	UP	DOWN	N-acetylneuraminate lyase, putative
SPD_1215	UP	UP	DOWN	UP	cytoplasmic alpha-amylase
SPD_1299	DOWN	DOWN	UP	DOWN	hypothetical protein SPD_1299
SPD_1300	DOWN	DOWN	UP	DOWN	thiamine biosynthesis protein ApbE, putative

D39 locus_Tag	MixPulseGlc vs Mix	GlcNAcPulseGlc vs GlcNAc	ManPulseGlc vs Man	GalPulseGlc vs Gal	Annotation_D39
SPD_1301	DOWN	DOWN	UP	DOWN	NADPH-dependent FMN reductase
SPD_1496	DOWN	DOWN	UP	DOWN	PTS system, IIBC components
SPD_1497	DOWN	DOWN	UP	DOWN	N-acetylmannosamine -6-phosphate 2-epimerase
SPD_2009	DOWN	DOWN	UP	DOWN	hypothetical protein SPD_2009
SPD_2012	DOWN	DOWN	DOWN	DOWN	alpha-glycerophosphate oxidase
SPD_2013	DOWN	DOWN	DOWN	DOWN	glycerol kinase
SPD_2033	DOWN	DOWN	UP	UP	ribosomal subunit interface protein

Supporting Figures

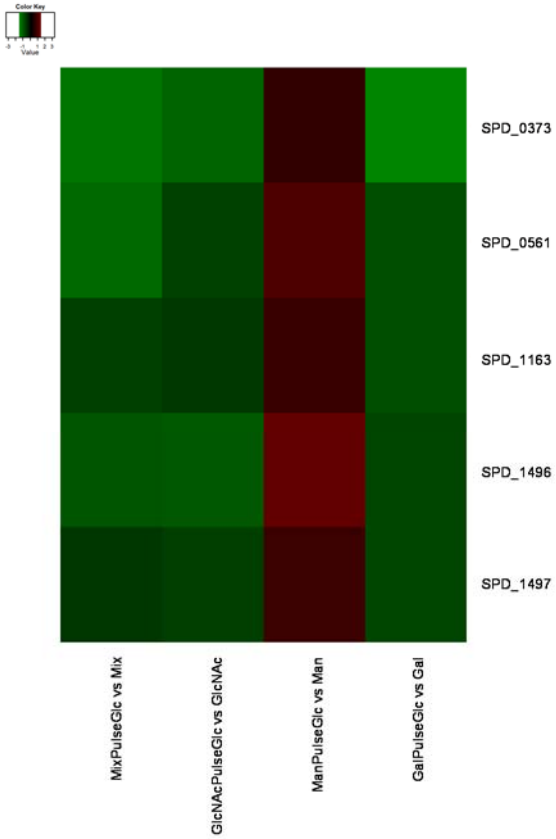

Figure S3.1. Visual representation of the clustering analysis performed for monosaccharides challenged with a pulse of glucose *versus* unchallenged cells, targeting the selected categories of genes.

Colour scale: ln-ratio of expression. Red, upregulated gene in the microarrays; green, downregulated gene in the microarrays. The figure was generated targeting the gene categories of interest (glycolysis, pyruvate metabolism, sugar dedicated transporters and catabolic genes as reviewed by Paixão *et al*., 2015, (Chapter 2), classical virulence factors). According to NCBI annotation: SPD_0373, hypothetical protein; SPD_0561, PTS system transporter subunit IIC; SPD_1163, N-acetylneuraminate lyase; SPD_1496, PTS system transporter subunit IIBC; SPD_1497, N-acetylmannosamine-6-phosphate 2-epimerase (*nanE-1*). Glc, glucose; Man, mannose; Gal, galactose; GlcNAc, N-acetylglucosamine; Mix, mixture of Gal, Man and GlcNAc.

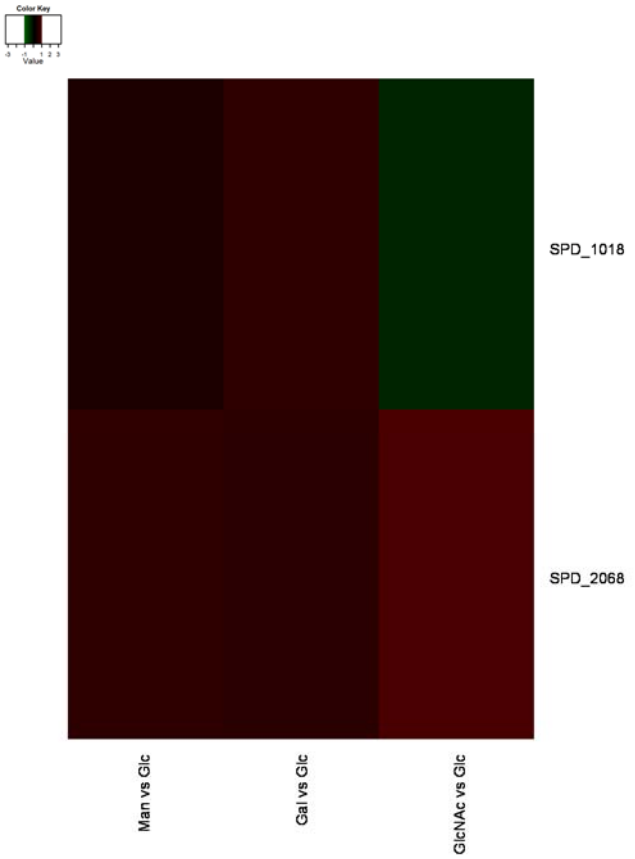

Figure S3.2. Visual representation of the clustering analysis performed for Gal, Man or GlcNAc *versus* Glc, targeting the selected categories of genes.

Colour scale: ln-ratio of expression. Red, upregulated gene in the microarrays; green, downregulated gene in the microarrays. The figure was generated targeting the gene categories of interest (glycolysis, pyruvate metabolism, sugar dedicated transporters and catabolic genes as reviewed by Paixão *et al.*, 2015, (Chapter 2), classical virulence factors). According to NCBI annotation: SPD_1018, immunoglobulin A1 protease (*iga*); SPD_2068, serine protease. Glc, glucose; Man, mannose; Gal, galactose; GlcNAc, N-acetylglucosamine.

Chapter 4

Overview and concluding remarks

Chapter 4 – Contents

Streptococcus pneumoniae is a common asymptomatic commensal of the nasopharynx. However, this bacterium is better known as a leading cause of bacterial meningitis, pneumonia, septicaemia and otitis media. The ever-increasing antibiotic resistance issues and the re-emergence of non-type vaccine strains call for the identification of new targets for the development of novel therapeutic and preventive drugs. Accumulating evidence strengthens the view that pathogenesis and central metabolism are profoundly interconnected, and thus the barrier between basic pneumococcal physiology and virulence is now more diffuse. The focus of this thesis was to deepen our understanding of carbon metabolism and its regulation in *S. pneumoniae*. Carbon metabolism is central to the physiology of this heterotroph bacterium, which relies on the efficient acquisition of sugars for energy generation and production of catabolic intermediates needed for biosynthesis. This work further contributed to disclose interdependencies between carbohydrate metabolism and *S. pneumoniae* virulence.

Living on mucins and the particular case of the mucin-degrading *S. pneumoniae*

The highly hydrated mucus gel overlaying the epithelial surfaces of the human body (*e.g.* respiratory, oral, gastrointestinal tracts) is a first line of defence against invading microorganisms, impurities, chemical (toxins), enzymatic and mechanical disruptions. Besides being a physical barrier it is also a matrix rich in host antimicrobial molecules (*e.g.* lysozyme, IgA, lactoferrin) [1]. The mucus major components are the high molecular weight glycoprotein mucins, which are constituted by a protein core heavily decorated with carbohydrate polymers of varied nature and size.

The carbohydrates present in mucins provide alternative binding sites to bacterial adhesins and, hence enable bacteria to thrive evading interactions with the underlying epithelium [2]. For example, the ability of the probiotic bacterium *Lactobacillus rhamnosus GG* to persist in the human gut as recently been associated with the ability of a protein in the pilli to bind host mucins [3]. Remarkably, mucins are also a valuable nutritional reservoir of carbon and energy sources particularly important in niches where free carbohydrates are limited, such as the nasopharynx or micro niches in the gastrointestinal tract, enabling bacterial survival and colonisation on these surfaces [2,4,5]. Mucins are heavily O-glycosylated glycoproteins, generally composed of the monosaccharides N-acetylgalactosamine (GalNAc), galactose (Gal), N-acetylneuraminic acid (NeuNAc), N-acetylglucosamine (GlcNAc) and fucose (Fuc) [6,7], which carbohydrate content can reach up to 80% of the mucin molecular mass [2]. Bacteria have evolved strategies to circumvent the mucin barrier and take advantage of this structure. Among others, those mechanisms encompass production of mucin-degrading enzymes that release carbohydrates from O- or N-linked oligosaccharide side chains (glycosidases) and proteins (proteases) that destabilize the mucus gel properties [1]. Thus, the ability to utilise mucin depends, to great extent, on these activities.

The ability to degrade mucin is present in a number of members of the human microbiota, and in particular of inhabitants of the nasal and oral cavity, and the gastrointestinal tract. Interestingly, it was estimated that only approximately 1% of the total human fecal microbiota was able to use mucin [8]. Among these are organisms belonging to the genera *Bifidobacterium, Ruminococcus, Clostridium* and *Bacteroides* [9,10] (for a detailed overview see [2]). Recently, a new species isolated from the gut, *Akkermansia muciniphila*, was shown to use mucin as sole carbon and energy source [4]. Despite possessing a number of glycosidases [2], *A.*

muciniphila only grows on a few monosaccharides (GalNAc, GlcNAc and Glc) and it strictly requires a protein source; in such semi-defined conditions the growth parameters are poorer than on mucin [4]. Accumulating evidence indicates that microbiota in general, such as the non-mucin degrading intestinal bacteria *E. coli*, can benefit from sugars derived from mucin-degrading organisms [9,11]. Furthermore, it has been shown that the joint action of mucin-degrading organism increases mucin degradation [12], which is likely to benefit all ecological partners.

Oral *Streptococcus* species are also able to use mucin (*e.g. S. mitis, S. sanguis, and S. milleri*) [13]. In *Streptococcus intermedius* UNS35, growth on mucin significantly increase the levels of several glycosidases and induced the activity of Man and GlcNAc PTSs. The authors suggested that these mechanisms may facilitate the persistence and growth of *S. intermedius in vivo* [14]. In contrast, its ecological cohabitant *Streptococcus mutans* is unable to use mucin as sole carbon and energy source [13]. However, enhanced survival was observed upon addition of mucin to sucrose-starved biofilms [15] or to a medium rich in amino acids [16]. In the latter, an intact tagatose 6-phosphate (T6P) pathway was also required for growth, suggesting that the mucin somehow provides a source of Gal. Thus, one can speculate that *S. mutans* may benefit from mucins once free carbohydrates become limited in the oral cavity. Of the mucin sugar constituents, *S. mutans* is able to use Man, GlcNAc and Gal as sole carbon sources [17–20].

The nasal cavity inhabitant *S. pneumoniae* possesses an incredible array of extracellular glycosidases with different substrate specificities (reviewed in [21]), which permits its growth on different glycoconjugates such as N-linked glycans and glycosaminoglycans (hyaluronic acid) [22,23]. Furthermore, *S. pneumoniae* is able to grow on mucin (O-linked glycan) as sole carbon source [24]. This ability is strictly associated with the expression of a number of glycosidases (Chapter 2), which act on the

mucin releasing neuraminic acids (NeuNAc and N-glycolylneuraminic acid), Gal and GalNAc, and to a less extent GlcNAc and Fuc [7]. Yesilkaya and co-authors showed that growth on mucin is heavily dependent on neuraminidase A (NanA) activity which releases the terminal N-acetylneuraminic acid of the oligosaccharide side chains [24], as this feature is seemingly essential for further breakdown of the carbohydrate polymers by other glycosidases [7,25,26]. Curiously, *nanA* was not among the differentially expressed genes on mucin as compared to Glc (Chapter 2). This finding leads us to propose that constitutive expression of *nanA* is sufficient to ensure the release of NeuNAc terminal moieties. Constitutive expression of glycosidase genes has been reported for enteric bacteria [9]. This mechanism was hypothesized to confer a selective advantage over organisms that do not express the glycosidases constitutively in conditions where the substrates are limiting for growth. We can speculate that the same holds true for *S. pneumoniae*, since it exclusively relies on carbohydrates to grow, particularly hexoses that are scarce in the airways.

In Chapter 2 of this thesis we identified Gal, Man and GlcNAc as the monosaccharide constituents of porcine gastric mucin (model glycoprotein) that can potentially sustain growth of *S. pneumoniae* strain D39 in the host. Based on a transcriptome analysis comparing mucin *vs*. Glc we singled out upregulated genes involved in the catabolism of sugars, and combined this information with the growth-sustaining monosaccharides identified in sugar phenotype assays containing representative mucin carbohydrate moieties. Interestingly, Gal processing genes represent the largest fraction of genes induced by mucin (Chapter 2), which emphasizes a cellular demand for Gal pathway functionality during growth on mucin. This finding is in line with an earlier study showing that upon pneumococcal growth the Gal content in porcine gastric mucin was reduced by 30%. Of the sugars capable of supporting growth of strain

D39, Gal suffered the largest decrease [7]. Thus, we propose that Gal is the main mucin moiety used for growth of the bacterium in the nasopharynx. Furthermore, Gal is a widespread sugar in glycoproteins.

We also observed induction of transporters specific for substrates in which the bacterium is unable to grow (*e.g*. NeuNAc) (Chapter 2). Similar observations have been reported for other organisms and *S. pneumoniae* and are associated with non-metabolic roles for the incoming substrate [11,27–29]. D39 has a frame shift mutation in the N-acetylneuraminate lyase gene of *nanAB* operon [30,31], and we (and others) have related this genotypic trait to its inability to grow on sialic acid. Recently, NeuNAc was found to act as a signalling molecule in the pneumococcus, including strain D39, that promotes increased colonisation, invasion of the host's lower respiratory tract and biofilm formation *in vitro* [32–34]. According to Gualdi *et al*. [31], the D39's inability to catabolise NeuNAc is not hindering the regulation of the *nanAB* locus or the strain's virulence. On the other hand, upregulation of NeuNAc transporters on mucin suggests that the amino sugar is still transported to exert exclusively regulatory functions or that the transporters display specificity for other sugars as well. A detailed biochemical characterization of each transporter to elucidate sugar specificity should be carried out in the future. Previously, Bidossi *et al*., [30] demonstrated that the ABC transporters encoded in sialic acid operon were also implicated in the uptake of ManNAc. This metabolite is the first intermediate in the sialic acid pathway (Chapter 2, Fig. 2.1).

We and others have shown that *S. pneumoniae* has the genetic potential, including glycosidases, transporters and catabolic pathways, for the use of the glycan-constituent sugars Gal, Man, GlcNAc as sole carbon sources (Chapter 2, [7,30,35,36]). However, experimental validation of the catabolic pathways was missing. In this study, we ascertained at the biochemical and genetic levels the *in silico* predictions (Fig. 4.1) for the

Gal, Man and GlcNAc catabolic pathways in *S. pneumoniae* strain D39 (Chapter 2).

The phosphorylated intermediates mannose 6-phosphate (Man6P) (Man pathway), N-acetylglucosamine 6-phosphate (GlcNAc6P) and glucosamine 6-phosphate (GlcN6P) (GlcNAc pathway), and tagatose 1,6-bisphosphate (TBP), galactose 6-phosphate (Gal6P) (T6P pathway for Gal) and α-galactose 1-phosphate (α-Gal1P) and α-glucose 1-phosphate (α-G1P) (Leloir pathway for Gal) were detected in ethanol extracts of exponentially growing cells. Moreover, induction of the dedicated enzymes of each pathway (ManA, NagA and NagB, GalK and LacD) was observed in sugar-grown cells (Chapter 2). Interestingly, ManA and NagB activities were also detected in Glc-grown cells, while the activities of GalK and LacD were only measured in Gal-grown cells. Constitutive expression of *manA* and *nagA* probably reflects the involvement of their functions in processes of cellular biosynthesis (Fig. 4.1).

The combined biochemical data (phosphorylated intermediates and enzyme activities) (Chapter 2) and the increased transcript levels of Leloir and T6P pathway specific genes (*galK*, *galT-2*, *galE-1*, *galM* and *lacBCD* on Gal-grown cells (Chapter 3); *lacABD* and *galM* on mucin (Chapter 2)) prove without doubt the simultaneous activity of both Gal pathways in *S. pneumoniae* (Fig. 4.1) [35]. Even though this behaviour is seemingly energetically costly, it is not a unique feature of the pneumococcus. *S. mutans*, *Streptococcus oligofermentans*, *Streptococcus gordonii* and *Lactococcus lactis* also possess both pathways and simultaneous activity has been demonstrated [18,37–39]. While in the oral *Streptococcus* the T6P pathways is apparently the preponderant route for Gal catabolism [18,37,38], in the dairy bacterium *L. lactis* this feature is strain dependent [39]. The assessment of the relative contribution of each pathway is not trivial and requires flux partitioning determination, using advanced labelling techniques coupled to mass spectrometry and/or nuclear

magnetic resonance detection. In *S. pneumoniae* this deserves further investigation, but our genetic data revealed that Gal catabolism requires at least an active galactokinase, as mutants in *galK* were unable to grow on Gal despite the presence of an intact T6P pathway (Chapter 2).

Mutations in *manA* and *nagA* rendered strains unable to grow on Man and GlcNAc, respectively, and a double knockout mutant D39Δ*lacDgalK* failed to grow on Gal. As a conclusion, mutant analysis demonstrated that *S. pneumoniae* D39 possesses no additional pathways for the catabolism of Man, GlcNAc and Gal.

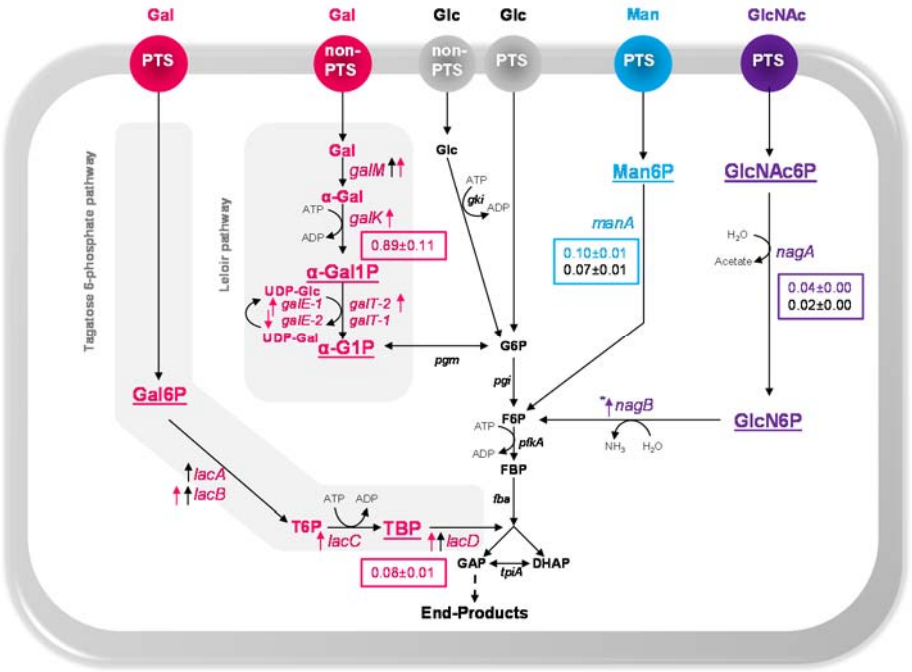

Figure 4.1. Schematic representation of the pathways for the dissimilation of galactose (Gal), mannose (Man) and N-acetylglucosamine (GlcNAc) in *S. pneumoniae* D39.

Reactions are catalysed by the following protein encoding genes: *galM*, aldolase 1-epimerase (mutarotase); *galK,* galactokinase; *galT-1, galT-2*, galactose 1-phosphate uridylyltransferase; *galE-1*, *galE-2*, UDP-glucose 4-epimerase; *pgm*, phosphoglucomutase/phosphomannomutase family protein; *lacA*, galactose 6-phosphate isomerase subunit LacA; *lacB*, galactose 6-phosphate isomerase subunit LacB; *lacC*, tagatose 6-phosphate kinase; *lacD*, tagatose 1,6-diphosphate aldolase; *pgi*, glucose 6-phosphate isomerase; *manA*, mannose 6-phosphate isomerase; *nagA*, N-

acetylglucosamine 6-phosphate deacetylase; *nagB*, glucosamine 6-phosphate isomerase; *gki*, glucokinase; *pgi*, glucose 6-phosphate isomerase; *pfkA*, 6-phosphofructokinase; *fba*, fructose-biphosphate aldolase; *tpiA*, triosephosphate isomerase. The lower glycolytic pathway is represented by a dashed arrow.
Intermediates: Gal, galactose; α-Gal, α-galactose; α-Gal1P, α-galactose 1-phosphate; α-G1P, α-glucose 1-phosphate; UDP-Glc, UDP-glucose; UDP-Gal, UDP-galactose; Gal6P, galactose 6-phosphate; T6P, tagatose 6-phosphate; TBP, tagatose 1,6-diphosphate; Man6P, mannose 6-phosphate; GlcNAc6P, N-acetylglucosamine 6-phosphate; GlcN6P, glucosamine 6-phosphate; Glc, glucose; G6P, glucose 6-phosphate; F6P, fructose 6-phosphate; FBP, fructose 1,6-biphosphate; GAP, glyceraldehyde 3-phosphate; DHAP, dihydroxyacetone phosphate.
Underlined intermediates represent the sugar-specific pathway intermediates determined in ethanol extracts of cells grown in the glycan-derived sugar.
Values are the specific activities (U $mgprotein^{-1}$) measured in glycan-derived sugar or in Glc-grown cells (black).
Black arrows indicate differential expression in mucin-grown cells as compared to Glc-grown cells. Coloured arrows indicate differential expression in the glycan-derived sugar as compared to Glc. The direction of the arrow indicates upregulation (up) or downregulation (down).
*Using a less restrictive criterion for microarrays analysis.
For the sake of simplicity the identity of putative transporters is not depicted in the figure.

Man, Gal and GlcNAc catabolic pathways are present and conserved among pneumococcal genomes (Tables S2.8 and S4.1), however events like single nucleotide polymorphisms that result in loss of activity cannot be excluded. A good example is provided by the inability of strain D39 to catabolise NeuNAc. Thus, while the high conservation of the pathways provides a measure of their physiological relevance, pathway activity needs to be confirmed in different pneumococcal serotypes.

The first step in sugar catabolism is transport across the cell envelope. The focus of this work was the intracellular metabolism, but our data, and in particular the expression data (Chapter 2 and 3) provide important information for the identification of sugar transporters. However, in most cases biochemical characterization is recommended to firmly ascertain substrate specificity.

Metabolism through the Leloir is usually associated with the entry of Gal via non-PTSs (secondary carriers or ABC). Indeed, Bidossi *et al*. [30] designated Gal uptake to a CUT1 family ABC transporter but further

experimentation is needed since a loss of function mutant displayed only mild reduction of the Gal phenotype [30] and our expression data revealed downregulation of the encoding genes on Gal (Chapter 3). Nevertheless, the ability of *ptsI* mutants to grow on Gal ([30], and our own unpublished data) further corroborates that *S. pneumoniae* internalizes Gal through still unknown non-PTSs permeases.

On the other hand, accumulation of Gal6P in growing (Chapter 2) and resting cells (Chapter 3) substantiates the entry of Gal through a PTS system, which is a requisite for T6P pathway activity. The increased expression levels of the galactitol-family PTS SPD_0559-0-1 on mucin (Chapter 2) and on Gal-adapted cells (Chapter 3) further supports the involvement of this system in Gal translocation [30,40]. This Gat-PTS has homology to the high affinity galactose-specific PTS present in *S. gordonii*, *S. oligofermentans* and *S. mutans* [37,38,41]. Regardless of the transporter identity in *S. pneumoniae*, the affinity of this uptake system(s) for Gal is low (Chapter 2).

S. mutans strain UA159 also lacks the high-affinity galactose-PTS, which correlates with inefficient dissimilation of Gal via the T6P pathway. Translocation of Gal in this strain occurs via the glucose–PTS permease EII^{Man} (ManLMN) and the lactose-PTS permease EII^{Lac} (LacFE), but the Gal-PTS activity is low [18]. In *S. pneumoniae*, Gal induced the expression of other PTSs genes including *lacE-2*, a lactose-PTS known to internalize Gal [35], and SPD_1057, a Gat-PTS also induced on mucin Chapter 2, hence their contribution for Gal translocation cannot be ruled out.

Man and GlcNAc transporters were not found differentially positively regulated in Man- and GlcNAc-grown cells, respectively (Chapter 3). Whether this behaviour is due to wrong assignment of the protein functions or that the genes encoding the uptake systems are constitutively expressed remains to be elucidated. As a concluding note, the importance of carbohydrates for the pneumococcal lifestyle is apparent form its

genomic potential: *S. pneumoniae* possesses the highest number of carbohydrate transporters, relative to its genome size, as compared to other sequenced prokaryote genomes [42]. Induction of transporters, other than the expected, reiterates the need for an in depth biochemical characterization of sugar uptake systems in *S. pneumoniae*.

The ability of *S. pneumoniae* to use mucin as sole carbon source and take advantage of mucin-constituent sugars reveals an evolutionary adaptation of *S. pneumoniae* to life in the nasopharynx.

Monosaccharide nutrition in the pneumococcus

S. pneumoniae is a strictly fermentative bacterium and therefore relies exclusively on carbohydrates to grow. In its natural habitat, the nasopharynx, free sugars are in general scarce. This is particularly true for the usually preferred carbohydrate of Gram-positive bacteria Glc, which content is below 1 mM [43–45]. However, we have experimentally proved that the pneumococcus has the catabolic pathways for the molecular breakdown of the monosaccharides Gal, Man and GlcNAc present in host glycoproteins, such as mucins (Chapter 2). Besides those three sugars we have shown that *S. pneumoniae* D39 has the ability to grow on GlcN as sole carbon source, but not on NeuNAc, GalNAc and GalN (Chapter 2). The lack of growth on NeuNAc has been discussed above, but the inability to use GalNAc and GalN was not investigated in detail. GalNAc accounts for up to 15% of the molecular mass of porcine gastric mucin, but is reduced by 35% in the mucin upon pneumococcal growth [7]. Catabolism of GalNAc in bacteria comprises transport by a PTS yielding N-acetylgalactosamine 6-phosphate (GalNAc6P), conversion to galactosamine 6-phosphate (GalN6P) by GalNAc6P

deacetylase, and finally isomerisation/deamination to T6P via GalN6P isomerase (coded by *agaS*) [46,47]. Genes encoding homologues of the GalNAc-PTS and *agaS* were in the genome sequence of D39, respectively SPD_0293-5-6-7 and SPD_0070. However, the only gene encoding an amino sugar deacetylase in D39 is *nagA* (GlcNAc catabolism) and a peptidoglycan GlcNAc deacetylase. In *E. coli* and *Lactobacillus casei* NagA can also catalyse the conversion of GalNAc6P to GalN6P [46–48]. Whether the specificity range is different (narrower) in *S. pneumoniae* or the inability to grow in GalNAc arises from a different mechanism remains to be investigated. More interestingly is the lack of growth on Fuc, despite the presence of a complete Fuc catabolic pathway [28]. However, *S. pneumoniae* apparently lacks the enzymes required for processing the terminal product of Fuc catabolism, L-lactaldehyde (Chapter 2, [30]). The transporter in the Fuc operon, SPD_1989-0-1-2, is selective for fucosylated-oligosaccharides which are then processed by intracellular glycosidases releasing Fuc [28,49], but specific import of the monosaccharide by other transporters cannot be excluded. The peculiar inability to use Fuc despite the genomic capacity suggests a role of Fuc on non-metabolic functions, such as virulence [50,51] or participation in a sensing mechanism for fucosylated-compounds [28] (*vide* introduction for a detailed description). Transport and intracellular hydrolysis of these oligosaccharides can provide a nutritional competitive advantage in a relatively monosaccharide poor environment, as the free sugars are released in the bacterium cytoplasm.

In the general survey conducted by Bidossi *et al*. [30], 32 different substrates, of which 8 were monosaccharides, were able to support pneumococcal growth, but strain variance was also reported. In our study a detailed characterization of growth on Gal, Man, GlcNAc and Glc is provided (Chapter 2). In both studies Glc supported the fastest growth, but differences on growth rates were observed for the other sugars

(Chapter 2 *vs.* [30]) which might stem from the use of rather dissimilar growth conditions or strain DP1004, a rough derivative of D39. Indeed, previous work in our lab established difference in growth rate between D39 and its rough derivative R6 growing in identical environmental conditions [52]. We found the specific growth rate to be independent of the initial substrate concentration for GlcNAc, Man and Glc. For Gal, however, the growth rate was considerably reduced (1.5-fold) in the lower sugar concentration and, in a sugar mixture, Gal was partially consumed and only after depletion of GlcNAc and Man (Chapters 2 and 3). The absence of a high affinity Gal transporter was evoked to explain these observations.

The presence of the high affinity Gal transporter in some strains of the cariogenic dental pathogen *S. mutans* and in the oral commensal *S. gordonii* has been proposed to give a competitive advantage for efficient use of Gal in ecological settings particularly in fasting periods [38,41]. In *S. mutans* efficient Gal uptake permits the creation of an acid environment detrimental for *S. gordonii* survival, whereas in *S. gordonii* efficient Gal metabolism permits a more effective antagonism likely through H_2O_2 production which inhibits *S. mutans* growth [38,41]. In the latter case Gal seems to promote a less cariogenic oral flora [38]. The absence of such a transporter in *S. pneumoniae* can be a drawback for efficient Gal metabolism in the host. Thus, it is tempting to speculate that in the nasopharynx Gal concentration is a not a limiting factor, most likely due to the activity of at least two pneumococcal galactosidases [7] or the galactosidase activity of other bacteria in the same niche, combined with Gal abundance in host glycoproteins. In support, Gal is one of the carbohydrates profusely released from the mucins upon the action of *S. pneumoniae* [7]. Moreover, despite being a less preferred sugar, the ATP_{yield} is higher in Gal-grown cells than in other carbohydrates, in line with higher amounts of acetate produced (Chapter 2). Indeed, growth in

non-preferential sugars (slow metabolizable carbon sources) is usually associated with mixed acid fermentation profiles in several *Streptococcaceae* [53,54]. In agreement, cells of *S. pneumoniae* D39 grown in Gal-containing medium, retrieved a pronounced shift towards a mixed acid fermentation products (Chapter 2, [35]), which was attributed to the activity of pyruvate formate lyase (PFL) and pyruvate formate-lyase activating enzyme (PFL-AE) [36]. The metabolic enzyme PFL competes with lactate dehydrogenase (LDH) for pyruvate. The concomitant generation of one more molecule of ATP (via acetate kinase) is certainly an advantage during the metabolism of slow metabolizable sugars. Overall, our results support the general idea that in laboratorial conditions Gal is a non-preferred substrate for bacterial proliferation [55], however in complex and ever-changing natural habitats a multitude of factors can skew the sugar preference palette to a primary use of Gal. Indeed, attenuation in animal models of disease of *S. pneumoniae* mutants on the galactose pathways provides strong evidence for the key role of Gal catabolism by *S. pneumoniae* in its natural habitat (Chapter 2).

In this study, Glc is proven the preferred sugar of the pneumococcus, as previously suggested by us and others [30,35]: i) glucose supports the fastest growth rates of all monosaccharides tested (Chapter 2); ii) in sugar mixtures, Glc is the first to be consumed (Chapter 3); iii) in pulse experiments, Glc utilization starts immediately after the stimulus, independently of the carbon source used for growth (Chapter 3). Since Glc is an abundant substrate in the bloodstream and infection sites [44,45], we hypothesize that the sugar is relevant in the development of disease as it favours fast growth. In contrast, we can speculate that growth on the non-preferential sugar Gal, abundant in the airway mucins, allows the pneumococcus to thrive in the host as a commensal coloniser. In this milieu poor in nutrients that can support fast growth, fast metabolic activity

is likely deterred by other niche adaptation features required for persistence.

The ability to co-metabolize sugars (*e.g.* Man and GlcNAc) (Chapter 2), the readiness to use Glc, and the smaller transcriptional response to Glc in cells adapted to grow on a sugar mixture (Chapter 3) indicate a relatively high metabolic flexibility of *S. pneumoniae*. Furthermore, the diversity of transporters and the broad range of catabolic substrates, the redundancy of the transport systems and of some catabolic pathways encoded in pneumococcal genomes empower the microbe to survive in varied conditions. This potential can present a fitness advantage in the pneumococcal ecological niche (nasopharynx) as well as when it has to cope with dramatic nutritional changes in the passage to invasive states. Tuning of the catabolic capabilities to sugar availability is a dynamic adaptive strategy that enables the pneumococcus to benefit from the carbon sources available and compete with the colonisers in the host. Indeed, efficient uptake and metabolism of sugars impacts the growth and the relative proportions of the colonising species [19,38,41].

Interestingly, as compared to the other nasopharyngeal colonisers *Haemophilus influenzae* and *Neisseria meningitides*, *S. pneumoniae* is able to use a larger diversity of substrates, a feature likely endowing the pneumococcus a competitive advantage. In this respect, *S. pneumoniae* is more similar to oral and intestinal microbiota [56]. Accumulating evidence sustains that the range of nutritional diversity is driven by niche specific adaptations [56–58]. For example, *S. thermophilus* adapted for growth in milk has a narrow substrate utilization capacity using lactose and saccharose preferentially, whereas Glc and fructose support poorer growth [59]. In contrast, the cariogenic microorganism *S. mutans* can metabolize a vast array of carbohydrates most of them common dietary sugars (*e.g.* glucose, fructose, maltose and sucrose) reflecting the nature of its habitat [20,60]. Apparently *S. pneumoniae* seems more adapted to

the nutritional environment in the nasopharynx than its counterparts *H. influenzae* and *N. meningitidis*. A full explanation for this observation cannot be put forward, but it is possible that *S. pneumoniae* may have inhabited other richer niches, like the oral cavity, where free sugars from host diet are available and thus acquired wide metabolic capabilities, which were not lost through genome reduction events in *S. pneumoniae.* Thus, the pneumococcal metabolic flexibility and redundancy in sugar transporters and pathways might represent a strategy to survive in environments with ever changing sugar availabilities.

Carbohydrate regulation in *S. pneumoniae*

Adaptation to changing host environments involves specific responses to varied cues that result in changes in gene regulation and metabolism. The pneumococcal response to carbohydrates was evaluated in this study.

Gal gene clusters are differently organized among LAB and regulatory mechanisms are variable and species-specific [61]. In *S. pneumoniae*, the Leloir genes are widespread in the chromosome whereas the T6P pathway genes are organized in two operons (Chapter 2, [62]). In our work, analysis of mutants in Gal catabolic pathways unravelled a subtle “regulatory” link between the Leloir and the tagatose 6-phosphate pathways (Chapter 2). We unexpectedly found that a *galK* pneumococcal mutant was unable to grow on Gal, despite possessing a complete T6P pathway. On the other hand, *lacD* deficient strain was able to grow on Gal after a prolonged lag phase (Chapter 2). The latter phenotype could be explained by alleviation of the repression mediated by the transcriptional regulator carbon catabolite protein A (CcpA) over the Leloir genes prior to

the functional expression of the pathway [35], and/or induction of a non-PTS system for Gal uptake. This hypothesis is substantiated by our own data showing nil GalK (and LacD) activity during growth on Glc (Chapter 2). Gal-mediated induction of Gal permeases has been reported for *L. lactis* [39].

The peculiar phenotype of the *galK* mutant is not easily explainable. A polar effect on the *galT-2* gene downstream of *galK*, resulting in the unintentional elimination of Gal1P uridylyltransferase activity, could lead to severe growth defects. However, growth on Glc was not affected by the *galK* mutation and complementation in *trans* with *galT-2* did not restore growth on Gal. A *galK* mutant of *S. mutans* strain UA159 displayed a similar phenotype [63]. In common, *S. pneumoniae* and *S. mutans* strain UA159 lack a high-affinity PTS for Gal. Even though the absence of a high-affinity PTS is expected to limit the pathway capacity, a complete blockage is unlikely. Furthermore, PTS-mediated transport of Gal occurs in *S. pneumoniae* D39, since Gal6P has been detected in extracts of cells metabolizing Gal as well as in resting cells by *in vivo* ^{13}C-NMR (Chapter 2, Chapter 3, [35]). In summary, in *S. pneumoniae* Gal catabolism requires a functional galactokinase and we suggest that Gal1P acts as an inducer of the expression of Gal catabolic genes (Chapter 2).

GalR has been reported as a transcriptional regulator of the Leloir pathway in other streptococci [64–66]. In *S. pneumoniae* it is responsive to carbohydrates (induced in Gal and repressed upon the Glc pulse) but its involvement in Gal regulation still needs to be addressed (Chapter 3). Recently, LacR was shown to be a repressor of the T6P pathway in Glc [62]. Firm identification of the molecular mechanisms underlying the coordination of Leloir and T6P pathways in the pneumococcus certainly deserves further investigation.

This work provides, for the first time, an integrated approach of the pneumococcal response to carbohydrate availability at different regulatory

layers, retrieving clues of possible metabolic constraints and hints on regulatory layers. Our results demonstrate that the transcriptional, metabolic and physiological responses to Gal, Man and GlcNAc are sugar-dependent (Chapters 2 and 3).

In GlcNAc no significant differences were observed at the transcriptional (glycolytic, fermentative and sugar-specific catabolic genes) and metabolic levels in comparison to Glc-grown cells. The end-products profile (lactate as main product) is in agreement with the generalized view that the fermentation of fast metabolizable sugars is homolactic. The underlying mechanism encompasses the accumulation of high amounts of FBP, a known LDH activator (Chapter 3). The rate of GlcNAc and Glc utilization in resting cells (anabolism uncoupled) was also similar. In light of these results it surprising that the growth rates on GlcNAc and Glc-grown are not identical, with Glc sustaining much faster growth (Chapter 2). A clue to this phenotype is provided by the accumulation of other phosphorylated metabolites in growing cells: fructose 6-phosphate, N-acetylglucosamine 6-phosphate and glucosamine 6-phosphate (Chapter 2). In particular, fructose 6-phosphate accumulated substantially. The large accumulation of phosphorylated metabolites in growing cells combined with the poorer performance of GlcNAc in supporting growth, indicate a metabolic bottleneck in anabolic processes.

In *S. pneumoniae*, likewise in *S. mutans,* differential regulation of *nagB* and *nagA* was observed in GlcNAc-adapted cells (Chapter 3, [67]) (Fig. 4.2).

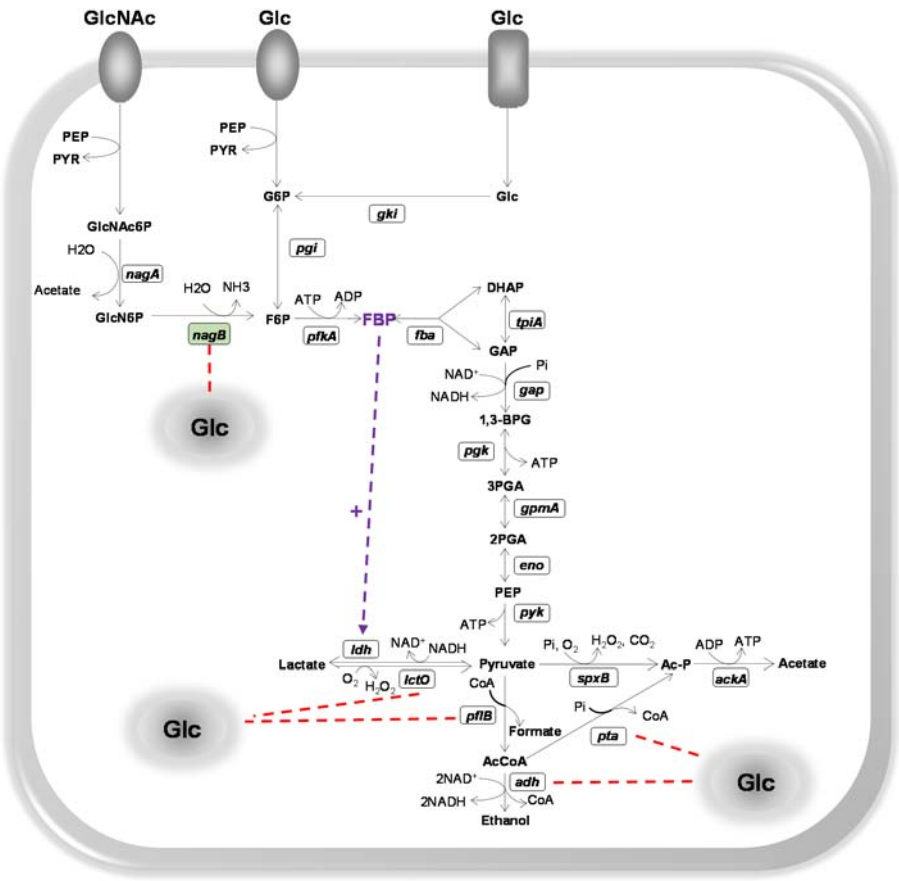

Figure 4.2. Model for transcriptional and metabolic regulation of central metabolic pathways in *S. pneumoniae* D39 during growth on GlcNAc.

Reactions are catalysed by the following protein encoding genes: *nagA*, N-acetylglucosamine 6-phosphate deacetylase; *nagB*, glucosamine 6-phosphate isomerase; *gki*, glucokinase; *pgi*, glucose 6-phosphate isomerase; *pfkA*, 6-phosphofructokinase; *fba*, fructose-biphosphate aldolase; *tpiA*, triosephosphate isomerase; *gap*, glyceraldehyde 3-phosphate dehydrogenase; *pgk*, phosphoglycerate kinase; *gpmA*, phosphoglyceromutase; *eno*, enolase; *pyk*, pyruvate kinase; *ldh*, L-lactate dehydrogenase; *spxB*, pyruvate oxidase; *lcto*, lactate oxidase; *pflB*, pyruvate formate-lyase; *pta*, phosphotransacetylase; *ackA*, acetate kinase; *adh*, bifunctional acetaldehyde-coA/alcohol dehydrogenase.
Intermediates: GlcNAc6P, N-acetylglucosamine 6-phosphate; GlcN6P, glucosamine 6-phosphate; G6P, glucose 6-phosphate; F6P, fructose 6-phosphate; FBP, fructose 1,6-biphosphate; GAP, glyceraldehyde 3-phosphate; DHAP, dihydroxyacetone phosphate; BPG, 1,3-biphosphoglycerate; 3-PGA, 3-phosphoglycerate; 2-PGA, 2-phosphoglycerate; PEP, phospho*enol*pyruvate.
Green boxes indicate upregulation in GlcNAc-grown cells as compared to Glc. *nagB* is upregulated using a less restrictive criterion for microarrays analysis. Red dashed lines

represent transcriptional repression in presence of Glc. Purple dashed arrow represent metabolic regulation of enzymes. Highlighted in big bold purple font is the glycolytic intermediate accumulated in resting cells as determined by *in vivo* ^{13}C-NMR.

It is well described that metabolism through non-preferential sugars generates mixed-acid fermentation profiles. Gal catabolism in *S. pneumoniae* was not the exception (Chapters 2 and 3, [35,36]). Results from our laboratory showed that in *S. pneumoniae*, the fermentative pathways are under the control of the transcriptional regulator CcpA [35]. CcpA activates *ldh* and represses *pta*, *ackA*, *adh* and *pflB*, hence favouring homolactic fermentation, *i.e*., fast growth by ensuring the efficient regeneration of reducing equivalents for glycolysis. However, repression of mixed acid genes is counterbalanced by Gal activation [35], suggesting other mechanisms in effect. In Chapter 3 we provide more evidence for the transcriptional regulation of Gal catabolism, however this type of regulation does not suffice to fully explain the observed phenotypes. Indeed, the gene expression pattern (only *pta* is upregulated in this study) does not fully correlate with the metabolic shift, which can only be explained through metabolic modulation of enzyme activities (Chapter 3).

The differences in gene expression profiles between this study and that of Carvalho *et al.* [35] can derive from the dissimilar analysis of the microarray data (criteria for significance and/or *in silico* comparative transcriptome) or the use of a different D39 isolate. Indeed, phenotypic differences between the two isolates are evident when comparing the work in this thesis with previous data [35], of which different growth rates and end-product profiles on Glc and Gal are obvious. This is not surprising, as the sequences of two isolates of *S. pneumoniae* D39 showed a number of mutations, which could be correlated with phenotypic traits of the isolates. For example, a mutation in the *spxB* in one of the

isolates correlated with lower H_2O_2 production and larger and less transparent colonies [68].

At metabolic level, the low FBP accumulation likely results in low levels of the known PFL inhibitors, DHAP and GAP, thus resulting in the alleviation of PFL activity and a consequent shift towards mixed acid (Fig. 4.3).

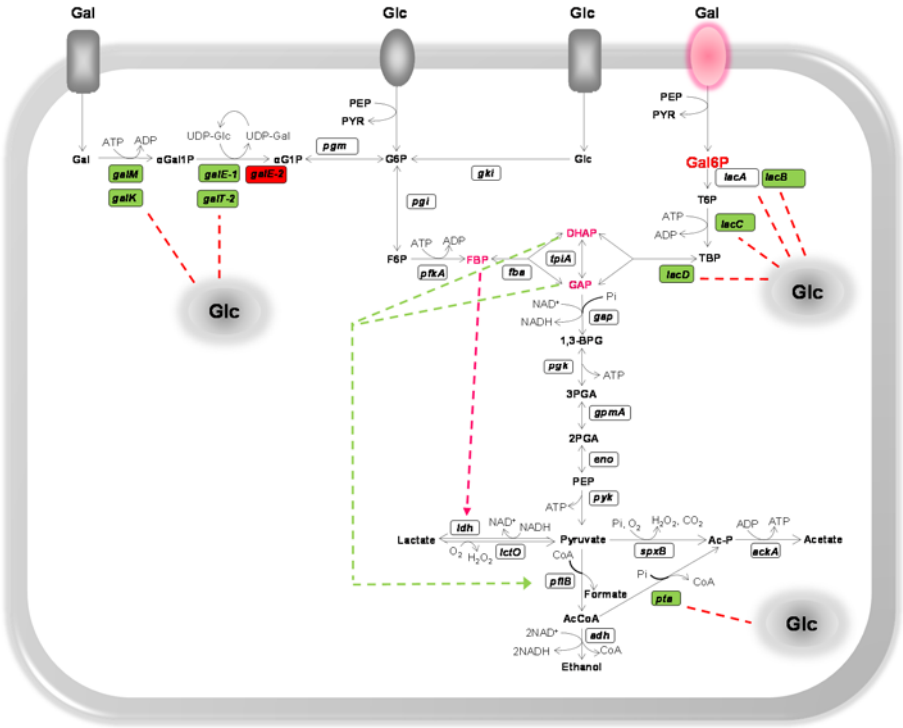

Figure 4.3. Model for transcriptional and metabolic regulation of central metabolic pathways in *S. pneumoniae* D39 during growth on Gal.

Reactions are catalysed by the following protein encoding genes: *galM*, aldolase 1-epimerase (mutarotase); *galK,* galactokinase; *galT-1, galT-2*, galactose 1-phosphate uridylyltransferase; *galE-1*, *galE-2*, UDP-glucose 4-epimerase; *pgm*, phosphoglucomutase/phosphomannomutase family protein; *lacA*, galactose 6-phosphate isomerase subunit LacA; *lacB*, galactose 6-phosphate isomerase subunit LacB; *lacC*, tagatose 6-phosphate kinase; *lacD*, tagatose 1,6-diphosphate aldolase; *gki*, glucokinase; *pgi*, glucose 6-phosphate isomerase; *pfkA*, 6-phosphofructokinase; *fba*, fructose-biphosphate aldolase; *tpiA*, triosephosphate isomerase; *gap*, glyceraldehyde 3-phosphate dehydrogenase; *pgk*, phosphoglycerate kinase; *gpmA*, phosphoglyceromutase; *eno*, enolase; *pyk*, pyruvate kinase; *ldh*, L-lactate dehydrogenase; *spxB*, pyruvate oxidase; *lcto*,

lactate oxidase; *pflB*, pyruvate formate-lyase; *pta*, phosphotransacetylase; *ackA*, acetate kinase; *adh*, bifunctional acetaldehyde-coA/alcohol dehydrogenase.
Intermediates: Gal, galactose; α-Gal, α-galactose; α-Gal1P, α-galactose 1-phosphate; α-G1P, α-glucose 1-phosphate; UDP-Glc, UDP-glucose; UDP-Gal, UDP-galactose; Gal6P, galactose 6-phosphate; T6P, tagatose 6-phosphate; TBP, tagatose 1,6-diphosphate; G6P, glucose 6-phosphate; F6P, fructose 6-phosphate; FBP, fructose 1,6-biphosphate; GAP, glyceraldehyde 3-phosphate; DHAP, dihydroxyacetone phosphate; BPG, 1,3-biphosphoglycerate; 3-PGA, 3-phosphoglycerate; 2-PGA, 2-phosphoglycerate; PEP, phospho*enol*pyruvate.
Green boxes indicate upregulation in Gal-grown cells as compared to Glc. Red box indicate downregulation in Gal-grown cells as compared to Glc. Red dashed lines represent transcriptional repression in presence of Glc. Pink transporter highlight a metabolic bottleneck in Gal catabolism. Highlighted in pink are the glycolytic and Gal-specific catabolic intermediates detected in resting cells by *in vivo* ^{13}C-NMR. The size of the font is indicative of the pool size. Accumulation of DHAP and GAP are not detected *in vivo* but low accumulation as compared to Glc-grown cells is inferred due to the reversibility of the reactions catalysed by FBP aldolase and triose 3-phosphate isomerase. Pink dashed lines represent relief of LDH activation. Green dashed lines represent relief of PFL inhibition.

In *S. pneumoniae*, the two pathways for Gal catabolism are transcriptionally regulated, with Gal acting as inducer and Glc inhibitor (Chapter 3). Previously, the Leloir pathway was found to be regulated in a CcpA-independent manner [35]. In the same study, the T6P pathway was induced by CcpA, but CcpA-independent regulation of the pathway has also been described [35,62]. The contribution of specific Gal transcriptional regulators should be experimentally addressed to understand these regulatory mechanisms. We show that expression of transcriptional regulator *galR* was modulated by Gal and Glc, while LacR was induced on Gal (Chapter 3). This regulator has been found to repress the T6P pathway in the absence of Gal and lactose and presence of Glc [62].

The inefficient Gal catabolism can be partially explained by the lack of a high affinity Gal transporter, but the intense accumulation of Gal6P in resting cells (as well as growing cells, only qualitative) suggests a metabolic bottleneck during the Gal molecular breakdown (Chapters 2

and 3). Which step(s) is inhibited remains to be elucidated. The inhibitory effect of Gal6P on growth of *S. mutans* is documented [18].

Interestingly, the slow metabolizable sugar Man only presented a modest shift to mixed acid fermentation, largely maintaining a homolactic fermentation, suggesting alternative mechanisms for regulation of the metabolic shift (Chapters 2 and 3). Man elicited a global effect on glycolytic (*fba*, *gap, pgk*, *eno* and *pyk*) and fermentative genes (induction of *adh*, *pflB* and *lctO*). The induction of glycolytic genes might be a way to alleviate the stress promoted by the high accumulation of Man6P. The deleterious effects of phosphorylated compounds in growth and metabolism are well-documented [69,70]. Our results strongly indicate a metabolic bottleneck likely at level of mannose 6-phosphate isomerase (Fig. 4.4) (Chapters 2 and 3).

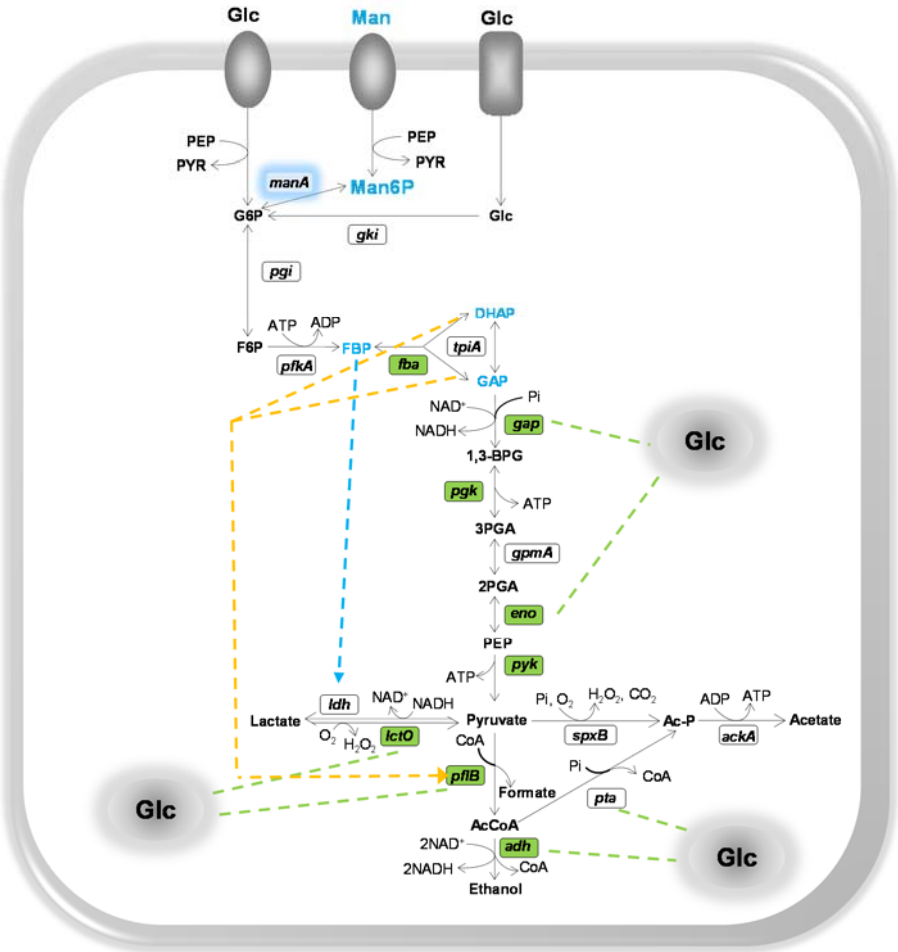

Figure 4.4. Model for transcriptional and metabolic regulation of central metabolic pathways in *S. pneumoniae* D39 during growth on Man.

Reactions are catalysed by the following protein encoding genes: *manA*, mannose 6-phosphate isomerase; *gki*, glucokinase; *pgi*, glucose 6-phosphate isomerase; *pfkA*, 6-phosphofructokinase; *fba*, fructose-biphosphate aldolase; *tpiA*, triosephosphate isomerase; *gap*, glyceraldehyde 3-phosphate dehydrogenase; *pgk*, phosphoglycerate kinase; *gpmA*, phosphoglyceromutase; *eno*, enolase; *pyk*, pyruvate kinase; *ldh*, L-lactate dehydrogenase; *spxB*, pyruvate oxidase; *lcto*, lactate oxidase; *pflB*, pyruvate formate-lyase; *pta*, phosphotransacetylase; *ackA*, acetate kinase; *adh*, bifunctional acetaldehyde-coA/alcohol dehydrogenase.
Intermediates: Man6P, mannose 6-phosphate; G6P, glucose 6-phosphate; F6P, fructose 6-phosphate; FBP, fructose 1,6-biphosphate; GAP, glyceraldehyde 3-phosphate; DHAP, dihydroxyacetone phosphate; BPG, 1,3-biphosphoglycerate; 3-PGA, 3-phosphoglycerate; 2-PGA, 2-phosphoglycerate; PEP, phospho*enol*pyruvate.

Green boxes indicate upregulation in Man as compared to Glc. Green dashed lines represent transcriptional repression in presence of Glc. Blue shadow highlight a metabolic bottleneck in Man catabolism.
Highlighted in blue are the glycolytic and Man-specific catabolic intermediates detected *in vivo* by ^{13}C-NMR. The size of the font is indicative of the size of the pool. Accumulation of DHAP and GAP is not detected *in vivo,* but a lower accumulation as compared to Glc-grown cells is inferred due to the reversibility of the reactions catalysed by FBP aldolase and triose 3-phosphate isomerase.
Blue dashed lines represent relief of LDH activation. Orange dashed lines represent relief of PFL inhibition.

The addition of Glc to cells adapted for growth on the glycan-constituent sugars generally repressed mixed acid fermentation, except for Man (Figs. 4.2, 4.3, 4.4). Interestingly transcript levels of *ldh* were not increased in any of the conditions examined. The transcriptional response to Glc was sugar-dependent. Clearly downregulation of Gal catabolism supports the hypothesis that Glc displays a repressing effect over Gal catabolism. In opposition Gal, Man and GlcNAc do not repress Glc metabolism, as denoted by the instantaneous utilization of the sugar upon the Glc challenge (Chapter 3).

Overall, our data shows that exposure to different carbohydrates and the underlying adaptation involves specific mechanisms comprising both genetic and metabolic regulation. The acquisition and catabolism of nutrients is a hierarchical and orchestrated process tuned to allow the bacterium to persist and in opportune conditions cause disease. The work in this thesis contributes to expand our still limited understanding of this complex phenomenon.

Sugar metabolism and virulence

Growing evidence from studies on human bacterial pathogens indicate that central carbon metabolism can dramatically impact the pathogenic potential and emphasize the role of sugar acquisition and catabolism on the *in vivo* fitness of the bacterium. Indeed, the expression of sugar specific metabolic pathways is required for survival in different niches by allowing the pneumococcus to exploit the available carbohydrates, but a sugar stimulus also influences in a specific fashion the virulence potential of the bacterium by modulating the expression of genes encoding virulence factors.

In this work we found that Gal catabolism is of key importance for pneumococcal growth in the nasopharynx and subsequent invasive states. This conclusion stems out from our observations that mutants in Gal catabolic genes, particularly D39Δ*lacD*Δ*galK*, showed attenuated ability to colonise and reduced virulence following intranasal infection in mouse models of colonisation and disease (bronchopneumonia with bacteraemia) (Chapter 2). In contrast, mutans in Man (D39Δ*manA*) or GlcNAc (D39Δ*nagA*) pathways, performed essentially as the wild-type strain D39. The lack of any effect upon direct administration of mutant strains in blood, indicates that Gal catabolism is key in the nasopharynx but not in the blood. Gal catabolic genes represent the highest fraction of genes induced by mucin (Chapter 2), an observation that is in agreement with the hypothesis that Gal is the primary carbon source for *S. pneumoniae* D39 in the nasal cavity. We suggested that deficient Gal catabolism could impact the expression of virulence traits, such as capsule. In an earlier study, Gal-grown cells were show to produce the double amount of capsule as compared to Glc-grown, but whether it is the capsule or other factor remains to be elucidated. Indeed, Gal induced well-

established virulence genes (*e.g. bgaA*) as well as the new herein proposed (*lacD*, *galK*) (Chapter 3).

Surprisingly, during this work we found that *S. pneumoniae* cultures growing on Gal formed visible aggregates, which led us to inspect the cells under the microscope. Unexpectedly, Gal-grown cells displayed a different morphology as compared to Glc-grown cells. We went further and used different molecular dyes to assess cell morphology under fluorescence microscopy. Cells were grown in CDM supplemented with Gal or Glc and samples were taken at mid-exponential and early stationary phases of growth (Fig. 4.5). Interestingly, we observed that Gal-grown cells have an elongated shape with sharp poles, and that this phenotype becomes more pronounced at later stages of growth or under lower Gal concentrations. Concomitantly, formation of chains is observed (Fig. 4.5). We hypothesised that this morphological adaptation might confer a strategic advantage for the pneumococcus to survive in the nasopharynx, while benefiting from Gal residues of mucins. It was shown that long pneumococcal chains are selected for stable colonisation by enhancing adherence to epithelial cells. In opposition, short chains are more likely to evade complement deposition (less complement activation) and subsequent phagocytosis, and therefore may be selected to invade the host, accounting for the diplococcal morphology in clinical samples [71,72]. Rodriguez *et al.,* [71] hypothesised that the environmental niche provide a signal for long chain formation, thus enhancing adherence of the pneumococcus. Here we propose that Gal, might be that signal.

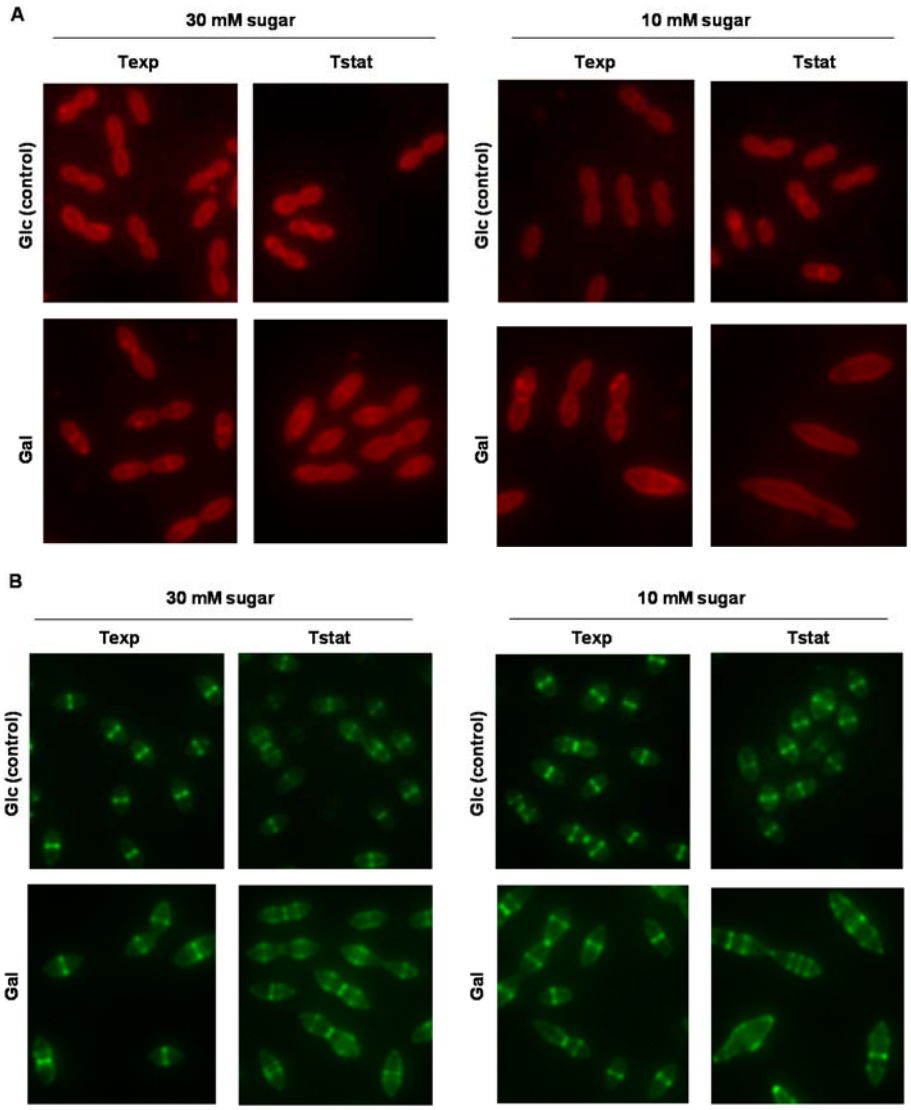

Figure 4.5. Cell morphology of *S. pneumoniae* grown in Gal in comparison to Glc.

Cells were grown in CDM with 30 and 10 mM of Gal or Glc. Samples were collected at mid-exponential and early stationary phases of growth. For direct comparison optical density at 600 nm was adjusted to 0.5 with fresh medium. For membrane labelling Nile Red was used (**A**). To assess side wall elongation VanFL was used (probe for peptidoglycan synthesis) (**B**). Visualization was carried out on a Zeiss Axiovert microscope. Exposure times were: phase contrast 100 msec; Texas Red and GFP 1000 msec. Abbreviations: Texp, mid-exponential growth phase; Tstat, early stationary growth phase.

We also observed that unlike Glc-grown cells, on Gal-grown cells the nascent peptidoglycan was not only positioned at the division site in the midcell (division septum) or at the constriction site between sister cells, which will form the new cell poles once division is complete. In Gal cultivations, several septa were observed and this effect was more pronounced at the stationary phase of growth in cultures with lower Gal concentration. These results suggest that peptidoglycan synthesis takes place at multiple division sites along the elongated cell. A model for sidewall elongation in which peptidoglycan insertion occurs simultaneously at multiple Z-ring-associated sites was proposed for the ovococci *L. lactis*. Moreover, filamentation resulted from septation inhibition and the contribution of penicillin binding proteins PBP2x (septal growth) and PBP2b (peripheral growth (elongation)) was described [73]. The biological role of filamentation in bacteria is wide (reviewed in [73]). In particular, filamentation increases the total bacterial surface, and this can be rationalized as a response to maximize nutritional uptake [74]. In *S. pneumoniae* the elongated filamentous phenotype can be perceived as a physiological advantage in the the nasopharynx milieu, where free sugars are scarce. The altered shape of the pneumococcus in response to carbohydrates is novel and certainly deserves future characterization.

A Glc stimulus during exponential growth of *S. pneumoniae* produced sugar specific responses on expression of virulence genes. However, Glc exerted mostly negative regulation over the known virulence genes (*bgaA, pflA, pflB, galK*), suggesting that these factors are required for colonisation, but not in disease states.

The profile and dynamics of gene expression presented in Chapter 3 highlight that the virulence potential of the pneumococcus is clearly influenced by the carbon source either by modulation of catabolic pathways and/or classical virulence factors.

Concluding note

This work provides a valuable contribution to the comprehension of carbohydrate metabolism in *S. pneumoniae* and its influence in pneumococcal colonisation and disease. The challenging goals set out in the beginning of this endeavour were at most achieved by a combined approach comprising a detailed physiological characterization, metabolic profiling, transcriptional profiling, mutant characterization, and virulence studies in animal models of disease. The data generated at the different "omic" layers has just begun to be analysed in the framework mathematical representations. The multi-level data herein generated can be used to fuel mathematical models of metabolism and regulation [75], which are expected to predict factors essential during colonisation and invasive states. The application of genome scale model to predict novel drug targets for cancer therapies has been reported [76]. Thus, new strategies could be followed aimed at developing therapeutics targeting sugar catabolic pathways to fight pneumococcal disease. Collectively, our data powerfully strengthens the link between physiology and pathogenesis. Furthermore, our research paves the way for new lines of investigation. Certainly the unexpected changes in *S. pneumoniae* cell shape in response to Gal deserve future scrutiny. Questions such as "is this response specific to Gal?", "does the altered morphology impact the ability to colonise and cause disease?, "what is the molecular mechanism?" and "what is the physiological relevance?" should be addressed in the future. We speculate that a meticulous and targeted analysis of the transcriptome data will unveil some clues to initiate such studies.

Also intriguing was the inability of a *galK* mutant to grow on Gal. Considering the role of Gal catabolism in the ability to colonise and cause disease we imagine that unravelling the molecular mechanism is of

importance to further our understanding of carbon metabolism in the host. Furthermore, the production of virulence factors, including capsule, should be assessed in Gal-catabolic mutants. How the catabolic mutants perform in mucin containing medium should also be examined and the derived knowledge is expected to corroborate our findings in the animal models.

Inspiration for future research in the field of pneumococcal physiology and metabolism is provided by the many pointers deriving from our transcriptome studies. For example, the genes SPD_0502 and *celBCD* were induced by Glc in all the conditions tested, and hence a role on Glc transport can be surmised. Experimental validation can be accomplished by mutating these genes in a *S. pneumoniae* Glc/Man-PTS mutant. In fact, the hypothesis that SPD_0502 and *celBCD* are involved in Glc uptake has been tested in our laboratory, in a larger effort to unravel the complement of Glc transporters in *S. pneumoniae*.

In conclusion, the data presented in this thesis extends considerably our knowledge on *S. pneumoniae* basic physiology and on how carbohydrate acquisition and metabolism influences the pathogenic potential of the bacterium. Growing evidence supports a strong intertwinement between central metabolism and virulence. Additionally, this thesis raises new research questions that can advance our understanding of the interactions between S. *pneumoniae* and its host.

References

1. Linden, S. K., McGuckin, M.A. Microbes at the host surface. Current research, technology and education topics in applied microbiology and microbial biotechnology.

A. Méndez-Vilas. Badajoz, Spain: Formatex Research Center; 2010. pp. 591–596. Available: http://www.formatex.org/microbiology2/index.html

2. Derrien M, van Passel MW, van de Bovenkamp JH, Schipper RG, de Vos WM, Dekker J. Mucin-bacterial interactions in the human oral cavity and digestive tract. Gut Microbes. 2010;1: 254–268. doi:10.4161/gmic.1.4.12778
3. Kankainen M, Paulin L, Tynkkynen S, von Ossowski I, Reunanen J, Partanen P, et al. Comparative genomic analysis of *Lactobacillus rhamnosus GG* reveals pili containing a human- mucus binding protein. Proc Natl Acad Sci U S A. 2009;106: 17193–17198. doi:10.1073/pnas.0908876106
4. Derrien M. Akkermansia muciniphila gen. nov., sp. nov., a human intestinal mucin-degrading bacterium. Int J Syst Evol Microbiol. 2004;54: 1469–1476. doi:10.1099/ijs.0.02873-0
5. Thornton DJ. From mucins to mucus: toward a more coherent understanding of this essential barrier. Proc Am Thorac Soc. 2004;1: 54–61. doi:10.1513/pats.2306016
6. Rose MC, Voynow JA. Respiratory tract mucin genes and mucin glycoproteins in health and disease. Physiol Rev. 2006;86: 245–278. doi:10.1152/physrev.00010.2005
7. Terra VS, Homer KA, Rao SG, Andrew PW, Yesilkaya H. Characterization of novel β-galactosidase activity that contributes to glycoprotein degradation and virulence in *Streptococcus pneumoniae*. Infect Immun. 2010;78: 348–357. doi:10.1128/IAI.00721-09
8. Miller RS, Hoskins LC. Mucin degradation in human colon ecosystems. Fecal population densities of mucin-degrading bacteria estimated by a “most probable number” method. Gastroenterology. 1981;81: 759–765.
9. Hoskins LC, Agustines M, McKee WB, Boulding ET, Kriaris M, Niedermeyer G. Mucin degradation in human colon ecosystems. Isolation and properties of fecal strains that degrade ABH blood group antigens and oligosaccharides from mucin glycoproteins. J Clin Invest. 1985;75: 944–953. doi:10.1172/JCI111795
10. Salyers AA, West SE, Vercellotti JR, Wilkins TD. Fermentation of mucins and plant polysaccharides by anaerobic bacteria from the human colon. Appl Environ Microbiol. 1977;34: 529–533.
11. Fabich AJ, Jones SA, Chowdhury FZ, Cernosek A, Anderson A, Smalley D, et al. Comparison of carbon nutrition for pathogenic and commensal *Escherichia coli* strains in the mouse intestine. Infect Immun. 2008;76: 1143–1152. doi:10.1128/IAI.01386-07
12. Willis CL, Cummings JH, Neale G, Gibson GR. *In vitro* effects of mucin fermentation on the growth of human colonic sulphate-reducing bacteria. Anaerobe. 1996;2: 117–122. doi:10.1006/anae.1996.0015
13. Van der Hoeven JS, van den Kieboom CW, Camp PJ. Utilization of mucin by oral *Streptococcus* species. Antonie Van Leeuwenhoek. 1990;57: 165–172.
14. Homer KA, Whiley RA, Beighton D. Production of specific glycosidase activities by *Streptococcus intermedius* strain UNS35 grown in the presence of mucin. J Med Microbiol. 1994;41: 184–190.
15. Renye JA, Piggot PJ, Daneo-Moore L, Buttaro BA. Persistence of *Streptococcus mutans* in stationary-phase batch cultures and biofilms. Appl Environ Microbiol. 2004;70: 6181–6187. doi:10.1128/AEM.70.10.6181-6187.2004

16. Mothey D, Buttaro BA, Piggot PJ. Mucin can enhance growth, biofilm formation, and survival of *Streptococcus mutans*. FEMS Microbiol Lett. 2014;350: 161–167. doi:10.1111/1574-6968.12336
17. Abranches J, Chen Y-YM, Burne RA. Characterization of *Streptococcus mutans* strains deficient in EIIABMan of the sugar phosphotransferase system. Appl Environ Microbiol. 2003;69: 4760–4769. doi:10.1128/AEM.69.8.4760-4769.2003
18. Zeng L, Das S, Burne RA. Utilization of lactose and galactose by *Streptococcus mutans*: transport, toxicity, and carbon catabolite repression. J Bacteriol. 2010;192: 2434–2444. doi:10.1128/JB.01624-09
19. Homer KA, Patel R, Beighton D. Effects of N-acetylglucosamine on carbohydrate fermentation by *Streptococcus mutans* NCTC 10449 and *Streptococcus sobrinus* SL-1. Infect Immun. 1993;61: 295–302.
20. Ajdić D, McShan WM, McLaughlin RE, Savić G, Chang J, Carson MB, et al. Genome sequence of *Streptococcus mutans* UA159, a cariogenic dental pathogen. Proc Natl Acad Sci U S A. 2002;99: 14434–14439. doi:10.1073/pnas.172501299
21. King SJ. Pneumococcal modification of host sugars: a major contributor to colonization of the human airway? Mol Oral Microbiol. 2010;25: 15–24. doi:10.1111/j.2041-1014.2009.00564.x
22. Burnaugh AM, Frantz LJ, King SJ. Growth of *Streptococcus pneumoniae* on human glycoconjugates is dependent upon the sequential activity of bacterial exoglycosidases. J Bacteriol. 2008;190: 221–230. doi:10.1128/JB.01251-07
23. Marion C, Stewart JM, Tazi MF, Burnaugh AM, Linke CM, Woodiga SA, et al. *Streptococcus pneumoniae* can utilize multiple sources of hyaluronic acid for growth. Infect Immun. 2012;80: 1390–1398. doi:10.1128/IAI.05756-11
24. Yesilkaya H, Manco S, Kadioglu A, Terra VS, Andrew PW. The ability to utilize mucin affects the regulation of virulence gene expression in *Streptococcus pneumoniae*. FEMS Microbiol Lett. 2008;278: 231–235. doi:10.1111/j.1574-6968.2007.01003.x
25. Corfield AP, Wagner SA, Clamp JR, Kriaris MS, Hoskins LC. Mucin degradation in the human colon: production of sialidase, sialate O-acetylesterase, N-acetylneuraminate lyase, arylesterase, and glycosulfatase activities by strains of fecal bacteria. Infect Immun. 1992;60: 3971–3978.
26. King SJ, Hippe KR, Weiser JN. Deglycosylation of human glycoconjugates by the sequential activities of exoglycosidases expressed by *Streptococcus pneumoniae*. Mol Microbiol. 2006;59: 961–974. doi:10.1111/j.1365-2958.2005.04984.x
27. Liu M, Durfee T, Cabrera JE, Zhao K, Jin DJ, Blattner FR. Global transcriptional programs reveal a carbon source foraging strategy by *Escherichia coli*. J Biol Chem. 2005;280: 15921–15927. doi:10.1074/jbc.M414050200
28. Higgins MA, Suits MD, Marsters C, Boraston AB. Structural and functional analysis of fucose-processing enzymes from *Streptococcus pneumoniae*. J Mol Biol. 2014;426: 1469–1482. doi:10.1016/j.jmb.2013.12.006
29. Chan PF, O'Dwyer KM, Palmer LM, Ambrad JD, Ingraham KA, So C, et al. Characterization of a novel fucose-regulated promoter (PfcsK) suitable for gene essentiality and antibacterial mode-of-action studies in *Streptococcus pneumoniae*. J Bacteriol. 2003;185: 2051–2058. doi:10.1128/JB.185.6.2051-2058.2003
30. Bidossi A, Mulas L, Decorosi F, Colomba L, Ricci S, Pozzi G, et al. A functional genomics approach to establish the complement of carbohydrate transporters in

Streptococcus pneumoniae. Miyaji EN, editor. PLoS ONE. 2012;7: e33320. doi:10.1371/journal.pone.0033320

31. Gualdi L, Hayre J, Gerlini A, Bidossi A, Colomba L, Trappetti C, et al. Regulation of neuraminidase expression in *Streptococcus pneumoniae*. BMC Microbiol. 2012;12: 200. doi:10.1186/1471-2180-12-200
32. Trappetti C, Kadioglu A, Carter M, Hayre J, Iannelli F, Pozzi G, et al. Sialic acid: a preventable signal for pneumococcal biofilm formation, colonization, and invasion of the host. J Infect Dis. 2009;199: 1497–1505. doi:10.1086/598483
33. Marion C, Burnaugh AM, Woodiga SA, King SJ. Sialic acid transport contributes to pneumococcal colonization. Infect Immun. 2011;79: 1262–1269. doi:10.1128/IAI.00832-10
34. Parker D, Soong G, Planet P, Brower J, Ratner AJ, Prince A. The NanA neuraminidase of *Streptococcus pneumoniae* is involved in biofilm formation. Infect Immun. 2009;77: 3722–3730. doi:10.1128/IAI.00228-09
35. Carvalho SM, Kloosterman TG, Kuipers OP, Neves AR. CcpA ensures optimal metabolic fitness of *Streptococcus pneumoniae*. Horsburgh MJ, editor. PLoS ONE. 2011;6: e26707. doi:10.1371/journal.pone.0026707
36. Yesilkaya H, Spissu F, Carvalho SM, Terra VS, Homer KA, Benisty R, et al. Pyruvate formate lyase is required for pneumococcal fermentative metabolism and virulence. Infect Immun. 2009;77: 5418–5427. doi:10.1128/IAI.00178-09
37. Cai J, Tong H, Qi F, Dong X. CcpA-dependent carbohydrate catabolite repression regulates galactose metabolism in *Streptococcus oligofermentans*. J Bacteriol. 2012;194: 3824–3832. doi:10.1128/JB.00156-12
38. Zeng L, Martino NC, Burne RA. Two gene clusters coordinate galactose and lactose metabolism in *Streptococcus gordonii*. Appl Env Microbiol. 2012;78: 5597–5605. doi:10.1128/AEM.01393-12
39. Neves AR, Pool WA, Solopova A, Kok J, Santos H, Kuipers OP. Towards enhanced galactose utilization by *Lactococcus lactis*. Appl Env Microbiol. 2010;76: 7048–7060. doi:10.1128/AEM.01195-10
40. Kaufman GE, Yother J. CcpA-dependent and -independent control of beta-galactosidase expression in *Streptococcus pneumoniae* occurs via regulation of an upstream phosphotransferase system-encoding operon. J Bacteriol. 2007;189: 5183–5192. doi:10.1128/JB.00449-07
41. Zeng L, Xue P, Stanhope MJ, Burne RA. A galactose-specific sugar: phosphotransferase permease is prevalent in the non-core genome of *Streptococcus mutans*. Mol Oral Microbiol. 2013;28: 292–301. doi:10.1111/omi.12025
42. Tettelin H, Nelson KE, Paulsen IT, Eisen JA, Read TD, Peterson S, et al. Complete genome sequence of a virulent isolate of *Streptococcus pneumoniae*. Science. 2001;293: 498–506. doi:10.1126/science.1061217
43. Görke B, Stülke J. Carbon catabolite repression in bacteria: many ways to make the most out of nutrients. Nat Rev Microbiol. 2008;6: 613–624. doi:10.1038/nrmicro1932
44. Shelburne SA, Davenport MT, Keith DB, Musser JM. The role of complex carbohydrate catabolism in the pathogenesis of invasive streptococci. Trends Microbiol. 2008;16: 318–325. doi:10.1016/j.tim.2008.04.002
45. Philips BJ, Meguer J-X, Redman J, Baker EH. Factors determining the appearance of glucose in upper and lower respiratory tract secretions. Intensive Care Med. 2003;29: 2204–2210. doi:10.1007/s00134-003-1961-2

46. Hu Z, Patel IR, Mukherjee A. Genetic analysis of the roles of *agaA*, *agaI*, and *agaS* genes in the N-acetyl-D-galactosamine and D-galactosamine catabolic pathways in *Escherichia coli* strains O157:H7 and C. BMC Microbiol. 2013;13: 94. doi:10.1186/1471-2180-13-94
47. Leyn SA, Gao F, Yang C, Rodionov DA. N-Acetylgalactosamine utilization pathway and regulon in proteobacteria: genomic reconstruction and experimental characterization in *Shewanella*. J Biol Chem. 2012;287: 28047–28056. doi:10.1074/jbc.M112.382333
48. Bidart GN, Rodríguez-Díaz J, Monedero V, Yebra MJ. A unique gene cluster for the utilization of the mucosal and human milk-associated glycans galacto- *N* -biose and lacto- *N* -biose in *L actobacillus casei*: Galacto- and lacto- *N* -biose utilization in *Lactobacillus*. Mol Microbiol. 2014;93: 521–538. doi:10.1111/mmi.12678
49. Higgins MA, Whitworth GE, El Warry N, Randriantsoa M, Samain E, Burke RD, et al. Differential recognition and hydrolysis of host carbohydrate antigens by *Streptococcus pneumoniae* family 98 glycoside hydrolases. J Biol Chem. 2009;284: 26161–26173. doi:10.1074/jbc.M109.024067
50. Hava DL, Camilli A. Large-scale identification of serotype 4 *Streptococcus pneumoniae* virulence factors. Mol Microbiol. 2002;45: 1389–1406.
51. Embry A, Hinojosa E, Orihuela CJ. Regions of Diversity 8, 9 and 13 contribute to *Streptococcus pneumoniae* virulence. BMC Microbiol. 2007;7: 80. doi:10.1186/1471-2180-7-80
52. Carvalho SM, Kuipers OP, Neves AR. Environmental and nutritional factors that affect growth and metabolism of the pneumococcal serotype 2 strain D39 and its nonencapsulated derivative strain R6. Horsburgh MJ, editor. PLoS ONE. 2013;8: e58492. doi:10.1371/journal.pone.0058492
53. Thomas TD, Turner KW, Crow VL. Galactose fermentation by *Streptococcus lactis* and *Streptococcus cremoris*: pathways, products, and regulation. J Bacteriol. 1980;144: 672–682.
54. Garrigues C, Loubiere P, Lindley ND, Cocaign-Bousquet M. Control of the shift from homolactic acid to mixed-acid fermentation in *Lactococcus lactis*: predominant role of the NADH/NAD+ ratio. J Bacteriol. 1997;179: 5282–5287.
55. Deutscher J, Francke C, Postma PW. How phosphotransferase system-related protein phosphorylation regulates carbohydrate metabolism in bacteria. Microbiol Mol Biol Rev. 2006;70: 939–1031. doi:10.1128/MMBR.00024-06
56. Buckwalter CM, King SJ. Pneumococcal carbohydrate transport: food for thought. Trends Microbiol. 2012;20: 517–522. doi:10.1016/j.tim.2012.08.008
57. Rohmer L, Hocquet D, Miller SI. Are pathogenic bacteria just looking for food? Metabolism and microbial pathogenesis. Trends Microbiol. 2011;19: 341–348. doi:10.1016/j.tim.2011.04.003
58. Price CE, Zeyniyev A, Kuipers OP, Kok J. From meadows to milk to mucosa - adaptation of *Streptococcus* and *Lactococcus* species to their nutritional environments. FEMS Microbiol Rev. 2012; 36(5):949-71. doi:10.1111/j.1574-6976.2011.00323.x
59. Vaillancourt K, LeMay J-D, Lamoureux M, Frenette M, Moineau S, Vadeboncoeur C. Characterization of a galactokinase-positive recombinant strain of *Streptococcus thermophilus*. Appl Environ Microbiol. 2004;70: 4596–4603. doi:10.1128/AEM.70.8.4596-4603.2004

60. Ajdic D, Pham VTT. Global transcriptional analysis of *Streptococcus mutans* sugar transporters using microarrays. J Bacteriol. 2007;189: 5049–5059. doi:10.1128/JB.00338-07
61. Grossiord B, Vaughan EE, Luesink E, de Vos WM. Genetics of galactose utilisation via the Leloir pathway in lactic acid bacteria. Le Lait. 1998;78: 77–84. doi:10.1051/lait:1998110
62. Afzal M, Shafeeq S, Kuipers OP. LacR is a repressor of *lacABCD* and LacT an activator of *lacTFEG*, constituting the lac-gene cluster in *Streptococcus pneumoniae*. Appl Environ Microbiol. 2014; doi:10.1128/AEM.01370-14
63. Abranches J, Chen Y-YM, Burne RA. Galactose metabolism by *Streptococcus mutans*. Appl Env Microbiol. 2004;70: 6047–6052. doi:10.1128/AEM.70.10.6047-6052.2004
64. De Vin F, Radstrom P, Herman L, De Vuyst L. Molecular and biochemical analysis of the galactose phenotype of dairy *Streptococcus thermophilus* strains reveals four different fermentation profiles. Appl Environ Microbiol. 2005;71: 3659–3667. doi:10.1128/AEM.71.7.3659-3667.2005
65. Vaillancourt K, Moineau S, Frenette M, Lessard C, Vadeboncoeur C. Galactose and lactose genes from the galactose-positive bacterium *Streptococcus salivarius* and the phylogenetically related galactose-negative bacterium *Streptococcus thermophilus*: organization, sequence, transcription, and activity of the gal gene products. J Bacteriol. 2002;184: 785–793. doi:10.1128/JB.184.3.785-793.2002
66. Ajdić D, Ferretti JJ. Transcriptional regulation of the *Streptococcus mutans* gal operon by the GalR repressor. J Bacteriol. 1998;180: 5727–5732.
67. Moye ZD, Burne RA, Zeng L. Uptake and metabolism of N-acetylglucosamine and glucosamine by *Streptococcus mutans*. Appl Env Microbiol. 2014; doi:10.1128/AEM.00820-14
68. Lanie JA, Ng W-L, Kazmierczak KM, Andrzejewski TM, Davidsen TM, Wayne KJ, et al. Genome sequence of Avery's virulent serotype 2 strain D39 of *Streptococcus pneumoniae* and comparison with that of unencapsulated laboratory strain R6. J Bacteriol. 2007;189: 38–51. doi:10.1128/JB.01148-06
69. Andersen HW, Solem C, Hammer K, Jensen PR. Twofold reduction of phosphofructokinase activity in *Lactococcus lactis* results in strong decreases in growth rate and in glycolytic flux. J Bacteriol. 2001;183: 3458–3467. doi:10.1128/JB.183.11.3458-3467.2001
70. Vanderpool CK, Gottesman S. The novel transcription factor SgrR coordinates the response to glucose-phosphate stress. J Bacteriol. 2007;189: 2238–2248. doi:10.1128/JB.01689-06
71. Rodriguez JL, Dalia AB, Weiser JN. Increased chain length promotes pneumococcal adherence and colonization. Infect Immun. 2012;80: 3454–3459. doi:10.1128/IAI.00587-12
72. Dalia AB, Weiser JN. Minimization of bacterial size allows for complement evasion and is overcome by the agglutinating effect of antibody. Cell Host Microbe. 2011;10: 486–496. doi:10.1016/j.chom.2011.09.009
73. Pérez-Núñez D, Briandet R, David B, Gautier C, Renault P, Hallet B, et al. A new morphogenesis pathway in bacteria: unbalanced activity of cell wall synthesis machineries leads to coccus-to-rod transition and filamentation in ovococci:

Filamentation of *Lactococcus lactis*. Mol Microbiol. 2011;79: 759–771. doi:10.1111/j.1365-2958.2010.07483.x

74. Young KD. The selective value of bacterial shape. Microbiol Mol Biol Rev MMBR. 2006;70: 660–703. doi:10.1128/MMBR.00001-06
75. Lerman JA, Hyduke DR, Latif H, Portnoy VA, Lewis NE, Orth JD, et al. In silico method for modelling metabolism and gene product expression at genome scale. Nat Commun. 2012;3: 929. doi:10.1038/ncomms1928
76. Ghaffari P, Mardinoglu A, Asplund A, Shoaie S, Kampf C, Uhlen M, et al. Identifying anti-growth factors for human cancer cell lines through genome-scale metabolic modeling. Sci Rep. 2015;5: 8183. doi:10.1038/srep08183

Supporting Information_Chapter 4

Supporting Table

Table S4.1. Conservation of Man and GlcNAc metabolic genes in different *S. pneumoniae* strains.

D39	SPD_0641|**manA**|YP_816136.1|GeneID:4442605	SPD_1866|**nagA**|YP_817273.1|GeneID:4441513	SPD_1246|**nagB**|YP_816713.1|GeneID:4441482
TIGR4	SP_0736|SP_0736|NP_345235.1|GeneID:930686|0.0|1	SP_2056|SP_2056|NP_346480.1|GeneID:930327|0.0|1	SP_1415|SP_1415|NP_345873.1|GeneID:931420|4e-171|1
R6	spr0647|pmi|NP_358241.1|GeneID:934184|0.0|1	spr1867|nagA|NP_359458.1|GeneID:933992|0.0|1	spr1272|nagB|NP_358865.1|GeneID:934489|3e-173|1
G54	SPG_0668|SPG_0668|YP_002037383.1|GeneID:6480018|0.0|1	SPG_1971|nagA|YP_002038638.1|GeneID:6480298|0.0|1	SPG_1356|nagB|YP_002038063.1|GeneID:6479779|2e-172|1
670_6B	SP670_0786|manA|YP_003878954.1|GeneID:9729508|0.0|1	SP670_2195|nagA|YP_003880347.1|GeneID:9730908|0.0|1	SP670_0882|SP670_0882|YP_003879047.1|GeneID:9729602|2e-172|1
70585	SP70585_0782|manA|YP_002740060.1|GeneID:7683193|0.0|1	SP70585_2144|nagA|YP_002741324.1|GeneID:7684933|0.0|1	SP70585_1454|SP70585_1454|YP_002740690.1|GeneID:7682925|3e-173|1
A026	T308_03440|T308_03440|REF_PRJNA222882:T308_03440|GeneID:17439128|0.0|1	T308_09740|T308_09740|REF_PRJNA222882:T308_09740|GeneID:17440375|0.0|1	T308_03955|T308_03955|REF_PRJNA222882:T308_03955|GeneID:17439231|1e-172|1
AP200	SPAP_0712|SPAP_0712|YP_003876307.1|GeneID:9726728|0.0|1	SPAP_2082|SPAP_2082|YP_003877633.1|GeneID:9728096|0.0|1	SPAP_1446|SPAP_1446|YP_003877034.1|GeneID:9727461|3e-173|1
ATCC_700669	SPN23F_06600|pmi|YP_002510687.1|GeneID:7328278|0.0|1	SPN23F_20790|SPN23F_20790|YP_002511925.1|GeneID:7328021|0.0|1	SPN23F_13800|nagB|YP_002511308.1|GeneID:7329127|2e-172|1
CGSP14	SPCG_0685|SPCG_0685|YP_001835402.1|GeneID:6217724|0.0|1	SPCG_2023|nagA|YP_001836740.1|GeneID:6217147|0.0|1	SPCG_1403|nagB|YP_001836120.1|GeneID:6218481|4e-172|1
gamPNI0373	HMPREF1038_00750|manA|YP_006742940.1|GeneID:13694048|0.0|1	HMPREF1038_02053|HMPREF1038_02053|YP_006744154.1|GeneID:13695363|0.0|1	HMPREF1038_01402|nagB|YP_006743558.1|GeneID:13694687|7e-173|1
Hungary19A_6	SPH_0837|manA|YP_001694201.1|GeneID:6029252|0.0|1	SPH_2211|nagA|YP_001695407.1|GeneID:6029467|0.0|1	SPH_1546|SPH_1546|YP_001694850.1|GeneID:6028655|2e-172|1
INV104	INV104_06120|pmi|YP_006062290.1|GeneID:12888886|0.0|1	INV104_17720|INV104_17720|YP_006063379.1|GeneID:12890044|0.0|1	INV104_12080|nagB|YP_006062845.1|GeneID:12889480|1e-172|1
INV200	SPNINV200_06500|pmi|YP_006065975.1|GeneID:12893422|0.0|1	SPNINV200_18690|SPNINV200_18690|YP_006067121.1|GeneID:12894672|0.0|1	SPNINV200_12600|nagB|YP_006066545.1|GeneID:12894063|5e-172|1
JJA	SPJ_0675|manA|YP_002735757.1|GeneID:7679287|0.0|1	SPJ_2062|nagA|YP_002737057.1|GeneID:7679563|0.0|1	SPJ_1314|SPJ_1314|YP_002736374.1|GeneID:7680146|2e-172|1
OXC141	SPNOXC_06670|pmi|YP_006064146.1|GeneID:12891046|0.0|1	SPNOXC_18120|SPNOXC_18120|YP_006065200.1|GeneID:12891545|0.0|1	SPNOXC_12470|nagB|YP_006064670.1|GeneID:12892230|1e-172|1

P1031	SPP_0748|manA|YP_002737925.1|GeneID:7681554|0.0|1	SPP_2094|nagA|YP_002739141.1|GeneID:7681476|0.0|1	SPP_1434|SPP_1434|YP_002738561.1|GeneID:7681114|2e-172|1
SPN034156	SPN034156_17160|pmi|YP_007765953.1|GeneID:15313753|0.0|1	SPN034156_08930|SPN034156_08930|YP_007765194.1|GeneID:15313442|0.0|1	SPN034156_03330|nagB|YP_007764674.1|GeneID:15314387|1e-172|1
SPN034183	SPN034183_06680|pmi|YP_007814306.1|GeneID:15314916|0.0|1	SPN034183_18160|SPN034183_18160|YP_007815357.1|GeneID:15315434|0.0|1	SPN034183_12450|nagB|YP_007814827.1|GeneID:15314731|1e-172|1
SPN994038	SPN994038_06570|pmi|YP_007812482.1|GeneID:15316733|0.0|1	SPN994038_18050|SPN994038_18050|YP_007813537.1|GeneID:15316611|0.0|1	SPN994038_12340|nagB|YP_007813005.1|GeneID:15317826|1e-172|1
SPN994039	SPN994039_06580|pmi|YP_007763156.1|GeneID:15320331|0.0|1	SPN994039_18060|SPN994039_18060|YP_007764211.1|GeneID:15318631|0.0|1	SPN994039_12350|nagB|YP_007763679.1|GeneID:15318797|1e-172|1
SPNA45	SPNA45_01065|pmi|YP_006701504.1|GeneID:13652410|0.0|1	SPNA45_00165|SPNA45_00165|YP_006700672.1|GeneID:13651515|0.0|1	SPNA45_00790|nagB|YP_006701249.1|GeneID:13652136|9e-171|1
ST556	MYY_0772|MYY_0772|YP_006252968.1|GeneID:12900206|0.0|1	MYY_1975|MYY_1975|YP_006254165.1|GeneID:12901239|0.0|1	MYY_0875|MYY_0875|YP_006253071.1|GeneID:12900309|1e-172|1
Taiwan19F_14	SPT_0752|manA|YP_002742223.1|GeneID:7685790|0.0|1	SPT_2051|nagA|YP_002743384.1|GeneID:7686377|0.0|1	SPT_0859|SPT_0859|YP_002742314.1|GeneID:7685472|2e-172|1
TCH8431_19A	HMPREF0837_11020|pmi|YP_003724462.1|GeneID:9344276|0.0|1	HMPREF0837_10052|manD|YP_003723494.1|GeneID:9343277|0.0|1	HMPREF0837_11132|nagB|YP_003724574.1|GeneID:9344388|1e-172|1

The table was obtained by a unidirectional Blast search, where the genes of *S. pneumoniae* D39 was used a query to find homologs in the 25 other genomes. Only the best hit in each genome is shown. Each cell contains the locus tag, e-value and the number of blast hits. The e-value is reflected in the blue colour code. The darker the blue colour, the lower the e-value (and more significant hit).
This table is also available on the CD.

ITQB-UNL | Av. da República, 2780-157 Oeiras, Portugal
Tel (+351) 214 469 100 | Fax (+351) 214 411 277

www.itqb.unl.pt